Fall 9-15-2022

The Essential Roles of AMP-Activated Protein Kinase in the Control of Regulatory T Cells

Junqing An

The Essential Roles of AMP-Activated Protein Kinase in the Control of Regulatory T Cells

by

Junqing An

Under the Direction of Ming-Hui Zou, MD, Ph.D.

A Thesis/Dissertation Submitted in Partial Fulfillment of the Requirements for the Degree of

Doctor of Philosophy

in the Institute for Biomedical Sciences

Georgia State University

2022

ABSTRACT

Regulatory T cells (Tregs) are an essential subtype of immune cells that controls self-tolerance, inflammatory responses, and tissue homeostasis. In tumor immunity, Treg cells are involved in tumor development and progression by inhibiting antitumor immunity. Therapeutically targeting Treg cells in inflammation-related diseases and cancers will therefore require the identification of context-specific mechanisms that guide their functions. The AMP-activated protein kinase (AMPK) functions as a master sensor and modulator of cellular energy and redox homeostasis, both of which are vital to various immune cells including Tregs. However, whether and how AMPK plays its roles in Tregs was unknown. My dissertation aims to elucidate the contributions of AMPK in the regulation of Tregs function in different mouse disease status.

In the first part of this dissertation, I established the essential roles of AMPK in the regulation of immune homeostasis from AMPKα1 global knock-out mice. By using both bone marrow transplantation and the adoptive Treg transfer experiment, I discovered that both Treg dysfunction and the autoimmune diseases occurred in AMPKα1 global knock-out mice. By using Treg-specific AMPKα1 knock-out mice, I further uncovered the indispensable roles of AMPK in the regulation of Treg functions, as the Treg-specific AMPKα1 knock-out mice develops autoimmune disease in livers. Mechanistically, I found that AMPK regulates normal functions of Treg by maintaining the protein stability of Foxp3, a critical transcriptional factor of Tregs.

In the second part, I studied the roles of AMPK in Tregs in tumor growth and metastasis. Treg-specific AMPKα1 knock-out mice exhibited delayed tumor progression and enhanced antitumor T cell immunity. Further experiments showed that AMPKα1 maintains the functional integrity of Treg cells and prevents interferon-γ production in tumor-infiltrating Tregs cells, indicating that AMPK promotes tumor growth by maintaining high levels of Foxp3 in infiltrating Tregs in tumor tissues. Mechanistically, AMPKα1 maintains the protein stability of FOXP3 in Tregs cells by downregulating the expression of E3 ligase CHIP (*STUB1*). Our results suggest that selective inhibition of AMPK in Tregs cells might be an effective anti-tumor therapy.

In the third part of the dissertation, I interrogated the role of AMPK in Tregs senescence and aging, as a decline of AMPK has been widely described in aged animals and humans. Compared to non-senescent Tregs, senescent Tregs showed fewer protective effects on arterial inflammation and atherosclerosis development. Treg-specific AMPKα1 knock-out mice displayed accelerated Treg senescence and arterial inflammation. Hypercholesterolemia, an established risk factor of cardiovascular diseases, promoted Treg senescence, resulting in the formation of plasticity Tregs with uncontrolled production of interferon-γ and impaired suppressive function. Selective activation of AMPK in Tregs restrained Treg senescence, downregulated the levels of reactive oxygen species (ROS) in aortic walls, and suppressed high fat diets-induced atherosclerosis in mice in vivo. Taken together, my results demonstrates that AMPK activation in Tregs might be a valid target for treating aging related diseases including atherosclerosis.

In conclusion, in this dissertation I have established essential roles of AMPK in maintaining Tregs functions and deregulated AMPK with consequent Tregs dysfunctions plays causative roles in the initiations and progressions of autoimmune liver diseases, cancer, and atherosclerosis-related cardiovascular diseases.

INDEX WORDS: Regulatory T cells, AMPK, Foxp3, Autoimmune liver disease, Anti-tumor immunity, Senescence, Atherosclerosis

The Essential Roles of AMP-Activated Protein Kinase in the Control of Regulatory T Cells

by

Junqing An

Committee Chair: Ming-Hui Zou

Committee: Ping Song

Andrew Ted Gewirtz

Leszek Ignatowicz

Electronic Version Approved:

Office of Academic Assistance – Graduate Programs

Institute for Biomedical Sciences

Georgia State University

September 2022

DEDICATION

This dissertation is dedicated to my parents, Rugang An and Herui Cheng, and my wife, ChaoShan Han. Your love and tolerance inspire me to be the best version of myself.

ACKNOWLEDGEMENTS

First and foremost, I would like to express my sincere thanks to my Ph.D. mentor Dr. Ming-Hui Zou, for his continued support, guidance, and valuable scientific expertise. I truly appreciate you for accepting me as your trainees and putting in the extra time to shape me into a better scientist. You are an amazing mentor, and I would not be where I am without your help.

I would also like to thank Dr. Ping Song, who is not only committee member but also supports my research work as a mentor. Thank you for spending time to help me revise my manuscript and provide scientific and professional advice all the way through my Ph.D. studying. My great thanks also go to my committee members, Dr. Andrew Gewirtz and Dr. Leszek Ignatowicz, for their valuable advice and guidance on this journey. I truly appreciate you putting in the time to help me write the reference letters when I applied for AHA fellowship and your scientific guidance on my dissertation is invaluable to me.

Next, I would like to thank all the past and present members in Dr. Zou's lab. I have experienced such a wonderful time to work with you. Thanks for your time, patience, and valuable reagents to help me solve my scientific problems and excel in my career. I would like to give special thanks to all the lab mangers. Without your effort, the lab could not function so smoothly and the working experience here could not be so great.

Finally, I would like to give my best appreciate to my parents and my wife. Thank you for your generous support. Thank you for being the person who are always there to help so that I can do anything I wanted to in life. Without your encouragement and love, I would not be here today.

TABLE OF CONTENTS

LIST OF TABLES

LIST OF FIGURES

LIST OF ABBREVIATIONS

ACC	Acetyl-CoA Carboxylase
ADaM	Allosteric drug and metabolite
ADP	Adenosine diphosphate
AICAR	5-aminoimidazole-4-carboxamide ribonucleotide
AIDS	Acquired immunodeficiency syndrome
AIH	Autoimmune hepatitis
ALT	Alanine aminotransferase
AMP	Adenosine monophosphate
AMPK	AMP-activated protein kinase
AMPKα1	AMP-activated protein kinase alpha 1
$AMPK\alpha1^{Treg-/-}$	Treg-specific AMPKα1 deletion mice
$AMPK\alpha1^{Treg-/-}$	Treg-specific AMPKα1 deletion
ANA	Antinuclear antibodies
ApoE	Apolipoprotein E
ATG9	Autophagy-related protein 9
ATP	Adenosine triphosphate
BAECs	Bovine aortic endothelial cells
$C_{12}FDG$	β-galactosidase substrate, 5-Dodecanoylaminofluorescein Di-β-D-Galactopyranoside
CA AMPK	Constitutive active AMPK
CAMMK2	Calcium/calmodulin dependent protein kinase kinase 2
CBM	Carbohydrate-binding module
CBS	Cystathionine β-synthase repeats
CD25	High-affinity IL-2 receptor α-chain
CDK	Cyclin-dependent kinase
CHX	Cycloheximide
CMV	Cytomegalovirus
CoREST	REST corepressor 1
CTLA-4	Cytotoxic T-lymphocyte antigen-4
CVD	Cardiovascular disease
DCAF1	DDB1-and CUL4-associated factor
DUB	Deubiquitinases
EAE	Experimental autoimmune encephalomyelitis
ECs	Endothelial cells
ER stress	Endoplasmic reticulum stress
ERRs	Estrogen-related receptors
ETC	Electron transport chain
ex-Treg	Loss of Foxp3 expression in Treg cells
FACS	Fluorescent-activated cell sorting
FAO	fatty acid oxidation
FBP	Fructose-1,6-bisphosphate
Fox	Forkhead box
Foxp3	Forkhead Box P3
GITR	Tumor necrosis factor receptor superfamily, member 18
GSH	Glutathione
GSTP1	Gutathione S-transferase pi gene
H/R	Hypoxia-reoxygenation
HDACs	Histone deacetylases
HIV	Human immunodeficiency virus
HMGCR	HMG-CoA reductase
HUVECs	Human umbilical vein endothelial cells

ICOS	Inducible T cell costimulator
IFN-γ	Interferon-γ
IL-17a	Interleukin 17a
IPEX	Immune dysregulation polyendocrinopathy enteropathy X-linked syndrome
iTreg	Induced Treg cells
KD	Kinase domain
KO	Knockout
LAG3	Lymphocyte activating 3
LCFA	Long-chain fatty acid
LKB1	Liver Kinase B1
LLCs	Lewis lung carcinoma cells
MDSC	Myeloid-derived suppressor cells
MMPs	Matrix metalloproteinases
mTOR	Mechanistic target of rapamycin kinase
NAD+	Nicotinamide adenine dinucleotide
NAFLD	Nonalcoholic fatty liver disease
NFAT	Nuclear factor of activated T-cells
NO	Nitric oxide
NOS	Nitric oxide synthase
NOX	Nicotinamide adenine dinucleotide phosphate oxidase
Nrp1	Neuropilin 1
OXPHOS	Oxidative phosphorylation
pACC	phosphorylated Acetyl-CoA Carboxylase
PBC	Primary biliary cholangitis
PBMCs	Peripheral blood mononuclear cells
PD1	Programmed cell death protein 1
PDHc	Pyruvate dehydrogenase complex
PD-L1	Programmed cell death 1 ligand 1
PGC1	Proliferator-activated receptor-γ co-activator 1
PI3K	Phosphatidylinositol 3-kinase
PLD1	Phospholipase D1
PMA	Phorbol 12-myristate 13-acetate
PPARγ	Peroxisome proliferator activated receptor gamma
Prkaa1	Protein kinase AMP-activated catalytic subunit alpha 1
$Prkaa1^{-/-}$	AMPKα1 global knockout mice
$Prkaa1^{fl/fl}$	Mice carrying a loxP-flanked Prkaa1 allele
Prkaa2	Protein kinase AMP-activated catalytic subunit alpha 2
PSC	Primary sclerosing cholangitis
PTM	Post-translational modification
qRT-PCR	Quantitative realtime PCR
RIMs	Regulatory subunit-interacting motifs
RNS	Reactive nitrogen species
ROS	Reactive oxygen species
SA β-gal	Senescence-associated beta-galactosidase
SASP	Senescence-associated secretory phenotype
SIRT1	Sirtuin 1
STUB1	STIP1 homology and U-box containing protein 1
TCA	Tricarboxylic acid cycle
Tconv	Conventional T cells
TCR	T cell receptor
Teff	Effector T cells
Tfam	Mitochondrial transcription factor A
TFAM	Mitochondrial transcription factor A
Th1	Type 1 helper T

Th17	T helper 17
TIL	Tumor infiltration lymphocytes
TME	Tumor microenvironment
Tmem	Memory T cell
Tregs	Regulatory T cells
TSC2	TSC complex subunit 2
TXNIP	Thioredoxin interacting protein
UCP2	Uncoupling protein 2
ULK1	Unc-51 like autophagy activating kinase 1
VPS34	Vacuolar protein sorting 34
WT	Wild-type
YFP	Yellow fluorescent protein

1 INTRODUCTION

Cell constantly needs to adjust its metabolism to meet the energy demands via an availability of nutrients (Von Bertalanffy, 1950). A series of specialized biochemical processes have been evolved to extract, reuse and store chemical energy in the form of ATP. When the cellular ATP levels decrease, cells need to lower energy consumption or restore energy supply, such as activating energy supply pathway or turning over of energetic content. The serine/threonine kinase adenosine monophosphate (AMP)-activated protein kinase (AMPK) is the primary cellular energy sensor through cellular adenosine triphosphate (ATP) levels that evolved across all eukaryotic organisms.(Hardie et al., 2012). In response to low energy supply, AMPK is activated by an allosteric mechanism through binding with AMP or ADP(Hardie et al., 2012). Once activated, AMPK regulates a network of downstream substrates toward increased catabolism and decreased anabolism. In addition to regulating cellular metabolism, AMPK is also activated in response to oxidant stress, caloric restriction and exercise, etc., maintaining organismal metabolism (Handschin, 2016).

1.1 The Structure of AMPK

AMP-activated protein kinase (AMPK) is a highly conserved heterotrimeric serine/threonine-protein kinase composed of α, β, and γ subunits. The α-subunit contains the catalytic kinase domain and a critical residue (Thr172) phosphorylated by upstream kinases. The β subunit contains a carbohydrate-binding module (CBM) that allows the interactions of AMPK with glycogen and an αγ binding domain at the C terminus (Hudson et al., 2003). A myristylation site at the N terminus of the β subunit facilitates AMPK target to cellular membranes(Hudson et al., 2003). The γ subunit contains four cystathionine β-synthase repeats (CBS) that allow

AMPK to bind to nucleotide and acquire the ability to sense the cell's energy state(Xiao et al., 2007). In mammals, each subunit is encoded by different isoforms; the α subunit contains α1 and α2 isoforms, which are encoded by *Prkaa1* and *Prkaa2* (Stapleton et al., 1996); the β subunit has β1 and β2 isoforms, encoded by *Prkab1* and *Prkab2* (Thornton et al., 1998); the γ subunit has three isoforms, γ1, γ2, and γ3, encoded by *Prkag1*, *Prkag2*, *and Prkag3*(Cheung et al., 2000). Each AMPK contains one α, one β, and one γ leading to 12 possible AMPK complexes(Ross et al., 2016). *In vivo*, the expression of each isoform varies across tissues and cells, affecting the activation of AMPK in response to different stress stimuli(Rajamohan et al., 2016).

Multiple studies have shown that the crystal structure of AMPK is essential for its activation. The regulatory subunit-interacting motifs (RIMs) of the α subunit create a conformational link between the α subunit and γ subunit CBS domains, which is essential for nucleotide binding and AMPK activation (Yan et al., 2018). Another important feature of the AMPK structure is the allosteric drug and metabolite (ADaM), which is located at the interface of α subunit kinase domain (KD) and the β subunit CBM. This site has been identified as the primary location for binding a host of small-molecule activators of AMPK (Ngoei et al., 2018). This site has attracted considerable interest for its capacity for mediating the activation of AMPK by synthetic ligands such as A-769662(Cool et al., 2006) and compound 991(Xiao et al., 2013). In addition, a recent study showed that the interaction of long-chain fatty acid (LCFA) CoA esters with this site is also capable of stimulating AMPK activation (Pinkosky et al., 2020). Multiple pre-clinical programs have targeted this motif to develop pan-AMPK activators as potential metabolic therapies for type 2 diabetes(Steneberg et al., 2018).

1.2 Regulation of AMPK

1.2.1 Regulation of AMPK by AMP/ATP Ratios

Under cellular stress, AMPK can be activated in response to decreased ATP production and increased ATP consumption. The increased AMP level bound to the γ subunit promoted the activity of AMPK through three mechanisms (Hawley et al., 2003; Hawley et al., 1995). Firstly, AMP has been shown to promote the phosphorylation of Thr172 by directly stimulating the upstream kinase activity of AMPK, such as LKB1 and CAMMK2(Fujiwara et al., 2016; Woods et al., 2003). The tumor suppressor LKB1 and the calcium-sensitive kinase CAMKK2 are the primary two upstream kinases for AMPK activity. LKB1 is responsible for most AMPK activation under mitochondrial insults and low-energy conditions(Shackelford and Shaw, 2009). However, AMPK can also be active in response to calcium flux by CAMKK2. Studies of LKB1 null cells indicate that CAMKK2 can maintain some AMPK activity independently of LKB1(Fogarty et al., 2010). Secondly, AMP prevents the dephosphorylation of Thr172 and caused allosteric activation of AMPK already phosphorylated on Thr172 to enhance AMPK activity (Davies et al., 1995; Suter et al., 2006). Lastly, AMP can activate AMPK by both allosteric activation and enhancing net phosphorylation. AMP can cause over 10-fold allosteric activation even at lower concentrations than ATP. And the allosteric activation by AMP can increase pACC under conditions in which there is no change in Thr172 phosphorylation (Gowans et al., 2013).

A variety of physiological conditions lead to the activation of AMPK, including mitochondrial inhibition, nutrient starvation and exercise, through modulating the AMP/ATP ratio(Herzig and Shaw, 2018). In addition, several small molecule activators of AMPK, such as A-769662,

compounds 991, PF-739 and MK-8722, have been developed to activate AMPK independently of nucleotide levels.

1.2.2 Regulation of AMPK by Reactive Oxygen Species (ROS)

ROS are plenty of free radicals and chemically reactive molecules which are most generated from oxygen molecule. The function of ROS can be both beneficial and detrimental, which is closely related to cell survival. Excessive production of ROS, usually termed oxidative stress, can lead to numerous diseases such as diabetes, cancer, neurodegenerative disease, and cardiovascular disease (CVD)(Brieger et al., 2012). Recent study has also demonstrated excess production of ROS provokes energy stress by disrupting the TCA cycle and mitochondrial function, which strongly activates AMPK(Zhao et al., 2017). The activity of AMPK was increased in a dose-dependent manner under hydrogen peroxide (H_2O_2) treatment, which was associated with an increased AMP-to-ATP ratio(Hinchy et al., 2018). However, overexpression AMPKγ2 R531G， an AMP-insensitive AMPK complex, can prevent H_2O_2 induced AMPK activation(Hawley et al., 2010). These data suggest that activation of AMPK by H_2O_2 may not target AMPK itself, but through changes to ADP, AMP, and ATP.

In addition, study showed that ROS can induce direct S-glutathionylation of AMPKα subunit at Cys299 and Cys304, which contributes to AMPK activation without affecting the ATP-to-AMP/ADP ratios(Zmijewski et al., 2010). However, the replacement of cysteine residues with insensitive alanine residues does not affect H_2O_2-induced AMPK activation(Hinchy et al., 2018).

1.2.3 Regulation of AMPK by Reactive Nitrogen Species (RNS)

Both Nitric oxide (NO) and its derivative RNS have also been implicated in AMPK activation. NO is produced by nitric oxide synthase (NOS) from L-arginine in cells. The interaction between NO and superoxide will generate peroxynitrite which reacts with other molecules to produce RNS, including dinitrogen trioxide, nitrogen dioxide, and other types of chemically reactive molecules.

In cultured endothelial cells (ECs), NO endogenously activates AMPK via elevating Ca^{2+} levels through activating soluble guanylyl cyclase(Zhang et al., 2008). Treat ECs with chemically synthesized peroxynitrite acutely and significantly increased phosphorylation of AMPK and its downstream target ACC without affecting cellular AMP level(Zou et al., 2003). Inhibition of NOS or overexpression of SOD prevent hypoxia-reoxygenation (H/R) induced AMPK activation in cultured bovine aortic endothelial cells (BAECs), suggesting a required role of peroxynitrite in H/R induced AMPK activation(Zou et al., 2003).

These effects of NO and RNS on AMPK activation is probably related to their role in suppressing mitochondrial ATP production. NO can react with complex I and cytochrome c oxidase, modulating physiologically the mitochondrial respiratory or OXPHOS efficiency(Sarti et al., 2012). RNS can induce cysteine S-nitrosylation or tyrosine nitration in almost all the complexes of mitochondrial ETC(Almeida et al., 2005).

1.3 The Functions of AMPK

Once activated, AMPK can phosphorylate downstream molecules to promote energy conservation via inhibiting anabolic processes that consume ATP and stimulating catabolic

pathways to generate ATP(Ma et al., 2017).

1.3.1 Inhibition of Anabolic Pathways

Acetyl-CoA Carboxylase (ACC) is a well-known AMPK substrate that blocks the oxidation of fatty acids and promotes synthesis (Kahn et al., 2005). Phosphorylation of ACC by AMPK inhibits its activity, promoting lipid oxidation and blocking *de novo* lipogenesis (Davies et al., 1990). Additionally, activation of AMPK inhibits phosphorylation of HMG-CoA reductase (HMGCR), which catalyzes the rate-limiting step of cholesterol synthesis(Carling et al., 1987). The essential role of AMPK in regulating lipid and sterol synthesis has significant implications in the treatment of diseases associated with excess fatty acid production, such as nonalcoholic fatty liver disease (NAFLD)(Smith et al., 2016).Under long-term conditions of reduced energy, AMPK maintains cellular energy by inhibiting gluconeogenesis. AMPK phosphorylates class IIa HDACs (HDAC4, 5, and 7) and prevents nucleus translocation resulting in decreased gluconeogenesis and increased glycogen storage(Mihaylova et al., 2011).

AMPK can also regulate energy consumption via modulation of mTOR, a master regulator of cell growth and protein translation. AMPK inhibits mTORC1 via phosphorylation and activation of the negative mTORC1 regulator TSC2 (Inoki et al., 2003), whereas phosphorylation and inhibition of the mTORC1 subunit RAPTOR(Gwinn et al., 2008). In response to energy-shortage conditions, increased AMPK activity leads to a decrease in mTOR activity, leading to decreased cell growth and protein synthesis to maintain or restore the cell's energy balance. Therefore, activation of AMPK limits ATP consumption by inhibiting anabolic glucose, lipid, and protein synthesis pathways under energy stress.

1.3.2 Activation of Catabolic Pathways

In addition to inhibiting anabolic pathways, AMPK also stimulates glucose utilization, mobilization of lipid stores, and turnover of macromolecules by autophagy to replenish ATP stores. AMPK stimulates glucose utilization via phosphorylating several downstream targets involved in glucose uptake, including TXNIP(Wu et al., 2013), TBC1D1(Chavez et al., 2008), and PLD1(Kim et al., 2010). For lipid mobilization, AMPK can stimulate lipases to release free fatty acids for β-oxidation and this process is dependent on the phosphorylation of ACC at Ser 79 and Ser 221 (Fullerton et al., 2013).

Growing evidence has shown that AMPK regulates various aspects of autophagy machinery to replenish nutrient stores during energy stress. Regulation of autophagy by AMPK through two independent mechanisms: the inhibition of mTOR signaling and directly phosphorylation of ULK1. ULK1 is an essential kinase for autophagy induction, whose activation phosphorylates several proteins involved in the execution of autophagy(Egan et al., 2015). AMPK has been shown to phosphorylates ULK1 on at least four residues: Ser467, Ser555, Thr574, and Ser637, and the phosphorylation of ULK1 by AMPK is essential for autophagy and cell survival during starvation and metabolic stress(Kim et al., 2011). Once activated, both AMPK and ULK1 can direct phosphorylate downstream PI3K-related VPS34 and the subunit Beclin1, a part of the autophagy initiation complex(Egan et al., 2015; Kim et al., 2013). Additionally, AMPK and ULK1 have also been reported to phosphorylate another rate-limiting autophagy protein, ATG9, to modulate autophagosome formation (Weerasekara et al., 2014).

1.3.3 AMPK Regulates Mitochondria Biogenesis

Mitochondrial biogenesis occurs in response to increased energy expenditure to produce more ATP. AMPK has been shown to participate in the process of mitochondria biogenesis. Mice with a dominant-negative mutant of AMPK failed to induce mitochondria biogenesis (O'Neill et al., 2011), whereas overexpression of a constitutively active AMPK in mice promotes mitochondria biogenesis(Garcia-Roves et al., 2008).These studies establish AMPK as a critical regulator of mitochondrial biogenesis. Several downstream molecules of AMPK are involved in the regulation of mitochondrial biogenesis, with most of genes seem to be under the control of the peroxisome proliferator-activated receptor-γ co-activator 1 (PGC1) family(Wu et al., 1999). AMPK activates PGC1α via direct phosphorylation at Thr177 and Ser538 or through several indirect mechanisms involving AMPK-dependent modulation of p38 MAPK, HDAC5, or SIRT1(O'Neill et al., 2013). Activation of PGC1α interacts with PPARγ or estrogen-related receptors (ERRs) to promote mitochondrial biogenesis genes(Eichner and Giguere, 2011). The effect of AMPK has great therapeutic implications in multiple pathological situations, including muscular dystrophy and mitochondrial myopathy (Ljubicic and Jasmin, 2013; Peralta et al., 2016).

1.3.4 AMPK Regulates Autophagy/Mitophagy

AMPK has been shown to regulate autophagy both in yeast(Wang et al., 2001) and in mammalian cells(Meley et al., 2006) through two different steps. First, activation of AMPK reduces mTOR activity through directly phosphorylating the mTOR upstream regulator TSC2 on Thr1227 and Ser1345 and the mTOR subunit RAPTOR on Ser722 and Ser792.

Subsequently, the reduced mTOR activity lost their inhibition on ULK1 to activate autophagy(Chan, 2009). Second, AMPK was shown to be essential for autophagy and cell survival during starvation and metabolic stress through direct phosphorylating ULK1 on at least four residues: Ser467, Ser555, Thr574, and Ser637(Egan et al., 2011).

Not only for general autophagy, activation of AMPK is also crucial for mitophagy. Inhibition of AMPK-ULK1 axis promotes the accumulation of defective mitochondria in cells(Egan et al., 2011). Activation of AMPK significantly reduce alcohol-induced liver injury and enhances hepatocytes' mitophagy level through enhancing *UQCRC2* gene transcription(Lu et al., 2021). Another pathway controlling mitophagy is the PINK1-Parkin-mediated elimination of depolarized mitochondria, PINK1 is selectively stabilized on impaired mitochondria which in turn recruits and phosphorylates the E3 ligase Parkin for mitochondria degradation by the autophagy machinery(Eiyama and Okamoto, 2015). In cardiomyocytes, overexpression of AMPKα2 rescues the impaired mitophagy after phenylephrine stimulation via directly phosphorylation of PINK1 at Ser495. The phosphorylation of PINK1 recruits the E3 ligase Parkin to remove depolarized mitochondria to prevent the progression of heart failure(Wang et al., 2018).

1.3.5 AMPK and Redox Homeostasis

AMPK is not only functional as a redox sensor, but also plays an essential role in protecting the oxidative stress. Activation of AMPK suppress oxidative stress through diminishing the superoxide production or upregulating antioxidant gene expression. Activation of AMPK by either salicylate or 5-aminoimidazole-4-carboxamide ribonucleotide (AICAR) prevents palmitate induced endothelial dysfunction by suppressing mitochondrial ROS-associated

endoplasmic reticulum stress (ER stress)(Li et al., 2015). The anti-diabetic drug miglitol can prevent oxidative stress induced endothelial cell apoptosis and vascular relaxation via enhancing AMPK activity(Aoki et al., 2012). In addition to mitochondria function, AMPK can also regulate ROS production via suppressing nicotinamide adenine dinucleotide phosphate oxidase (NOX). Deficiency of AMPKα2 in human umbilical vein endothelial cells (HUVECs) increase NOX expression and the subsequent superoxide production, 26S proteasome activity, kappa Bα degradation, and nuclear translocation of nuclear factor kappa B(Wang et al., 2010).

Treatment of MEFs with AMPK activator A-769662 blocks glucose starvation induced mitochondrial ROS production via promoting PGC-1α dependent antioxidant response(Rabinovitch et al., 2017). Similar, metformin normalizes hyperglycemia-induced mitochondrial ROS production by induction of manganese superoxide dismutase (MnSOD) and promotion of mitochondrial biogenesis through activation of AMPK-PGC1α pathway(Kukidome et al., 2006). Both metformin and AICAR can suppress superoxide production in HUVECs via increasing the expression of antioxidant gene *UCP2*(Xie et al., 2008). All these data suggest activation of AMPK increases antioxidant potentials, which provides potential value for treating oxidative stress-related disease in clinic.

1.3.6 AMPK in Cancers

AMPK acts as either a tumor suppressor or a tumor promoter, depending on the text. Genetic loss of AMPK before tumors development exacerbating the disease(Vara-Ciruelos et al., 2019), while inhibition of AMPK after the disease established attenuates it(Kishton et al., 2016).

The idea that AMPK function as a tumor suppressor come from the findings that LKB1 is an

essential upstream kinase required for AMPK activation(Hawley et al., 2003). LKB1 has been identified a few years earlier to be a tumor suppressor(Collins et al., 2000). Following the discovery of the link between AMPK and LKB1, the use of AMPK activator metformin to treat type 2 diabetes was found to be associated with reduced risk of cancers(Noto et al., 2012). Recent study showed that activation of AMPK by metformin induces phosphorylation and degradation of PD-L1 in cancer cells, thereby promoting protective T-cell immunity(Cha et al., 2018). However, these studies using metformin may have an AMPK-independent effects, and not all confirm that AMPK is necessary by gene knockout. Thus, the genetic loss of AMPK is needed to identify its role in cancer development in vivo. One of the first approach using AMPK α1 global knockout mice suggests the expression of AMPKα1 prevent the development of B cell lymphoma(Faubert et al., 2013). The following T cell specific AMPKα1 deletion mice further demonstrates the anti-tumor effects of AMPK in lymphoma development(Vara-Ciruelos et al., 2019).

In contrast to the tumor suppressor, AMPK can also promote tumor development in certain contexts. Stimulation of AMPK by aerobic glycolysis in breast tumors promotes tumor-associated myeloid cell (MDSC) expansion, which contributes to cancer development(Li et al., 2018). Activation of AMPK in mouse metastasis models drives pyruvate dehydrogenase complex (PDHc) activation to promote cancer metastasis by adapting cancer cells to metabolic and oxidative stresses (Cai et al., 2020). In a model of T cell acute lymphoblastic leukemia/lymphoma, knocking out AMPK after tumor establishment results in a lower recovery of T-ALL cells(Kishton et al., 2016). In lung epithelial cells, knocking out LKB1 enhanced KRas mutated tumor growth, while by contrast, knockout of both AMPKα1 and α2 was found to

reductions in the size and numbers of lung tumors. These data suggest that LKB1 is a tumor suppressor in non-small-cell lung cancer, while presence of AMPK promote tumor growth (Eichner et al., 2019).

1.3.7 AMPK, Cellular Senescence, and Aging

Cellular senescence is state of permanent cell-cycle arrest while continuing viability and metabolic activity(Shakeri et al., 2018). Accumulation of senescent cells in tissues create a proinflammatory environment which favors the onset and progression of age-related diseases(Sharpless and Sherr, 2015). Cell senescence can be triggered by various detrimental stimulus, including oxidative stress, shortened telomeres, DNA damage, mitochondrial dysfunction, abnormal metabolism, and gene mutation(Matthews et al., 2006; Regulski, 2017). There are two types of cell senescence. The first one is called replicative senescence which characterized by irrevocable cell proliferation arrest, which is mediated by telomere shortening(Kuilman et al., 2010). The second is stress-induced premature senescence (SIPS), which is induced by distinct endogenous or exogenous(Kuilman et al., 2010). Senescent cells have both beneficial and deleterious functions for the organism which are treated as potential powerful targets for antiaging approaches(Soto-Gamez and Demaria, 2017).

Effective regulation of metabolic homeostasis is crucial to prevent cellular senescence. As an important energy sensor, activation of AMPK has been shown to prevent aging or senescence in many studies(Fang et al., 2018; Lee et al., 2015b; Salminen and Kaarniranta, 2012). Decreased AMPK has been observed in aging and age-related disease(Funakoshi et al., 2011; Qiang et al., 2007), while overexpression of AMPK extends the lifespan in *C.elegans*

or *Drosophila*(Apfeld et al., 2004; Funakoshi et al., 2011). Activation of AMPK by its pharmacological activators, such as metformin, ACIAR, and berberine, have been characterized to have therapeutic potential for age-related disease(Funakoshi et al., 2011; Son et al., 2016). In humans, the application of metformin has been performed in clinical study to evaluate its antiaging capacity, such as delaying the progression of age-related diseases(Funakoshi et al., 2011; Konopka and Miller, 2019).

The singling targets of AMPK and their role in the regulation of aging process have been extensive explored during the last ten years. AMPK has been shown to prevent senescence and aging through activation of SIRT1, FOXO and PGC-1α(Salminen and Kaarniranta, 2012), as well as the suppression of mTOR(Burkewitz et al., 2014). SIRT1 is a major regulator of cellular energy metabolism which can enhance the cellular stress resistance and against the aging process(Le Bourg, 2009). Activation of AMPK stimulates the functional activity of SIRT1 through increasing the intracellular concentration of NAD+, which activates several downstream targets, e.g., PGC-1α, FoxP1 and FoxO3 and maintains mitochondrial biogenesis(Nakahata et al., 2009). The mammalian FoxO family of Forkhead transcription factors are involved in the regulation of several crucial cellular functions, which was observed as a key player in longevity regulation(Lin et al., 1997). AMPK has been demonstrated to directly phosphorylate FoxO3 protein at six threonine/serine residues, which promotes the activation of FoxO3-mediated transcription and extends the lifespan in *C. elegans*. (Greer et al., 2007). Activation of p53 pathway clearly prevents aging process and reduces age-related damage via increasing expression of antioxidant genes(Matheu et al., 2007). AMPK controls both the expression level and transactivation capacity of p53 via directly phosphorylation,

which prevents IL-1-associated SASP production(Wiley et al., 2016).

Autophagy is a cellular mechanism that is required for cell survival when cells encounter stress(Anding and Baehrecke, 2017). In general, autophagy appears to be constitutively active while its activity decreases during aging process, which occurs in attenuated autolysosomes and autophagic flux (Abdellatif et al., 2018). Growing evidence indicates that decreased autophagy results in cellular senescence. Deficiency of the critical autophagy gene Atg7 in VSMC causes accumulation of SQSTM1/p62 and promotes the development of stress-induced premature senescence, resulting in acceleration of ligation-induced neointima formation and diet-induced atherogenesis(Grootaert et al., 2015). In contrast, activation of autophagy by rapamycin was shown to inhibit replicative senescence via decreasing mTOR signaling(Tan et al., 2016). AMPK is a major inducer of autophagy associated with the reduction of energy metabolism(Egan et al., 2011). Activation of AMPK was shown to prevent oxidative stress-induced cellular senescence via restoring autophagic flux and intracellular NAD^+ elevation(Han et al., 2016). In addition, activation of AMPK can also restrain the production of pro-inflammatory SASP via suppression of the mTOR-NF-κB signaling loop(van Vliet et al., 2021). All these data suggest the significant role of AMPK in maintaining cellular housekeeping by autophagy and in that way can extend the organismal lifespan.

1.4 The Role of AMPK in T cells

1.4.1 AMPK in T cells

As we mentioned above, the catalytic α subunit of AMPK contains two isoforms (α1 and α2), which are encoded by *Prkaa1* and *Prkaa2* genes, respectively. In T cells, AMPKα1 is the

predominant isoform of the AMPKα subunit, whereas the expression of AMPKα2 is too low to be detected in both resting and activated lymphocytes (MacIver et al., 2011; Tamas et al., 2006). During T cell activation under TCR-CD3 stimulation, the activity of AMPK is increased in a time-dependent manner, which indicates an essential role of AMPK in T cells (Zheng et al., 2009). Indeed, activation of AMPK is required for T cells' long-term fitness and proliferation via the regulation of ROS production (Lepez et al., 2020). However, genetic models using AMPKα1 global knockout mice established that AMPKα1 is dispensable for T cell development or the homeostasis of mature T cells(Mayer et al., 2008).

As with other cell types, metabolic stressors such as metformin, AMPK agonists, and nutrient limitation can activate AMPK in T cells independent of immune stimulation(Pearce et al., 2009; Rolf et al., 2013). Even though AMPK activity is controlled by LKB1 in T cells, LKB1 also exerts distinct effects on T cell biology through AMPK-independent pathways. The deficiency of LKB1 disrupts T cell development and leads to enhanced $CD4^+$ Th1 responses not observed in AMPKα1-deficient $CD4^+$ T cells(MacIver et al., 2011).

1.4.2 Regulation of T cell Metabolism by AMPK

Activated T cells need to produce sufficient ATP to meet their increased biosynthetic demands of proliferation. AMPK is also required for T cells' metabolic adaptation and effector responses as an essential metabolic regulator. Deficiency of AMPKα1 in T cells impaired mitochondrial bioenergetics and ATP production in response to glucose limitation or pathogenic challenges (Blagih et al., 2015). In response to the low glucose situation, AMPK suppresses mTORC1-dependent IFNγ translation and induces cells to use glutamine to fuel the TCA cycle and OXPHOS (Blagih et al., 2015). AMPKα1-deficient Teff cells show less

efficiency in inducing colitis in Rag2-/- mice and T cell-specific AMPKα1 knockout mice have less ability to generate effective primary T cell responses to viral and bacterial infections (Blagih et al., 2015).

1.4.3 Regulation of T Cell Fate by AMPK

Metabolic changes in cells have been broadly associated with inflammation and AMPK is known as an essential regulator in anti-inflammatory immune responses(O'Neill and Hardie, 2013). Considerable evidence indicates that AMPK can influence T cell differentiation and fate. AMPK has been linked to the proper generation of $CD8^+$ memory T cell (Tmem). Impaired TNFR/TLR signaling leads to defective $CD8^+$ Tmem generation due to loss of AMPK activation during Teff cell contraction (Pearce et al., 2009), and AMPKα1-deficient $CD8^+$ OT-1 cells fail to generate effective memory responses during bacterial infection(He et al., 2021). The impact of AMPK on Tmem cell fate could be due to differential AMPK activity between Teff and Tmem cells. Compared to Teff cells, Tmem cells have higher AMPK activity but lower mTORC1 activity, promoting long-term T cell survival (Pearce et al., 2009). In response to nutrient limitations, deficiency of fructose-1,6-bisphosphate (FBP) promotes AMPK activation, which further activates SENP1-Sirt3 signaling and enhances the survival and development of Tmem cells(He et al., 2021). In this light, stimulating AMPK activity during initial T cell activation may enhance Tmem cell differentiation. Indeed, administration of AMPK agonist metformin promotes Tmem cell generation and consequently improves the efficacy of an experimental anti-cancer vaccine(Pearce et al., 2009).

1.4.4 AMPK in Regulatory T cells

Naturally occurring $CD4^+$ regulatory T cells (Tregs) are a functionally distinct T cell subpopulation engaged in maintaining of immunological self-tolerance and homeostasis (Josefowicz et al., 2012; Sakaguchi, 2004). Tregs with specifically CD25 on the cell surface and Foxp3 in their nucleus played an essential role in suppressing aberrant self-immune against immune responses. Abnormal Treg cells can not only cause classical immunological diseases but are also involved in the progress of tumors, obesity, atherosclerosis, tissue regeneration, and degenerative disease(Sakaguchi et al., 2020). Thus, a further understanding of the intracellular mechanism in controlling the adaptability and heterogeneity of Tregs will provide state-of-art strategies for disease therapy.

The role of AMPK in regulatory T cells (Tregs) is still controversial. AMPK-dependent control of fatty acid metabolism impacts the balance between T helper 17 (Th17) and Treg cells. Compared to conventional T cells (Tconvs), Tregs have a higher activated AMPK (Michalek et al., 2011). AMPK-dependent activation of fatty acid oxidation (FAO) and oxidative metabolic supports the differentiation of Treg cells (Michalek et al., 2011). During autoimmune development, the expression of AMPKα1 was decreased in Treg cells, and loss of AMPK exacerbated the disease progression of autoimmune encephalomyelitis (Nath et al., 2009b). Moreover, activation of AMPK by Pioglitazone promotes the induction of Foxp3 and generation of Tregs, which stabilize atherosclerotic plaque(Tian et al., 2017).

However, genetic deletion of AMPK in Tregs does not lead to any obvious abnormalities in mice before 1-year-old under normal conditions, which is different with its upstream LKB1 (He et al., 2017). Deletion of LKB1, one of the well-known AMPK upstream, disrupted the metabolic

and functional fitness of Treg cells and induced lethal autoimmunity(Yang et al., 2017). Furthermore, LKB1 is also required to maintain Foxp3 expression by preventing CNS2 methylation(Wu et al., 2017). All these data suggest a distinct function of LKB1 and AMPK in Treg cells. The precise role of AMPK in Treg cells is still far more known, which requires further study.

1.4.5 AMPK and Anti-tumor Immunity

With the development of immune checkpoint inhibitors, cancer immunotherapy has succeeded in clinical cancer treatment. T cells' responses to tumor antigens significantly contribute to cancer immunosurveillance and anti-tumor immunity. Recent work suggests that metabolic constrains in the tumor microenvironment (TME) can negatively affect anti-tumor T cell responses, in part by competition of nutrients between tumor infiltration lymphocytes (TIL) and tumor cells(Chang et al., 2015). Glucose starvation promotes PD1 expression on activated T cells, which reduces IFN-γ production and induces T cell exhaustion(Chang et al., 2013). However, the production of lactic acid in the highly glycolytic TME upregulates PD1 expression in Treg cells which function as an active checkpoint for the function of Treg in TME(Kumagai et al., 2022). Therefore, this high glucose consumption and lactate production TME promotes tumor immune escape by depriving effector T cells and supporting regulatory populations.

As an important metabolic regulator, the activity of AMPK shows both pro- and anti-tumor T cell immunity. The immunomodulatory cytokines, IL-10, can suppress glycolytic metabolism in immune cells, which triggers an AMPK-mediated metabolic checkpoint to suppress Teff cell function(Krawczyk et al., 2010; Sag et al., 2008). However, other work indicates that metformin

treatment enhances T cell-mediated tumor rejection with increased recruitment of functional CD8+ tumor infiltrated T cells (TIL)(Eikawa et al., 2015). Meanwhile, metformin treatment potentiates anti-PD1 immunotherapy efficacy through reversing TIL exhaustion(Scharping et al., 2017). One disadvantage of these studies is that metformin may work through either AMPK-independent pathway in T cells or effects on whole-body metabolism. Thus, the T cells specific AMPK deficient mice is needed to further investigate the role of AMPK in anti-tumor T cells immunity.

1.5 T cell Senescence and Atherosclerosis

Because of the highly increased life quality, the life expectancy of a human is significantly increased. However, with increased life expectancy, advanced age is emerging as a risk factor for chronic fatal diseases, such as cancer, autoimmunity, and cardiovascular disease (CVD) (Niccoli and Partridge, 2012). Accumulation of senescent cells in diseased or impaired cardiovascular systems plays an essential role in the pathogenesis of age-related CVD, including atherosclerosis(Matthews et al., 2006).

1.5.1 Features of Cellular Senescence

Senescent cells show general characteristics with flattened and enlarged morphology, upregulated senescence-associated beta-galactosidase (SA β-gal) activity, accumulation of *p16ink4a*, *p19Arf*, and *p21Cip1*, and telomere attrition. Besides these, senescent cells also display the senescence-associated secretory phenotype (SASP), secreting a variety of pro-inflammatory cytokines, growth factors, chemokines, and matrix metalloproteinases (MMPs) (Song et al., 2020). These secreted SASPs enable the communication of senescent cells with

their neighboring cells and promote the senescence of these neighboring cells, tissue regeneration, and embryonic development (Munoz-Espin et al., 2013). Another essential feature of senescent cells is that they are more resistant to pro-apoptotic stimulation, probably due to pro-survival BH2 family proteins (Yosef et al., 2016).

1.5.2 Hallmarks of T cell Senescence

Proper and effective T cell responses are essential to the success of adaptive immunity during the aging process. However, considerable evidence has suggested that T cells are one of the major cell types which may undergo aging-related functional changes (Goronzy and Weyand, 2019). T cell aging may be one of the primary manifestations of immunosenescence, displaying the impaired ability to eliminate the harmful elements while increasing pro-inflammatory cytokine production that leads to autoimmune disease (Hakim et al., 2004). Senescent T cells acquire general features of senescence, including short telomeres, DNA damage, apoptosis resistance, and upregulated β-galactosidase activity. In addition, decreased expression of the costimulatory molecules CD27 and CD28 and increased terminal-differentiation markers have also been identified in senescent T cells(Akbar et al., 2016). These increased senescent T cells secret abundant pro-inflammatory cytokines, such as TNF and interferon-γ, reminiscent of a senescence-associated secretory phenotype (SASP)(Callender et al., 2018).

Compared to $CD4^+$ T cells, $CD8^+$ T cells are more likely to acquire an immunosenescent phenotype, perhaps due to the declined mitochondrial quality(Callender et al., 2020). Recent studies showed that Treg cells are more likely to be senescence than effector T cells during aging. Aged Tregs show less suppressive activity in restraining Teff proliferation and

immunological aging while acquiring proinflammatory cytokines(Guo et al., 2020). Deficiency of DDB1-and CUL4-associated factor (DCAF1) expression in Tregs promotes aberrant ROS production via facilitating GSTP1 function, which leads to Treg senescence(Guo et al., 2020). Overexpression of GSTP1 and ROS scavengers can recover these hallmarks of aged Treg cells.

Age-associated mitochondrial dysfunction makes a great contribution to the acquisition of a senescent phenotype in T lymphocytes. Even though T cells from older individuals contains more mitochondrial proteins than those from young controls, they exhibit impaired oxidative phosphorylation(Bektas et al., 2019). Genetic deletion of the mitochondrial transcription factor A (TFAM) in T cells results in mitochondrial dysfunction and ultimately promotes age-associated T cell dysfunction. Moreover, TFAM-deficient T cells display type 1 helper T (Th1) proinflammatory phenotype, thus exacerbating inflammaging and promoting physical disabilities and premature death(Desdin-Mico et al., 2020). Patients with AIDS accompany with accelerated T cell senescence which contributes to the high mortality rate even when active HIV infection is under control(Deeks and Phillips, 2009). Reduced mitochondrial fitness in Tregs from HIV-infected people cause impaired Treg function, resulting failing to restore CD4+ T cells pool during antiretroviral therapy(Younes et al., 2018). As an essential metabolic modulator, activation of AMPK has also been shown to regulate glutamine-dependent mitochondrial metabolism to maintain T cell bioenergetics and viability(Blagih et al., 2015). However, whether activation of AMPK is essential to restrain T cell, especially Treg senescence is still unknown.

With the development of individual aging, the immune system experiences profound

changes that significantly impact health and survival (Grubeck-Loebenstein et al., 1998). Immunological aging refers to immunosenescence (declined immunity) and inflammaging (chronic nonspecific inflammation), which are considered major contributing factors to the morbidity and mortality of elderly individuals (Fulop et al., 2017). The immunosenescence causes declined immune response in later life, contributing to reduced efficacy of vaccination and reactivation of latent viruses and tumors (Partridge et al., 2018). Despite the impaired responsiveness of the immune system, a low-grade, chronic, and systemic pro-inflammatory state is frequently observed in the elderly (so-called “inflammaging”)(Goronzy and Weyand, 2012). The inflammaging has been shown as an essential factor in the pathogenesis of many age-related diseases, including cardiovascular disease and neurodegenerative syndromes (Costantini et al., 2018; Liberale et al., 2020).

1.5.4 Immunosenescence in Atherosclerosis

Atherosclerosis is the leading cause of the cardiovascular disease (CVD), resulting in much morbidity and mortality worldwide (Libby et al., 2019). With a high incidence of atherosclerosis in elderly patients, the relationship between age-related immune changes and the pathophysiology process of atherosclerosis has attracted significant research interest. *Macrophages* are the primary immune cells that play critical roles in atherosclerotic plaque development, collagen content, and necrotic core formation (Stoneman et al., 2007). During the development of atherosclerosis, the accumulation of senescent macrophages in the sub-endothelial space was shown to de deleterious at all stages of atherosclerosis (Childs et al., 2016). Accumulation of these senescent macrophages promoted the plaque instability with decreased cap thickness, reduced collagen content, and increased the necrotic score by

elevating SASP components, including MMP3 and MMP13. Interestingly, selective removal of these senescent cells via genetic or pharmacological strategies can reverse atherosclerosis in mice (Childs et al., 2016).

1.5.5 T cell Senescence and Atherosclerosis

Despite macrophages, accumulating evidence suggests that senescent T cells are also implicated in the pathogenesis of atherosclerosis. Accelerated telomere shortening has been shown to present in the peripheral blood mononuclear cells (PBMCs) and T cells of patients with atherosclerosis (Samani et al., 2001). Infection with cytomegalovirus (CMV) has been extensively investigated in the progression of immunosenescence (Pawelec, 2014). Patients who have a higher frequency of senescent $CD8^{+}CD28^{null}$ T cells after CMV infection have been shown to have impaired vascular function and a high risk of atherosclerosis (Grahame-Clarke et al., 2003; Zhu and Liu, 2020). A multiethnic study has found that increased senescent memory $CD4^{+}$ T cells are associated with subclinical atherosclerosis, such as coronary artery calcification and carotid artery intimal media thickness (Olson et al., 2013). These findings are consistent with another study that a higher frequency of $CD8^{+}CD28^{null}CD57^{+}$ T cells in HIV-infected patients was associated with an increased prevalence of carotid artery disease (Kaplan et al., 2011). However, the direct role of senescent T cells in atherosclerosis development is still not clear right now. In this regard, it has been hypothesized that senescent T cells directly contribute to the pathophysiology of atherosclerosis by secreting IFN-γ to induce macrophage activation or secreting perforin and granzymes to destroy endothelial and vascular smooth muscle cells (Johnson, 2007; Leon and Zuckerman, 2005). Recent study demonstrates that compare to conventional T cells (Tconv) cells Tregs are more likely to be

senescence during aging, which shows less efficient in preventing Tconv aging(Guo et al., 2020). However, whether and how senescent Tregs play their functions in the development of atherosclerosis is unknown. Given the essential role of Tregs in preventing atherosclerosis, studies focusing on the role of senescent Tregs in atherosclerosis may present a novel therapeutic target for preventing atherosclerotic artery disease.

1.6 Gaps of Knowledge

Recent work established that AMPK is activated in T cells by immunological and environmental stimuli, and activation of AMPK is required to maintains T cell metabolic adaption and effector responses(Blagih et al., 2015). Despite both natural and inducible Treg exhibit elevated levels of AMPK activity compared with Teff and naïve T cells, the role of AMPK in Treg cells on the development of autoimmunity and cancer is still not clear.

Evidence suggest that Treg cells contribute to the anti-inflammatory response during anthogenesis(Ait-Oufella et al., 2006; Gotsman et al., 2006). Recent studies indicated that Treg cells would become plasticity during atherogenesis(Butcher et al., 2016). Recent data suggests that senescent Tregs are dysfunctional and express high levels of inflammatory cytokines. The contributions of Tregs senescence in atherosclerosis remained to be determined. Finally, whether and how senescent Tregs become more plasticity remained to be elucidated.

1.7 Research Objectives

Chapter 1: Activation of AMPKα1 is essential for regulatory T cell function and preventing autoimmune liver disease

The objective of project 1 was to investigate the role of AMPKα1 in regulatory T cells and autoimmune disease. We plan to use AMPKα1 global knock out (Prkaa1$^{-/-}$) mice, bone marrow transplantation mice model, adoptive Treg transfer mice model, and Treg-specific AMPKα1 deletion (AMPKα1$^{Treg-/-}$) mice to investigate the role of AMPK in Tregs and autoimmune liver disease. We will also detect whether AMPK regulates Treg survival, differentiation, proliferation, and function both *in vitro* and *in vivo*. Finally, we plan to determine whether and how AMPK regulates the expression of Foxp3 in Treg cells.

Chapter 2: AMP-activated protein kinase alpha 1 promotes tumor development via FOXP3 elevation in tumor-infiltrating Treg cells.

The objective of project 2 was to determine the role of AMPKα1 in Treg cells and tumor development. We plan to construct tumor models in Treg-specific AMPKα1 deletion () mice and their littermate control mice to investigate the role of AMPK in Tregs and anti-tumor immunity. We will also investigate whether expression of AMPK can maintain Foxp3 expression in tumor infiltrated Tregs. Finally, we will investigate the mechanism on how AMPK regulates Foxp3 expression in Treg cells.

Chapter 3: Hypercholesterolemia-driven inhibition of AMP-activated protein kinase alpha 1 induces Treg senescence during atherosclerosis.

The goal of project 3 was to investigate the role of AMPKα1 in Treg senescence and the development of atherosclerosis. Firstly, we will detect the expression of senescent Treg cells in atherosclerosis developing mice. Secondly, we will adoptively transfer senescent Tregs and non-senescent Tregs to investigate their role in the development of atherosclerosis. Thirdly, we will detect whether AMPK regulates Treg senescence during atherogenesis both *in vitro*

and *in vivo*. Next, we will construct the ApoE Treg-specific AMPKα1 deletion mice ($ApoE^{-/-}$ $AMPK\alpha1^{Treg-/-}$) to test the role of AMPK in Tregs and atherosclerosis development. Finally, we plan to adoptive transfer constitutive active AMPK (CA) AMPK-Tregs to western diet-fed $ApoE^{-/-}$ mice to test their protective role on atherosclerosis.

2 Activation of AMPKα1 is Essential for Regulatory T cell Function and Preventing Autoimmune Liver Disease

Zhu H, Liu Z, An J, et al. Cell Mol Immunol. 2021 Dec;18(12):2609-2617.

Huaiping Zhu[1 2#], Zhaoyu Liu[1 3#*], Junqing An[1#], Miao Zhang[4], Yu Qiu[1], Ming-Hui Zou[1]

[1]Center for Molecular and Translational Medicine, Georgia State University, Atlanta, GA 30303, USA

[2]The First Affiliated Hospital of USTC, Anhui Provincial Key Laboratory of Blood Research and Applications, Division of Life Sciences and Medicine, University of Science and Technology of China, Hefei, Anhui, 230001, P.R. China

[3] Medical Research Center, Guangdong Provincial Key Laboratory of Malignant Tumor Epigenetics and Gene Regulation, Sun Yat-Sen Memorial Hospital, Sun Yat-Sen University, Guangzhou, Guangdong, 510120, P.R. China

[4]Department of Medicine, University of Oklahoma Health Sciences Center, Oklahoma City, OK 73117, USA

Keywords: AMPK, Treg, autoimmune liver diseases, Foxp3

#All authors contributed equally to this work

2.1 Abstract

Regulatory T cells (Treg cells) are crucial for maintaining immune tolerance. Compromising the regulatory function of Treg cells can lead to autoimmune liver disease. However, how Treg function is regulated is still not fully clarified. Here we report that global knockout (KO) mice of AMP-activated protein kinase alpha 1 (AMPKα1) spontaneously develop immune-mediated liver injury, with massive lymphocyte infiltration in the liver, elevated serum alanine aminotransferase level and higher production of autoantibody. Both transplantation of wild type bone marrow and adoptive transfer of wild type Treg cells can rescue AMPKα1 KO mice from the liver injury. In addition, Treg-specific AMPKα1 KO mice display histological features resembling autoimmune liver disease, higher production of autoantibody and hyperactivation of $CD4^+$ T cells. AMPKα1 deficiency significantly impairs Treg cell suppressive function while not affecting Treg cell differentiation and proliferation. Furthermore, AMPK is activated upon T cell receptor (TCR) stimulation, which triggers Foxp3 phosphorylation, suppressing Foxp3 ubiquitination and proteasomal degradation. Importantly, the frequency of Treg cells and the phosphorylation levels of AMPK at T172 from circulating blood is significantly lower in patients with autoimmune liver diseases. ***Conclusion***: Our data suggest that AMPK maintains the immune-suppressive function of Treg cells and confers protection from autoimmune liver disease.

2.2 Introduction

Autoimmune liver disease is immune-mediated liver injury (hepatocellular or hepatobiliary) such as autoimmune hepatitis (AIH), primary biliary cholangitis (PBC), and primary sclerosing cholangitis (PSC)(Krawitt, 2006; Trivedi and Adams, 2013). Although the pathogenesis of autoimmune liver disease is not fully understood, it is generally recognized that impairment of immunoregulatory networks plays a crucial role(Lapierre and Lamarre, 2015; Liberal et al., 2015). In a healthy population, circulating autoreactive T cells are suppressed by peripheral tolerance mechanisms to limit autoimmune tissue damage, among which regulatory T cell (Treg cell)-

exerted immune suppression plays a key role(Liberal et al., 2017; Sakaguchi et al., 2010). Patients with autoimmune liver diseases display a reduced Treg cell frequency or function compared to healthy subjects(Ferri et al., 2010; Grant et al., 2014; Longhi et al., 2004; Longhi et al., 2009). In addition, adoptive transfer of ex vivo expanded Treg cells has been shown to restore peripheral tolerance in an autoimmune hepatitis murine model(Lapierre et al., 2013). Therefore, understanding the molecular mechanisms underlying Treg cell regulation is important for the treatment of this disease.

AMP-activated protein kinase (AMPK) is a highly conserved serine/threonine protein kinase that functions as a key energy sensor and metabolic regulator to maintain cellular energy balance(Hardie, 2007, 2011). Recent work has established that AMPK is activated in T cells by both immunological and environmental stimuli, and plays an important role in T cell metabolism(Ma et al., 2017). Global deletion of AMPKα1 increased T cell glycolysis and enhanced production of interferon-γ (IFN-γ) and interleukin 17a (IL-17a)(MacIver et al., 2011). More recently, AMPK was shown to be necessary for effector T cell response during viral and bacterial challenge (Blagih et al., 2015) and to drive oxidative metabolism in leukemic T cells(Kishton et al., 2016). AMPK has also been implicated in Treg cell regulation. Stimulation of AMPK *in vivo* with the AMPK activator metformin has been shown to increase Treg cells(Michalek et al., 2011), attenuate experimental autoimmune encephalomyelitis (EAE) and suppress systemic autoimmunity(Lee et al., 2017; Sun et al., 2016). However, the mechanism behind AMPK's effects on Treg cells and its therapeutic potential in treating autoimmune liver disease is not yet known.

Forkhead Box P3 (Foxp3) is a lineage-specific transcription factor of Treg cells and is crucial for developing mature Treg cells, and maintaining their immunosuppressive function (Rudensky, 2011). Foxp3 expression, stability, and activity are tightly modulated in cellular systems. This regulation involves many epigenetic and post-translational modifications associated with the immunosuppressive activity of Treg cells(Chen et al., 2013; Li et al., 2007; Liu et al., 2013; van Loosdregt et al., 2013; van Loosdregt et al., 2010). Phosphorylation of Foxp3 is generally

decreased in patients with rheumatoid arthritis and can affect Treg activity and cellular functions(Nie et al., 2013). Foxp3 phosphorylation by proto-oncogene PIM2 and cyclin-dependent kinase (CDK) cascade has been demonstrated to affect Foxp3 stability and immune tolerance(Deng et al., 2015; Morawski et al., 2013). However, other kinase(s) responsible for Foxp3 phosphorylation, especially those involved in autoimmune liver disease, remains undefined.

In this study, we found that globally knockout and Treg specific deletion of AMPKα1 impairs Treg suppressive activity and leads to the development of autoimmune liver disease in mice. Mechanistically, we found that AMPK activation triggers the phosphorylation of Foxp3 and maintains Foxp3 protein stability. Clinically, patients with autoimmune liver diseases showed less Treg frequency and AMPK phosphorylation. All these results demonstrated a critical role of AMPK in Treg cells and that selective activation of AMPK in Treg might be a therapeutic target for the treatment of autoimmune liver diseases.

2.3 Materials and Methods

2.3.1 Patients

Peripheral blood was collected from healthy control and primary biliary cholangitis (PBC) patients. The diagnosis of PBC was based upon internationally accepted criteria. Briefly, 2 of the following 3 criteria had to be met for a diagnosis of PBC: (1) serum AMA (titer>1:40) and/or ANA, (2) a cholestatic pattern of liver biochemistry with at least 1 of serum bilirubin, alkaline phosphatase, or gamma-glutamyl transpeptidase above the reference range, and (3) diagnostic or compatible liver histology. PBC patients were classified into early stage PBC, moderate PBC, and advanced-stage PBC according to the Rotterdam criteria(Kuiper et al., 2009). Clinical characteristics of the patients were provided in **Table 1.**

Table 1 Clinical characteristics of healthy control and PBC patients

	Healthy control	PBC patients
Number	12	21
Sex(male/female)	5/7	4/17
Age	47.0±13.0	56.1±10.4
Early stage	N	1
Moderate stage	N	8
Advanced state	N	12
Treated with UDCA	N	17

2.3.2 Mice

Prkaa1$^{-/-}$ and *Prkaa2*$^{-/-}$ mice were generated as previously described(Jorgensen et al., 2004; Viollet et al., 2003), and backcrossed into C57BL/6 background for at least ten generations. *Prkaa1*$^{flox/flox}$, *Foxp3*$^{YFP\text{-}cre}$, *Alb1*^{cre}, *LysM*^{cre}, *Rag1*$^{-/-}$, CD45.1^{+}C57BL/6, C57BL/6 mice were purchased from Jackson Laboratory (Bar Harbor, ME). Treg-specific AMPK α1 knock out (KO) mice were obtained by crossing mice carrying a loxP-flanked *Prkaa1* allele (*Prkaa1*$^{fl/fl}$) with *Foxp3*^{cre} mice expressing yellow fluorescent protein-Cre (YFP-Cre) recombinase fusion protein under the control of the Foxp3 promoter (referred to herein as *Prkaa1*$^{fl/fl}$ *Foxp3*^{cre}). Myeloid-specific AMPK α1 KO mice were generated by crossing *Prkaa1*$^{fl/fl}$ mice with LysM^{cre} transgenic mice. All mice were housed in specific pathogen-free conditions in the animal facilities at Georgia State University. The animal protocol was reviewed and approved by Georgia State University Institute Animal Care and Use Committee.

2.3.3 Bone Marrow Transplantation

Eight-week-old WT and *Prkaa1*$^{-/-}$ mice were subjected to 11-Gy lethal total-body irradiation (two doses of 5.5 Gy within an interval of 4 h) to eliminate endogenous bone marrow stem cells and bone marrow-derived cells, and immediately reconstitute with 5 × 10^6 donor bone marrow cells isolated from the femurs and tibias of WT or *Prkaa1*$^{-/-}$ mice. The hematologic parameters and liver tissue of recipient mice were analyzed 12 weeks after bone marrow transplantation.

2.3.4 Adoptive Treg Transfer

$CD4^+CD45RB^{hi}$ naive T cells were induced to develop into Treg cells by exposure to anti-CD3/CD28 antibodies in presence of TGFβ, IL-2, all-trans retinoic acid for 4 days. Induced Treg cells (iTreg) were then adoptively transferred into *Prkaa1*$^{-/-}$ mice. Six weeks later, mice were sacrificed and analyzed.

2.3.5 *In Vitro* Treg Cell Suppressive Assay

Sorted naive $CD4^+CD25^-CD62L^{hi}CD44^{lo}$T cells ($5 \times 10^4$ cells) were labeled with 5 μM CellTrace Violet (Invitrogen, Carlsbad, CA) for 10 minutes at 37°C in PBS, wash twice in 0.1% BSA PBS, and were then cocultured with sorted Tregs from *Prkaa1*$^{+/+}$ *Foxp3*^{cre} or *Prkaa1*$^{fl/fl}$ *Foxp3*^{cre} mice in the presence of T cell-depleted splenocytes (1×10^5 cells) and soluble anti-CD3 (2 μg/ml, Invitrogen, Carlsbad, CA). Four days later, cells were harvested, and violet dilution was measured by flow cytometric analysis.

2.3.6 *In Vivo* Treg Cell Suppressive Assay

Rag1$^{-/-}$ mice were i.v. injected with 4×10^5 Teff cells ($CD4^+CD45RB^{hi}$ $CD25^-$), either alone or with 1×10^5 Treg cells from *Prkaa1*$^{+/+}$ *Foxp3*^{cre} (WT) or *Prkaa1*$^{fl/fl}$ *Foxp3*^{cre}(KO) mice. Recipient *Rag1*$^{-/-}$ mice were monitored weekly for 10 weeks. Cells from mesenteric lymph node were subjected to cytometry analysis. Colon tissues were collected for H&E staining.

2.3.7 Serum Alanine Aminotransferase Level Measurement

Serum alanine aminotransferase levels were measured in Alanine Transaminase Colorimetric Activity Assay Kit (Cayman, Ann Arbor, MI) according to manufacturer's protocol. After ALT Initiator was added to wells, absorbance at 340 nm was read immediately and every minute following for a period of 5 minutes.

2.3.8 Autoantibody Detection

For detection of ANA or dsDNA-specific antibodies, ELISA plates (Thermo Fisher Scientific, Waltham, MA) were pre-coated with 5 µg/ml nuclear extract or double strand DNA from WT mouse liver. The plates were incubated with 1:100 diluted serum samples, and the assay was developed with HRP-labeled goat anti-mouse IgG (Thermo Fisher Scientific, Waltham, MA). Serum was diluted to 1:10000. Total IgG levels were detected by incubating plates with biotinylated anti-mouse IgG (Thermo Fisher Scientific, Waltham, MA) followed by streptavidin-peroxidase (eBioscience, San Diego, CA). Ig isotypes were detected by Isotyping multiplex assay (Millipore, Billerica, MA).

2.3.9 Histopathology Staining

Mice were sacrificed, and their organs/ tissues were dehydrated, embedded in paraffin, sectioned, and stained with H&E. Embedded samples were then sectioned and stained with appropriate antibodies.

2.3.10 Flow Cytometry Analysis

The frequency and phenotypic properties of Treg cells or Teff were determined by flow cytometry on a Becton Dickinson fluorescent activated cell sorter (FACScalibur, FACSCanto II or LSRFortessa, Becton Dickinson, CA). FlowJo 2 or FACSDiva (Treestar Inc) software were used for analysis. Each reaction was performed with 1×10^6 cells, and a minimum of 3×10^5 events were recorded. Isotype controls were included for each sample tested. The antibodies used include: fluorochrome-conjugated anti-mouse CD45 (Biolegend, San Diego, CA), CD4 (Biolegend), CD44 (Biolegend), CD62L (Biolegend), Foxp3 (eBiosceince, San Diego, CA), IL17 (Biolegend); anti-human CD25 (BD Bioscience), CD127 (eBiosceince), CD4 (Becton Dickinson, CA), CD45 (BD).

Intracellular staining: the frequency of cells positive for Treg cells were determined by

intracellular staining after cell fixation and permeabilization with Cytofix/Cytoperm (BD Bioscience) and counterstaining with PE-conjugated anti-FOXP3, FITC-conjugated anti-CD4 antibodies. The frequency of IL17 producing cells was detected after exposure to phorbol 12-myristate 13-acetate (PMA) (10ng/ml)/Ionomycin (50ng/ml), incubation with Brefeldin A (10μg/ml, all from Sigma Aldrich Company, St. Louis, MO) for 4 hours and counterstaining with fluorochrome-conjugated anti- IL17 and CD4 monoclonal antibodies. To assess the phosphor-AMPK (T172) in Treg cells, cells were initially stained with fluorochrome-conjugated anti-CD4, CD25 and CD127 monoclonal antibodies, then treated with intracellular Cytofix/Cytoperm. After incubation at room temperature for 30 minutes and centrifugation at *500g* for 5 minutes, cells were stained with anti-p-AMPK (Cell Signaling Technology, MA) at room temperature for 45 minutes, washed twice with Cytoperm buffer, then stained with PE-conjugated anti-rabbit IgG and washed twice with Cytoperm buffer. Flow cytometry was performed as above.

2.3.11 RNA Extraction and qRT-PCR

RNA was extracted by using RNeasy Mini Kit (QIAGEN, Hilden, Germany) according to the manufacturer's instructions. cDNA was synthesized using iScript cDNA Synthesis Kit (Bio-rad, Hercules, CA). The expression of Foxp3 mRNAs was determined using quantitative realtime PCR (qRT-PCR). Each cDNA sample was amplified using SYBR Green (Bio-rad, Hercules, CA) on Bio-rad CFX96 Touch Realtime PCR detection system. Primer sequences for Foxp3 were forward, 5'-CACAGCAACAGCACTGGAAC-3'; reverse, 5'-TTTTGGGCATTGCTTGAGGC-3'.

2.3.12 Western Blot Analysis

Antibodies against AMPKα, phospho-AMPKα (Thr172) were purchased from Cell Signaling Technology (Danvers, MA). Anti-Foxp3 antibody was purchased from eBioscience (San Diego, CA). Anti-phospho-serine/threonine antibody was from Abcam (Cambridge, UK) and anti-actin was purchased from Santa Cruz Technology (Dallas, TX). Cells were lysed with NP-40 lysis buffer (1% NP-40, 20 mM Tris-HCl, pH 7.5, 150 mM NaCl, 5 mM EDTA, 50 mM NaF, 2 mM Na3VO4,

and 10 μg/ml each of aprotinin and leupeptin) or were lysed with 1X SDS sample buffer (50 mM Tris-HCl, pH 6.8, 100 mM DTT, 2% SDS, and 10% glycerol). Proteins were separated by SDS-PAGE and transferred to nitrocellulose membranes (Millipore, Billerica, MA). Membranes were visualized with an enhanced chemiluminescence detection system (Thermo Fisher Scientific, Waltham, MA).

2.3.13 *In Vitro* Kinase Assay

In vitro kinase assay was performed as previously described(Shaw et al., 2004). Briefly, GST-FOXP3 recombinant protein (Abnova, Taiwan) was incubated in the absence or presence of AMPKα1β1γ1 recombinant protein (a kind gift from Dr. Dietbert Neumann of Maastricht, the University in Netherlands) in the kinase buffer (50 mM Tris, pH 7.5/10 mM $MgCl_2$/1 mM DTT/200 μm AMP/200 μm ATP) at 37°C for 20 min. Reactions were stopped by addition of SDS sample buffer, and samples were then subjected to SDS-PAGE and western blot analysis.

2.3.14 Statistical Analysis

All statistical analyses were performed using GraphPad Prism version 5 (GraphPad Software, CA). Results were analyzed with a student's *t*-test (two groups) or ANOVA (more than two groups). Data are present as mean values ± SD. A P value of <0.05 was statistically significant.

2.4 Results

2.4.1 AMPKα1 Deletion Leads to Liver Injury

AMPK is a conserved serine/threonine kinase consisting of α, β and γ subunits. The α subunit, for which two isoforms exist (α1 and α2), is responsible for the catalytic activity of the heterotrimeric complex. AMPK α1 is encoded by the *Prkaa1* gene and AMPK α2 is encoded by the *Prkaa2* gene. We found that the liver of *Prkaa1*$^{-/-}$ mice exhibited white spots by gross appearance (**Figure 1A**). Further histological analysis showed massive inflammatory cell infiltration (**Figure 1B**). Moreover, total number of infiltrated leukocytes in the liver was

dramatically increased in *Prkaa1*$^{-/-}$ mice (**Figure 1C**). However, all these abnormal liver phenotypes were absent in *Prkaa2*$^{-/-}$ mice (**Figure 2**). We further analyzed serum level of alanine aminotransferase (ALT) and found that it was higher in *Prkaa1*$^{-/-}$ mice than in WT mice (**Figure 1D**). In addition, serum level of total immunoglobulin G (IgG) was much higher in *Prkaa1*$^{-/-}$ mice than in WT mice (**Figure 1E**). Further, *Prkaa1*$^{-/-}$ mice showed higher concentrations of serum IgG2a, IgG2b and IgA (**Figure 1F**), as well as antinuclear antibodies (ANA) (**Figure 1G**). Proportions of $CD4^+$ T helper 17 (Th17) lymphocytes, which are key effector cells in autoimmune diseases, were significantly increased in the liver of *Prkaa1*$^{-/-}$ mice (**Figure 1H**). Moreover, the frequency of Treg cells in liver tissue was decreased in *Prkaa1*$^{-/-}$ mice than in WT mice (**Figure 1I**), however, the absolute number of Treg cells was slightly increased rather than decreased in liver organ of *Prkaa1*$^{-/-}$ mice (**Figure 1J**), this is likely due to more infiltrated leukocyte in liver organ of *Prkaa1*$^{-/-}$ mice. However, the frequency of Treg cells in peripheral blood was markedly lower in *Prkaa1*$^{-/-}$ mice than in WT mice (**Figure 1K**). Collectively, these data suggest that AMPKα1 deletion in mice causes increased immune cell infiltration, resulting in immune-mediated liver injury.

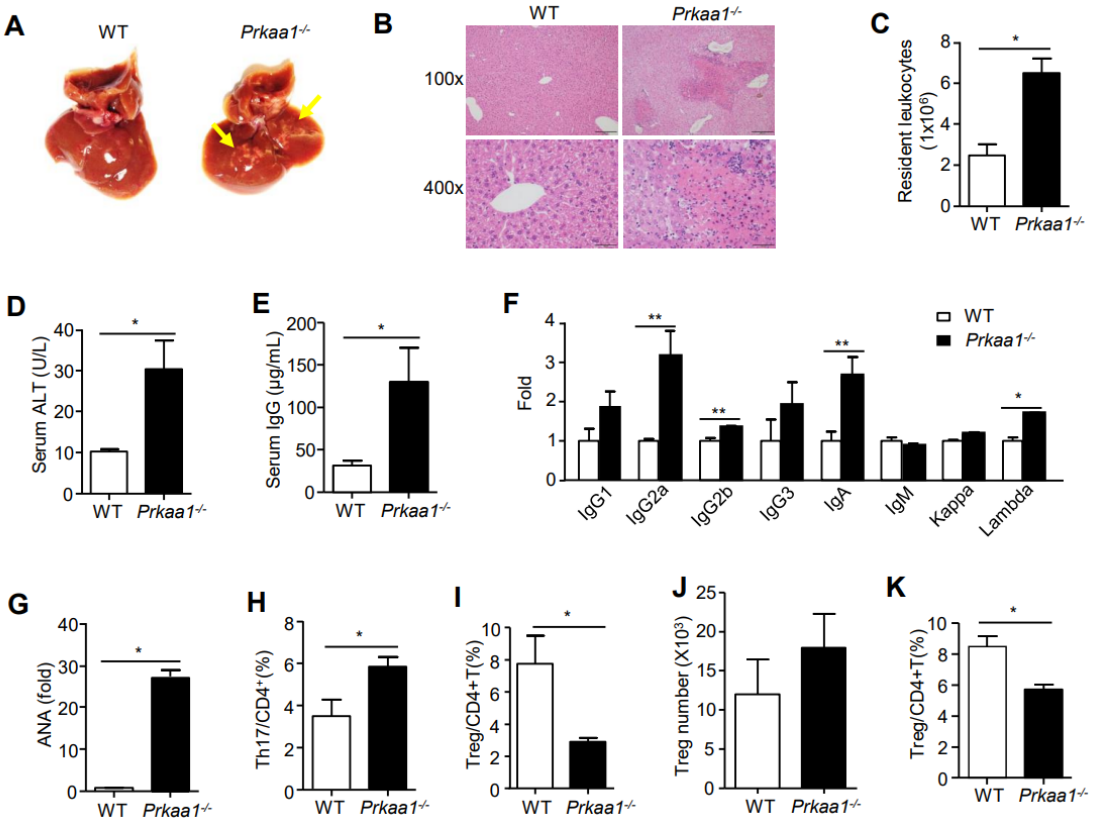

Figure 1 AMPKα1 deletion leads to liver injury.
A Photograph of livers from 3-month-old WT and Prkaa1-/- mice. B H&E staining of liver. C Total number of leukocytes isolated from whole livers (N = 5-7). D Serum level of alanine aminotransferase (N = 19–32). E Quantified serum levels of total IgG in 8-month-old WT and Prkaa1-/- mice (N = 7–8). F Quantified serum levels of Ig isotypes in 8-month-old WT and Prkaa1−/− mice (N = 3–4). G Quantified serum level of ANA antibody in 8-month-old WT and Prkaa1-/- mice (N = 8–12). H IL17+/CD4+ cell population in livers (N = 4). *p < 0.05; **p < 0.01 vs. WT. I Treg cell+/CD4+ cell population in livers (N = 4). J Absolute number of Treg cells in livers. K The frequency of Treg cells in peripheral blood

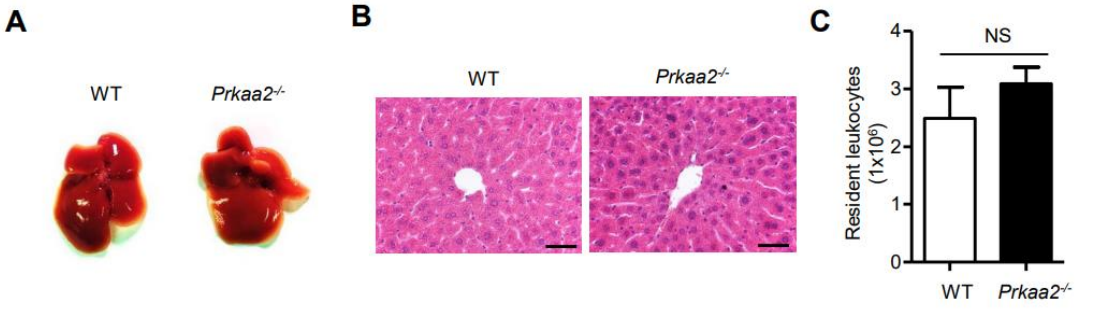

Figure 2 AMPKα2 deletion does not lead to liver injury.
A,Photography of liver from 3 month-old WT and *Prkaa2-/-* mice. B, H&E staining of liver (scale bar=50μm). C, Total number of leukocytes isolated from whole livers (N=5-7).

2.4.2 Bone Marrow Transplantation and Adoptive Treg Transfer Rescue *Prkaa1*$^{-/-}$ Mice from Liver Injury

We next investigated which cell type(s) contributes to the liver injury in *Prkaa1*$^{-/-}$ mice. We first examined the liver-specific AMPK α1 knockout (KO) mice. As shown in **Figure 3**, liver-specific AMPK α1 KO mice exhibited normal liver histology and no inflammatory cell infiltration, suggesting that liver cells are not responsible for the injury. We then tested whether AMPK α1 deficiency in hematopoietic cells may lead to the liver injury. To this end, we performed reciprocal bone marrow transplantation between WT and *Prkaa1*$^{-/-}$ mice, in which bone marrow cells were transplanted into irradiated mice. As shown in **Figure 4A**, liver inflammatory injury in *Prkaa1*$^{-/-}$ mice was completely resolved after 12 weeks engraftment of WT bone marrow, whereas bone marrow from *Prkaa1*$^{-/-}$ mice induced liver injury in WT mice. In addition, serum IgG levels in *Prkaa1*$^{-/-}$ mice received WT bone marrow decreased to the same level as in WT mice, whereas serum IgG levels in WT mice that received *Prkaa1*$^{-/-}$ bone marrow increased to the same level as in *Prkaa1*$^{-/-}$ mice (**Figure 4B**). These data suggest that lack of AMPKα1 expression in bone marrow-derived cells leads to liver inflammatory injury.

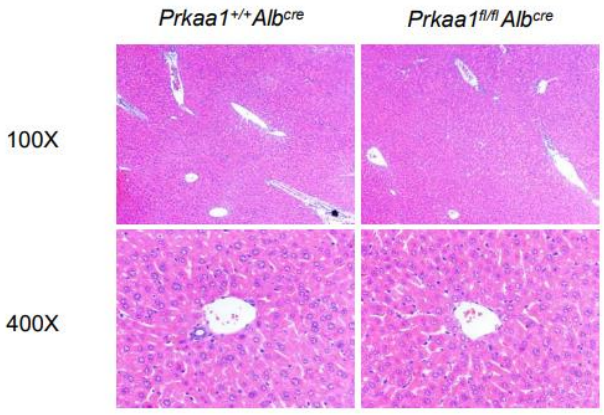

Figure 3 Liver-specific AMPKα1 deletion does not lead to liver injury.
H&E staining of liver from 3-month-old *Prkaa1*$^{+/+}$ *Alb*^{cre} or *Prkaa1*$^{fl/fl}$ *Alb*^{cre} mice (N=8).

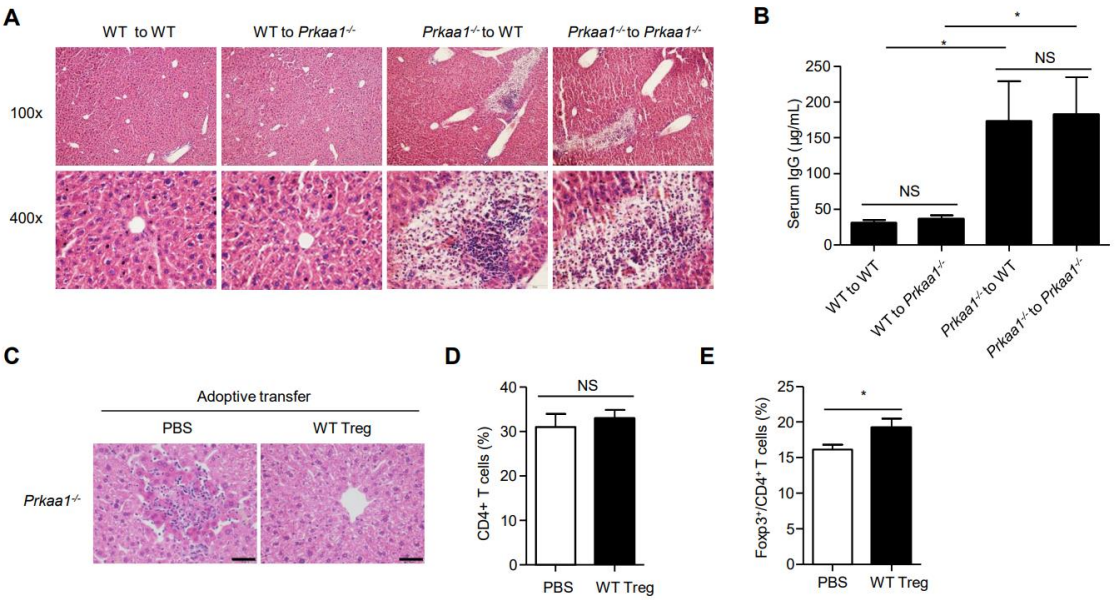

Figure 4 Bone marrow transplantation and adoptive Treg cell transfer prevent liver injury in Prkaa1-/- mice.
A H&E staining of liver sections obtained 12 weeks after irradiated mice were transplanted with bone marrow from WT or Prkaa1-/- mice. B Quantified serum level of total IgG from transplanted mice (N = 5). C H&E staining of livers from Prkaa1-/- mice adoptively transferred with PBS or WT Foxp3+ iTreg cells (scale bar = 50 μm). D CD4+ cell population in the lymph nodes of Prkaa1-/- recipient mice. E Foxp3+/CD4+ cell population in the lymph nodes of Prkaa1−/− recipient mice (N = 9). *P < 0.05

We then examined myeloid-specific AMPK α1 knockout (KO) mice. As shown in **Figure 5**, deletion of AMPK α1 in myeloid cells does not result in liver injury, suggesting that other immune cells may be involved. Since Tregs have been suggested to play an essential role in suppressing liver inflammation in animal model studies(Bochtler et al., 2008; Kido et al., 2008; Lapierre et al., 2013), we next tested whether the rescue effect of WT bone marrow on *Prkaa1*$^{-/-}$ mice is due to the activity of Treg cells. To this end, induced Treg cells (iTreg) were adoptively transferred into *Prkaa1*$^{-/-}$ mice. Six weeks later, *Prkaa1*$^{-/-}$ mice that received transfer of PBS as a control still exhibited liver inflammatory injury, whereas *Prkaa1*$^{-/-}$ mice received transfer of WT iTreg cells showed no more liver injury (**Figure 4C**). Compared to mice that received control, *Prkaa1*$^{-/-}$ mice that received WT iTreg cells had similar levels of $CD4^+$ T cells (**Figure 4D**), but higher levels of Treg cells (**Figure 4E**). All these results suggest that deficiency of AMPK α1 in Tregs may contribute to the liver injury in *Prkaa1*$^{-/-}$ mice.

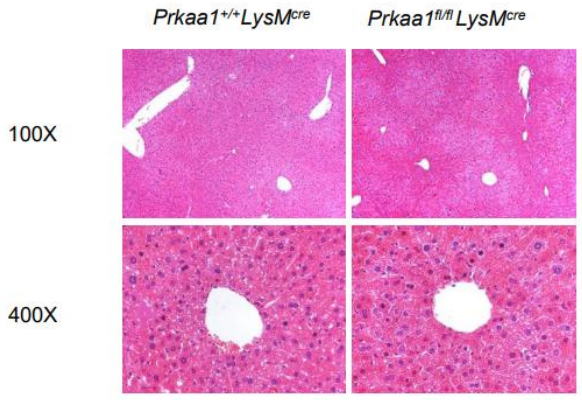

Figure 5 Myeloid-specific AMPKα1 deletion does not lead to liver injury.
H&E staining of liver from 3-month-old *Prkaa1*$^{+/+}$ *LysM*^{cre} or *Prkaa1*$^{fl/fl}$ *LysM*^{cre} mice (N=5).

2.4.3 Treg-specific AMPK α1 Deletion Leads to Autoimmune Liver Disease

To understand more precisely the role of AMPKα1 in Treg cells, we crossed mice carrying a loxP-flanked *Prkaa1* allele (*Prkaa1*$^{fl/fl}$) with *Foxp3*^{cre} mice expressing yellow fluorescent protein-Cre (YFP-Cre) recombinase fusion protein under the control of the Foxp3 promoter (referred to herein as *Prkaa1*$^{fl/fl}$ *Foxp3*^{cre}) (**Figure 6A**). The genotype was confirmed by PCR (**Figure 6B**). Immunoblot analysis confirmed efficient and specific deletion of AMPKα1 in sorted YFP^{+} Treg cells, but not YFP^{-} conventional T cells from *Prkaa1*$^{fl/fl}$ *Foxp3*^{cre} mice (**Figure 6C**). Interestingly, we found that *Prkaa1*$^{fl/fl}$ *Foxp3*^{cre} mice displayed histological features resembling human autoimmune liver disease, including portal inflammation (presence of inflammatory infiltrates surrounding hepatic portal tracts), interface hepatitis (portal infiltrates extending into the lobule), and lobular inflammation (infiltrates within the liver parenchyma) (**Figure 6D**). In addition to those histological manifestations, serum immunoglobulin G (IgG) level, serum antinuclear antibodies (ANA) and anti-double stranded DNA (anti-dsDNA) levels were also significantly increased in *Prkaa1*$^{fl/fl}$ *Foxp3*^{cre} mice as compared to their wild type of littermate control (**Figure 6E-6G**). Moreover, *Prkaa1*$^{fl/fl}$ *Foxp3*^{cre} mice had a greater frequency of memory and effector CD4^{+} T cells (CD44^{+} CD62L^{-} CD4^{+}), with a concomitantly lower frequency of naïve CD4^{+} cells (CD44^{-} CD62L^{+} CD4^{+}) (**Figure 6H-6I**), suggesting an activated phenotype in these mice. Consistent with these findings, *Prkaa1*$^{fl/fl}$ *Foxp3*^{cre} mice had a significant increase of CD4^{+} cells producing IL-17(**Figure**

6J), whose elevation has been detected in both human and mouse autoimmune hepatitis(Yu et al., 2010; Zhao et al., 2011). Collectively, all these data suggest that deficiency of AMPKα1 in Treg cells leads to autoimmune liver disease.

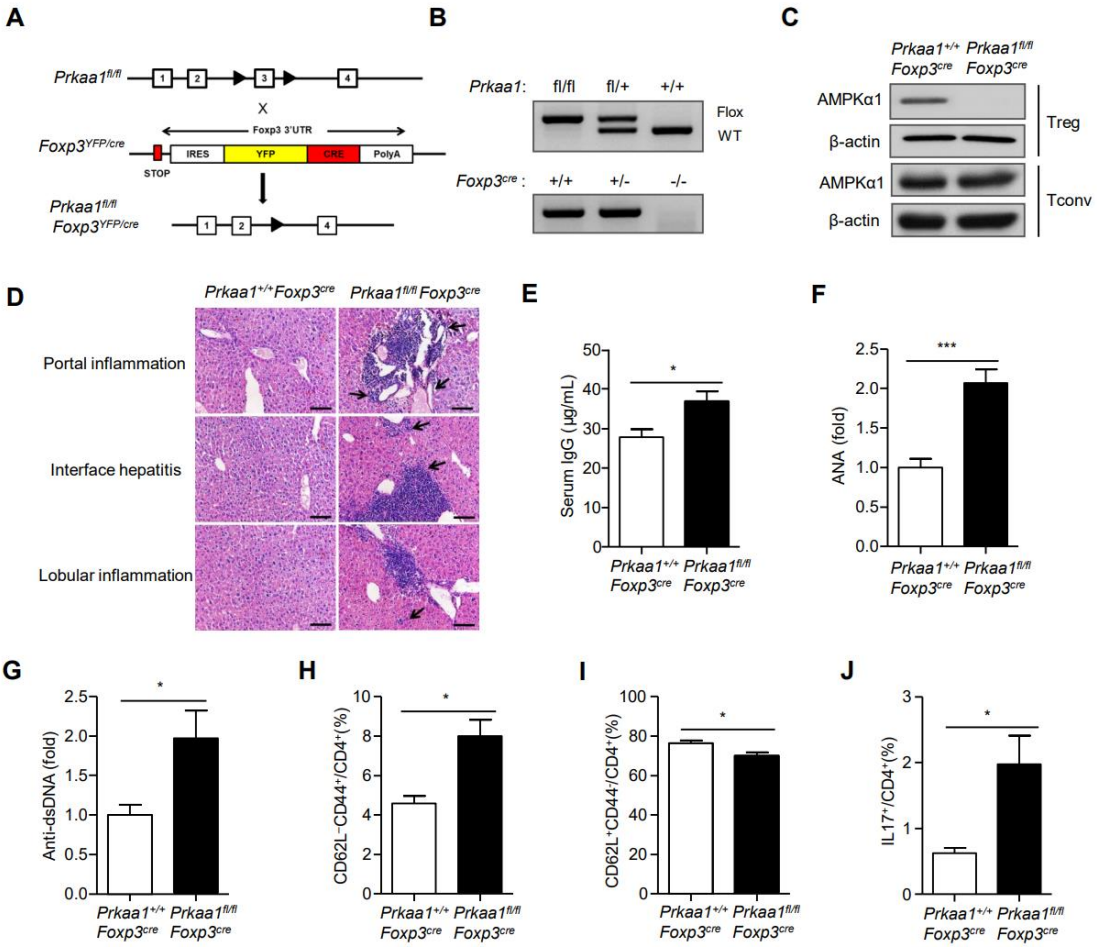

Figure 6 Treg-specific AMPK α1 deletion leads to autoimmune liver diseases.
A, Breeding scheme for generation of Treg specific AMPKa1 KO mice. B. PCR identification of conditional KO mice. C, Immunoblot identification of knockout efficiency in T regulatory cells (Treg) and conventional T cells (Tconv). D, H&E staining of liver sections in one year-old *Prkaa1*$^{+/+}$ *Foxp3*^{cre} and *Prkaa1*$^{fl/fl}$ *Foxp3*^{cre} mice (N=8-9). E-G, Quantified serum levels of total IgG (E), ANA antibody (F), and anti-double strand DNA antibody (G) in *Prkaa1*$^{+/+}$ *Foxp3*^{cre} and *Prkaa1*$^{fl/fl}$ *Foxp3*^{cre} mice (N=13-20). H-I, FACS analysis of CD62L, CD44 expression in conventional T cells from MLN in 8-week-old *Prkaa1*$^{+/+}$ *Foxp3*^{cre} and *Prkaa1*$^{fl/fl}$ *Foxp3*^{cre} mice. J, FACS analysis of IL17 production in CD4^{+} T cells from MLN of *Prkaa1*$^{+/+}$ *Foxp3*^{cre} and *Prkaa1*$^{fl/fl}$ *Foxp3*^{cre} mice (N=12). *, p<0.05.

2.4.4 AMPKα1 Deletion does not Affect Treg Cell Differentiation or Proliferation

Disruption of Treg homeostasis has previously been associated with autoimmune liver disease(Diestelhorst et al., 2017; Ferri et al., 2010; Longhi et al., 2004), we thus next explored whether AMPKα1 regulate Treg homeostasis. As shown in **Figure 7A**, Treg frequency in the

thymus is comparable in *Prkaa1*$^{-/-}$ and WT mice, suggesting that AMPKα1 deletion does not affect Treg differentiation. To further confirm this hypothesis, CD4^{+}CD45RB^{hi} naive T cells were induced to develop into Treg cells by exposure to anti-CD3/CD28 antibodies in presence of TGFβ, IL-2, all-trans retinoic acid for 2 or 4 days. As shown in **Figure 7B**, naive T cells from *Prkaa1*$^{-/-}$ mice showed similar differentiation to those from WT mice. We further examined Treg cell proliferation by using sorted Treg cells treated with anti-CD3/CD28 antibodies and IL-2. As shown in **Figure 7C**, Treg cells from *Prkaa1*$^{-/-}$ mice also showed a similar proliferation rate as Treg cells from WT mice, suggesting that AMPKα1 does not regulate Treg cell proliferation.

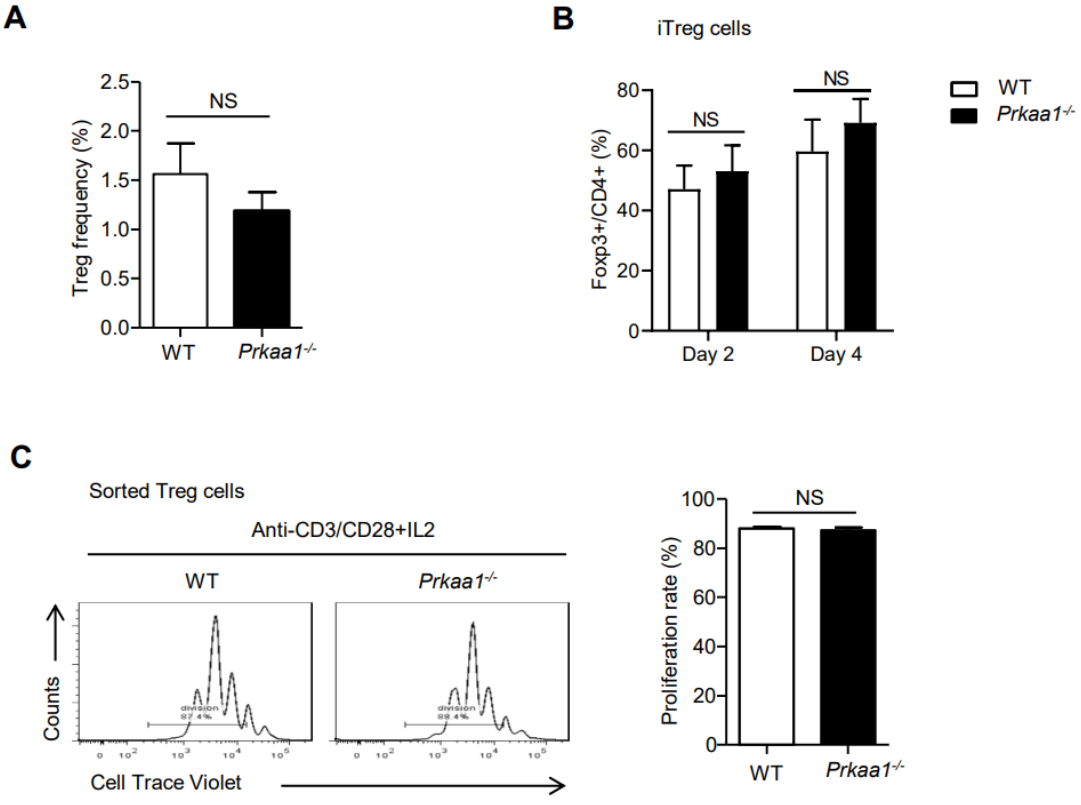

Figure 7 AMPKα1 deletion does not affect Treg cell differentiation or proliferation.
A, Treg frequency in thymus from WT or *Prkaa1*$^{-/-}$ mice mice (N=6). B, FACS-sorted CD4^{+}CD45RB^{hi} naive T cells were induced into Treg with anti-CD3/CD28 antibodies in presence of TGFβ, IL-2 and all-trans retinoic acid for 2 or 4 days (N=4). C, Sorted YFP+ Treg cells were stimulated with anti-CD3/CD28 antibodies and IL-2 for 4 days. Cell Trace Violet dilution was examined by flow cytometry (N=4).

2.4.5 AMPKα1 Deletion Compromises Treg Suppressive Activity

Since Treg cells play a crucial role in maintaining immunological tolerance by actively

suppressing self-reactive lymphocytes, we then examined whether AMPKα1 deficiency impairs Treg suppressive function. To this end, an *in vitro* suppressive assay was first performed. As shown in **Figure 8A**, Treg cells from AMPKα1-deficient mice did not inhibit the proliferation of Teff cells as efficiently as their WT counterparts. We also tested the suppressive function of AMPKα1 deficient Tregs *in vivo* in a well-characterized Teff transfer-induced colitis model ($CD4^+CD45RB^{hi}$ cells injected into *Rag1*$^{-/-}$ mice, **Figure 8B**). As shown in Figure **Figure 8C-8D**, the transfer of Teff cells alone elicited colitis in *Rag1*$^{-/-}$ recipient mice, as manifested by gradual weight loss, splenomegaly and lymphadenopathy. However, co-transfer of WT Treg cells, but not AMPKα1-deficient Treg cells, effectively suppressed weight loss and enlargement of the spleen and mesenteric lymph nodes. Consistent with these findings, histological analysis of *Rag1*$^{-/-}$ mice that received WT Tregs showed a lower degree of colon inflammation compared with mice that received AMPKα1-deficient Treg cells (**Figure 8E**). These results suggest that AMPKα1 is required for Treg suppressive activity.

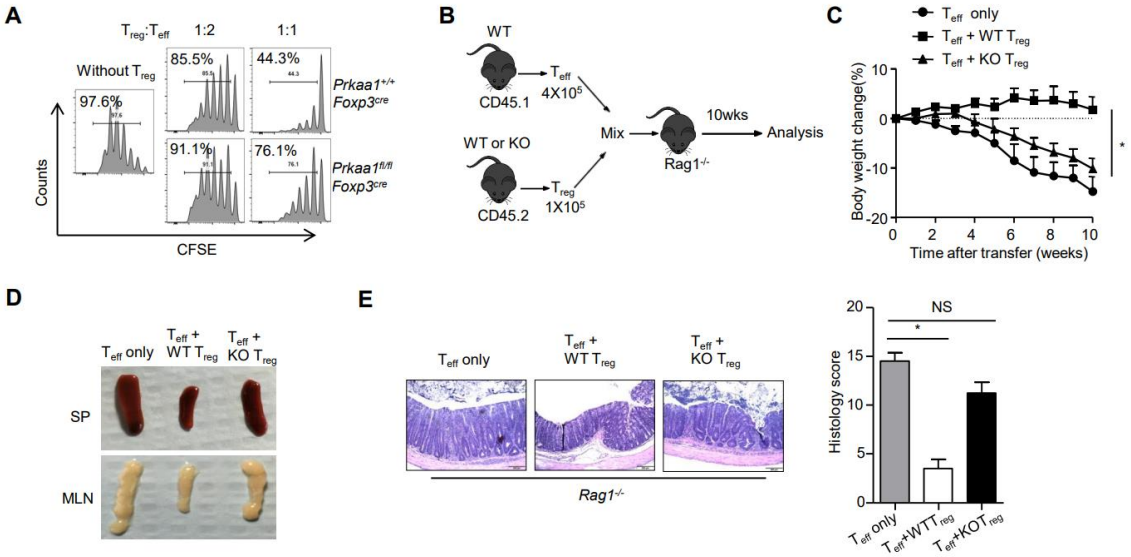

Figure 8 AMPKα1 deletion compromises Treg suppressive activity.
A, Sorted naïve $CD4^+YFP^-CD62L^+CD44^-$ T cells from *Prkaa1*$^{+/+}$ *Foxp3*^{cre} and *Prkaa1*$^{fl/fl}$ *Foxp3*^{cre} mice were labeled with violet, then co-cultured with $CD4^+$ YFP^+ T regulatory cells at 1:2 or 1: 1 ratio in the presence of T cell-depleted splenocytes and anti-CD3. Violet dilution was assessed 4 days later by flow cytometry. Data are representative of three independent experiments. B-E, $CD4^+CD45RB^{hi}$ naïve T cells (T_{eff}) were transferred together with or without sorted Treg cells from *Prkaa1*$^{+/+}$ *Foxp3*^{cre} (WT) or *Prkaa1*$^{fl/fl}$ *Foxp3*^{cre} (KO) mice into *Rag1*$^{-/-}$ mice. C, Body weight of individual mouse was monitored every week for 10 weeks. Data are compiled from three independent experiments. D, Representative images of spleen and MLNs from *Rag1*$^{-/-}$ recipient mice. E, H&E staining of colon section and histology scores of sections from *Rag1*$^{-/-}$

recipient mice (N=6, *p<0.05).

2.4.6 Activation of AMPK Phosphorylates Foxp3 and Regulates its Stability

As Foxp3 is essential for the suppressive properties of Treg cell, we tested whether AMPKα1 regulates Foxp3. As shown in **Figure 9A**, Foxp3 protein levels were significantly decreased in Treg cells isolated from *Prkaa1*$^{fl/fl}$ *Foxp3*^{cre} mice as compared to WT mice. Conversely, the mRNA levels of Foxp3 were not changed (**Figure 9B**), suggesting that AMPKα1 may regulate Foxp3 at the post-transcriptional level.

It has been reported that TCR stimulation controls phosphorylation of Foxp3(Nie et al., 2013). In sorted YFP^{+} Treg cells, TCR stimulation (anti-CD3/anti-CD28) increased AMPK phosphorylation at threonine 172, which indicates AMPK activation, in a time-dependent manner (**Figure 9C**). As AMPK is a serine/threonine kinase, we hypothesized that AMPK may be the direct upstream kinase of Foxp3. To test this hypothesis, we performed an *in vitro* kinase assay. As shown in **Figure 9D**, Foxp3 was phosphorylated by recombinant AMPK in a dose-dependent manner. To further establish if AMPK phosphorylation alters Foxp3 levels in intact cells, 293A cells were transfected to overexpress with a vector control or Foxp3 plasmid. Twenty-four hours after transfection, the cells were stimulated with AMPK activator A769662 or the AMPK inhibitor Compound C for 12 hours. As shown in **Figure 9E**, activation of AMPK by A769662 significantly increased Foxp3 level. Conversely, inhibition of AMPK activity by Compound C significantly decreased Foxp3 levels. Importantly, sorted Treg cells treated with A769662, or Compound C showed similar results (**Figure 9F**). As Foxp3 expression is tightly regulated by polyubiquitination-mediated proteasomal degradation(Chen et al., 2013; van Loosdregt et al., 2013), we further examined if AMPK regulates Foxp3 ubiquitination. As shown in **Figure 9G**, activation of AMPK with A769662 significantly decreased Foxp3 ubiquitination, whereas selective AMPK inhibition with Compound C had the opposite effect, abolishing the A769662-regudced Foxp3 ubiquitination. Moreover, MG132, a potent 26S proteasome inhibitor, normalized AMPK-regulated Foxp3 levels (**Figure 9H**). Taken together, these results imply that AMPK activation maintains Foxp3 stability

in Treg cells.

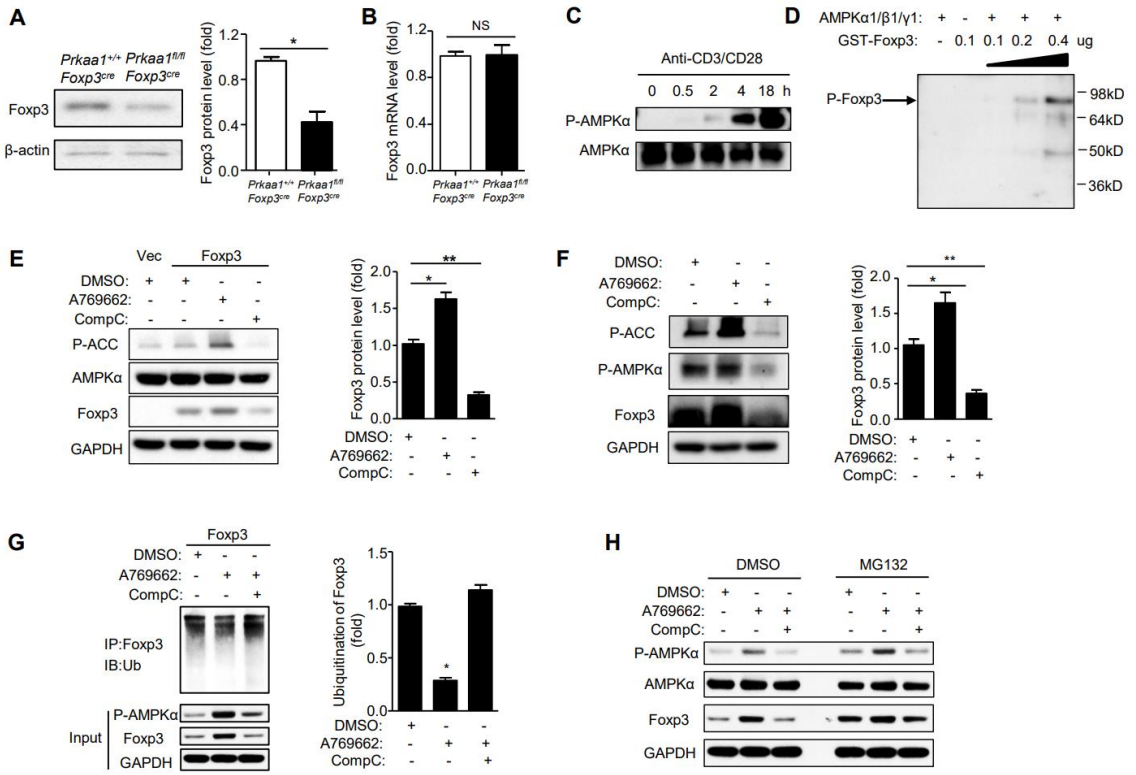

Figure 9 Activation of AMPK phosphorylates Foxp3 and regulates its stability.
A, Immunoblot analysis of Foxp3 protein level in sorted Treg cells isolated from *Prkaa1*$^{+/+}$ *Foxp3*^{cre} or *Prkaa1*$^{fl/fl}$ *Foxp3*^{cre} mice (N=6, *p<0.05 versus control mice). B, Quantitative RT-PCR analysis of Foxp3 mRNA level in sorted Treg cells. C, Sorted Treg cells were stimulated with anti-CD3/CD28 antibodies for indicated times. D, *In vitro* kinase assay to determine phosphorylation of Foxp3 by recombinant AMPK. E, 293A cell were transfected with vector control or Foxp3 overexpressing plasmid, and then stimulated with AMPK activator A769662 or AMPK inhibitor compound C for 12 hours. F, Sorted Treg cells were stimulated with A769662 or compound C for 12 hours. G, Ubiquitination of Foxp3 in 293A cells transfected with Foxp3 plasmid and stimulated with A769662 or compound C for 12 hours. H, 293A cell transfected with Foxp3 plasmid were stimulated with A769662 or compound C in the presence or absence of proteasome inhibitor MG132. All immunoblot results are representative of at least three independent experiments. *p<0.05.

2.4.7 Reduced Treg cells and Decreased AMPK Phosphorylation in Treg Cells from Primary Biliary Cholangitis (PBC) Patients

To test the relevance of our findings in human disease, we further obtained peripheral blood from patients with primary biliary cholangitis (PBC) and healthy controls and assessed the frequency of Treg cells and the level of phosphorylated AMPK in Treg cells. Fluorescent-activated cell sorting (FACS) analysis indicated that the frequency of Treg cells from circulating blood is significantly lower in PBC patients than in healthy controls (**Figure 10A**), moreover, the phosphorylation levels of AMPK at T172 were decreased in PBC patients compared to controls

(**Figure 10B-10C**), This finding further implies a crucial role for AMPK activation in autoimmune liver disease.

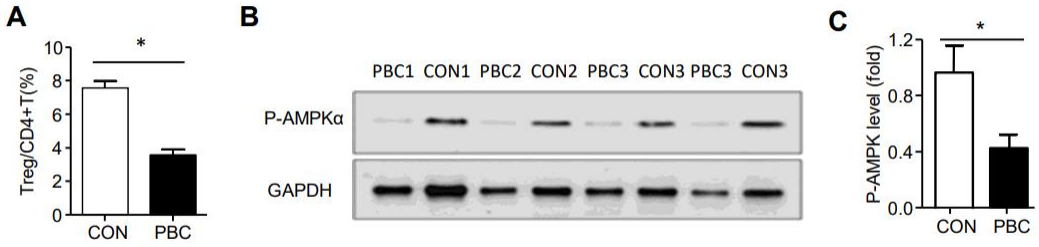

Figure 10 Reduced Treg cells and decreased AMPK phosphorylationin in Treg cells from primary biliary cholangitis (PBC) patients.
A, FACS analysis of frequency of Treg cells (CD4+CD25+CD127low) in peripheral blood from healthy control and PBC patients, N=16-21, *p<0.05 versus control group. B, Western blot for p-AMPK (T172) in CD4+CD25+CD127low population of peripheral blood from healthy control and PBC patients. C, Western was used to quantitatively evaluate the phosphorylation of AMPK at Thr-172 in CD4+CD25+CD127low population of peripheral blood from healthy control and PBC patients, GAPDH as loading control. *p<0.05 versus control group.

2.5 Discussion

AMP-activated protein kinase (AMPK) is a crucial regulator in energy metabolism and stress response pathways(Hardie, 2007, 2008; Hardie and Carling, 1997). Here we report that AMPKα1 plays a novel role in the control of Treg cell suppressive activity and prevention of autoimmune liver disease.

During an immune response, changes in the proliferative and functional state of T cells are accompanied by profound modifications in energy metabolism(Jones and Thompson, 2007). As a central regulator of energy homeostasis, AMPK thus has long been implicated in regulating T cell function(Ma et al., 2017). AMPKα1-deficient T cells displayed reduced metabolic plasticity in response to glucose limitation in vitro and reduced metabolic activity and lower ATP levels during pathogenic challenge in vivo(Blagih et al., 2015). However, T cells isolated from AMPKα1-deficient mice display normal responses to mitogenic stimulation in vitro(MacIver et al., 2011), whereas exacerbated T cell-mediated pathology was observed in an *in vivo* model of autoimmunity with whole-body AMPKα1 deletion(Nath et al., 2009b). These results suggest that AMPK might play an important role in regulatory immune cells. Indeed, it has been reported that

in vivo administration of metformin, a pharmacological activator of AMPK, suppresses systemic autoimmunity and attenuates the induction of experimental autoimmune encephalomyelitis (EAE) in C57BL/6 mice(Lee et al., 2017; Nath et al., 2009a; Sun et al., 2016). In these studies, metformin was found to either inhibit T cell-mediated immune responses and the production of Th1 or Th17 cytokines or suppress B cell differentiation into plasma cells and thus decrease serum levels of anti-double stranded DNA antibodies. These studies suggest that AMPK may regulate Treg function and indirectly, the development of autoimmunity. Consistent with this hypothesis, we found that AMPKα1 deficiency impairs Treg suppressive function. Mice with Treg-specific deletion of AMPKα1 spontaneously developed autoantibodies, hyperactivation of T cell responses, and autoimmune liver disease. This is also consistent with a recent report that Berberine, a compound which can activate AMPK, can attenuate Concanavalin A-induced autoimmune hepatitis in mice(Wang et al., 2017). More importantly, we found that in patients with primary biliary cholangitis (PBC), one of the major types of autoimmune liver disease, the phosphorylation of AMPK is dramatically decreased, and correspondingly, the frequency of Treg cells is significantly decreased. This finding further suggest that AMPK activation is important for the maintenance of Treg function and the prevention of autoimmune liver disease.

Moreover, we found that AMPKα1 phosphorylates Foxp3 and maintains Foxp3's stability. As the main transcriptional regulator of Treg cells, Foxp3 establishes Treg cell function and acts largely as a repressor(Arvey et al., 2014). However, how Foxp3 in Treg cells is regulated remains not entirely clear. Previously, intense investigation has been focused on transcriptional activation at the *Foxp3* locus. Recently, various studies have started to define important roles for post-translational modification, especially phosphorylation, in Foxp3 regulation and Treg function(van Loosdregt and Coffer, 2014). Indeed, TCR engagement triggers a signaling cascade with rapid phosphorylation events and reprograms the proteomes and bioenergetic features for T cell activation, proliferation, and differentiation(Tan et al., 2017). Here we showed that TCR stimulation triggers the activation of serine/threonine kinase AMPK, which directly phosphorylates Foxp3 and

decreases its ubiquitination and degradation. Therefore, our findings have revealed AMPK as a novel kinase for phosphorylating and maintaining protein stability of Foxp3 under disease settings, which may provide the molecular mechanism for pharmacological activation of AMPK in treating autoimmune disorders.

In conclusion, we have identified AMPKα1 as a new regulator of Treg suppressive function and autoimmune liver disease and our studies suggest the possibility of pharmacological activation of AMPK in the treatment of this disorder.

2.6 Author Contributions

M.-H.Z. conceived the project, H.Z., Z.L., J.A., M.Z., Y.Q. designed the experiments, carried out experiments and analyzed data, Z.L. and H.Z. wrote the manuscript.

2.7 Financial Support

This study was supported in part by the following grants: NHLBI (HL079584, HL080499, HL089920, HL110488, HL128014, and HL132500), NCI (CA213022), NIA (AG047776), NSFC (31870897), and NSFC (81900387). Dr. M.H. Zou is an eminent scholar of the Georgia Research Alliance.

2.8 Competing Interests

The authors declare no competing interests.

3 AMP-Activated Protein Kinase Alpha1 Promotes Tumor Development via FOXP3 Elevation in Tumor-infiltrating Treg Cells.

An J, et al. iScience. 2021 Dec 4;25(1):103570.

Junqing An[1], Ye Ding[1], Changjiang Yu[1], Jian Li[1], Shaojin You[1], Zhixue Liu[1], Ping Song[1*], Ming-Hui Zou[1,2*]

[1]Center for Molecular and Translational Medicine, Georgia State University, 157 Decatur Street SE. Atlanta, GA 30303

[2]Lead contact

*Corresponding author. Ping Song, Ph.D., 157 Decatur Street SE, Atlanta, GA 30303, Tel:1-404-413-6636, E-mail: psong@gsu.edu. Ming-Hui Zou, M.D., Ph.D., 157 Decatur Street SE, Atlanta, GA 30303, Tel:1-404-413-6637, E-mail: mzou@gsu.edu

3.1 Summary

Overwhelming evidence indicate that infiltration of tumors by Treg cells with elevated levels of FOXP3 suppresses the host antitumor immune response. However, the molecular mechanisms that maintain high expression of FOXP3 in tumor-infiltrating Treg cells remain elusive. Here, we report that AMP-activated protein kinase alpha1 (AMPKα1) enables high FOXP3 expression in tumor-infiltrating Treg cells. Mice with Treg-specific AMPKα1 deletion showed delayed tumor progression and enhanced antitumor T cell immunity. Further experiments showed that AMPKα1 maintains the functional integrity of Treg cells and prevents interferon-γ production in tumor-infiltrating Treg cells. Mechanistically, AMPKα1 maintains the protein stability of FOXP3 in Treg cells by downregulating the expression of E3 ligase CHIP (*STUB1*). Our results suggest that AMPKα1 activation promotes tumor growth by maintaining FOXP3 stability in tumor-infiltrating Treg cells and that selective inhibition of AMPK in Treg cells might be an effective anti-tumor therapy.

Keywords: AMPK, antitumor immunity, Treg function, Foxp3

3.2 Introduction

The recognition of tumor antigens by the host immune system promotes antitumor immune responses (Carey et al., 1976). The promotion of tumor-specific T cell responses has been recognized as a promising strategy for cancer therapy (Borst et al., 2018). However, the increased expression of immunosuppressive molecules (PD1/PDL1) and enrichment of immunosuppressive cells (myeloid-derived suppressor cells, tumor-associated macrophages, and regulatory T (Treg) cells) in the tumor microenvironment (TME) limit antitumor immunity and promote tumor immune escape (Han et al., 2020; Kumar et al., 2016; Petty and Yang, 2017; Tanaka and Sakaguchi, 2017). Despite the great progress achieved with immune checkpoint blockers in cancer therapy, the molecular mechanisms that determine the immunosuppressive character of the TME are still not fully understood.

Treg cells are a heterogeneous population of lymphocytes that express the transcription factor Foxp3 and play an essential role in immune balance and tissue homeostasis (Bonney et al., 2015; Smigiel et al., 2014; Veiga-Parga et al., 2013). Stable expression of Foxp3 is required for the development and function of Treg cells, whereas deficiency or mutation of Foxp3 impairs Treg function and causes several autoimmunity disorders (Bacchetta et al., 2018; Bennett et al., 2001; Fontenot et al., 2003). In cancers, enrichment of Treg cells in the TME promotes tumor development, invasiveness, and metastasis (Hatziioannou et al., 2017), whereas depletion or inhibition of Treg cells in the TME has shown as a promise strategy for cancer therapy (Hatzioannou et al., 2020; Xiong et al., 2020). In contrast to Treg cells in peripheral blood and other tissues, Treg cells that infiltrate the TME are predominantly $Foxp3^{high}$ effector Treg (eTreg) cells, the accumulation of which is linked to poor prognosis of various cancers (Wing et al., 2019). Multiple studies showed that destabilized FOXP3 in Treg cells promotes antitumor immunity and suppresses tumor development (Cortez et al., 2020; Overacre-Delgoffe and Vignali, 2018; Yang et al., 2020). Conversely, elevated Foxp3 expression in tumor-infiltrating Treg cells suppressed

the proliferation of effector T cells and promoted gastric cancer progression (Yuan et al., 2010). The molecular mechanism that maintains high Foxp3 expression in tumor-infiltrating Treg cells is still unknown.

AMP-activated kinase (AMPK) is an essential energy sensor activated by the AMP/ATP ratio (Herzig and Shaw, 2018). The activation of AMPK signaling has emerged as a controversial regulator of tumor development (Hardie, 2015). One study showed that AMPK could suppress lymphomagenesis by negatively regulating the Warburg effect (Faubert et al., 2013). Conversely, other studies showed that deletion of AMPK was detrimental to the growth of $Kras^{G12D}p53^{f/f}$ tumors (Eichner et al., 2019), and inhibition of AMPK activity by Compound C blocked cell cycle progression and prevented B16F1 melanoma growth (Lee et al., 2019). In addition to its effects on cancer cells, AMPK was shown to increase the antitumor activity of tumor-infiltrating CD8+ T cells by suppressing the transcription of *Pdcd1* (Zhang et al., 2020). The relationship between AMPK and Foxp3 and the role of AMPK in tumor-infiltrating Treg cells remain poorly understood.

We used *in vitro* and *in vivo* experiments to analyze the role of AMPKα1 in the tumor-promoting effects of Treg cells. Mice with Treg-specific AMPKα1 deficiency showed increased antitumor immunity and delayed tumor progression. Conditional deletion of AMPKα1 impaired the immunosuppressive capacity of Treg cells. Furthermore, AMPKα1 deficiency increased the expression of E3 ligase CHIP and promoted the ubiquitination and proteasomal degradation of FOXP3 in Treg cells. Although further studies are necessary, our results indicate that AMPK suppression in Treg cells might be an effective strategy for cancer immunotherapy.

3.3 Results

3.3.1 AMPKα1 is Upregulated in Tumor-Infiltrating Treg Cells but is Dispensable for T cell Development.

AMPK is a heterotrimeric complex kinase consisting of α, β, and γ subunits, the former of which is responsible for the catalytic activity of the enzyme (Steinberg and Carling, 2019). The two

isoforms of AMPKα, AMPKα1, and AMPKα2, are encoded by the *Prkaa1* and *Prkaa2* genes, respectively (Steinberg and Carling, 2019). AMPKα1 is the predominant isoform in T cells, which also express AMPKα2 but at lower levels (Mayer et al., 2008; Tamas et al., 2006). To explore the regulation and function of AMPK signaling in tumor-infiltrating Treg cells, we monitored AMPKα1 expression in Treg cells from tumors and spleens of mice bearing B16F10 melanoma tumors. Flow cytometry revealed that the frequency of Treg cells was higher in the TME than in the spleen (**Figure 11A**) and that the AMPKα1 expression level was higher in Treg cells from tumors than in Treg cells from the spleen (**Figure 11B**).

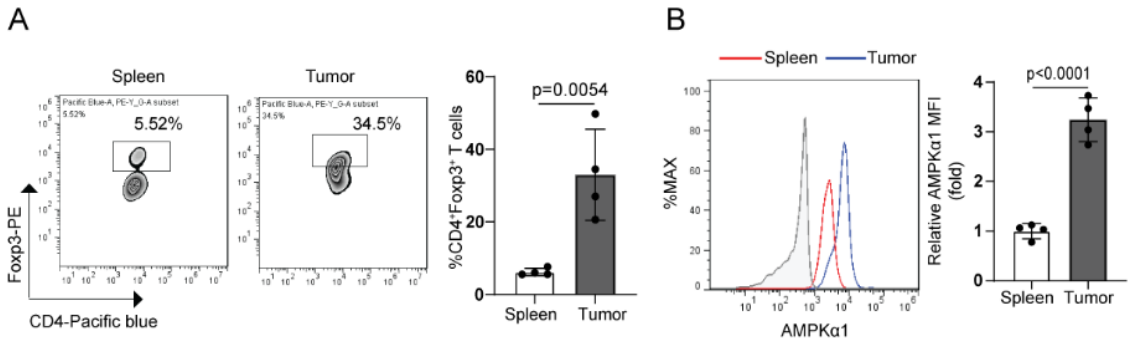

Figure 11 AMPKα1 is upregulated in tumor-infiltrating Tregs.
(A) Representative flow cytometry images and quantification of $CD4^+Foxp3^+$ frequency in mouse spleens and tumors on day 10 after B16F10 melanoma implantation (n = 4 in each group; data are presented as individual values and mean ± SD and analyzed by Student's t test). (B) Representative flow cytometry images and quantification of AMPKα1 mean fluorescence intensity (MFI) in Treg cells from mouse spleens and tumors (n = 4 in each group; data are presented as individual values and mean ± SD and analyzed by Student's t test).

To further examine the role of AMPKα1 in Treg cells, we generated Treg-specific AMPKα1-deficiency mice ($Prkaa1^{fl/fl}Foxp3^{Cre/YFP}$, hereafter referred to as $AMPKα1^{Treg-/-}$) by crossing mice bearing loxp-flanked *Prkaa1* alleles with Foxp3-*Cre/YFP* mice (littermate controls $Prkaa1^{+/+}Foxp3^{Cre/YFP}$ referred to as $AMPKα1^{Treg+/+}$). We then confirmed that the AMPKα1 protein level was deleted in Foxp3-YFP^+ Treg cells but not in $CD4^+$Foxp3-YFP^- Tconv cells (T conventional cells) from the $AMPKα1^{Treg-/-}$ mice (**Figure 12A**). Flow cytometry analysis showed no difference in the frequencies of Treg cells and other T cell phenotypes in the thymus between

the AMPKα1$^{Treg-/-}$ mice and the AMPKα1$^{Treg+/+}$ mice (**Figure 12B-12D**), implying that AMPKα1 plays a dispensable role in the development of Treg cells.

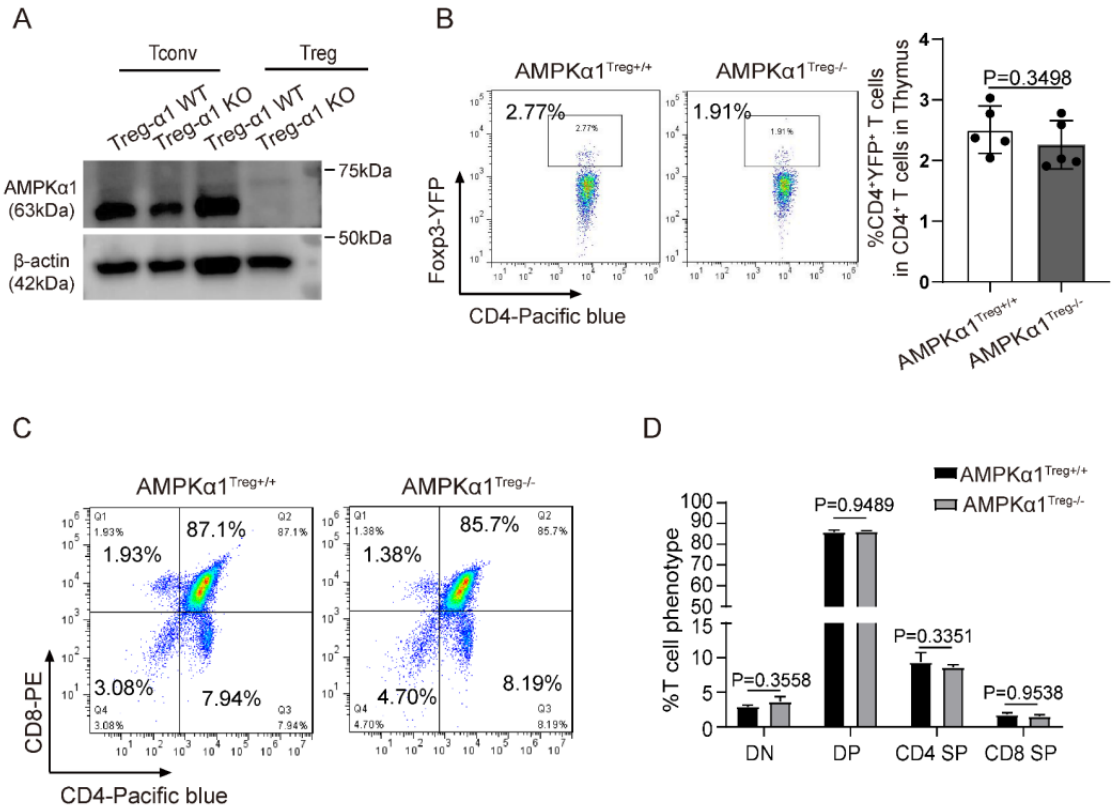

Figure 12 AMPKα1 deficiency has a mild effect on the development of different T cell phenotypes. (A) Immunoblot identification of knockout efficiency in conventional T cells (Tconv) and T regulatory cells (Treg). (B) Representative FACS plot and frequency of CD4$^+$Foxp3-YFP$^+$ Treg cells in thymus of AMPKα1$^{Treg+/+}$ and AMPKα1$^{Treg-/-}$ mice. (n = 5 in each group; data are presented as individual values and mean ± SD and analyzed by Student's *t* test).(C) Representative FACS plot of different T cell phenotypes in thymus of AMPKα1$^{Treg+/+}$ and AMPKα1$^{Treg-/-}$ mice. (D) Frequency of different T cell phenotypes in thymus (n = 5 in each group; data are presented as individual values and mean ± SD and analyzed by Student's *t* test).

3.3.2 AMPK Deletion in Treg Cells Suppresses Tumor Progression.

We challenged AMPKα1$^{Treg-/-}$ mice and AMPKα1$^{Treg+/+}$ mice with B16F10 melanoma cells to explore how AMPKα1 expression in Treg cells affects tumor development. Compared with the AMPKα1$^{Treg+/+}$ mice, the AMPKα1$^{Treg-/-}$ mice showed decreased tumor size (**Figure 13A**). Furthermore, the growth of the melanoma cells was largely attenuated in the AMPKα1$^{Treg-/-}$ mice relative to that in the AMPKα1$^{Treg+/+}$ mice (**Figure 13B**). Moreover, AMPKα1$^{Treg-/-}$ mice had lower tumor weight (**Figure 13C**), less tumor blood vessel formation (**Figure 13D**), and lower

frequencies of Ki-67^{+} proliferating cells in their tumors (**Figure 13E**). Similarly, AMPKα1$^{Treg-/-}$ mice showed decreased tumor sizes and delayed tumor progression when compared with AMPKα1$^{Treg+/+}$ mice after implantation with Lewis lung carcinoma cells (LLCs; **Figure 14A-14C)**. These findings indicate that deficiency of AMPKα1 in Treg cells impairs tumor progression in mice.

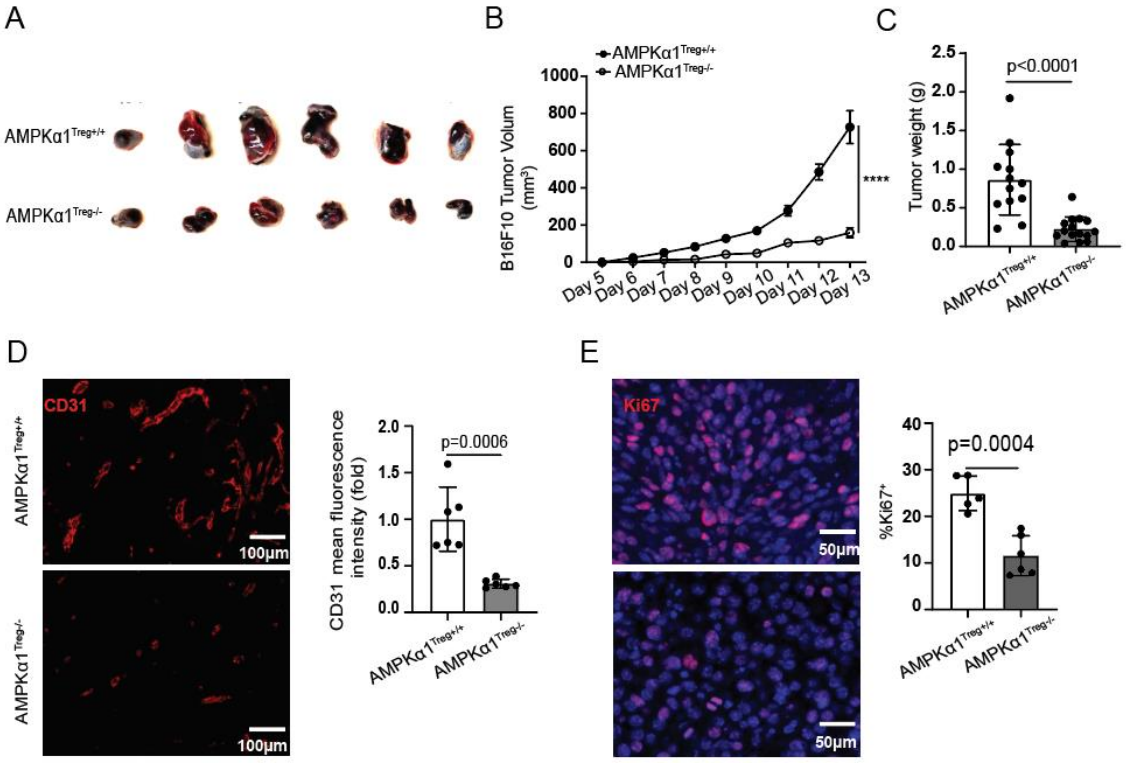

Figure 13 Deficiency of AMPKα1 in Treg prevent tumor development.
(A) Representative images of tumors from AMPKα1$^{Treg+/+}$ and AMPKα1$^{Treg-/-}$ mice on day 13 after implantation with B16F10 cells. (B) Tumor volume in AMPKα1$^{Treg+/+}$ and AMPKα1$^{Treg-/-}$ mice after implantation with B16F10 cells (n = 13 in AMPKα1$^{Treg+/+}$ group and n = 15 in AMPKα1$^{Treg-/-}$ group; data are presented as mean ± SEM and analyzed by two-way ANOVA). (C) Tumor weight in AMPKα1$^{Treg+/+}$ and AMPKα1$^{Treg-/-}$ mice on day-13 after implantation with B16F10 cells (n=13 in AMPKα1$^{Treg+/+}$ group and n = 15 in AMPKα1$^{Treg-/-}$ group; data are presented as individual values and mean ± SD and analyzed by Student's t test). (D) Representative images of immunofluorescence and quantification of CD31 intensity in tumors from AMPKα1$^{Treg+/+}$ and AMPKα1$^{Treg-/-}$ mice on day 10 after implantation with B16F10 cells (n = 6 in each group; data are presented as individual values and mean ± SD and analyzed by Student's t test). Three or more fields per tumor were quantified. Scale bar: 100 μm.(E) Representative images of immunofluorescence and percentage of Ki67^{+} cells in tumors from AMPKα1$^{Treg+/+}$ and AMPKα1$^{Treg-/-}$ mice on day 10 after implantation with B16F10 cells (n = 5 in AMPKα1$^{Treg+/+}$ group and n = 6 in AMPKα1$^{Treg-/-}$ group; data are presented as individual values and mean ± SD and analyzed by Student's t test). Three or more fields per tumor were quantified. Scale bar: 50 μm.

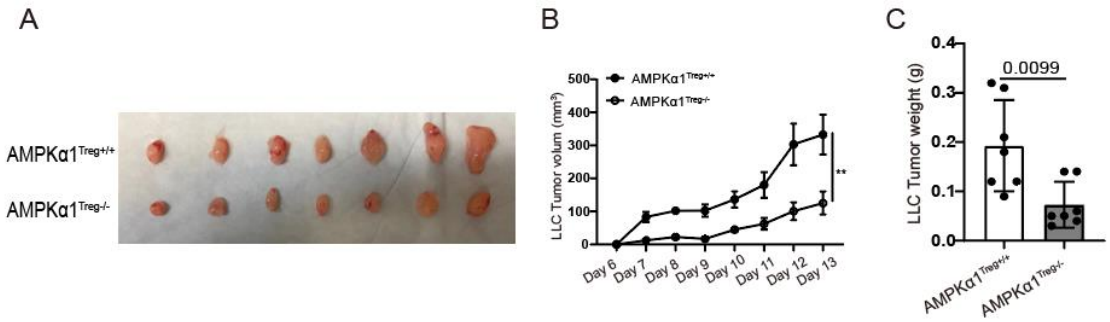

Figure 14 Mice with Treg-specific AMPKα1 deletion showed delayed tumor progression.
(A) Representative images of tumors from AMPKα1$^{Treg+/+}$ and AMPKα1$^{Treg-/-}$ mice on day 13 after LLC tumor inoculation. (B) Tumor volumes of AMPKα1$^{Treg+/+}$ and AMPKα1$^{Treg-/-}$ mice after LLC inoculation (n = 7 in each group; data are presented as mean ± SEM and analyzed by two-way ANOVA). (C) Tumor weights from AMPKα1$^{Treg+/+}$ and AMPKα1$^{Treg-/-}$ mice on day 13 after LLC tumor inoculation (n = 7 in each group; data are presented as individual values and mean ± SD and analyzed by Student's *t* test).

3.3.3 AMPKα1 Deficiency in Treg Cells Promotes Antitumor T Cell Responses.

Histological analysis revealed that tumor tissues from AMPKα1$^{Treg-/-}$ mice had more inflammatory cells infiltration than those from AMPKα1$^{Treg+/+}$ mice (**Figure 15A**). Further analysis showed the tumors from the AMPKα1$^{Treg-/-}$ mice had more CD3$^+$, CD4$^+$ and CD8$^+$ T cell infiltration than the tumors from the AMPKα1$^{Treg+/+}$ mice (**Figure 15B and 15C**); however, the frequency of tumor-infiltrating B cells was comparable between the two mouse strains (**Figure 15D**). These data indicate an enhanced antitumor immunity in the AMPKα1$^{Treg-/-}$ mice.

Next, we performed flow cytometry analysis of the tumors to further explore the antitumor effects of AMPKα1 deletion in Treg cells (**Figure 16A**). Compared with the tumors from the AMPKα1$^{Treg+/+}$ mice, the tumors from the AMPKα1$^{Treg-/-}$ mice had increased numbers of CD45$^+$ leukocytes, CD3$^+$ T cells, CD4$^+$ T cells, and CD8$^+$ T cells (**Figure 16B**). Meanwhile, the proportions of CD45$^+$ cells in tumors and the frequency of CD3$^+$ and CD8$^+$ T cells in CD45$^+$ cells significantly increased in tumor tissues from AMPKα1$^{Treg-/-}$ mice (**Figure 16C**). The expression of IFN-γ, an important cytotoxic cytokine, by tumor-infiltrating CD8$^+$ T cells was also higher in AMPKα1$^{Treg-/-}$ mice than that in AMPKα1$^{Treg+/+}$ mice (**Figure 16D and 16E**). However, the frequency and numbers of tumor-infiltrating CD45$^+$IFNγ$^+$ and CD4$^+$IFNγ$^+$ T cells were comparable between AMPKα1$^{Treg+/+}$ mice and AMPKα1$^{Treg-/-}$ mice (**Figure 16F and 16G**). These findings

suggest that the absence of AMPKα1 in Treg cells promotes $CD8^+$ T cells mediated antitumor immunity.

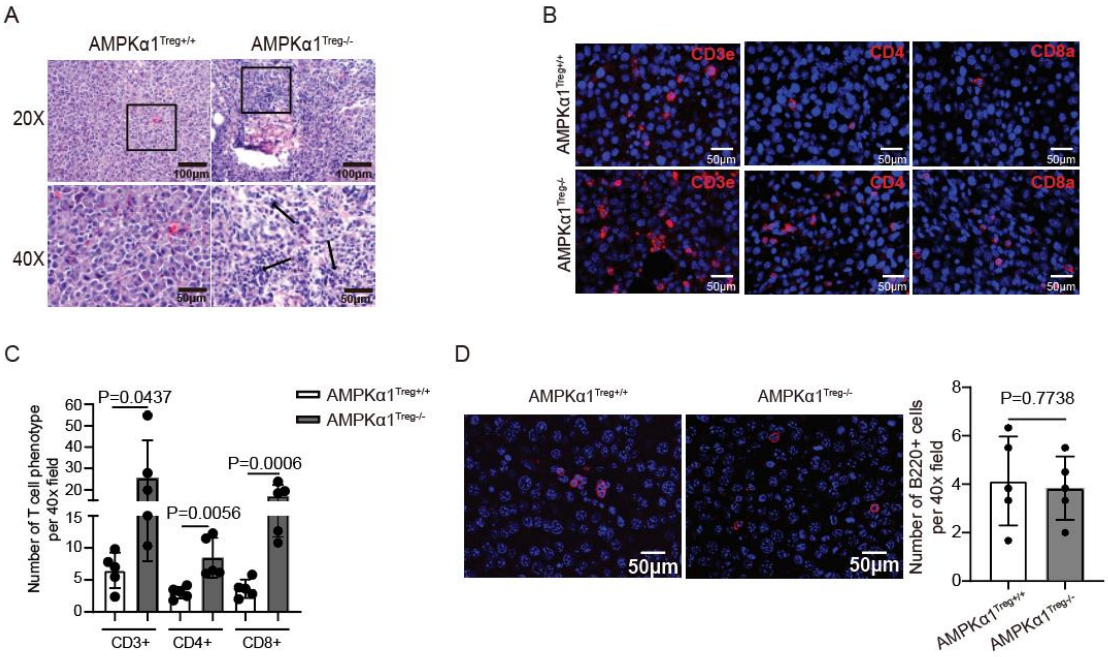

Figure 15 Deficiency of AMPKα1 in Treg cells had mild effects on B cell infiltration in tumors.
(A) Representative H&E images of day-10 B16F10 induced tumors from $AMPK\alpha1^{Treg+/+}$ and $AMPK\alpha1^{Treg-/-}$ mice (Black arrows indicate inflammatory cell infiltrations). Scar bar, 20X, 100μm, 40X, 50μm. (B) Representative immunofluorescence staining images of CD3e, CD4, and CD8a in tumor sections from $AMPK\alpha1^{Treg+/+}$ and $AMPK\alpha1^{Treg-/-}$ mice. Scale bar: 50 μm.(C) Cell numbers of $CD3^+$, $CD4^+$, and $CD8^+$ T cells per 40× field in tumor sections from $AMPK\alpha1^{Treg+/+}$ and $AMPK\alpha1^{Treg-/-}$ mice (n = 5 in each group; data are presented as individual values and mean ± SD and analyzed by Student's t test). Five or more fields per tumor were quantified. (D) Representative B220 immunofluorescent image and number of $B220^+$ B cells in tumor sections per 40× field from day-10 B16F10 tumors of $AMPK\alpha1^{Treg+/+}$ and $AMPK\alpha1^{Treg-/-}$ mice (n = 5 in each group; data are presented as individual values and mean ± SD and analyzed by Student's *t* test). Scar bar, 50 μm.

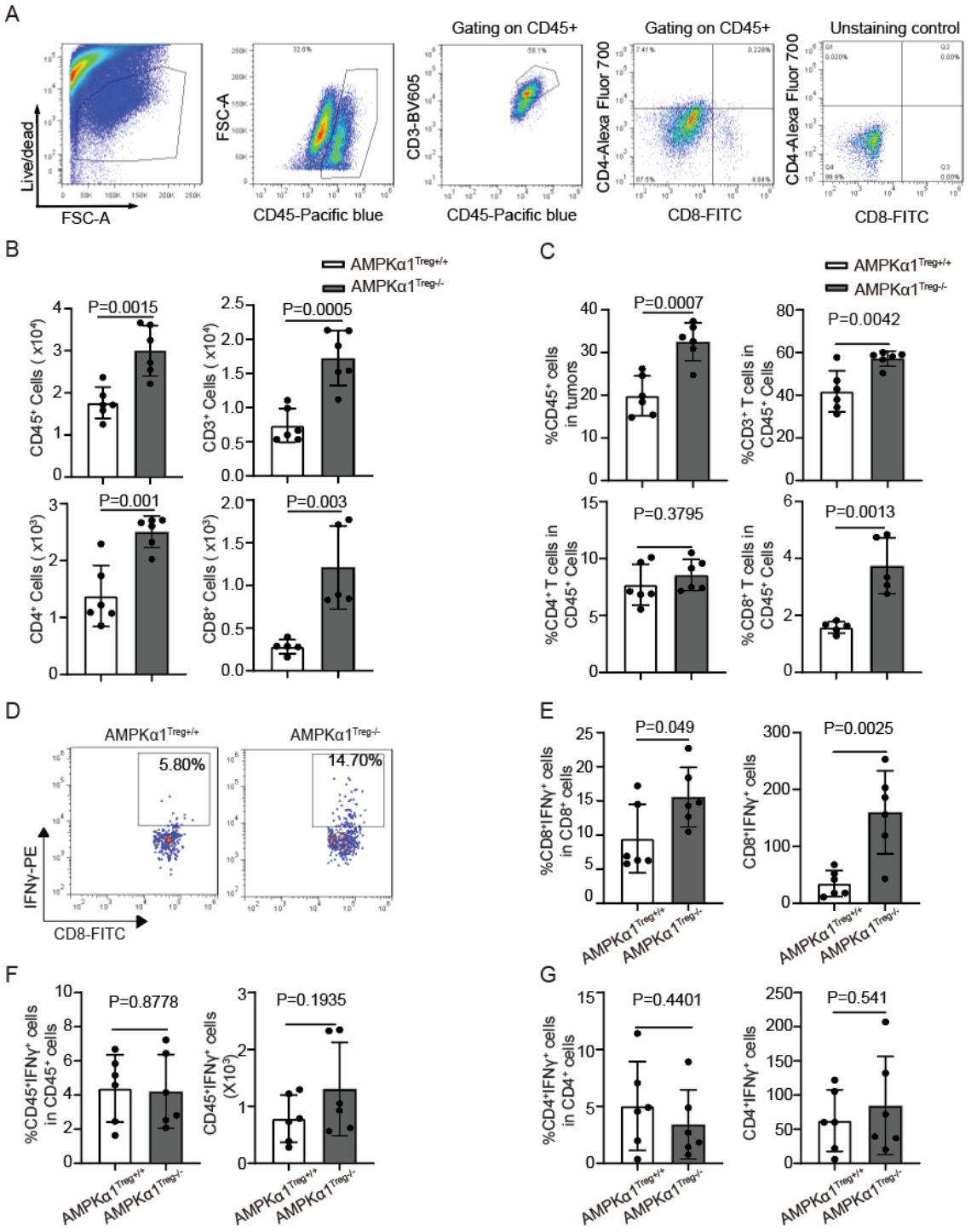

Figure 16 Treg-specific AMPKα1 deficient mice show increased antitumor immunity.
(A) Gating strategy of CD45⁺ lymphocytes, CD3⁺, CD4⁺, and CD8⁺ T cells in tumor tissues.(B) Cell numbers of CD45⁺ (n = 6), CD3⁺ (n = 6), CD4⁺ (n = 6), and CD8⁺ (n = 5) T cells per 1 × 10^6 tumor cells from day-13 tumor tissues of AMPKα1$^{Treg+/+}$ and AMPKα1$^{Treg-/-}$ mice measured by flow cytometry (data are presented as individual values and mean ± SD and analyzed by Student's t test). (C) Proportions of CD45⁺ (n = 6), CD3⁺ (n = 6), CD4⁺ (n = 6), and CD8⁺ (n = 5) T cells in day-13 tumor tissues of AMPKα1$^{Treg+/+}$ and AMPKα1$^{Treg-/-}$ mice analyzed by flow cytometry (data are presented as individual values and mean ± SD and analyzed by Student's t test). (D) Representative FACS images of IFN-γ–producing CD8⁺ cells from day-13 tumor tissues of AMPKα1$^{Treg+/+}$ and AMPKα1$^{Treg-/-}$ mice. (E) Frequency and numbers of IFN-γ–producing CD8⁺

cells per 1×10^6 tumor cells from tumor tissues of AMPKα1$^{Treg+/+}$ and AMPKα1$^{Treg-/-}$ mice (n = 6 in each group; data are presented as individual values and mean ± SD and analyzed by Student's t test). (F) Frequency and numbers of IFN- γ –producing CD45$^+$ cells per 1×10^6 tumor cells from tumor tissues of AMPKα1$^{Treg+/+}$ and AMPKα1$^{Treg-/-}$ mice (n = 6 in each group; data are presented as individual values and mean ± SD and analyzed by Student's t test). (G) Frequency and numbers of IFN- γ –producing CD4$^+$ cells per 1×10^6 tumor cells from tumor tissues of AMPKα1$^{Treg+/+}$ and AMPKα1$^{Treg-/-}$ mice (n = 6 in each group; data are presented as individual values and mean ± SD and analyzed by Student's t test).

3.3.4 AMPKα1-Deficient Treg Cells Present a 'Fragile' Phenotype in TME.

Our observations of increased antitumor immunity in AMPKα1$^{Treg-/-}$ mice led us to assess possible changes in the Treg populations. Intra-tumoral Treg cells can present a 'fragile' phenotype, marked by aberrant IFN-γ expression but loss of Treg signature genes, was shown to promote more efficient antitumor immunity (Lim et al., 2021; Overacre-Delgoffe et al., 2017). Next, we tested whether AMPK could influence the formation of 'fragile' Treg cells in TME. Several cell surface markers are related to the immunosuppressive function of Treg cells and have been exploited as cancer therapeutic targets (Ohue and Nishikawa, 2019). Analysis these cell surface markers revealed decreases in CD25, CTLA-4, and PD1 expression in AMPKα1-deficient Treg cells in TME compared with that in wild-type (WT) Treg cells **(Figure 17A-17C)**. In addition, both the frequency and mean fluorescence intensities (MFIs) of IL-10, an inhibitory cytokine expressed by Treg cells, were decreased in tumor infiltrating CD4$^+$Foxp3-YFP$^+$ Treg cells after AMPKα1 deletion **(Figure 17D-17E)**. These data indicate that the functional integrity of Treg cells was compromised after AMPKα1 deficiency in TME. Analysis the expression of IFN-γ in tumor infiltrating Treg cells, we found an increased frequency of IFN-γ$^+$ Treg cells in tumors from AMPKα1$^{Treg-/-}$ mice compared with controls **(Figure 17F)**. Meanwhile, the expression of IFN-γ in tumor-Treg cells also showed increased in AMPKα1$^{Treg-/-}$ mice **(Figure 17G)**. Overall, these data point towards an essential role of AMPKα1 in maintaining the function profile of Treg cells in TME and preventing the induction of fragile Treg cells.

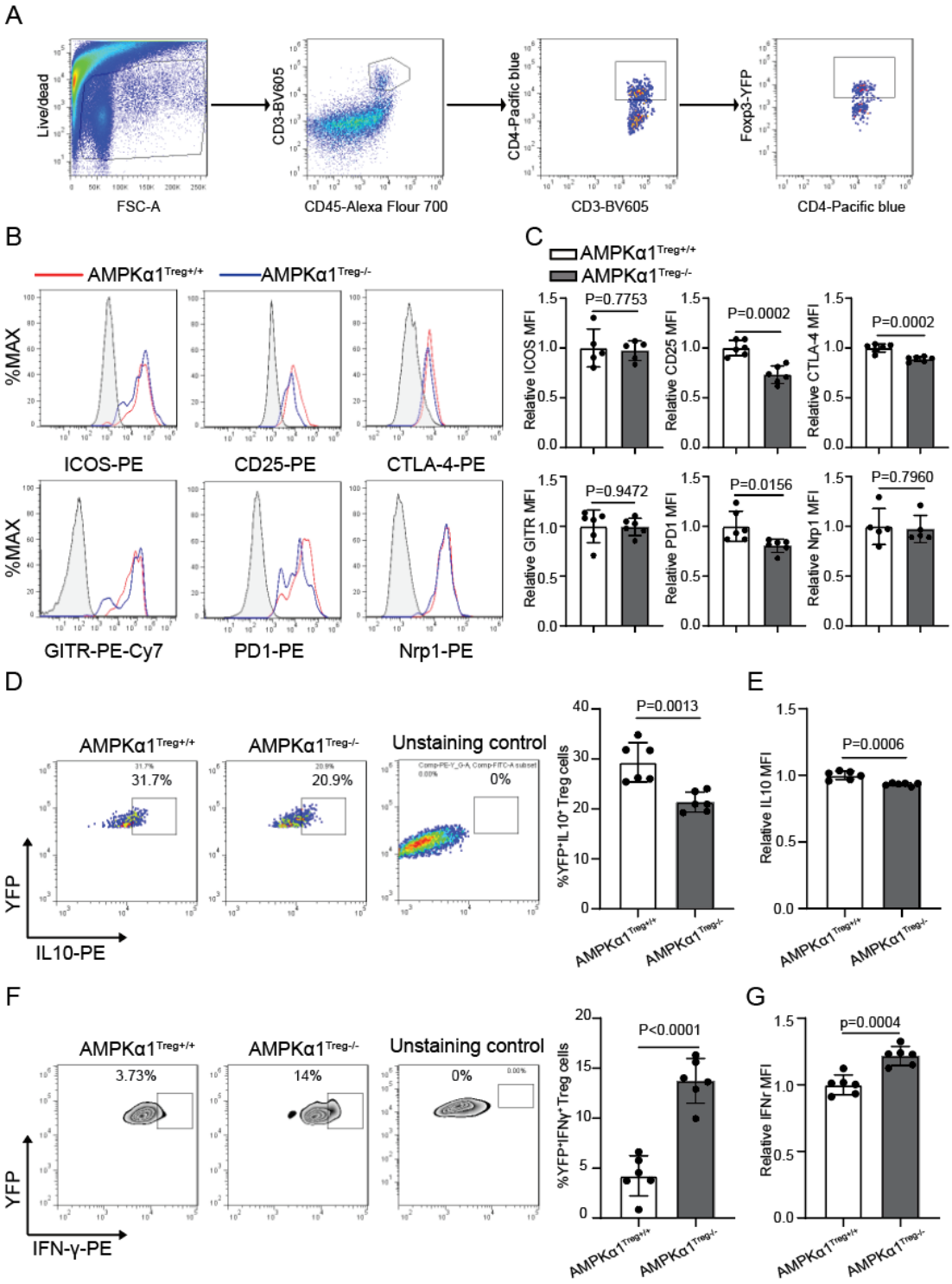

Figure 17 AMPKα1-deficient Treg cells present a 'fragile' phenotype in TME.
(A) Gating strategy of CD4⁺YFP⁺ Treg cells from tumor tissues. (B) Representative FACS images of ICOS, CD25, CTLA-4, GITR, PD1 and Nrp1 expression on CD4⁺Foxp3-YFP⁺ Treg cells from day 13 tumor tissues of AMPKα1$^{Treg+/+}$ and AMPKα1$^{Treg-/-}$ mice. (C) Relative MFI of cell surface ICOS (n = 5), CD25 (n = 6), CTLA-4 (n = 6), GITR (n = 6), PD1(n = 6) and Nrp1 (n = 5) on CD4⁺Foxp3-YFP⁺ Treg cells from day 13 tumor tissues of AMPKα1$^{Treg+/+}$and AMPKα1$^{Treg-/-}$mice. (Data are presented as individual values and mean ± SD

and analyzed by Student's t test). (D) Representative FACS images and frequency of $YFP^+IL\text{-}10^+$ Treg cells in $CD4^+Foxp3\text{-}YFP^+$ Treg cells from day 13 tumor tissues of $AMPK\alpha1^{Treg+/+}$and $AMPK\alpha1^{Treg-/-}$mice. (n = 6 in each group, data are presented as individual values and mean ± SD and analyzed by Student's t test). (E) Relative MFI of IL-10 in $CD4^+Foxp3\text{-}YFP^+$ Treg cells from day 13 tumor tissues of $AMPK\alpha1^{Treg+/+}$and $AMPK\alpha1^{Treg-/-}$mice. (n = 6 in each group, data are presented as individual values and mean ± SD). (F) Representative FACS images and frequency of $YFP^+IFN\text{-}\gamma^+$ Treg cells in $CD4^+Foxp3\text{-}YFP^+$ Treg cells from day 13 tumor tissues of $AMPK\alpha1^{Treg+/+}$and $AMPK\alpha1^{Treg-/-}$mice. (n = 6 in each group, data are presented as individual values and mean ± SD and analyzed by Student's t test). (G) Relative MFI of IFN-γ in $CD4^+Foxp3\text{-}YFP^+$ Treg cells from day 13 tumor tissues of $AMPK\alpha1^{Treg+/+}$and $AMPK\alpha1^{Treg-/-}$mice. (n = 6 in each group, data are presented as individual values and mean ± SD and analyzed by Student's t test).

3.3.5 AMPKα1 Maintains FOXP3 Expression in Treg Cells.

As a key transcriptional factor, *Foxp3* controls the development and functional integrity of Treg cells(Fontenot et al., 2003). Unstable FOXP3 expression promotes IFN-γ transcription in Treg cells (Yang et al., 2020). Immunofluorescence staining of FOXP3 showed similar numbers of $Foxp3^+$ cells in tumor sections from $AMPK\alpha1^{Treg+/+}$ and $AMPK\alpha1^{Treg-/-}$ mice (**Figure 18A**). Nonetheless, the FOXP3 fluorescence intensity in $Foxp3^+$ cells from the tumors of $AMPK\alpha1^{Treg-/-}$ mice was lower than that from the tumors of $AMPK\alpha1^{Treg+/+}$ mice (**Figure 18A and 18B**), indicating that AMPKα1 deficiency decreases FOXP3 protein level in in Treg cells during tumor development.

To establish the role AMPK in Foxp3 regulation in Treg cells, we analyze the expression of yellow fluorescent protein (YFP), a reporter of transcriptional induction of Foxp3. We found that deficiency of AMPKα1 has a mild effect on the frequency of $CD4^+YFP^+$ cells and the MFIs of YFP, but significantly decreased FOXP3 expression in tumor infiltrated $CD4^+YFP^+$ Treg cells (**Figure 18C and 18D**). These data suggest that deletion of AMPKα1 does not affect the induction of the *Foxp3* gene, but it compromises the expression of the FOXP3 protein after tumor implantation.

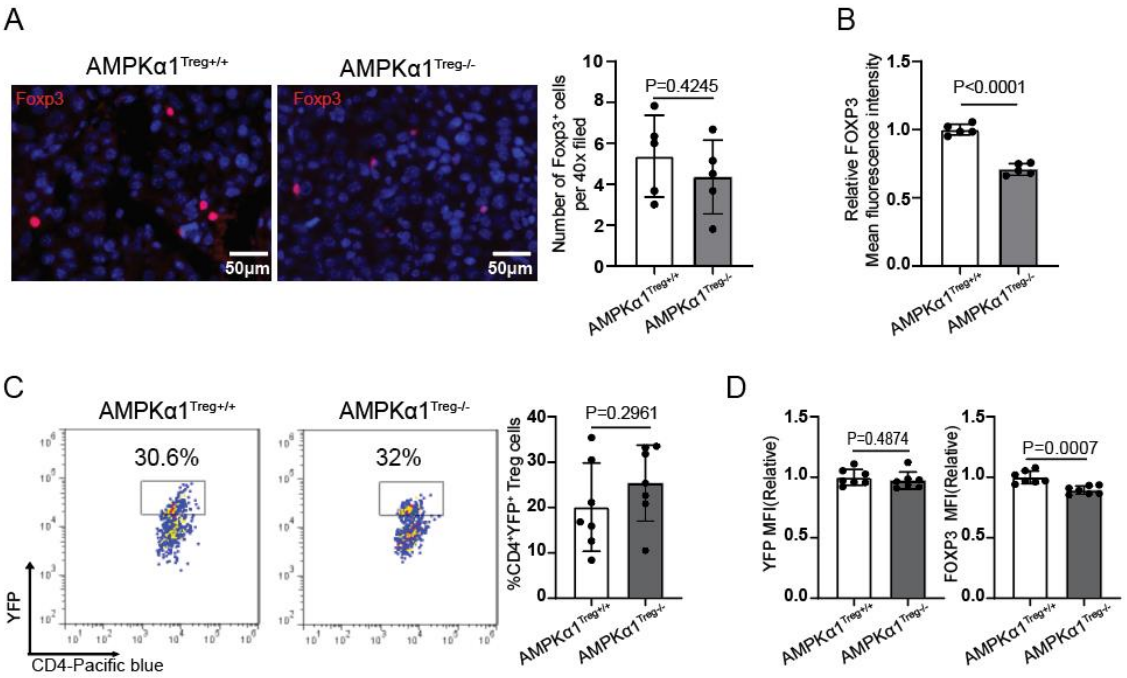

Figure 18 AMPKα1 deficiency impairs FOXP3 expression in tumor-infiltrated Treg cells.
(A) Representative immunofluorescence images of FOXP3 and quantification of Foxp3$^+$ cell numbers on tumor sections from AMPKα1$^{Treg+/+}$ and AMPKα1$^{Treg-/-}$ mice (n = 5 in each group; data are presented as individual values and mean ± SD and analyzed by Student's t test). Five or more fields per tumor were quantified. Scale bar: 50 μm. (B) Quantification of FOXP3 fluorescence intensity in Foxp3$^+$ cells. (n = 5 in each group; data are presented as individual values and mean ± SD and analyzed by Student's t test). Five or more field per tumor were quantified. (C) Representative FACS images and percentage of CD4$^+$YFP$^+$ Treg cells in day-13 tumor tissues of AMPKα1$^{Treg+/+}$ and AMPKα1$^{Treg-/-}$ mice (n = 7 in each group; data are presented as individual values and mean ± SD and analyzed by Student's t test). (D) Relative MFI of YFP and FOXP3 in tumor infiltrated CD4$^+$YFP$^+$ Treg cells of AMPKα1$^{Treg+/+}$ and AMPKα1$^{Treg-/-}$ mice (n = 7 in each group; data are presented as individual values and mean ± SD and analyzed by Student's t test).

To test whether this effect also happened in steady state, we used both GFP antibody (YFP signal can be detected by GFP antibody) and Foxp3 antibody to analyze the CD4$^+$YFP$^+$ and CD4$^+$Foxp3$^+$ Treg frequency respectively in the spleen of AMPKα1$^{Treg+/+}$ and AMPKα1$^{Treg-/-}$ mice without tumor implantation. Both the frequency of CD4$^+$YFP$^+$ Treg cells and expression of YFP were comparable between both strains, while the frequency of CD4$^+$Foxp3$^+$ Treg cells and expression of Foxp3 were significant decreased in AMPKα1$^{Treg-/-}$ mice **(Figure 19A-19D)**. Therefore, both in TME and stable state, AMPKα1 is required for Foxp3 protein level but not affect the survival/proportion of Treg cells.

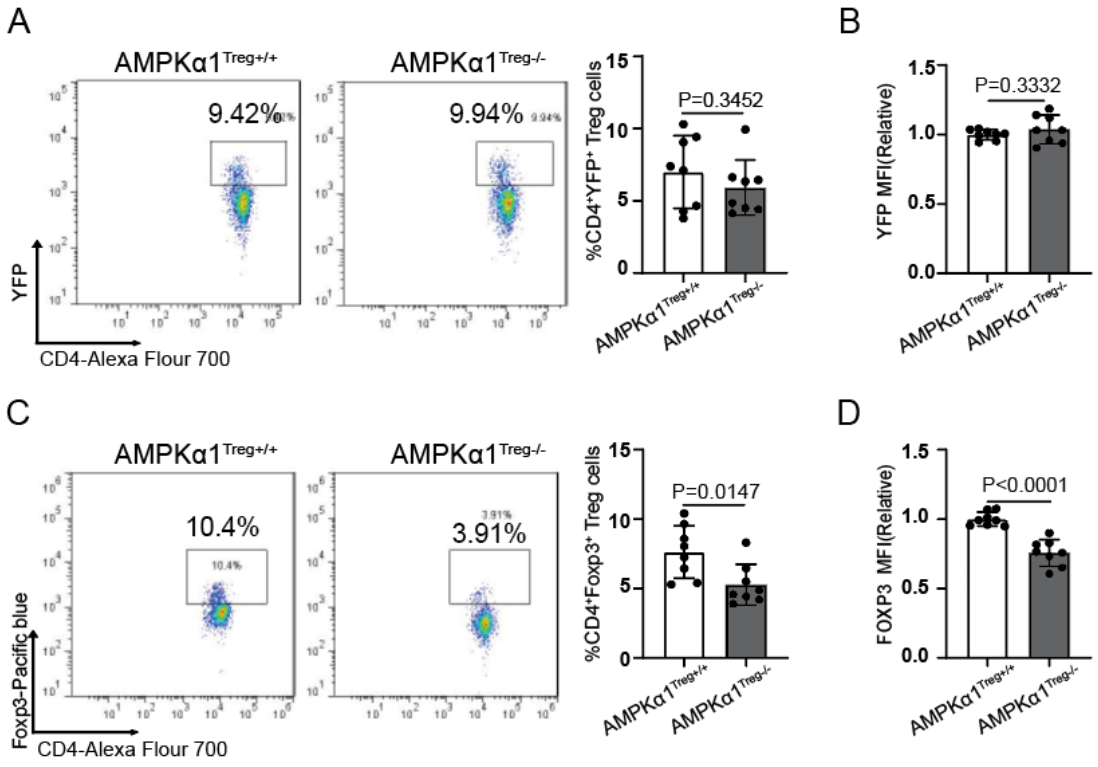

Figure 19 AMPKα1 is required Foxp3 protein expression in basal condition.
(A) Representative FACS images and frequency of CD4$^+$YFP$^+$ Treg cells in the spleens of AMPKα1$^{Treg+/+}$ and AMPKα1$^{Treg-/-}$ mice under steady state (n=8 in each group; data are presented as individual values and mean ± SD and analyzed by Student's t test). (B) Relative MFI of YFP in CD4$^+$YFP$^+$ Treg cells from AMPKα1$^{Treg+/+}$ and AMPKα1$^{Treg-/-}$ mice under steady state (n =8 in each group; data are presented as individual values and mean ± SD and analyzed by Student's t test). (C) Representative FACS images and frequency of CD4$^+$Foxp3$^+$ Treg cells in the spleens of AMPKα1$^{Treg+/+}$ and AMPKα1$^{Treg-/-}$ mice under steady state (n = 8 in each group; data are presented as individual values and mean ± SD and analyzed by Student's t test). (D) Relative MFI of FOXP3 in Treg cells from AMPKα1$^{Treg+/+}$ and AMPKα1$^{Treg-/-}$ mice under steady state (n = 8 in each group; data are presented as individual values and mean ± SD and analyzed by Student's t test).

3.3.6 Deficiency of AMPKα1 Impairs FOXP3 Protein Stability.

T cell receptor (TCR) signaling is required for Foxp3 expression, either through induction of *Foxp3* transcription or through post-translational modification (Ono, 2020). Activation of TCR signaling by CD3/CD28 Dynabeads promoted AMPKα1 expression in AMPKα1-sufficient (WT) Treg cells but not in AMPKα1-deficient (KO) Treg cells (**Figure 20A and 20B**). Although FOXP3 expression was also increased in both types of Treg cells after CD3/CD28 treatment, the folds of increase in the AMPKα1-deficient (KO) Treg cells were smaller than that those of the AMPKα1-sufficient (WT) Treg cells (**Figure 20C and 20D**). These data suggest that AMPKα1 is partially required for TCR-induced FOXP3 upregulation.

To further investigate the intracellular mechanism by how AMPKα1 regulates Foxp3 expression in Treg cells, we isolated Treg cells from AMPKα1$^{Treg+/+}$ and AMPKα1$^{Treg-/-}$ mice and compared the protein and mRNA levels of Foxp3. We found that the FOXP3 protein level was much lower in the AMPKα1$^{-/-}$ Treg cells than those in the AMPKα1$^{+/+}$ Treg cells (**Figure 20E**), whereas the *Foxp3* mRNA level was similar (**Figure 20F**).

Next, we asked whether AMPK regulates FOXP3 protein stability. We transfected human embryonic kidney (HEK) 293 cells with Flag-Foxp3 plasmid together with AMPKα1 plasmid or AMPKα1 siRNA (**Figure 20G and 20H**). We found that AMPKα1 overexpression prevented cycloheximide (CHX)-induced reduction of FOXP3 levels (**Figure 20G**), whereas AMPKα1 silencing decreased the protein stability of FOXP3 (**Figure 20H**). These data suggest that AMPKα1 stabilizes the FOXP3 protein through post-translational modification.

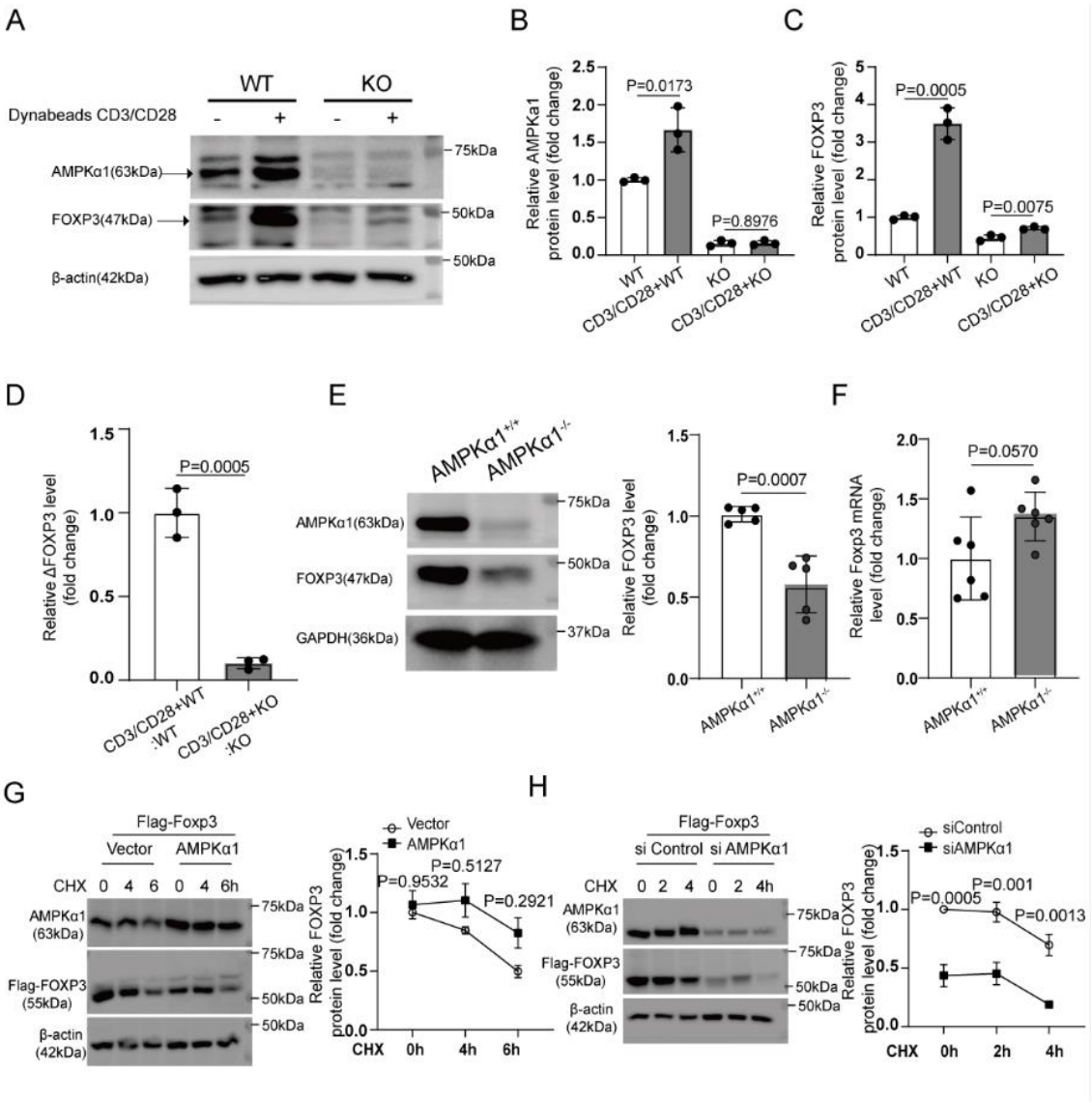

Figure 20 AMPKα1 maintains the protein stability of FOXP3.

(A) Isolated primary Treg cells ($CD4^+YFP^+$) from $AMPK\alpha1^{Treg+/+}$ (WT) and $AMPK\alpha1^{Treg-/-}$ (KO)mice were treated with Dynabeads CD3/CD28 beads at 1:1 ratio for 24 h. The expression of AMPKα1 and FOXP3 were detected by western blot. (B) Quantification of relative AMPKα1 expression in Treg cells from $AMPK\alpha1^{Treg+/+}$ (WT) and $AMPK\alpha1^{Treg-/-}$ (KO) mice stimulated with or without Dynabeads CD3/CD28 (n = 3 in each group; data are presented as individual values and mean ± SD and analyzed by Student's t test). (C) Quantification of relative FOXP3 expression in Treg cells from $AMPK\alpha1^{Treg+/+}$ (WT) and $AMPK\alpha1^{Treg-/-}$ (KO) mice stimulated with or without Dynabeads CD3/CD28 (n = 3 in each group; data are presented as individual values and mean ± SD and analyzed by Student's t test). (D) Quantification of the increased FOXP3 level (ΔFoxp3) after CD3/CD28 treatment between Treg cells from $AMPK\alpha1^{Treg+/+}$ (WT) and $AMPK\alpha1^{Treg-/-}$ (KO)mice (n = 3 in each group; data are presented as individual values and mean ± SD and analyzed by Student's t test). (E) Representative western blot and quantification of FOXP3 protein levels in $AMPK\alpha1^{+/+}$ and $AMPK\alpha1^{-/-}$ Tregs (n = 5 in each group; data are presented as individual values and mean ± SD and analyzed by Student's t test). (F) Quantification of relative *Foxp3* mRNA levels in in $AMPK\alpha1^{+/+}$ and $AMPK\alpha1^{-/-}$ Tregs (n = 6 in each group; data are presented as individual values and mean ± SD and analyzed by Student's t test). (G) Western blot and quantitative analysis of relative FOXP3 protein levels in HEK293T cells treated with cycloheximide (CHX) in combination with control vector or AMPKα1 plasmid (n = 3 in each group/time point; data are presented as mean ± SEM and analyzed by two-way ANOVA). (H) Western blot and quantitative analysis of relative FOXP3 protein levels in HEK293T cells treated with CHX

in combination with siControl or siAMPKα1 (n = 3 in each group/time point; data are presented as mean ± SEM and analyzed by two-way ANOVA).

3.3.7 Deficiency of AMPKα1 Promotes FOXP3 Degradation through E3 Ligase CHIP.

The stability of FOXP3 is tightly regulated by proteasomal degradation (Barbi et al., 2015). We therefore asked whether the reduced protein level of FOXP3 in AMPKα1-deficient Treg cells could be recovered by blocking proteasomal degradation. As shown in **Figure 21A**, treatment with the proteasome inhibitor MG132 normalized Foxp3 levels in Treg cells from AMPKα1$^{Treg-/-}$ and AMPKα1$^{Treg+/+}$ mice. Since post-translational ubiquitination of FOXP3 affects FOXP3 stability and Treg function (Barbi et al., 2015), we determined whether AMPKα1 regulates FOXP3 ubiquitination. To this end, flag-Foxp3 plasmid were transfected into HEK 293T cells after being transfected with either control siRNA or AMPKα1 siRNA. We then treated the cells with MG132 and performed flag-Foxp3 pull-down and immunoblot to assess ubiquitin species. We found that ubiquitination of FOXP3 was increased when AMPKα1 was knocked down (**Figure 21B**). These results imply that deficiency of AMPKα1 promotes Foxp3 degradation through polyubiquitination-mediated proteasomal degradation, which results in a decrease of Foxp3 levels in Treg cells.

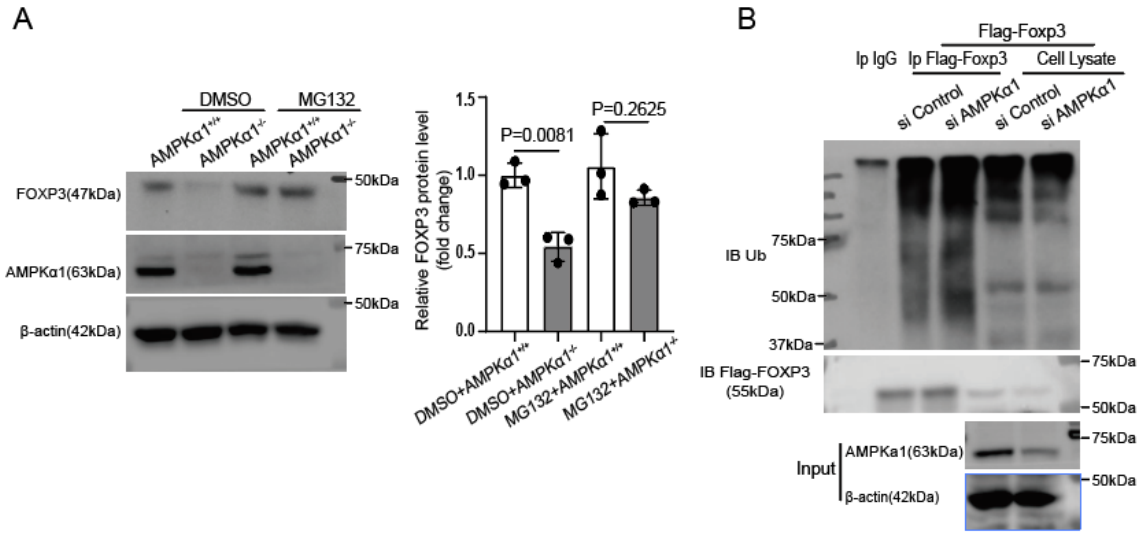

Figure 21 Deficiency of AMPKα1 promotes FOXP3 ubiquitination and proteasome degradation.
(A) Western blot and quantitative analysis of FOXP3 in AMPKα1-suficient (AMPKα1$^{+/+}$) and AMPKα1-deficienct (AMPKα1$^{-/-}$) Treg cells (CD4^{+}YFP^{+}) in the presence or absence of proteasome inhibitor MG132 (n = 3 in each group; data are presented as individual values and mean ± SD and analyzed by Student's t test). (B) Effect of AMPKα1 knockdown on FOXP3 ubiquitination. Flag-Foxp3 together with siControl or siAMPKα1 were transfected into HEK293T cells. The cells were then treated with 5 μM MG132 for 4 h before harvest and lysis. Ubiquitination of FOXP3 proteins was detected by western blot.

Finally, we investigated how AMPK regulates FOXP3 ubiquitination and degradation. The polyubiquitination and degradation of FOXP3 are controlled by E3 ligase CHIP (*STUB1*) and deubiquitinase USP7 (Chen et al., 2013; van Loosdregt et al., 2013). We found that the expression of deubiquitinase USP7 was comparable between WT and AMPKα1-deficient Treg cells (**Figure 22A**); however, both the protein and mRNA level of CHIP were higher in AMPKα1-deficient Treg cells than those in WT Treg cells (**Figure 22B and 22C**). We observed a similar effect in tumor infiltrating Treg cells, which showed increased CHIP expression after AMPKα1 deletion (**Figure 22D and 22E**). Furthermore, CHIP knockdown by shCHIP lentivirus partially recovered the reduced Foxp3 expression in AMPKα1-deficient Treg cells (**Figure 22F and 22G**). These results indicated that CHIP is only partially responsible for the modulation of Foxp3 protein stability by AMPKα1.

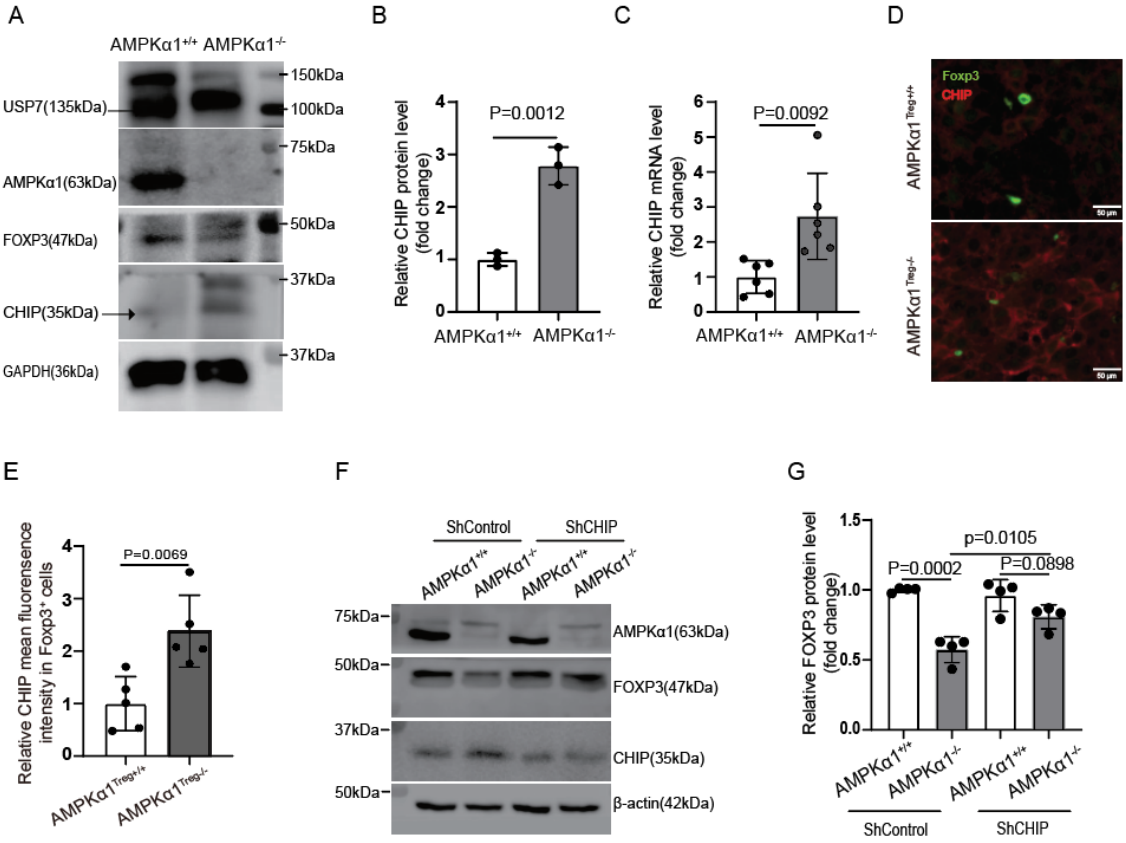

Figure 22 Deficiency of AMPKα1 promotes FOXP3 degradation through E3 ligase CHIP.
(A) Western blot analysis of AMPKα1, USP7, CHIP, and FOXP3 protein levels in sorted AMPKα1-suficient

(AMPKα1$^{+/+}$) and AMPKα1-deficienct (AMPKα1$^{-/-}$) Treg cells (CD4^{+}YFP^{+}). (B) Quantification of relative CHIP expression in sorted AMPKα1-suficient (AMPKα1$^{+/+}$) and AMPKα1-deficienct (AMPKα1$^{-/-}$) Treg cells (CD4^{+}YFP^{+}) (n = 3 in each group; data are presented as individual values and mean ± SD and analyzed by Student's t test). (C) Quantification of relative *CHIP* mRNA levels in sorted AMPKα1-suficient (AMPKα1$^{+/+}$) and AMPKα1-deficienct (AMPKα1$^{-/-}$) Treg cells (CD4^{+}YFP^{+}) (n = 6 in each group; data are presented as individual values and mean ± SD and analyzed by Student's t test). (D) Representative immunofluorescence images of FOXP3 (Green) and CHIP (Red) from day-10 tumors of AMPKα1Treg+/+ and AMPKα1Treg-/- mice. Scar bar, 50 μm. (E) Quantification of relative CHIP mean fluorescence intensity in Foxp3+ cells from day-10 tumors of AMPKα1Treg+/+ and AMPKα1Treg-/- mice (n = 5 in each group; data are presented as individual values and mean ± SD and analyzed by Student's t test). Five or more fields per tumor were quantified. (F) Western blot analysis of FOXP3 protein levels in AMPKα1-suficient (AMPKα1$^{+/+}$) and AMPKα1-deficienct (AMPKα1$^{-/-}$) Treg cells (CD4^{+}YFP^{+}) in the presence of shControl lentivirus or shCHIP lentivirus. (G) Quantification of relative FOXP3 expression in AMPKα1-suficient (AMPKα1$^{+/+}$) and AMPKα1-deficienct (AMPKα1$^{-/-}$) Treg cells (CD4^{+}YFP^{+}) in the presence of shControl or shCHIP lentivirus (n = 4 in each group; data are presented as individual values and mean ± SD and analyzed by Student's t test).

3.4 Discussion

Accumulating evidence suggest that cell-intrinsic molecules that potentiate Foxp3 expression in tumor-infiltrating Treg cells can provide new targets for cancer therapy (Cortez et al., 2020; Hatzioannou et al., 2020; Xiong et al., 2020). In this study, we found that AMPKα1 is highly expressed in tumor-infiltrating Treg cells and is indispensable in these cells for FOXP3 expression and functional integrity of Treg cells in TME. Tumor-exposed Treg-specific AMPKα1 deficiency mice exhibited increased numbers of tumor-infiltrating T cells and more efficient antitumor immunity. AMPKα1 maintained the protein stability of FOXP3 while not affecting the transcription of *Foxp3* in Treg cells. Furthermore, increased E3 ligase CHIP (*STUB1*) expression in AMPKα1-deficient Treg cells promote the ubiquitination and proteasomal degradation of FOXP3, decreasing FOXP3 levels in Treg cells.

AMPK signaling activates both antitumor and protumor immune responses in the TME. Activation of AMPK by its agonist, metformin, promotes the phosphorylation and degradation of PD-L1, which promotes antitumor immunity (Cha et al., 2018). Conversely, inhibition of AMPK activity in tumor-bearing mice, as well as conditional deletion of AMPKα1 in myeloid cells, improves protective T cell immunity by suppressing the immunoregulatory function of myeloid-derived suppressor cells (Trillo-Tinoco et al., 2019). In addition, AMPK inhibition reduces immunosuppressive phenotypes in tumor-associated macrophages and unleashes an antitumor

effector T cell response (Wang et al., 2019; Xu et al., 2018). Thus, the modulation of AMPK has combined effects in different cell populations within the TME. The nutrient sparse, hypoxic, and acidic environment of tumor tissues negatively affects T effector cell function while supporting Treg cell function (Watson et al., 2021; Zappasodi et al., 2021). AMPK is upregulated and activated in the hypoxic and nutrient-limited TME (Gutierrez-Salmeron et al., 2020; Hao et al., 2015); however, the regulation and role of AMPK in tumor-infiltrating Treg cells are largely unknown. Our results show that AMPK upregulation in tumor-infiltrating Treg cells prevents antitumor T cell response and thus promotes tumor progression, suggesting that specific inhibition of AMPK signaling in Treg cells might have therapeutic value for cancer treatment.

Our results support AMPKα1 is required for FOXP3 protein stability and functional integrity of Treg cells in TME. Consistently with our observations, Michalek et al. reported showed that p-AMPK expression was higher in Treg cells than in conventional T cells, and that AMPK activation promoted the generation of Treg cells *in vivo* by regulating fatty acid oxidation (FAO) (Michalek et al., 2011). Consistent with these findings, pioglitazone and metformin were shown to enhance Treg cell expansion and inhibit the progression of plaque instability and autoimmune encephalomyelitis through activation of AMPK signaling (Sun et al., 2016; Tian et al., 2017). By contrast, other studies showed that absence of AMPKα1 and AMPKα2 had only a mild impact on immune homeostasis and the survival of Treg cells (Timilshina et al., 2019; Yang et al., 2017). The discrepancy between our results and the previous results might be due to different animal models, as the previous studies were mainly focused on the autoimmune disease caused by LKB1 and used very young mice in steady state. In addition, recent studies showed that SREBPs or CoREST (REST corepressor 1) deletion in Treg cells could promote antitumor effects while having limited impacts on immune homeostasis in steady state (Lim et al., 2021; Xiong et al., 2020), which matches the heterogeneous results regarding AMPK deletion. The role of AMPK in Treg cells warrants further investigation.

Stabilization of Foxp3 maintains Treg lineage plasticity and hampers the antitumor immune

response (Martin et al., 2010). Uncovering the fundamental regulators that control Foxp3 expression is therefore essential for understanding and exploiting efficient Treg therapies for cancer treatment (Cortez et al., 2020). Loss of *Foxp3* expression transforms Treg cells into so-called ex-Treg cells, which have no immunosuppressive ability but acquire effector Th cell-like phenotypes (Hori, 2014). This has potential clinical relevance, because the accumulation of ex-Treg cells in the TME potentiates immunotherapy (Hatzioannou et al., 2020; Li et al., 2020a). The decreased FOXP3 protein stability and normal *Foxp3* gene induction observed in AMPKα1-deficient Treg cells in our study is not fully in accordance with the phenotype of ex-Treg cells; however, impaired FOXP3 protein stability without impairment of *Foxp3* gene expression was also shown to impair Treg lineage stability and promote ex-Treg transformation in one recent study (Liu et al., 2019). It would therefore be interesting to investigate the effect of AMPKα1 deficiency on ex-Treg transformation by crossing *Prkaa1*$^{fl/fl}$ mice with Treg lineage-tracking *Foxp3*$^{IRES\text{-}YFP\text{-}Cre\text{-}Rosa26\text{-}loxp\text{-}td\text{-}RFP\text{-}loxp}$ mice (Gaddis et al., 2018). Fragility of Treg cells in TME was shown to promote antitumor immunity which potentiates the therapeutic effects of immune checkpoint therapy (Hatzioannou et al., 2020; Lim et al., 2021). However, the intracellular mechanism on how intratumoral Treg cells to prevent fragile IFN-γ-expressing Treg cells in TME remains largely unknown. Our findings demonstrate an essential role of AMPK in the prevention of induction of fragile Treg cells during tumor development.

FOXP3 ubiquitination and Treg function are tightly regulated by the E3 ubiquitin ligase CHIP (*STUB1*) (Chen et al., 2013). We found that AMPKα1 deficiency upregulated CHIP expression in Treg cells *in vivo* and *in vitro*; however, the increased CHIP expression in tumors of AMPKα1$^{Treg\text{-}/\text{-}}$ mice was not confined to Foxp3^{+} Treg cells but also appeared in non-Treg cells. A previous study showed that *CHIP* transcription and expression were tightly correlated with inflammatory cytokines (Chen et al., 2013). Therefore, we hypothesize that the increased CHIP expression in non-Treg cells in our experiments was due to the strong inflammatory conditions in the tumors of the AMPKα1$^{Treg\text{-}/\text{-}}$ mice. In addition to inflammatory cytokines, *CHIP* transcription is linked to

different stresses such as heat shock and oxidative damage (Chen et al., 2013; Paul and Ghosh, 2014; Stankowski et al., 2011). Because of the crucial role of AMPK in oxidative stress regulation, the upregulation of *CHIP* in AMPKα1-deficient Treg cells might be due to increased oxidative stress (Ren et al., 2020). Some post-translational modifications were also reported to regulate the expression or activity of CHIP (Paul and Ghosh, 2014; Zemanovic et al., 2018). Furthermore, one previous study showed a direct association between CHIP and AMPK levels in cardiomyocytes (Schisler et al., 2013), suggesting that another possible mechanism of CHIP regulation is direct phosphorylation of CHIP by AMPK. Although the E3 ligase function of CHIP is well known, the mechanism by which CHIP itself is regulated is much less clear. Further experiments are needed to determine how AMPK regulates CHIP in Treg cells.

In conclusion, AMPKα1 is a critical mediator controlling FOXP3 stability and the functional integrity of Treg cells in TME. Further studies are warranted to investigate whether therapeutic inhibition of AMPK activity in Treg cells bolsters antitumor immunity.

3.5 Limitation of Study

In this study, we showed that AMPKα1 promotes tumor development through elevation the protein stability of Foxp3 in Treg cells. Mechanismly, AMPKα1 downregulates CHIP, a well-known E3 ligase of Foxp3, which prevents Foxp3 ubiquitination and degradation. However, this specific mechanism on how AMPK regulates CHIP expression in Treg cells still lack exploitation. It is meaningful to further investigate how AMPK regulates CHIP expression in Treg cells. In addition, the exploitation of AMPK role in Treg cells in clinical value need to be further studied

3.6 Acknowledgments

This study was supported by the National Institutes of Health grants (HL079584, HL080499, HL089920, HL110488, HL128014, HL132500, HL137371, HL153333 and HL142287), National Cancer Institute (CA213022), National Institute on Aging (AG047776) (to M.-H. Z.) and HL140954 (P. S.)). Dr. Zou is a Georgia Research Alliance Eminent Scholar in Molecular Medicine.

3.7 Author Contributions

J.A., P.S., and M.-H.Z. designed the experiments. J.A., C.Y., J.L., and S.Y. carried out all the experiments. J.A. and P.S. wrote the manuscript and prepared figures and tables. Z.L. constructed the pCHD1-Flag-SBP-Foxp3 plasmid. J.A., Y.D., Z.L., and S.Y., analyzed the data. M.-H.Z. conceived the project and revised the manuscript. All authors had final approval of the submitted and published version.

3.8 Declaration of Interests

The authors declare no conflicts of interest.

3.9 Star Methods

3.9.1 Resource Availability

Lead contact

Requests for further information and reagents may be directed to the lead contact, Ming-Hui Zou (mzou@gsu.edu).

Materials availability

Unique reagents generated in this study are available from the lead contact with a completed Material Transfer Agreement. All antibodies, reagents, and resources are list on **table 2**.

Table 2 Key resource table

REAGENT or RESOURCE	SOURCE	IDENTIFIER
Antibodies		
Flow cytometry: PE anti-mouse CD45 antibody (30-F11)	BioLegend	103106
Flow cytometry: Pacific blue anti-mouse CD45 antibody (30-F11)	BioLegend	103126
Flow cytometry: Alexa Fluor 700 anti-mouse CD45 antibody (30-F11)	BioLegend	103128
Flow cytometry: Brilliant Violet 605™ anti-mouse CD3e antibody (17A2).	BioLegend	100237
Flow cytometry: Pacific blue anti-mouse CD4 antibody (RM4-5)	BioLegend	100531

Flow cytometry: PE/Cyanine 7 anti-mouse CD4 antibody (GK1.5)	BioLegend	100422
Flow cytometry: Alexa Fluor 488 anti-mouse CD8a (53-6.7)	BioLegend	100723
Flow cytometry: Alexa Fluor 488 anti-mouse/rat/human Foxp3 antibody (150D)	BioLegend	320012
Flow cytometry: PE anti-mouse Foxp3 antibody (MF-14)	BioLegend	126404
Flow cytometry: Alexa Fluor 488 anti-mouse Foxp3 antibody (MF-14)	BioLegend	126406
Flow cytometry: Alexa Fluor 488 anti-GFP (FM264G)	BioLegend	338008
Flow cytometry: PE anti-GFP(FM264G)	BioLegend	338004
Flow cytometry: PE Rat anti-mouse CD25(3C7)	BioLegend	101904
Flow cytometry: PE CD278(iCOS) (15F9)	BioLegend	107705
Flow cytometry: PE anti-mouse IFN-γ(XMG1.2)	BioLegned	505808
Flow cytometry: PE-Cy7 anti-mouse CD357 (GITR) (YGITR 765)	BioLegend	120222
Flow cytometry: PE anti-mouse CD152 (CTLA-4) (UC10-4B9)	BioLegend	106305
Flow cytometry: PE anti-mouse CD279 (PD1) (RMP1-30)	BioLegend	109103
Flow cytometry: PE anti-mouse IL10 (JES5-16E3)	BioLegend	505008
Flow cytometry: PE anti-mouse CD304 (Nrp1) (3E12)	BioLegend	145204
Western blot: Rabbit anti-FOXP3 antibody	abcam	Ab75763
Western blot: FOXP3 Monoclonal Antibody (150D/E4)	eBioscience	14-4774-82
Immunofluorescence: FOXP3 (D608R) rabbit	Cell Signaling	12653S
Flow cytometry/Western blot/ Immunohistochemistry: Recombinant anti-AMPK alpha 1 antibody	Abcam	ab32047
Immunohistochemistry: Recombinant anti-AMPK alpha 1 antibody	Abcam	Ab110036
Western blot: Goat AMPKa1(C-20)	Santa Cruz	Sc-19128
Immunofluorescence: CD3e Monoclonal antibody (SP7)	Thermo Fisher	MA5-14524
Immunofluorescence: Recombinant anti-CD8 alpha antibody	Abcam	Ab217344
Immunofluorescence: Recombinant anti-CD4 antibody	Abcam	Ab183685
Immunofluorescence: CD31(PECAM-1) (D8V9E) Rabbit mAb	Cell signaling	77699
Immunofluorescence: Recombinant anti-Ki-67 antibody (SP6)	Abcam	Ab16667
A Western blot: Anti β-actin antibody(C4)	Santa Cruz	Sc-47778

Western blot/Immunofluorescence: Anti-CHIP(Stub1) antibody	Santa Cruz	Sc-133066
Western blot: Anti-HAUSP(USP7) antibody (H-12)	Santa Cruz	Sc-137008
Western blot: Ubiquitin antibody	Cell signaling	3933
Immunofluorescence:CD45R(B220) Monoclonal Antibody (RA3-6B2)	Thermo Fisher	14-0452-85
Flow cytometry/Immunofluorescence: Goat anti-Rabbit IgG H&L (Alexa Fluor 488)	abcam	Ab150077
Chemicals, peptides, and recombinant proteins		
Anti-CD3/CD28 Dynabeads	ThermoFisher	11452D
IL2 Recombinant Mouse Protein	ThermoFisher	PMC0025
Fixable Viability Dye eFluor 660	ThermoFisher	65-0864-18
Fixable Viability Dye eFluor 780	ThermoFisher	65-0865-14
Cycloheximide	SIGMA	01810
MG132	SIGMA	133407-82-6
DNase I	SIGMA	10104159001
Collagenase D	SIGMA	11088866001
iScript cDNA Synthesis Kit	BioRad	170-8891
Lipofectamine 2000 Transfection Reagent	ThermoFisher	11668019
Lipofectamine RNAiMAX Transfection Reagent	ThermoFisher	13778075
Albumin, Bovine Fraction V (BSA)	RPI	A30075-100;CAS:9048-46-8
Fetal bovine serum (FBS)	Sigma-Aidrich	12303C
Penicillin-Streptomycin	ThermoFisher	15140122
RPMI 1640	CORNING	10-040-CV
DMEM	CORNING	10-013-CV
Critical commercial assays		
Dynabeads Mouse CD4+ CD25+ Treg isolation Kit	ThermoFisher	11463D
eBioscience Foxp3/Transcription Factor Staining Buffer Set	ThermoFisher	00-5523-00
eBioscience Protein Transport Inhibitor Cocktail (500x)	ThermoFisher	00-4980-03
eBioscience Cell Stimulation Cocktail (500x)	ThermoFisher	00-4970-03
Dynabeads Untouched Mouse CD4 Cells Kit	ThermoFisher	11416D
Experimental models: Cell lines		
HEK 293T cells	ATCC	CRL-11268
B16F10 melanoma	ATCC	CRL-6475-LUC2™
LL/2(LLC1)	ATCC	CRL-1642
Experimental models: Organisms/strains		
Mouse: C57BL/6J	The Jackson Laboratory	JAX:000664
Mouse: Prkaa1$^{fl/fl}$	The Jackson Laboratory	JAX:014141
Mouse: Foxp3$^{YFP/Cre}$	The Jackson Laboratory	JAX:016959

Oligonucleotides		
See Table S1 for RT-PCR primers of *Foxp3*, *CHIP*, and *GAPDH*	This paper	NA
Recombinant DNA		
pCHD1-Flag-SBP-Foxp3	This paper	NA
CHIP(STUB1) shRNA(m) Lentiviral Particles	Santa Cruz	Sc-44731-V
Software and algorithms		
GraphPad Prism 8	GraphPad Software	https://www.graphpad.com/
ImageJ Software	ImageJ	https://imagej.net/Welcome
FlowJo	FlowJo 7.6	https://www.flowjo.com/

Data and code availability

All data produced in this study are available from the lead contact upon request.

This paper has no original code.

Any additional information required to reanalyze the data showed in this paper is available from the lead Contact upon request.

3.9.2 Experimental Model and Subject Details

Cell lines

HEK 293T cells, B16-F10-luc2 cells, and LLC cells were cultured in Dulbecco's Modification of Eagle's Medium (CORNING) containing 4.5 g/L glucose, L-glutamine, and sodium pyruvate, supplemented with 10% FBS, 100 U/ml penicillin, and 100 μg/ml streptomycin in a 37℃ incubator with humidity and 5% CO_2. Moreover, primary mouse cells were isolated from 6–8 mice/group on the same day.

Mouse strains

Prkaa1fl/fl, Foxp3Cre/YFP, and C57BL/6 mice were purchased from Jackson Laboratory (Bar Harbor, ME). All genetic models had the C57BL/6 background. Prkaa1fl/flFoxp3Cre/YFP mice were used at 10-16 weeks of age unless otherwise noted. Age-matched and sex-matched Foxp3Cre/YFP mice were used as controls.

All mice were housed in specific pathogen-free conditions in the animal facilities at Georgia State University. The animal protocol was reviewed and approved by the Georgia State University Institutional Animal Care and Use Committee.

Tumor models

B16-F10 murine melanoma cells and LLC cells were purchased from the ATCC. First, we confirmed that the cell lines were negative for *Mycoplasma spp.* We subcutaneously implanted $5x10^5$ B16-F10 melanoma cells or $5x10^5$ LLC cells on the backs of 10–12-week-old male AMPKα1$^{Treg+/+}$ and AMPKα1$^{Treg-/-}$ mice. The mice were monitored every day, and tumor growth and tumor size were determined based on tumor volume (0.5 x width^2 x length). Tumors were collected 10-13 days after inoculation unless otherwise noted.

3.9.3 Method Details

Cell isolation from tumors and lymphoid organs

Tumor-infiltrating lymphocytes were isolated by incubating tumor tissues in collagenase D (1 mg/ml, Roche) and DNase I (0.25 mg/ml, Sigma) for one hour. Single-cell suspensions from tumors were generated by passing the digested tumor tissues through a 40-μm cell strainer. Single-cell suspensions from spleen and lymph nodes were obtained directly by passing the tissues through a 40-μm cell strainer.

Flow cytometry

Each reaction was performed with more than 1×10^6 cells, and a minimum of 1×10^5 events were recorded. Fluorescence-positive cells were analyzed with a FACScalibur or LSRFortessa device (Becton Dickinson, CA). Cells were processed for viability staining using eBioscience LIVE/DEAD fixable Dye eFluor 660 or eFluor 780 (Thermofisher). For analysis of cell surface markers, cells were stained in stain buffer (BD bioscience) with the appropriate antibodies. Information on antibodies, clones, and fluorophores is provided in the Key resources table. A Foxp3/transcription factor staining buffer set from eBioscience was used for intracellular staining.

For staining intracellular cytokines, cells were stimulated for 6-18 h with a cell stimulation cocktail (Thermofisher) conjunction with protein transport inhibitor cocktail (Thermofisher) before being stained. After stimulation, the cells were stained with appropriate antibodies following the manufacturer's instructions. For YFP staining, Alexa Fluor 488 anti-GFP or PE anti-GFP antibody from BioLegend was used.

Histopathology and immunofluorescent staining

Organs were fixed with 10% (v/v) neutral buffered formalin, embedded in paraffin, sectioned, and stained with hematoxylin and eosin. For immunofluorescent staining, 4-μm sectioned paraffin slides were subjected to xylene and alcohol for dehydration. Then, the slides were subjected to antigen retrieval, permeabilized with 0.2% Triton X-100, and blocked with protein block goat serum (BioGenex, Fremont, CA). Then, the slides were incubated with CD31, anti Ki67, Foxp3, CD3e, B220, CD4, CD8, or CHIP antibodies at 4℃ overnight. Alexa Fluor 555 and Alexa Fluor 488 goat anti-rabbit, anti-rat, or anti-mouse were used as secondary antibodies, incubated at room temperature for one h. Cell nuclei were stained with DAPI and mounted with VectaMountTMAQ (#5501, Vector Laboratories) for fluorescence microscopy. Quantification was performed using Image J software.

Cell purification and culture

Lymphocytes were isolated from spleens, and CD4+CD25+ Treg cells were isolated using a Dynabeads CD4+CD25+ Isolation Kit (ThermoFisher). CD4+ T cells were isolated using a Dynabeads CD4+ T cell Isolation Kit (ThermoFisher). Then, CD4+YFP+ Treg cells were purified by YFP (GFP staining) using FACSAria II (BD Bioscience). The purified cells were cultured in RPMI 1640 supplemented with 10% FBS, 100 U/ml penicillin, 100 mg/ml streptomycin, and β mercaptoethanol.

RNA extraction and qRT-PCR

According to the manufacturer's instructions, RNA was extracted using the RNeasy Mini Kit (QIAGEN, Hilden, Germany). cDNA was synthesized using the iScript cDNA Synthesis Kit. The

expression of Foxp3 and CHIP mRNAs was determined by quantitative real-time PCR (qRT-PCR). Each cDNA sample was amplified using SYBR Green (Bio-rad, Hercules, CA) on a Bio-rad CFX96 Touch Real-time PCR detection system.

Western blot analysis

Cells were lysed with NP-40 lysis buffer (1% NP-40, 20 mM Tris-HCl pH 7.5, 150 mM NaCl, 5 mM EDTA, 50 mM NaF, 2 mM Na_3VO_4, and 10 µg/ml each of aprotinin and leupeptin) or with 1× SDS sample buffer (50 mM Tris-HCl pH 6.8, 100 mM DTT, 2% SDS, and 10% glycerol). Proteins were separated by SDS-PAGE and transferred to nitrocellulose membranes (Millipore, Billerica, MA). Membranes were visualized with an enhanced chemiluminescence detection system (Thermo Fisher Scientific, Waltham, MA). When necessary, the membranes were stripped by incubation in stripping buffer (Thermo Fisher Scientific, Waltham, MA) for 15 - 30 min with constant agitation, washed, and then re-probed with various other antibodies.

Immunoprecipitation

For immunoprecipitation, HEK293T cells were transfected with lipo2000 or RNA iMAX. Forty-eight hours after transfection, the cells were treated with MG132 for six h and then lysed in lysis buffer (50 mM Tris-HCL pH 7.5, 0.5% Nonidet p40 (US Biological), 1 mM EDTA and 40 mM NaCl with 1% protease inhibitor cocktail (ThermoFisher)). Anti-FLAG M2 affinity gel was used for immunoprecipitation. The precipitated samples were then boiled and analyzed by western blot.

Lentiviral shRNA transduction

CHIP (Stub1) shRNA(m) lentiviral particles were obtained from Santa Cruz. Purified $CD4^+YFP^+$ Treg cells were activated with Dynabeads CD3/CD28 plus IL-2 (200 U/ml) for 48 h and then transduced with lentivirus in the presence of 10 µg/ml polybrene by centrifugation at 900 *g* for 3 h. The transduced cells were then cultured in RPMI 1640 medium for 48 h and subsequently lysed for western blot analysis.

Quantification and Statistical Analysis

All statistical analyses were performed using GraphPad Prism version 8 (GraphPad Software, CA). Student's t test was used for analysis comparing two samples. One-way ANOVA tested differences among multiple samples. Two-way ANOVA was applied to study the effect of two parameters (i.e., time and treatment) and their interaction. $P < 0.05$ was considered statistically significant.

4 Hypercholesterolemia-Driven Inhibition of AMP-Activated Protein Kinase α1 Induces Treg Senescence during Atherogenesis

Junqing An[1], Ming-Hui Zou[1*]

[1]Center for Molecular and Translational Medicine, Georgia State University, 157 Decatur Street SE. Atlanta, GA 30303

*Corresponding author. Ming-Hui Zou, M.D., Ph.D., 157 Decatur Street SE, Atlanta, GA 30303, Tel:1-404-413-6637, E-mail: mzou@gsu.edu

4.1 Abstract

Background: Aging is the most important and irreversible risk factor in cardiovascular diseases (CVD). Regulatory T cells (Tregs) senescence, which display plasticity-like phenotype, plays an important role in CVD. Elevated evidences suggest that atherosclerotic environments drives Treg plasticity and Tregs dysfunction. How Tregs becomes senescence and whether or not atherosclerotic environments promote Tregs senescence and plasticity remain unknown.

Methods: In a western diet-induced atherosclerosis mice model, the accumulation of senescent Tregs in the spleen, para-aorta lymph nodes and aorta tissues was monitored. The role of senescent Tregs in atherogenesis was determined by adoptive Treg transfer. The involvement of AMPK in Treg senescence was further evaluated in AMPKα1 global knockout (*Prkaa1*$^{-/-}$) mice and Treg-specific AMPKα1 deletion mice (AMPKα1$^{Treg-/-}$). The role of AMPK in Tregs and atherogenesis was analyzed by constructing *Apoe* (*apolipoprotein E*) knockout with specific deletion of AMPKα1 in Tregs and adoptive transfer CA AMPK (constitutive active AMPK) Tregs into western diet-induced atherosclerotic mice.

Results: We observed significantly increased senescent Tregs in spleen, para-aorta lymph node, and aorta tissues of western fed ApoE$^{-/-}$ mice. Compared to thoracic and abdominal aorta, Tregs in aorta arches showed higher levels of senescent related markers. Adoptive transfer of non-

senescent Tregs but not senescent Tregs significantly ablated the development of atherosclerosis. Compared to non-senescent Tregs, senescent Tregs are more likely to be plasticity and dysfunctional. Mechanically, we revealed that AMPKα1 was downregulated in Tregs from both aged and western diet-fed ApoE$^{-/-}$ mice and AMPK reduction promoted Treg senescence via upregulation of reactive oxygen species (ROS). Furthermore, a deficiency of AMPKα1 in Tregs promoted arterial inflammation and atherosclerosis in ApoE$^{-/-}$ mice. Finally, adoptive transfer of CA AMPK-Tregs significantly retarded atherosclerosis progression and reduced plaque vulnerability.

Conclusions: we conclude that AMPKα1 reduction in Tregs promotes Treg senescence, resulting in accumulation of dysfunctional plasticity Tregs that accentuated arterial inflammation and atherogenesis. Adoptive transfer of CA AMPK-Tregs could be a novel therapeutic method to treat atherosclerotic diseases and vulnerable plaques.

4.2 Introduction

Atherosclerosis is a chronic inflammatory disease and one of the major causes of vascular death worldwide (Herrington et al., 2016; Wolf and Ley, 2019). Accumulation of modified lipoproteins caused by hyperlipidemia induces abnormal vascular immune responses and drives atherosclerosis (Rao et al., 2015b; Yin et al., 2015). Familial hypercholesterolemia (FH), with 1 in 500 prevalence worldwide, is the epitomized disease that causes cholesterol deposition in arteries and premature atherosclerosis(Hopkins et al., 2011; Nordestgaard et al., 2013). Given the extensive immune-inflammatory activation, immunomodulation has emerged as a potential therapy method for atherosclerosis(Back et al., 2019). As an important immune regulator, regulatory T cells (Tregs) are shown to maintain the immune homeostasis to prevent tissue damage(Munoz-Rojas and Mathis, 2021). Presentation of Tregs within atherosclerotic plaques play protective roles on atherosclerosis via regulating immune cells activation and inflammation(Ait-Oufella et al., 2006). However, hyperlipidemia-induced Treg plasticity leads to

their impaired immunosuppressive function. The reshape of physiological Tregs into pathological Tregs dampens its protective effect on atherosclerosis progression and plaque stability(Butcher et al., 2016; Gaddis et al., 2018; Shao et al., 2021). However, it is still unclear how the hyperlipidemia environment dampens Treg function and increases Treg plasticity.

Recent studies showed cellular senescence is associated with atherosclerosis and is recognized as a risk factor for atherosclerosis formation and progression (Wang and Bennett, 2012; Wu et al., 2020). Accumulation of senescent immune cells such as macrophages and T cells in atherosclerotic lesions was detrimental throughout the disease pathogenesis. Selective removal of these senescent cells is emerging as a promising therapeutic strategy to prevent atherosclerosis progression(Childs et al., 2016; Childs et al., 2018; Song et al., 2020). A recent study showed Tregs senesce more severely than Tconv cells with age, with preferential upregulation of senescence-related markers. Senescent Tregs displayed less immunosuppressive activity while higher expression of inflammatory cytokines, which is similar to the plasticity of Tregs(Guo et al., 2020). However, it is unknown whether and how senescent Tregs play their roles in atherogenesis.

Here, we reported that Tregs senescence is a primary reason causing Treg plasticity in atherosclerosis. In addition, we found that age-related decline of AMPK caused Tregs senescence resulting in an uncontrolled aortic inflammation with enhanced atherosclerosis in mice in vivo.

4.3 Methods

4.3.1 Animals

Prkaa1$^{flox/flox}$, *Foxp3*$^{YFP\text{-}Cre}$, ApoE$^{-/-}$, and C57BL/6 mice were purchased from Jackson Laboratory (Bar Harbor, ME). *Prkaa1*$^{-/-}$ and Treg-specific AMPKα1 knock out mice (*Prkaa1*$^{fl/fl}$*Foxp3*$^{YFP/Cre}$) were generated as previous described(Jorgensen et al., 2004; Zhu et al., 2021). Treg-specific AMPKα1 knock out mice in ApoE$^{-/-}$ background (ApoE$^{-/-}$ *Prkaa1*$^{fl/fl}$*Foxp3*$^{YFP/Cre}$) were obtained by crossing ApoE$^{-/-}$ mice with *Prkaa1*$^{fl/fl}$*Foxp3*$^{YFP/Cre}$ mice. Mice were used for experiments at 8-10

weeks of age. Mice of both sexes were used, and all mice were randomly selected for different treatment groups. For atherosclerosis studies, ApoE-/- mice were fed a Western diet (42% from fat, 0.2% from cholesterol) (Research Diets, D12079B). All mice were housed in specific pathogen-free conditions in the animal facilities at Georgia State University. The animal protocol was reviewed and approved by Georgia State University Institute Animal Care and Use Committee.

4.3.2 Preparation of Cell Suspensions from Aorta and Lymphoid Organs

Single cell suspensions from aorta tissues were prepared by digesting cleaned aorta with 2 mg/ml collagenase I, 1 mg/ml collagenase XI, 120 U/ml hyaluronidase, and 150 μg/ml DNase I in HBSS for 1 hour at 37℃ before passing the suspensions through a 40-μm cell strainer. Single cells from lymphoid organs such as spleen, peri-aortic lymph nodes, and peripheral lymph nodes were obtained directly by passing the tissues through a 40-μm cell strainer.

4.3.3 Flow Cytometry

Single cell suspensions were incubated with TruStain FcX™ PLUS (anti-mouse CD16/CD32) antibodies for 15 minutes at room temperature before incubating with appropriate antibodies for 30 minutes for cell surface markers. Cells were processed for viability staining using eBioscience LIVE/DEAD fixable Dye eFluor 660 or eFluor 780 (Thermofisher). Intracellular staining was performed by using eBioscience™ Foxp3 transcription factor staining buffer set (00-5523-00) according to the manufacturer's instructions. For intracellular cytokine staining, the cell suspensions were stimulated with eBioscienceTM cell stimulation cocktail (00-4970-03) and eBioscienceTM protein transport inhibitor cocktail (00-4980-93) for 18 hours before staining with appropriate antibodies following intracellular staining procedure. For YFP staining, Alexa Fluor 488 anti-GFP or PE anti-GFP antibody from BioLegend was used. All the flow cytometry antibodies were listed in **table 3**. The staining cells were analyzed on the LSR-Fortessa machine (BD Bioscience).

Table 3 Primary antibody information

REAGENT or RESOURCE	SOURCE	IDENTIFIER
Antibodies		
Flow cytometry: PE anti-mouse CD45 antibody (30-F11)	BioLegend	103106
Flow cytometry: Pacific blue anti-mouse CD45 antibody (30-F11)	BioLegend	103126
Flow cytometry: Brilliant Violet 605™ anti-mouse CD3e antibody (17A2).	BioLegend	100237
Flow cytometry: Alexa Fluor 700 anti-mouse CD4 antibody (Gk1.5)	BioLegend	100430
Flow cytometry: Pacific blue anti-mouse CD4 antibody (RM4-5)	BioLegend	100531
Flow cytometry: PE/Cyanine 7 anti-mouse CD8 antibody (53-6.7)	BioLegend	100722
Flow cytometry: Alexa Fluor 488 anti-mouse CD8a (53-6.7)	BioLegend	100723
Flow cytometry: Alexa Fluor 488 anti-mouse/rat/human Foxp3 antibody (150D)	BioLegend	320012
Flow cytometry: PE anti-mouse Foxp3 antibody (MF-14)	BioLegend	126404
Flow cytometry: Pacific blue anti-mouse Foxp3 antibody (MF-14)	BioLegend	126410
Flow cytometry: Alexa Fluor 488 anti-GFP (FM264G)	BioLegend	338008
Flow cytometry: PE anti-GFP(FM264G)	BioLegend	338004
Flow cytometry: PE Rat anti-mouse CD25(3C7)	BioLegend	101904
Flow cytometry: APC anti-mouse CD25(PC61)	BD Pharmingen	557192
Flow cytometry: PE CD278(iCOS) (15F9)	BioLegend	107705
Flow cytometry: PE anti-mouse IFN-γ(XMG1.2)	BioLegned	505808
Flow cytometry: PE-Cy7 anti-mouse CD357 (GITR) (YGITR 765)	BioLegend	120222
Flow cytometry: PE anti-mouse CD152 (CTLA-4) (UC10-4B9)	BioLegend	106305
Flow cytometry: PE anti-mouse CD279 (PD1) (RMP1-30)	BioLegend	109103
Flow cytometry: PE anti-mouse IL10 (JES5-16E3)	BioLegend	505008
Flow cytometry: PE anti-mouse CD304 (Nrp1) (3E12)	BioLegend	145204
Flow cytometry: PE anti-mouse CD223 (LAG-3) (C9B7W)	BioLegend	125208

4.3.4 SA-β-gal Activity Assay in T cells

The SA-β-gal activity in T cells was detected by staining with the fluorescent β-galactosidase substrate C12FDG following previous protocol(Zhang et al., 2021). Briefly, fresh isolated

lymphocytes, $CD4^+$ T cells, or $CD4^+YFP^+$ Tregs were pretreated with 100 nM bafilomycin A1 (Millipore Sigma SML1661) before adding 33 μM C_{12}FDG (ab273642) for another 2 hours in 37 ℃ incubator. The cell suspensions were then washed with cold 1x PBS for 3 times and stained with appropriate antibodies following flow cytometry procedure.

4.3.5 Adoptive Treg Transfer Experiments

Splenic senescent Tregs ($C_{12}FDG^{high}$-Treg) and non-senescent Tregs ($C_{12}FDG^{low}$-Treg) were sterilely sorted from 8-week-old $ApoE^{-/-}$ mice fed with 20 weeks western diet. GFP-Tregs and GFP-CA AMPK-Tregs were obtained by transfecting pLenti-XI-Neo-eGFP-Constitutively Active AMPK, and pLenti-XI-Neo-eGFP lentivirus to fresh isolated Tregs. Then the cells were subsequently labeled with CSFE (ThermoFisher C34554) for 10 minutes at 37 ℃ and washed with 1x PBS for 3 times. The labeled cells ($2x10^5$ Tregs/mice) were then injected into 8-week-old ApoE-/- mice fed with 4 weeks western diet. After another 4 weeks western diet, the aorta, spleens, serum and hearts were collected for flow cytometry, lipid assay, and lesion size detection.

4.3.6 ROS Detection in T Cells

CM-H_2DCFDA was used to detect the ROS expression in T cells following previous described(Jackson et al., 2004).fresh isolated lymphocytes and T cells were washed with 1x PBS and seeded in prewarmed medium. 2 μM CM-H_2DCFDA (ThermoFisher C6827) was added into the medium and cells were cultured for 20 minutes. After that, cells were washed with 1x PBS for 3 times and staining with appropriate antibodies for flow cytometry. For ROS scavengers, cells were treated with 10 mM GSH (VWR, IC10181405) and 10 μM Mito TEMPO (Millipore Sigma SML0737) for 24 hours.

4.3.7 Cell Isolation

$CD4^+$ T cells were isolated from the spleen of mice by Dynabeads™ Untouched™ Mouse CD4 Cells Kit (ThermoFisher 11415D). For Treg isolation from Prkaa1+/+Foxp3YFP/Cre and

Prkaa1fl/flFoxp3YFP/Cre mice, splenocytes were stained with CD3, CD4, and GFP (for YFP staining) antibodies, and then CD3+CD4+GFP+ cells were sorted by Fortesea in the core facility of Georgia State University. For senescent and non-senescent Treg cell isolation, splenocytes were first isolated from the 20 weeks western diet fed ApoE-/- mice, and then staining with CD3, CD4, CD25 antibodies, and C12FDG fluorescence. Senescent and non-senescent Treg cells were sorted by $CD3^{+}CD4^{+}CD25^{+}C_{12}FDG^{high}$ and $CD3^{+}CD4^{+}CD25^{+}C_{12}FDG^{low}$ separately.

4.3.8 Quantification of Atherosclerotic Lesions

The aorta roots were embedded in OCT and then serially sectioned at 8-μm thickness. For oil red staining, six to eight serial cryosections were collected from each mouse and stained with Oil Red O for 1 hour in 37℃, and then counterstained with hematoxylin to visualize nuclei. The plaque images were captured using the Olympus microscope, and quantification was performed with Image J software (National Institute of Health). To assay the lesion are in while aorta, the intimal surface was exposed by a longitudinal cut from the ascending arch to the left subclavian artery. The aorta was stained with 0.5% Sudan IV in 35% ethanol and 50% acetone for 10 min, and then rinsed with phosphate-buffered saline.

4.3.9 Immunofluorescence Staining

For immunofluorescence staining, sliced aorta root tissues were rinsed with ddH2O and then fixed in ice-cold acetone for 10 minutes. After that, the slides were washed with PBS and blocked with protein block (BioGenex, HK112-9K) for 30 minutes. Then the slides were incubated with primary antibody (anti-CD68, Bio-rad, 1:200) at 4℃ overnight. Alexa Fluor 555 goat anti-rat was used as secondary antibodies, incubated at room temperature for one h. Cell nuclei were stained with DAPI and mounted with VectaMountTMAQ (#5501, Vector Laboratories) for fluorescence microscopy. Quantification was performed using Image J software.

4.3.10 RNA Extraction and qRT-PCR

According to the manufacturer's instructions, RNA was extracted using the RNeasy Mini Kit (QIAGEN, Hilden, Germany). cDNA was synthesized using the iScript cDNA Synthesis Kit. The expression of $p16^{Ink4a}$, $p19^{Arf}$, $p21^{Cip1}$, Prkaa1, IFNγ, IL6, IL1β, IL17, and TNFα mRNAs was determined by quantitative real-time PCR (qRT-PCR). The primers of these genes were listed in **table 4.** Each cDNA sample was amplified using SYBR Green (Bio-rad, Hercules, CA) on a Bio-rad CFX96 Touch Real-time PCR detection system.

Table 4 Primer's information

Oligo name	Oligo sequence
mAMPKα1 R	TCCTTTTCGTCCAACCTTCCA
mAMPKα1 F	TACTCAACCGGCAGAAGATTCG
mIL17R	CTTTCCCTCCGCATTGACA
mIL17F	GCTCCAGAAGGCCCTCAGA
mIL1b R	GTTCATCTCGGAGCCTGTAGTG
mIL1b F	TGGACCTTCCAGGATGAGGACA
m-Tnf-F	TAGCCCACGTCGTAGCAAAC
m-Tnf-R	GCAGCCTTGTCCCTTGAAGA
m-Il6-F	GCCTTCTTGGGACTGATGCT
m-Il6-R	TGCCATTGCACAACTCTTTTC
m-Ifng-F	GGAGGAACTGGCAAAAGGATGG
m-Ifng-R	ATGTTGTTGCTGATGGCCTGA
mGAPDH_F	ACTCCACTCACGGCAAATTC
mGAPDH_R	TCTCCATGGTGGTGAAGACA
mArf-F	GCCGCACCGGAATCCT
mArf-R	TTGAGCAGAAGAGCTGCTACGT
mINK4a-F	CCCAACGCCCCGAACT
mINK4a-R	GCAGAAGAGCTGCTACGTGAA
mCip1_F	CGAGAACGGTGGAACTTTGAC
mCip1_R	CAGGGCTCAGGTAGACCTTG

4.3.11 Western Blot Analysis

Cells were lysed with NP-40 lysis buffer (1% NP-40, 20 mM Tris-HCl pH 7.5, 150 mM NaCl, 5 mM EDTA, 50 mM NaF, 2 mM Na_3VO_4, and 10 μg/ml each of aprotinin and leupeptin) or with 1× SDS sample buffer (50 mM Tris-HCl pH 6.8, 100 mM DTT, 2% SDS, and 10% glycerol). Proteins were separated by SDS-PAGE and transferred to nitrocellulose membranes (Millipore, Billerica, MA).

Membranes were visualized with an enhanced chemiluminescence detection system (Thermo Fisher Scientific, Waltham, MA). When necessary, the membranes were stripped by incubation in stripping buffer (Thermo Fisher Scientific, Waltham, MA) for 15 - 30 min with constant agitation, washed, and then re-probed with various other antibodies.

4.3.12 Lentiviral Transduction

Lentiviral transduction was performed by transfecting HEK 293T cells with pLenti-XI-Neo-GST-Constitutively Active AMPK (addgene#139843), pLenti-XI-Neo-GST, pLenti-XI-Neo-eGFP-Constitutively Active AMPK, and pLenti-XI-Neo-eGFP lentiviral vectors along with packaging plasmids. For the transduction of $CD4^+$ T cells, purified $CD4^+$ T cells were activated with anti-CD3/CD28 beads for 24 hours and then transduced with lentivirus in the presence of 10μg/ml polybrene by spinning at 900g for 120 min. Cells were harvested 2 days after transduction and then treated with cholesterol for aging marker analysis. For Treg transduction, sorted $CD4^+CD25^+$ Tregs were activated with anti-CD3/CD28 beads supplemented with IL-2 (200U/ml) for 24 hours and then transduced with pLenti-XI-Neo-eGFP or pLenti-XI-Neo-eGFP-Constitutively Active AMPK in the presence of 10 μg/ml polybrene by spinning at 900g for 120 min. Cells were harvested for 2 more days after transduction and GFP^+ cells were then sorted to perform adoptive Treg transfer experiments.

4.3.12 Quantification and Statistical Analysis

All statistical analyses were performed using GraphPad Prism version 8 (GraphPad Software, CA). Student’s t test was used for analysis comparing two samples. One-way ANOVA tested differences among multiple samples. Two-way ANOVA was applied to study the effect of two parameters (i.e., time and treatment) and their interaction. $P < 0.05$ was considered statistically significant.

4.4 Results

4.4.1 Tregs are More Likely to be Senescence Under Hyperlipidemia Condition

To determine the role of senescent Tregs in the development of atherosclerosis, we performed an atherosclerosis mouse model by feeding ApoE$^{-/-}$ mice with 16-weeks western diet. After treatment, we comprehensively analyzed the cellular senescence of Tconv (conventional T cell) cells and Treg cells by detecting the expression of senescence-associated β-galactosidase (SA-β-gal) activity, a key marker of cellular senescence. We found that both Tconv cells and Treg cells from splenocytes of western diet-fed ApoE$^{-/-}$ mice displayed a higher expression of SA-β-gal activity compared to those from the chow diet-fed group (**Figure 23A and 23B**). In addition, compared with Tconv cells, the senescence marker was preferentially upregulated in Tregs (**Figure 23A and 23B**).

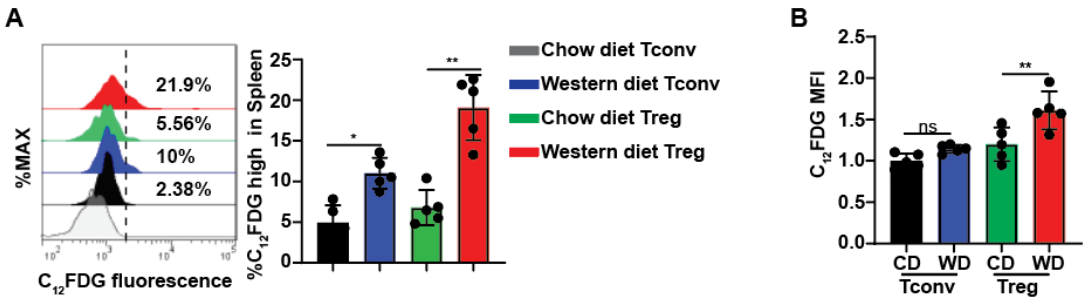

Figure 23 Preferential Treg senescence during atherogenesis.
8-week-old ApoE$^{-/-}$ mouse were treated with chow diet or western diet for 16 weeks. Senescent cells were assessed by flow cytometry with the fluorescent β-gal substrate C_{12}FDG. A, Percentage of senescent Treg (CD4^{+}Foxp3^{+}C_{12}FDG^{high}) and Tconv(CD4^{+}Foxp3^{-}C_{12}FDG^{high}) cells in the splenocytes of chow diet or western diet-feed ApoE$^{-/-}$ mice (n=5/group). B, Quantification analysis of relative C_{12}FDG MFI in Tconv (CD4^{+}Foxp3^{-}C_{12}FDG^{high}) and Treg (CD4^{+}Foxp3^{+}C_{12}FDG^{high}) cells in the splenocytes of chow diet or western diet-feed ApoE$^{-/-}$ mice (n=5/group). Data are presented as mean±SD, ns $p>0.05$, *$p<0.05$, and **$p<0.01$ by Student *t* test.

Next, we investigated the frequency of senescent Tregs in both para-aorta lymph nodes and single cells from whole aorta tissues. Compared to chow diet fed ApoE$^{-/-}$ mice, the SA-β-gal activity was found to be a significant increase in Tregs from western diet fed ApoE$^{-/-}$ mice (**Figure 24A-24D**). Consistent with the increased SA-β-gal activity, both the mRNA and protein level of senescence signature genes, including p16^{Ink4a} and ^{p21cip1}, were also increased in Tregs from the

western diet-treated ApoE$^{-/-}$ mice (**Figure 24E-24F**). When analyzing the expression of senescent Tregs in different part of the aorta, we found compared to thoracic aorta (low atherosclerosis plaque formation area), the activity of SA-β-gal was increased in Tregs from aorta arch (high atherosclerosis plaque formation area) (**Figure 24G**).

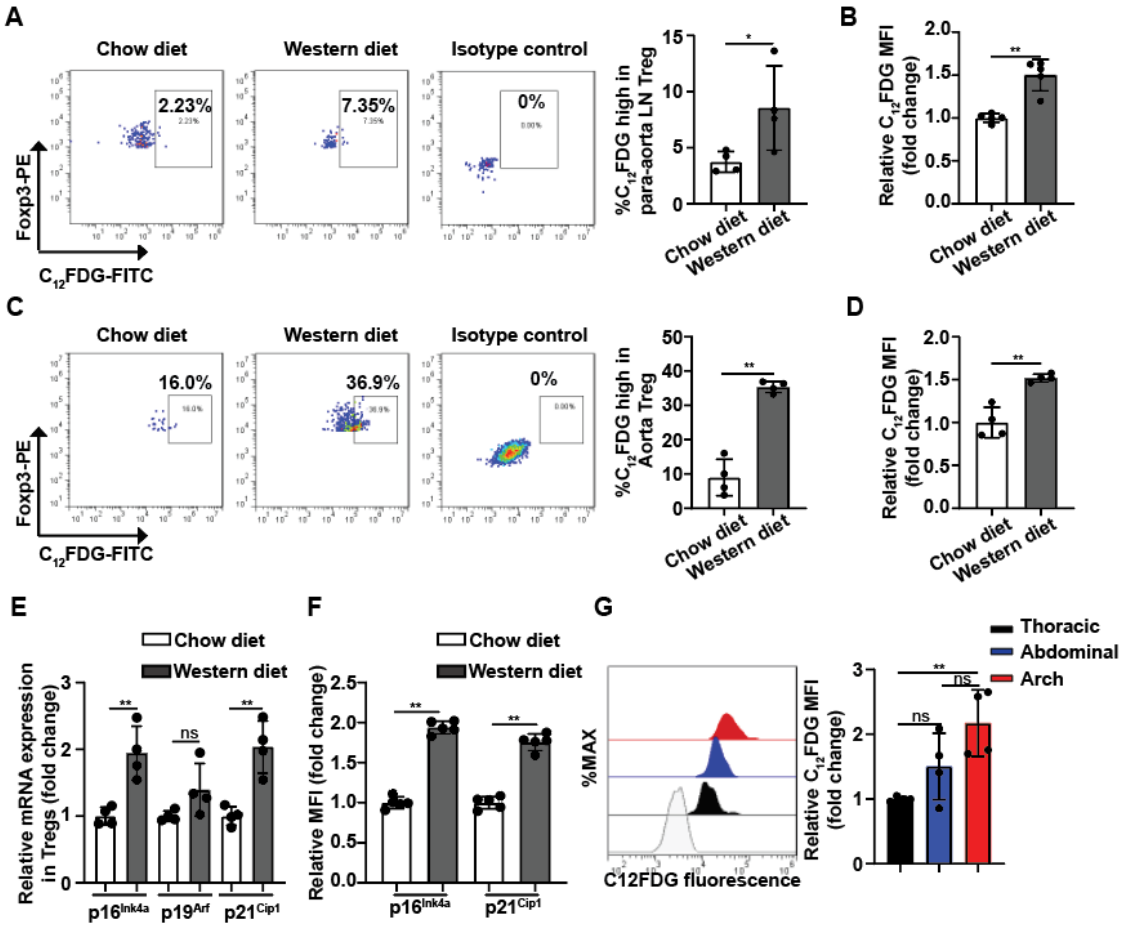

Figure 24 ***Senescent Tregs are increased during atherogenesis.***
A-B, Percentage of senescent Treg cells (A) and mean fluorescence intensity (MFI) of C_{12}FDG in Treg cells (B) from para-aorta lymph nodes of ApoE$^{-/-}$ mice feed with chow diet or western diet (n=4/group). C-D, Percentage of senescent Treg cells (C) and mean fluorescence intensity (MFI) of C_{12}FDG in Treg cells (D) from aorta single cells of ApoE$^{-/-}$ mice feed with chow diet or western diet (each sample contains 4 pooled aortas, n=4/group). E, Relative mRNA expression of p16^{Ink4a}, p19^{Art}, p21^{Cip1} in Treg cells (CD4^{+}CD25^{+}) isolated from ApoE$^{-/-}$ mice feeding with chow diet or western diet (n=4/group). F, Mean fluorescence intensity (MFIs) of p16^{Ink4a} and p21^{Cip1} in Treg cells (n=4/group). G, Quantification of relative C_{12}FDG MFIs in Treg cells from aorta arch, Thoracic aorta, and abdominal aorta of ApoE$^{-/-}$ mice feed with 16 weeks western diet (each sample contains 8 pooled aortas, n=3/group). Data are presented as mean±SD, ns p>0.05, *p<0.05, and **p<0.01 by Student *t* test (A-F) and one way ANOVA (G).

4.4.2 Western Diets Disrupt Immune Homeostasis in ApoE$^{-/-}$ Mice

During the development of aging, the increased senescent Tregs promotes the progression of immunological aging, with the hallmarks of decreased naïve T cells, increased effector T cells, and increased production of IFNγ in both CD4^{+} and CD8^{+} T cells(Guo et al., 2020). Analyzing the T cell function in chow diet or western diet feed ApoE$^{-/-}$ mice, we found both CD4^{+} and CD8^{+} T cells in western diet feed ApoE$^{-/-}$ mice adopted effector memory phenotypes, as well as higher production of IFNγ compared to chow diet feed mice (**Figure 25A-25D**). However, the frequency of Tregs in spleen, para-aorta lymph nodes, and aorta tissues was significant increase in western diet feed ApoE$^{-/-}$ mice (**Figure 26A-26C**), which may due to the chronic inflammation caused by western diet treatment. These data suggest that western diet disrupts the immunosuppressive function of Tregs and leads to immunological aging.

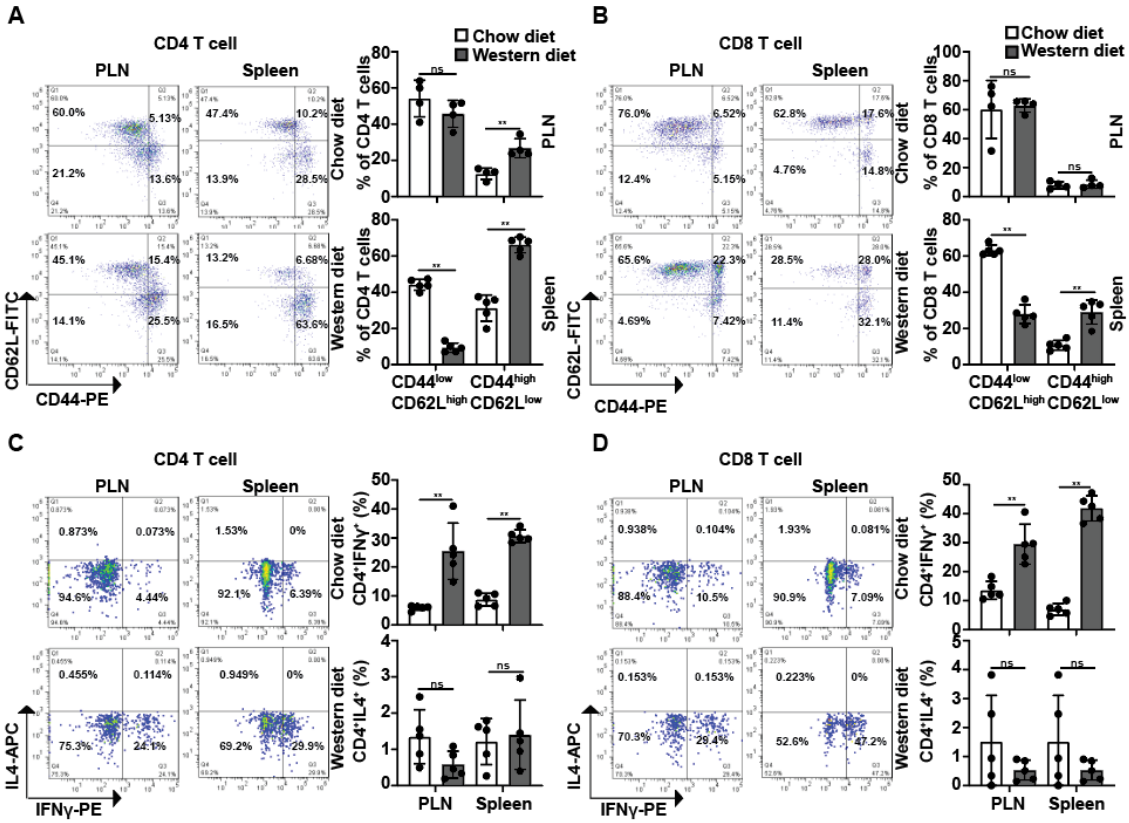

Figure 25 ***Hypercholesterolemias disturb T cell homeostasis in ApoE-/- mice.***
A-B, Representative flow images and quantification of naïve (CD44^{low}CD62L^{high}) and effector/memory

($CD44^{high}CD62L^{low}$) $CD4^+$ (A) and $CD8^+$ (B) T cells in peripheral lymph nodes (PLN) and spleens of 16 weeks chow diet or western diet treated $ApoE^{-/-}$ mice (n=4 per group). C-D, Representative flow images and quantification of IFNγ and IL-4 production $CD4^+$ (C) and $CD8^+$ (D) T cells in peripheral lymph nodes (PLN) and spleens of 16 weeks chow diet or western diet treated $ApoE^{-/-}$ mice (n=4 per group). Data are presented as mean±SD, ns p>0.05, *p<0.05, and **p<0.01 by Student *t* test.

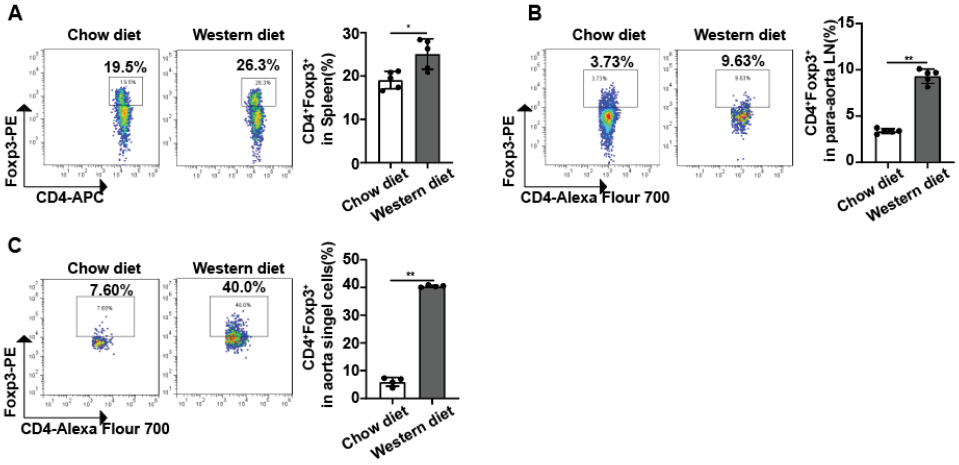

Figure 26 ***Increased Treg frequency in western diet feed ApoE-/- mice.***
A-C, Representative flow images and quantification of $CD4^+Foxp3^+$ Treg cells in spleens (A), para-aorta lymph nodes (B), and aorta tissues (C) of 16 weeks chow diet or western diet treated $ApoE^{-/-}$ mice (n=4 per group). Data are presented as mean±SD, ns p>0.05, *p<0.05, and **p<0.01 by Student *t* test.

4.4.3 Senescent Tregs Possess Less Protective Effect on Atherosclerosis Development

To directly test the role of Tregs senescence on atherosclerosis development, we performed *in vivo* adoptive Tregs transfer experiments following the previously described(Bonacina et al., 2021). 8-week-old $ApoE^{-/-}$ mice were fed with the western diet for four weeks and then received senescent Tregs ($C_{12}FDG^{high}$-Treg), and non-senescent Tregs ($C_{12}FDG^{low}$-Treg), which were sorted from $ApoE^{-/-}$ mice fed 20 weeks western diet (**Figure 27A**). The recipient mice were fed the western diet for four additional weeks. At the end of the treatment, we observed that the donor Tregs could be detected within the aorta tissue of the recipient $ApoE^{-/-}$ mice (**Figure 28A**). Interestingly, compared to $ApoE^{-/-}$ mice received medium alone, non-senescent-Treg recipients displayed a 4-fold reduction of plaque size, while senescence-Treg recipients presented a similar plaque size (**Figure 27B and 27C**). The serum cholesterol and triglycerides levels were comparable among different groups (**Figure 28B and 28C**). These data indicate an impaired protective role of senescence-Treg on atherosclerosis plaque formation.

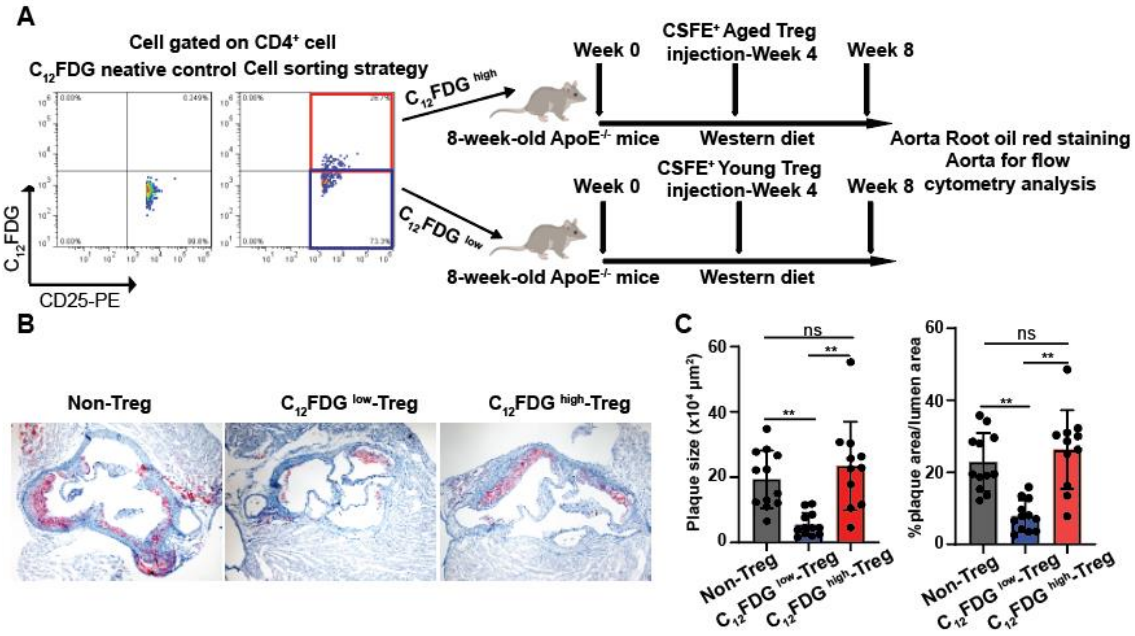

Figure 27. ***Senescence Treg cells show less protective effect on atherosclerosis development.***
A, Experiment design and schematic diagram of adoptive Treg transfer experiment. Western diet feeding 8-week-old ApoE$^{-/-}$ mice received medium alone (non-Treg), senescence ($C_{12}FDG^{high}$) or non-senescence ($C_{12}FDG^{low}$) Tregs. B, Representative oil red staining aorta root figures of ApoE$^{-/-}$ recipients in indicated groups. C, Quantification of plaque size and plaque area ratio of ApoE$^{-/-}$ recipients in indicated groups (n=12 in non-Treg and $C_{12}FDG^{low}$–Treg group and n=11 in $C_{12}FDG^{high}$–Treg group). Data are presented as mean±SD, ns p>0.05, *p<0.05, and **p<0.01 by one way ANOVA.

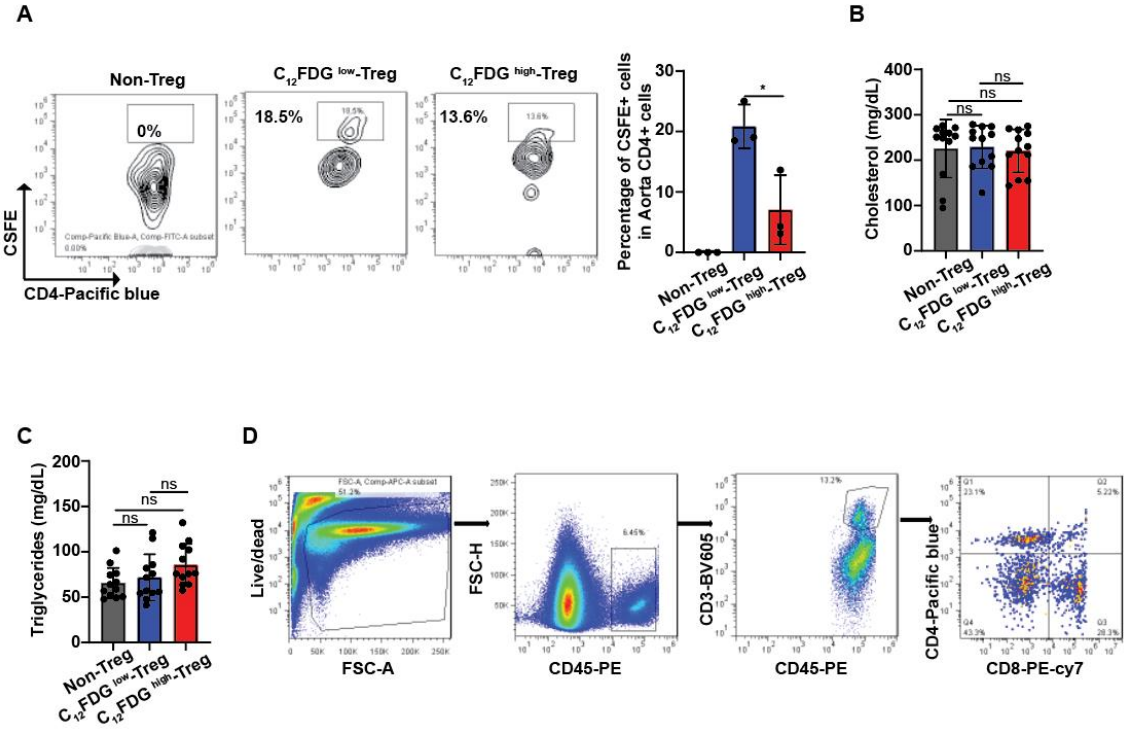

Figure 28 ***Adoptive transfer senescence Tregs show mild effect on serum lipid level.***
A, Representative flow images and quantification of CSFE^{+} Treg (donor Treg) in aortas of indicated groups

(each sample is pooled by three mice aortas, n=3/group). B-C, Quantification of serum cholesterol (B) and triglycerides (C) level of indicated groups (n=12 in each group, data are presented as mean±SD, ns p>0.05 by one way ANOVA). D, Gating strategy of $CD45^+$ cells, $CD3^+$ T cells, $CD4^+$ T cells, and $CD8^+$ T cells from aorta single cells. Data are presented as mean±SD, ns p>0.05, *p<0.05, and **p<0.01 by one way ANOVA.

To further analysis the immune cells' situation on the recipient mice. Flow cytometry analysis was performed on different groups' aorta tissues to investigate the impact of senescent-Treg and non-senescent-Treg on arterial inflammation (**Figure 28D**). Compared with medium alone, transfer both senescent and non-senescent-Tregs significant decreased the proportion and number of $CD45^+$ cells among aorta tissues. However, senescent-Tregs recipients showed higher frequency and numbers of $CD45^+$ cells compared to non-senescent Tregs (**Figure 29A**). For $CD3^+$ T cells, both senescent-Tregs and non-senescent Tregs transfer decreased the frequency and numbers of $CD3^+$ T cells, but senescent-Treg recipients showed higher numbers of $CD3^+$ T cells than non-senescent Treg recipients (**Figure 29B**). For $CD8^+$ T cells, transfer non-senescent Tregs but not senescent Tregs significant decreased the frequency and numbers of $CD8^+$ T cells (**Figure 29C and 29D**). Importantly, non-senescent Treg recipients but not senescent Treg recipients attenuated the macrophage content in the plaque area (**Figure 29E and 29F**). All these suggest compared to non-senescent Tregs, senescent Tregs are dysfunctional in suppressing arterial inflammation.

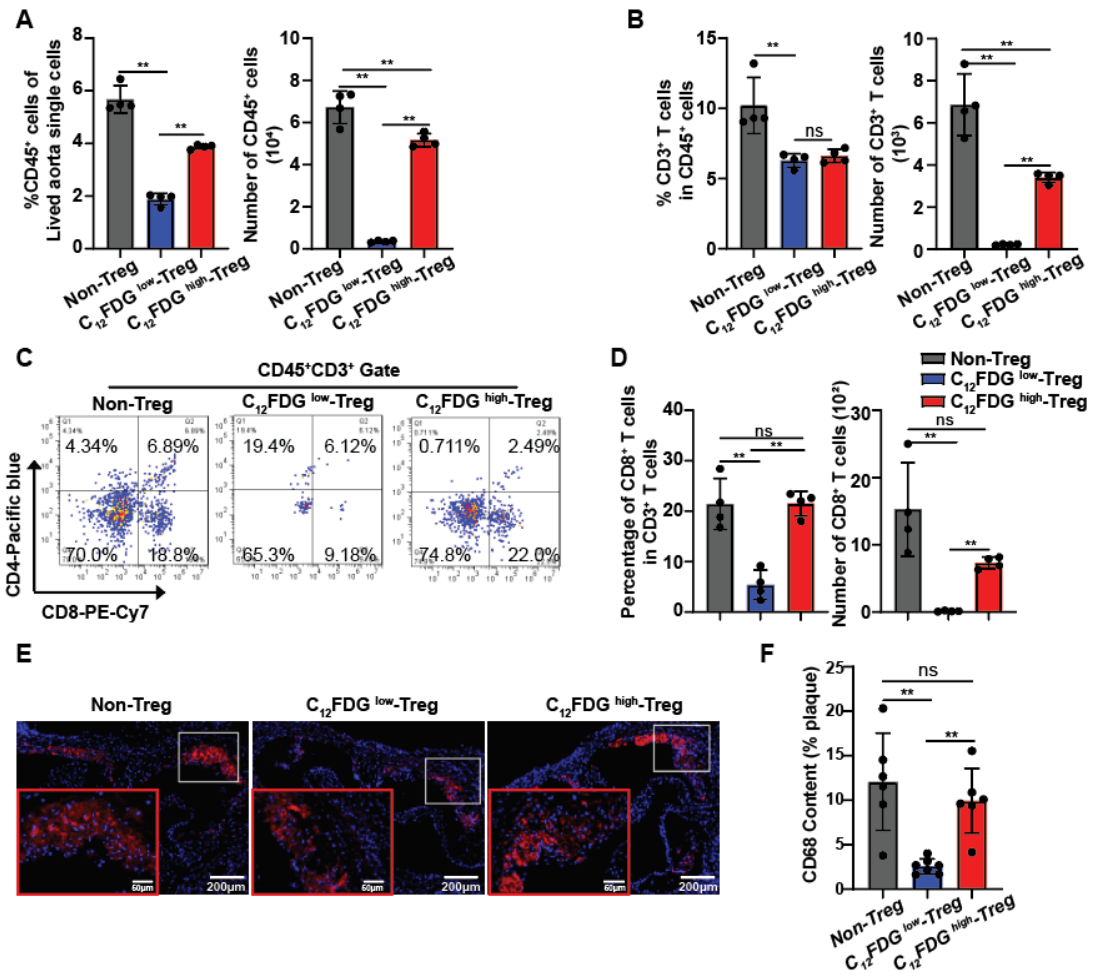

Figure 29 ***Senescent Tregs show fewer protective effects on arterial inflammation.***
A, Quantification of the percentage and the number of CD45+ cells among aorta single cells (n=4/group, each group pooled by three mice aorta). B, Quantification of the percentage of CD3+ T cells, CD4+CD8- T cells, and CD4-CD8+ T cells among CD45+ cells from aorta single cells (n=4/group, each group pooled by three mice aorta). C, Expression of $CD45^+CD3^+CD4^+$ T cells and $CD45^+CD3^+CD8^+$ T cells among aorta single cells were analyzed by flow cytometry. D, Quantification of the percentage and numbers of CD8+ T cells among CD45+ cells from aorta single cells (n=4/group, each group pooled by three mice aorta). E, Representative CD68 immunofluorescence staining figures of aorta root from indicated groups. F, Quantification of the CD68 content among plaque area (n=6 in each group). Data are presented as mean±SD, ns $p>0.05$, and $^{**}p<0.01$ one way ANOVA.

4.4.4 Senescent Tregs are More Likely to be Dysfunctional and Plasticity

Next, we were trying to investigate the mechanism of how senescent Tregs become dysfunctional during atherogenesis. Analysis of the expression of several Tregs suppressive activity related to cell surface molecules such as CD25, GITR, ICOS, LAG3, Nrp1, and PD1, we found most of them were dramatically decreased in senescent Tregs compared to non-senescent

Tregs. Significantly, the expression of Foxp3, the critical transcriptional factor of Tregs, was also decreased in senescent Tregs (**Figure 30A and 30B**).

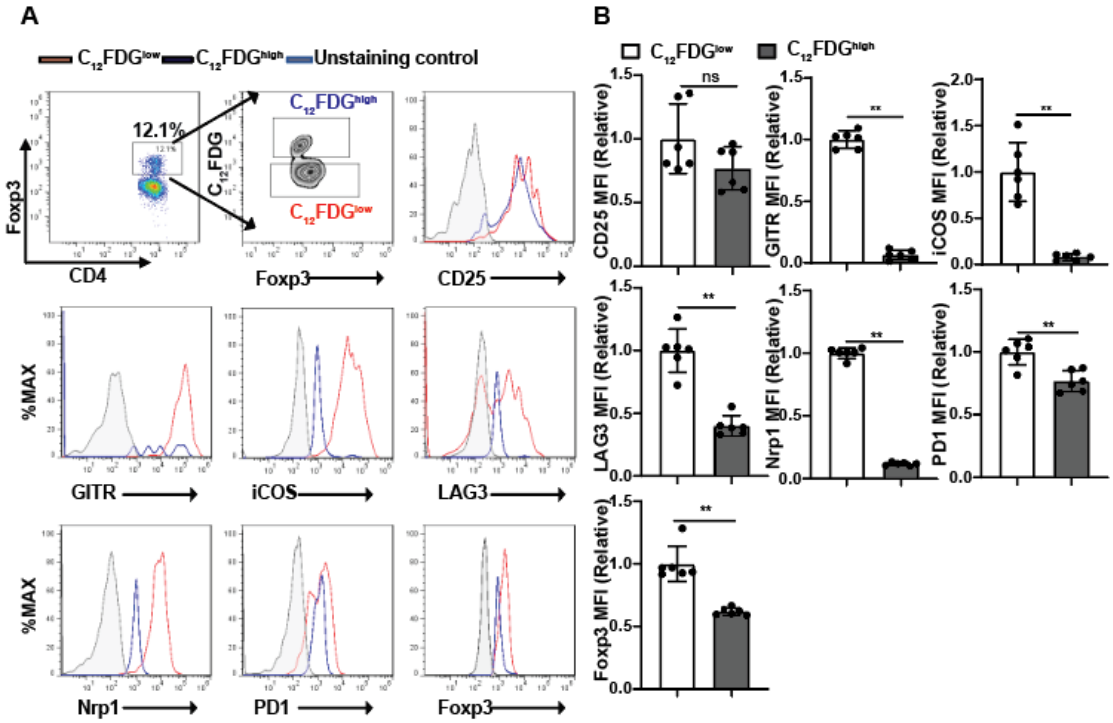

Figure 30 ***Senescent Tregs have decreased suppression markers.***
A, Representative histograms of CD25, GITR, iCOS, LAG3, Nrp1, PD1, and Foxp3 expression on senescence ($C_{12}FDG^{high}$) and non-senescence ($C_{12}FDG^{low}$) Treg cells from the spleen of 20 weeks western diet feed $ApoE^{-/-}$ mice. B, Relative mean fluorescence intensities (MFIs) of surface CD25, GITR, iCOS, LAG3, Nrp1, PD1, Foxp3 on senescence ($C_{12}FDG^{high}$) and non-senescence ($C_{12}FDG^{low}$) Treg cells from the spleen of 20 weeks western diet feed $ApoE^{-/-}$ mice (n=6 in each group). Data are presented as mean±SD, ns $p>0.05$, *$p<0.05$, and **$p<0.01$ by Student *t* test.

Furthermore, the frequency of IL-10^{+} Tregs and expression of IL-10, an essential immunosuppressive cytokine secreted by Tregs, were significantly decreased in senescence Tregs (**Figure 31A and 31B**). Atherosclerosis was shown to drive Treg plasticity and form IFNγ-producing Th1-like Tregs(Butcher et al., 2016). We then hypothesized whether senescent Tregs are more likely to be plasticity and form IFNγ-producing Tregs. Compared to non-senescent Tregs, we found a significantly increased frequency of IFNγ^{+} cells and IFNγ expression in senescent Tregs (**Figure 31C and 31D**). Thus, all these data suggest that decreased immunosuppressive markers and increased proinflammatory cytokine in senescent Tregs promote its plasticity and cause impaired protective function on arterial inflammation and atherosclerosis development.

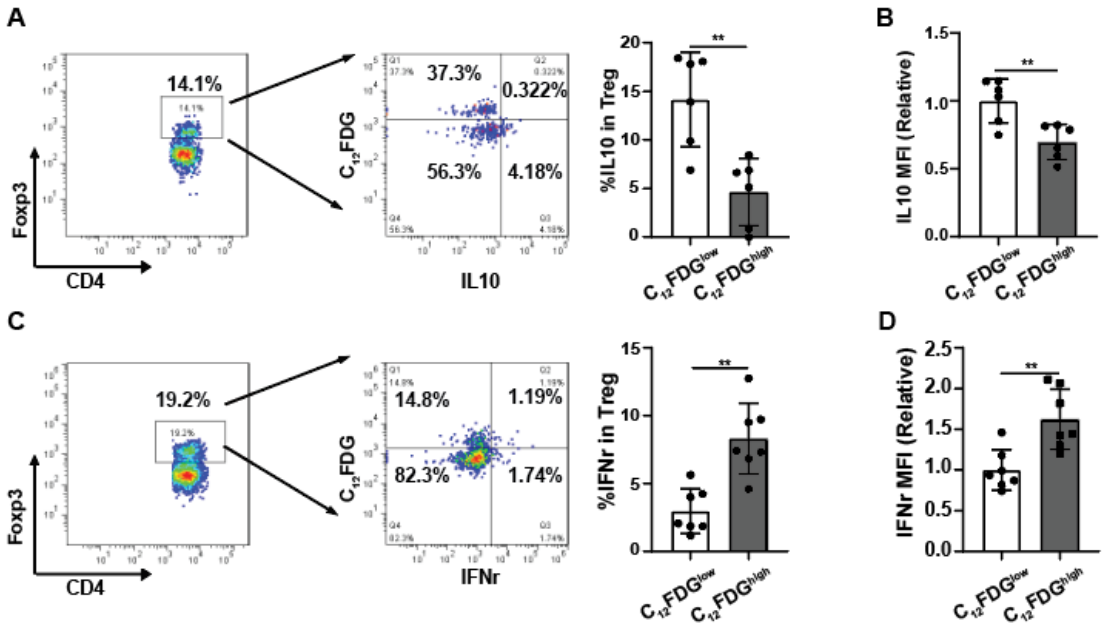

Figure 31 ***Senescent Tregs are more likely to be plasticity.***
A, Representative flow cytometry figure and quantification of IL10 expression in senescence ($C_{12}FDG^{high}$) and non-senescence ($C_{12}FDG^{low}$) Treg cells from the spleen of 20 weeks western diet feed $ApoE^{-/-}$ mice (n=6 in each group). B, Relative MFI of IL10 on senescence ($C_{12}FDG^{high}$) and non-senescence ($C_{12}FDG^{low}$) Treg cells from the spleen of 20 weeks western diet feed $ApoE^{-/-}$ mice (n=6 in each group). C, Representative flow cytometry figure and quantification of IFNγ expression in senescence ($C_{12}FDG^{high}$) and non-senescence ($C_{12}FDG^{low}$) Treg cells from the spleen of 20 weeks western diet feed $ApoE^{-/-}$ mice (n=7 in each group). D, Relative MFI of IFNγ on senescence ($C_{12}FDG^{high}$) and non-senescence ($C_{12}FDG^{low}$) Treg cells from the spleen of 20 weeks western diet feed $ApoE^{-/-}$ mice (n=7 in each group). Data are presented as mean±SD, ns $p>0.05$, and $^{**}p<0.01$ Student *t* test.

4.4.5 Cholesterol Accumulation Leads to Treg Senescence

To investigate the role of Cholesterol in the induction of Treg senescence, we firstly analyzed the cholesterol content in both Tconv cells and Treg cells from young (2 months) and aged (24 months) mice. We found both Tconv cells and Treg cells from aged mice showed higher cholesterol content in both their cell membrane and intracellular (**Figure 32A and 32B**). More interestingly, when we compared the cholesterol content between aged Tconv cells and aged Treg cells, we found aged Treg cells even showed higher cholesterol content in both their cell membrane and intracellular (**Figure 32A and 32B**). To further test the role of cholesterol in Treg senescence, we treated isolated $CD4^+$ T cells with different lipid components. We found compared to other lipid components, CD-CHO(Cholesterol-methyl-β-cyclodextrin), the most efficient manner to load cholesterol into cells in vitro, treatment shows the strongest effects on the induction of Treg

senescence (**Figure 32C**). CD-CHO complexes are the most efficient manner to load cholesterol into cells in vitro in T cells(Li et al., 2020b). Also, under different dose of CD-CHO treatment, Treg cells showed more sensitive to be senescence than Tconv cells (**Figure 32D**). Meanwhile, CD-CHO *in vitro* treatment dramatically increased the mRNA expression of $p16^{Ink4a}$, $p19^{Arf}$, and $p21^{Cip1}$ (**Figure 32E**). Furthermore, the protein expression of $p16^{Ink4a}$ and $p21^{Cip1}$ were also increased under CD-CHO treated Treg cells but not in Tconv cells (**Figure 32F and 32G**).

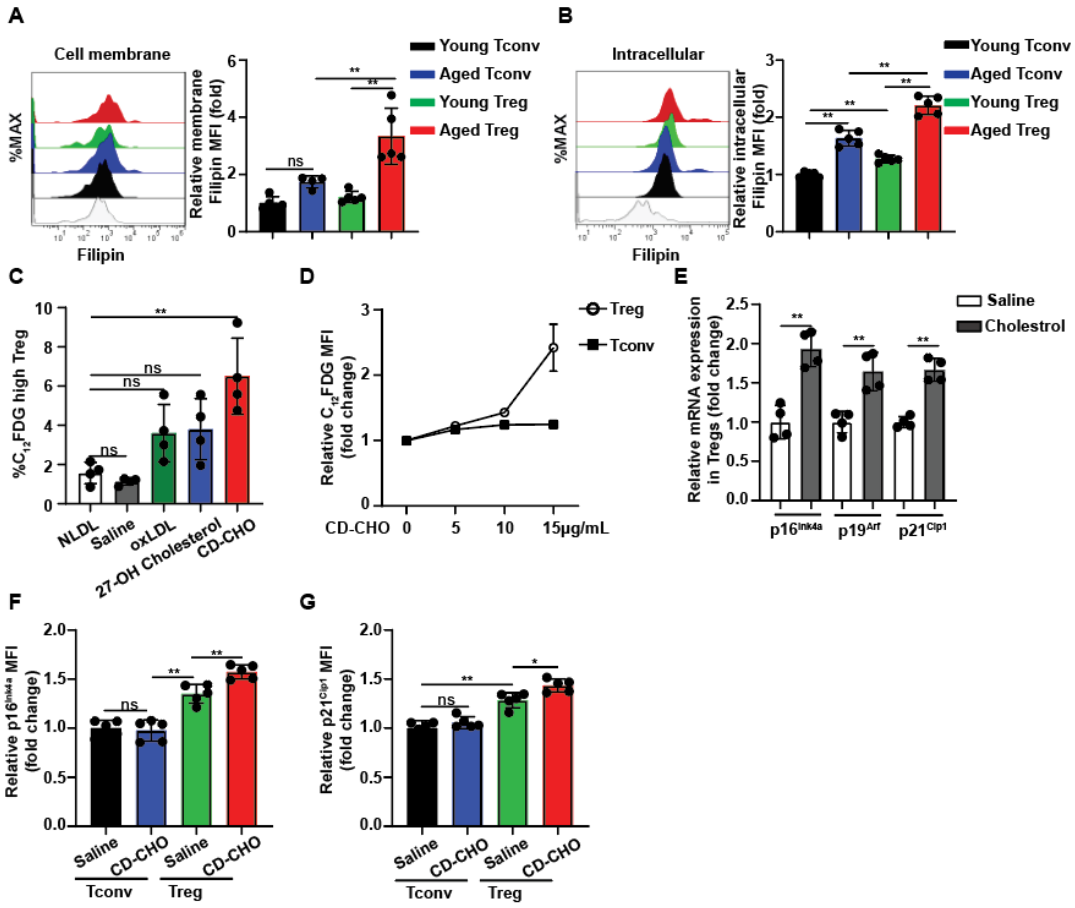

Figure 32. ***High cholesterol leads to Treg senescence***
The cholesterol content in both Tconvs and Tregs from young (2 months) and aged (24 months) wild-type mice were analyzed by filipin staining. A, Representative flow cytometry plots and quantification of cell membrane filipin staining on Tconvs and Tregs (n=4/group). B, Representative flow cytometry plots and quantification of intracellular filipin staining on Tconvs and Tregs (n=4/group). C, Isolated $CD4^+$ T cells were treated with normal LDL, saline, oxLDL, 27-OH cholesterol, and CD-CHO *in vitro* and quantification of senescent Treg cells were analysis by flow cytometry (n=4/group). D, Quantification of senescent Tconvs and Tregs under indicated dose of CD-CHO treatment (n=4/group/dose). E, Relative mRNA expression of $p16^{Ink4a}$, $p19^{Art}$, $p21^{Cip1}$ in sorted Treg cells ($CD4^+CD25^+$) treated with saline or cholesterol (n=4/group). F-G, Relative protein expression of $p16^{Ink4a}$ and $p21^{Cip1}$ in Tconvs and Tregs treated with saline or cholesterol (n=5/group). Data are presented as mean±SD, ns $p>0.05$, *$p<0.05$, and **$p<0.01$ by Student *t* test.

4.4.6 Decreased AMPKα1 Leads to Treg Senescence Under Hyperlipidemia Condition

Next, we explored the potential factor contributing to Treg senescence during atherogenesis and found the expression of AMPKα1, an essential factor to restrain cellular senescence(Ido et al., 2012; Inata et al., 2018), was decreased among aged Tregs (**Figure 33A**). Notably, decreased AMPKα1 protein expression was also observed in isolated Tregs from 16 weeks western diet fed ApoE-/- mice (**Figure 33B-33D**), or in Tregs after *in vitro* cholesterol and 7KC treatment (**Figure 33E**). However, the mRNA level of AMPKα1 was comparable between Tregs from chow diet or western diet feed ApoE$^{-/-}$ mice (**Figure 33F**), which indicate a posttranslational regulation of AMPKα1 by hypercholesterolemia. In contrast, the expression of AMPKα1 showed no reduction in Tconv (CD4^{+}CD25^{-}) cells after western diet treatment (**Figure 33G**). Therefore, these data suggest that AMPKα1 may involve in the progression of Treg senescence.

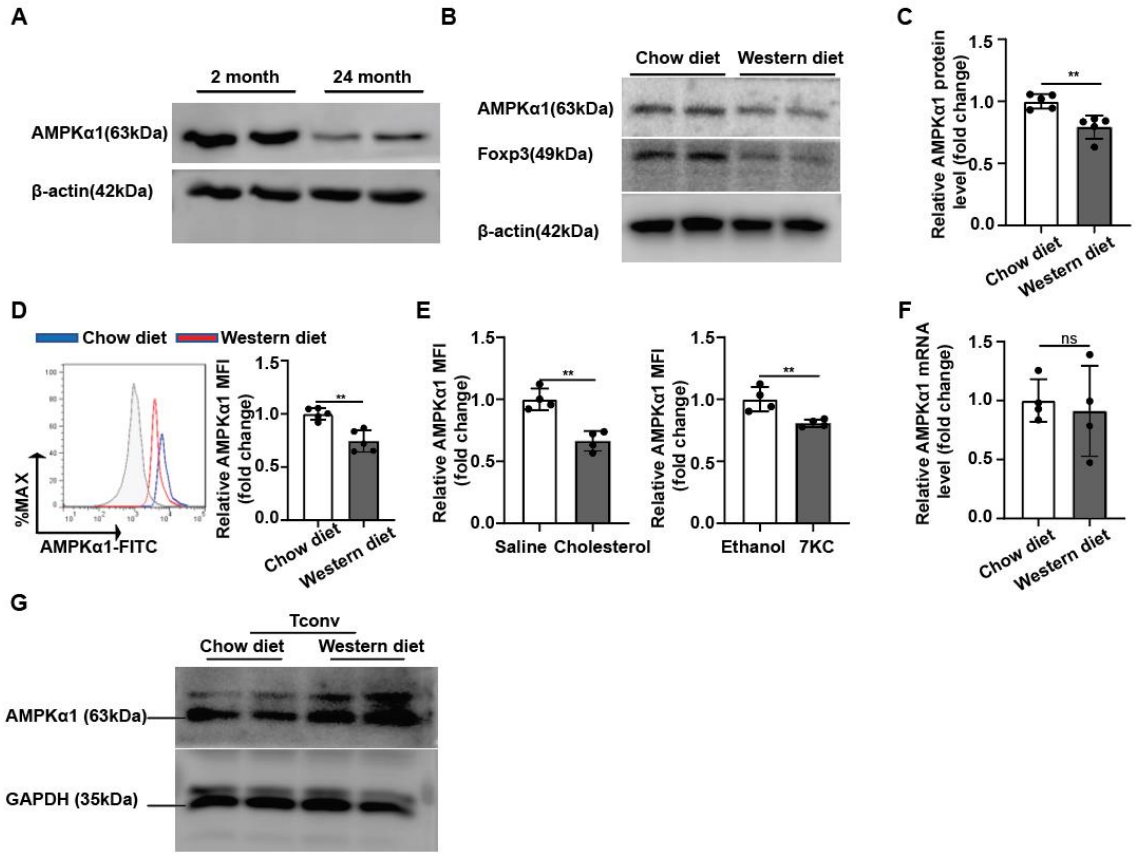

Figure 33. ***Decreased AMPKα1 protein level in aged and hypercholesterolemia-treated Tregs.***
A, Western bolt analysis of AMPKα1 expression in Treg cells isolated from the spleen of 2-month-old and 24-month-old C57 BL/6J mice. B-C, Representative western blot (B) and quantification (C) of relative

AMPKα1 expression in sorted Treg cells from splenocytes of 16 weeks chow diet or western diet treated ApoE$^{-/-}$ mice (n=4 in each group). D, Representative histogram and quantification of relative AMPKα1 expression in Tregs from splenocytes of 16 weeks chow diet or western diet treated ApoE$^{-/-}$ mice (n=4 in each group). E, Quantification of relative AMPKα1 expression in Treg cells treated with cholesterol and 7KC (n=4 in each group). F, Quantification of relative AMPKα1 mRNA level in sorted Treg cells from splenocytes of 16 weeks chow diet or western diet treated ApoE$^{-/-}$ mice (n=4 in each group). G, Western blot analysis of AMPKα1 expression in Tconv (CD4^{+}CD25^{-}) cells isolated from 16 weeks western diet or chow diet feed ApoE$^{-/-}$ mice. Data are presented as mean±SD, ns p>0.05, *p<0.05, and **p<0.01 by Student *t* test.

We next analyzed the role of AMPKα1 on Treg senescence and found both Tregs from AMPKα1 global knockout mice (*Prkaa1*$^{-/-}$) (**Figure 34A and 34B**) and Treg-specific AMPKα1 knockout mice (AMPKα1$^{Treg-/-}$) displayed a higher SA-β-gal activity (**Figure 34C and 34D**). Meanwhile, Tregs from AMPKα1$^{Treg-/-}$ mice showed higher mRNA levels of p16^{Ink4a}, p19^{Arf}, and p21^{Cip1}than those from AMPKα1$^{Treg+/+}$ mice, which presented a senescence phenotype (**Figure 34E**). In addition, mice with Treg-specific AMPKα1 deletion developed aging-related autoimmunity (**Figure 35A and 35B**). All these data indicate AMPKα1 is required to prevent Treg senescence, and deficiency of AMPKα1 may be responsible for the Treg senescence under cholesterol treatment. Indeed, we found that overexpression of CA-AMPK (constitutively active AMPK) (**Figure 35C**) prevented cholesterol-induced Treg senescence (**Figure 34F and 34G**). These findings collectively suggest that hyperlipidemia induces Treg senescence via downregulating AMPKα1 expression.

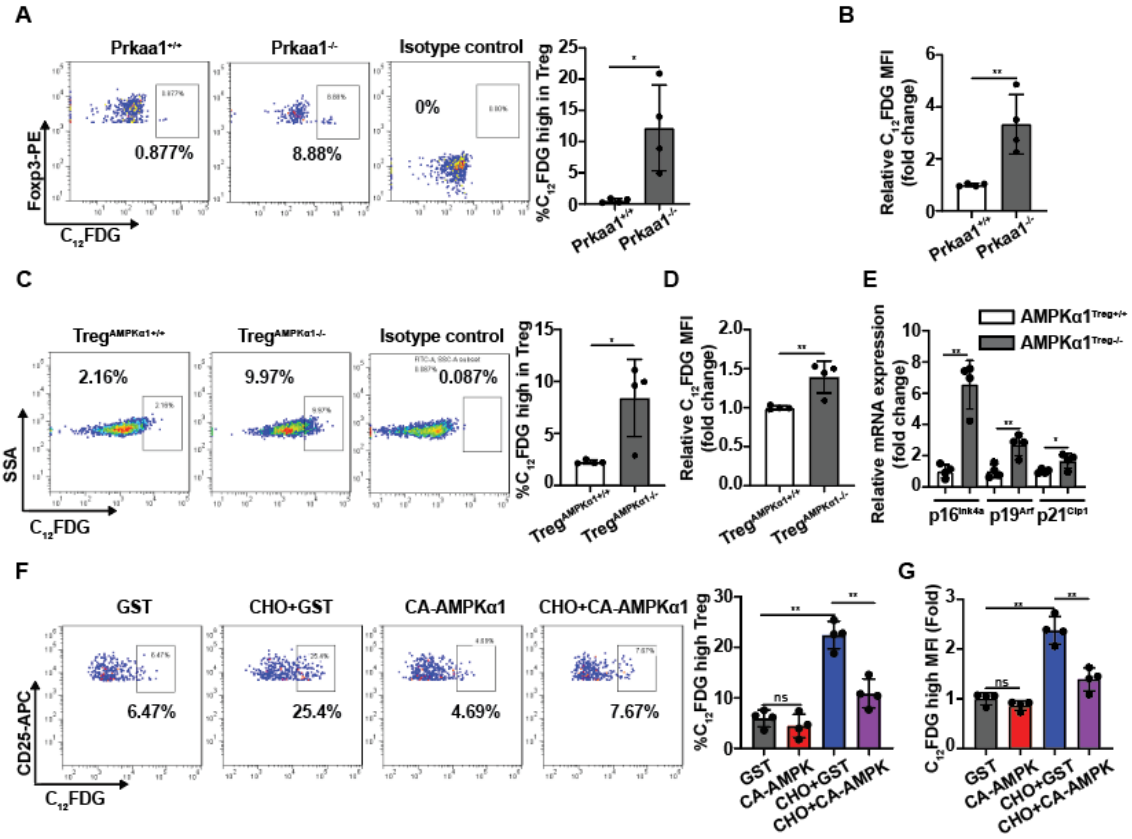

Figure 34. Selective *activation of AMPK prevents Treg senescence.*
A, Representative flow figures and quantification of percentage of C_{12}FDG high Treg cells among Treg cells from the splenocytes of 7-week-old Prkaa1$^{+/+}$ and Prkaa1$^{-/-}$ mice (n=4 in each group). B, Relative MFIs of C_{12}FDG in Tregs from Prkaa1$^{+/+}$ and Prkaa1$^{-/-}$ mice (n=4 in each group).C, Representative flow figures and quantification of percentage of C_{12}FDG high Treg cells among isolated Treg cells from 8-10-week-old AMPKα1$^{Treg+/+}$ and AMPKα1$^{Treg-/-}$ mice (n=4 in each group). D, Relative MFIs of C_{12}FDG in Tregs from AMPKα1$^{Treg+/+}$ and AMPKα1$^{Treg-/-}$ mice (n=4 in each group). E, Quantification of relative p16, p19, and p21 mRNA level in Treg cells isolated from 8-10-week-old AMPKα1$^{Treg+/+}$ and AMPKα1$^{Treg-/-}$ mice (n=4 in each group). F, Isolated CD4^{+} T cells from C57 BL/6J mice were transfected with lentivirus-GST control or lentivirus-GST-CA-AMPK, and then treated with cholesterol and saline for 24 hours. Percentage of C_{12}FDG high Treg cells in indicated groups were analyzed by flow cytometry (n=4 in each group). G, Relative MFIs of C_{12}FDG in Tregs of indicated groups (n=4 in each group). Data are presented as mean±SD, ns p>0.05, *p<0.05, and **p<0.01 by Student *t* test (A-E) and one way ANOVA (F and G).

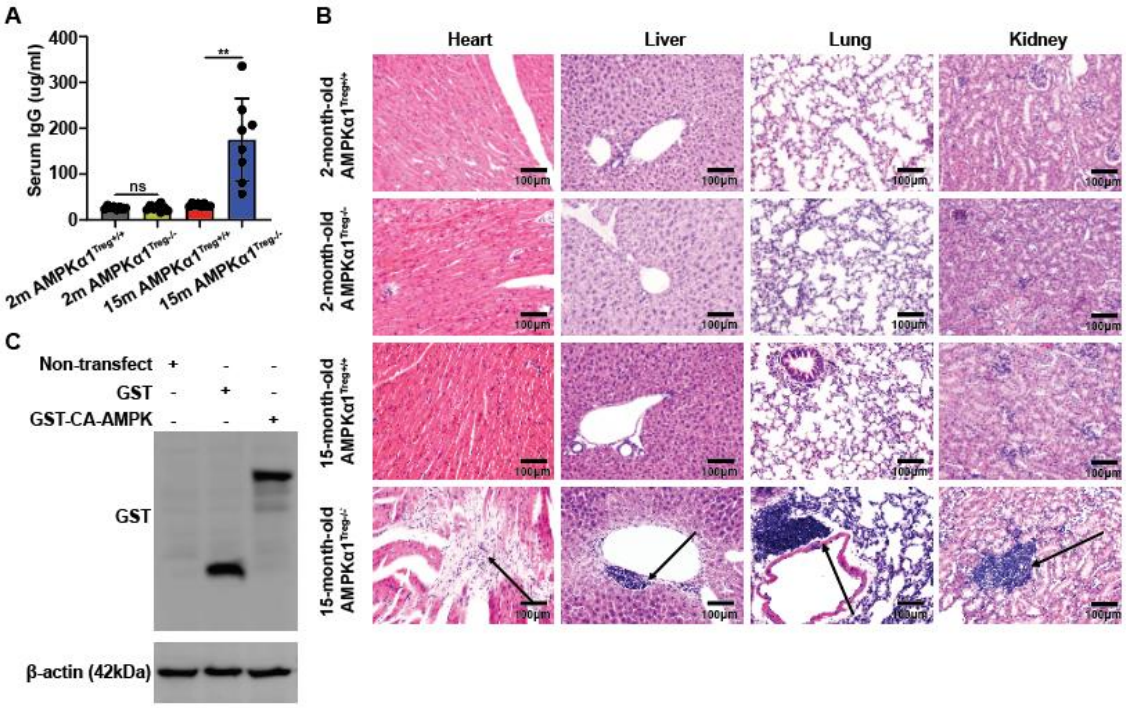

Figure 35. ***Deficiency of AMPKα1 in Tregs causes inflammaging.***
A, Quantification of serum total IgG level in 2-month-old and 24-month-old AMPKα1$^{Treg+/+}$ and AMPKα1$^{Treg-/-}$ mice (n=8 in each group). B, Representative H&E staining images for heart, liver, lung, and kidney from 2-month-old and 15-month-old AMPKα1$^{Treg+/+}$ and AMPKα1$^{Treg-/-}$ mice (arrow indicate immune cell infiltration, scar bar=100μm). C, Western blot analysis of GST expression in CD4^{+} T cells transfected with lentivirus-GST or lentivirus-GST-CA-AMPK. Data are presented as mean±SD, ns p>0.05 and **p<0.01 by student t test.

4.4.7 AMPKα1 Attenuates Treg Senescence via Restraining ROS Levels

Following the above findings, we further explored how AMPK regulates Treg senescence. Aberrant accumulation of ROS was shown as a predominant contributor to Treg senescence(Guo et al., 2020). Even though AMPK has been widely reported as an essential ROS regulator in different types of cells(Ren and Shen, 2019; Zhao et al., 2017), its role in ROS production of Tregs is still unknown. Here we found that Tregs from both AMPKα1$^{Treg-/-}$ and Prkaa1$^{-/-}$ mice displayed a significantly upregulated ROS level than those from their littermate control mice (**Figure 36A and 36B**). Meanwhile, the expression of mitochondria ROS was also significant increase in AMPKα1-deficient Tregs (**Figure 36C**). Furthermore, downregulation of ROS levels by its scavengers GSH and Mito TEMPO can effectively recover the senescence phenotype caused by AMPKα1 deletion in Treg cells (**Figure 36D-36E**). Thus, the excessive ROS production is a critical mechanism

underlying Treg senescence caused by AMPKα1 deletion.

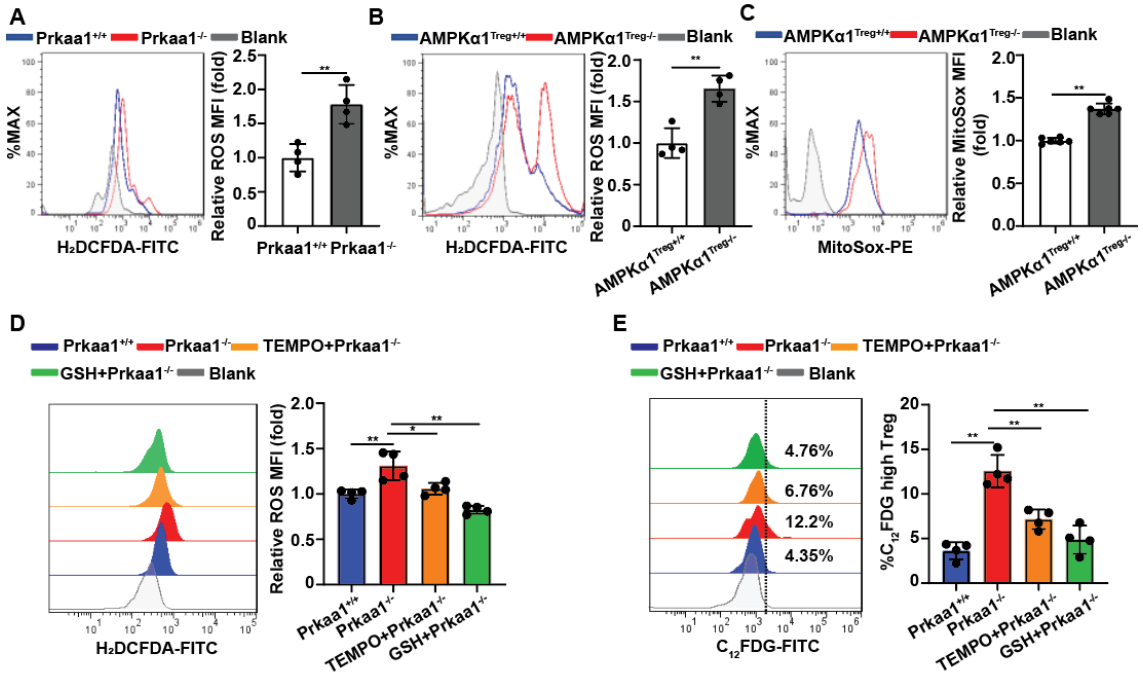

Figure 36. ***AMPK prevents Treg senescence via inhibition of ROS production.***
A, Representative histogram and quantification of relative ROS expression in expression in Treg cells from splenocytes of *Prkaa1*$^{+/+}$ and *Prkaa1*$^{-/-}$ mice (blank, no DCFDA, n=4 in each group). B, Representative histogram and quantification of relative ROS expression in Treg cells from splenocytes of AMPKα1$^{Treg+/+}$ and AMPKα1$^{Treg-/-}$ mice (blank, no DCFDA, n=4 in each group). C, Representative histogram and quantification of relative Mitochondria ROS expression in Treg cells from splenocytes of AMPKα1$^{Treg+/+}$ and AMPKα1$^{Treg-/-}$ mice (blank, no MitoSox, n=4 in each group). D, Representative histogram and quantification of ROS expression in Treg cells from splenocytes of *Prkaa1*$^{+/+}$ and *Prkaa1*$^{-/-}$ mice in the absence or presence of Mito TEMPO(10 μM) or GSH (10 mM) (blank, no DCFDA, n=4 in each group).E, Representative flow figures and quantification of C12FDG high Treg cells from splenocytes of *Prkaa1*$^{+/+}$ and *Prkaa1*$^{-/-}$ mice in the absence or presence of Mito TEMPO(10 μM) or GSH (10 mM) (n=4 in each group). , data are presented as mean±SD, ns p>0.05 and **p<0.01 by student t test (A and B) and one way ANOVA (C and D).

4.4.7 AMPKα1 Deficiency in Tregs Causes Disturbed Immune Homeostasis in ApoE$^{-/-}$ Mice

Intrigued by the essential role of AMPKα1 on the senescence of Tregs, we further explored the role of AMPKα1 in Tregs on atherosclerosis. We constructed the ApoE$^{-/-}$ Treg-specific AMPKα1 deletion (ApoE$^{-/-}$AMPKα1$^{Treg-/-}$) mice via breeding ApoE$^{-/-}$ mice with our previous AMPKα1$^{Treg-/-}$ mice, and their littermate was used as control (ApoE$^{-/-}$AMPKα1$^{Treg+/+}$). We found that ApoE$^{-/-}$ AMPKα1$^{Treg-/-}$ mice displayed disturbed T cell homeostasis at six months old under chow diet conditions, with upregulated effector/memory and downregulated naïve CD4^{+} and CD8^{+} T cells

(**Figure 37A and 37B**). Additionally, both $CD4^+$ and $CD8^+$ T cells from $ApoE^{-/-}AMPK\alpha1^{Treg-/-}$ mice showed higher expression of IFNγ but not IL-4 (**Figure 37C-3F**).

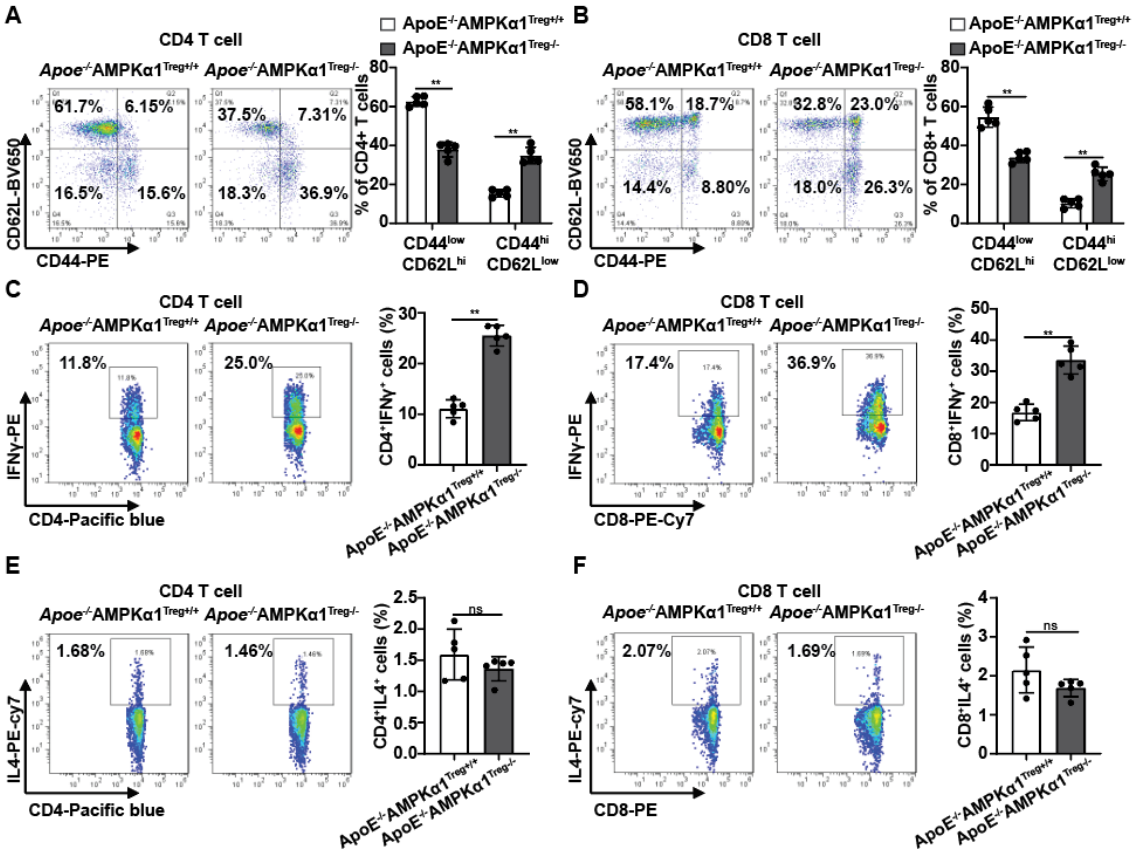

Figure 37 ***Deficiency of AMPKα1 disrupts T cell homeostasis in ApoE-/- mice.***
A-B, Representative flow images and quantification of naïve ($CD44^{low}CD62L^{high}$) and effector/memory ($CD44^{high}CD62L^{low}$) $CD4^+$ (A) and $CD8^+$ (B) T cells in spleens of 6-month-old $ApoE^{-/-}AMPK\alpha1^{Treg+/+}$ and $ApoE^{-/-}AMPK\alpha1^{Treg-/-}$ mice under chow diet condition (n=4 per group). C-D, Representative flow images and quantification of IFNγ production $CD4^+$ (C) and $CD8^+$ (D) T cells in spleens of 6-month-old $ApoE^{-/-}AMPK\alpha1^{Treg+/+}$ and $ApoE^{-/-}AMPK\alpha1^{Treg-/-}$ mice under chow diet condition (n=4 per group). E-F, Representative flow images and quantification of IL4 production $CD4^+$ (E) and $CD8^+$ (F) T cells in spleens of 6-month-old $ApoE^{-/-}AMPK\alpha1^{Treg+/+}$ and $ApoE^{-/-}AMPK\alpha1^{Treg-/-}$ mice under chow diet condition (n=4 per group). Data are presented as mean±SD, ns $p>0.05$, $^{**}p<0.01$, by Student's *t* test

Even though the frequency of $CD4^+YFP^+$ Tregs were comparable, the expression of Foxp3 was decreased in Tregs from $ApoE^{-/-}AMPK\alpha1^{Treg-/-}$ mice (**Figure 38A**). Moreover, compared to $ApoE^{-/-}AMPK\alpha1^{Treg+/+}$ mice, Tregs from $ApoE^{-/-}AMPK\alpha1^{Treg-/-}$ mice displayed less frequency of IL10+ cells while higher IFNγ+ cells (**Figure 38B and 38C**). These data suggest that AMPKα1 deletion induces Treg plasticity and disturbed immune homeostasis, which are similar to that of senescent Tregs caused by hyperlipidemia.

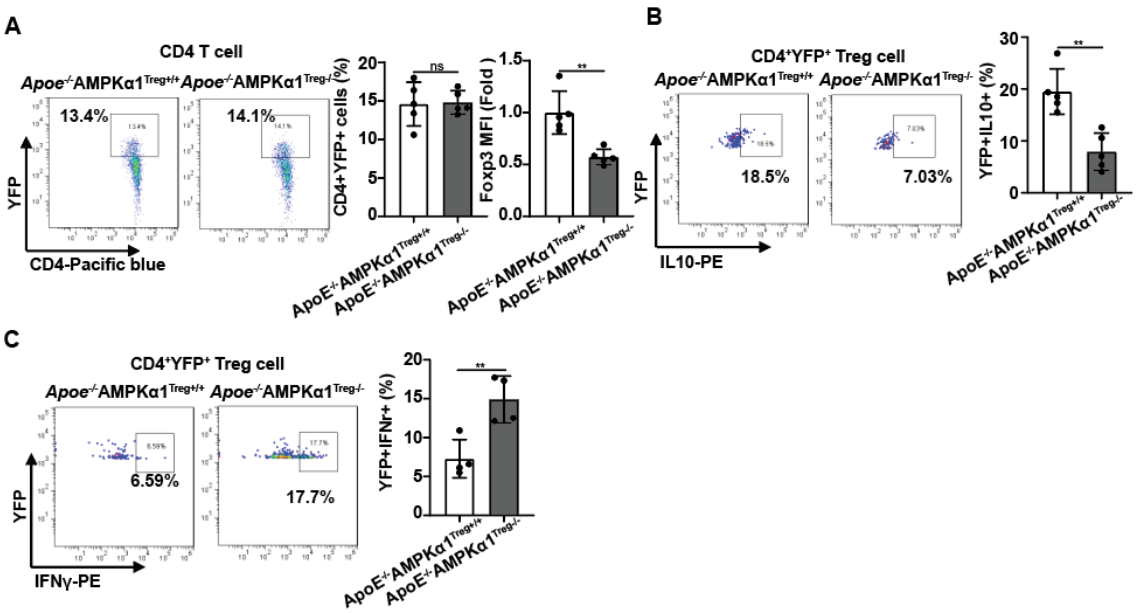

Figure 38 ***AMPKα1 is required to maintain Treg stability in ApoE-/- mice.***
A, Frequency of CD4+YFP+ Tregs in spleen and relative Foxp3 MFI in Tregs of 6-month-old ApoE$^{-/-}$AMPKα1$^{Treg+/+}$ and ApoE$^{-/-}$AMPKα1$^{Treg-/-}$ mice under chow diet condition (n=4 per group). B-C, Representative flow images and quantification of IL-10 production (B) and IFNγ (C) production Treg cells in spleens of 6-month-old ApoE$^{-/-}$AMPKα1$^{Treg+/+}$ and ApoE$^{-/-}$AMPKα1$^{Treg-/-}$ mice under chow diet condition (n=4 per group). Data are presented as mean±SD, ns p>0.05, **p<0.01, by Student's *t* test

4.4.8 Deficiency of AMPKα1 in Tregs Promotes Immune Cell Infiltration in the Aortas of ApoE$^{-/-}$ Mice

We next performed flow cytometry to analyze the immune cell infiltration in the aorta of 6-month-old ApoE$^{-/-}$AMPKα1$^{Treg+/+}$ and ApoE$^{-/-}$AMPKα1$^{Treg-/-}$ mice under chow diet condition (**Figure 39A**). Compared to ApoE$^{-/-}$AMPKα1$^{Treg+/+}$ mice, the immune cell infiltration was significant increase in the aorta of ApoE$^{-/-}$AMPKα1$^{Treg-/-}$ mice, including higher frequency and numbers of CD45^{+} cells (**Figure 39B and 39C**) and CD3^{+} T cells (**Figure 39D and 39E**). Further analysis showed that both the frequency and numbers of CD4^{+}CD8^{-} and CD4^{-}CD8^{+} T cells were significant increase in the aorta of ApoE$^{-/-}$AMPKα1$^{Treg-/-}$ mice (**Figure 39F-39H**). However, even though the frequency of Treg cells in aorta was comparable the total numbers of Tregs were increased in the arterials of ApoE$^{-/-}$AMPKα1$^{Treg-/-}$ mice, which could be due to the increased total numbers of T cells (**Figure 39I-39K**). These data suggest that AMPKα1 is required for Treg function but has mild effect on Treg survival in the aorta.

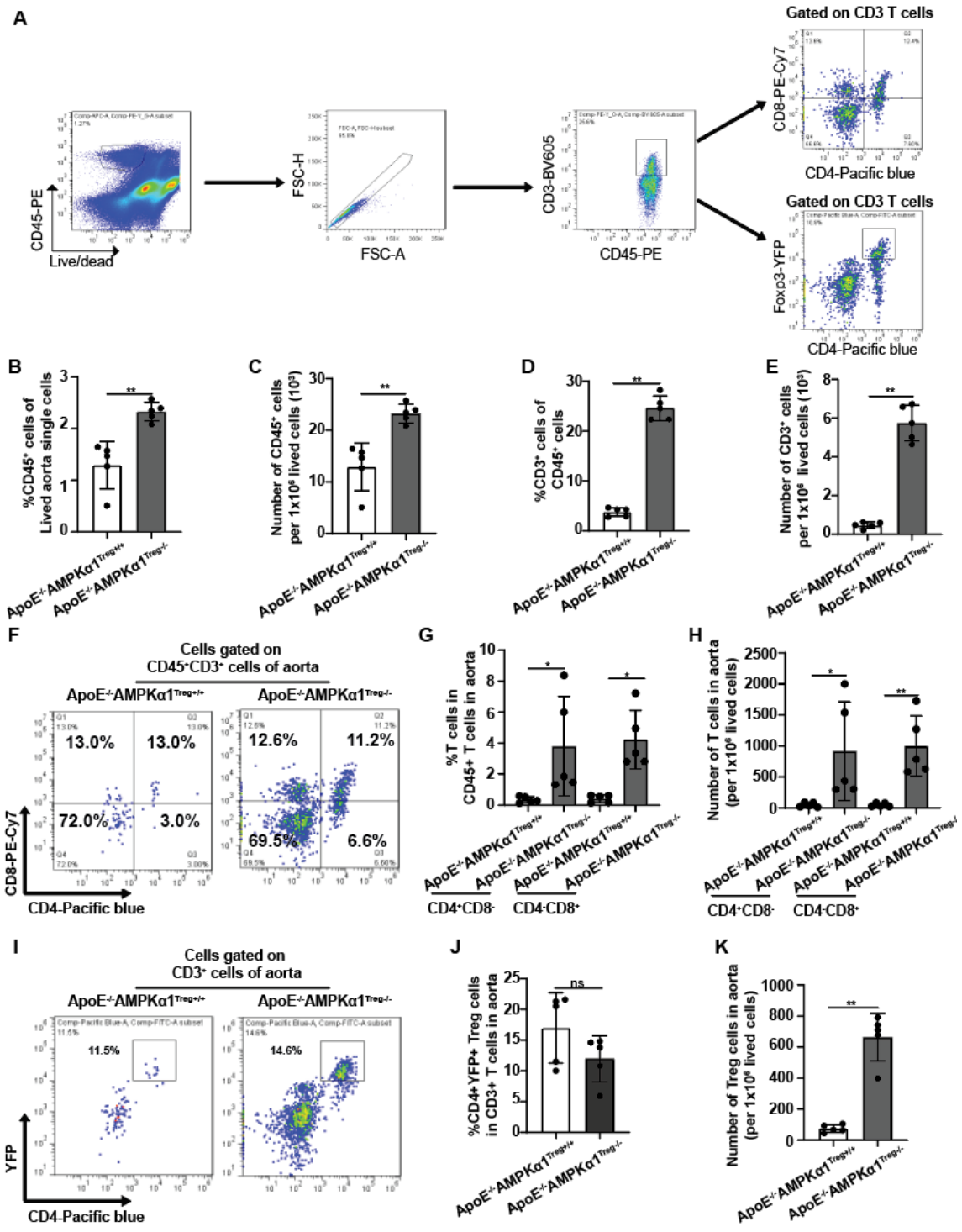

Figure 39. ***Deficiency of AMPKα1 in Tregs promotes immune cell infiltration in aorta of ApoE$^{-/-}$ mice.*** A, Gating strategy of CD45$^+$ cells, CD3$^+$, CD4$^+$, CD8$^+$ T cells, and CD4$^+$YFP$^+$ Treg cells from aorta single cells. B-C, Quantification of percentage (B) and number (C) of CD45$^+$ cells among aorta single cells from 6-month-old ApoE$^{-/-}$Treg$^{AMPKα1+/+}$ and ApoE$^{-/-}$Treg$^{AMPKα1-/-}$ mice under chow diet condition (each sample is pooled by four mice aorta, n=5 in each group). D-E, Quantification of percentage (D) and number (E) of CD3$^+$ cells among aorta single cells from 6-month-old ApoE$^{-/-}$Treg$^{AMPKα1+/+}$ and ApoE$^{-/-}$Treg$^{AMPKα1-/-}$ mice under chow diet condition (each sample is pooled by four mice aorta, n=5 in each group). F, Representative flow figures of CD45$^+$CD3$^+$CD4$^+$ T cells and CD45$^+$CD3$^+$CD8$^+$ T cells among aorta single cells were

analyzed by flow cytometry. G-H, Quantification of percentage (G) and number (H) of $CD4^+CD8^-$ T cells and $CD4^-CD8^+$ T cells among aorta single cells from 6-month-old $ApoE^{-/-}Treg^{AMPK\alpha1+/+}$ and $ApoE^{-/-}Treg^{AMPK\alpha1-/-}$ mice under chow diet condition (each sample is pooled by four mice aorta, n=5 in each group). I, Representative flow figures of $CD45^+CD3^+CD4^+$ YFP^+ Treg cells among aorta single cells were analyzed by flow cytometry. J-K, Quantification of percentage (J) and number (K) of Treg cells among aorta single cells from 6-month-old $ApoE^{-/-}Treg^{AMPK\alpha1+/+}$ and $ApoE^{-/-}Treg^{AMPK\alpha1-/-}$ mice under chow diet condition (each sample is pooled by four mice aorta, n=5 in each group). Data are presented as mean±SD, ns $p>0.05$, *$p<0.05$, and **$p<0.01$ by Student *t* test.

4.4.9 Deficiency of AMPKα1 in Tregs Promotes Arterial Inflammation and Atherosclerosis

We next aimed to investigate the effects of AMPK in Tregs on arterial inflammation and atherosclerosis. $ApoE^{-/-}AMPK\alpha1^{Treg-/-}$ mice and their littermate controls ($ApoE^{-/-}AMPK\alpha1^{Treg+/+}$) were fed chow diet and sacrificed at 6-month-old to detect the cytokine expression in aorta tissues and plaque formation. As shown in **Figure 41A and 41B,** no difference in serum cholesterol and triglyceride levels was observed in the two groups of mice, whereas $ApoE^{-/-}AMPK\alpha1^{Treg-/-}$ mice displayed significant increased mRNA level of IFN-γ, IL-1β， IL-17， and TNF-α in the aorta (**Figure 40A**).Moreover, $ApoE^{-/-}AMPK\alpha1^{Treg-/-}$ mice developed much more lesions area in whole aorta and aortic root area compared with $ApoE^{-/-}AMPK\alpha1^{Treg+/+}$ mice (**Figure 40B and 40C**). Similar changes were also observed in the female mice of these two groups (**Figure 41C**). Furthermore, the expression of macrophage, which was detrimental for plaque stability(Colin et al., 2014), were significant increase in the plaque area of $ApoE^{-/-}AMPK\alpha1^{Treg-/-}$ mice (**Figure 40D**). Thus, all these data demonstrated AMPKα1 in Tregs is required to prevent atherosclerosis plaque formation and vulnerability.

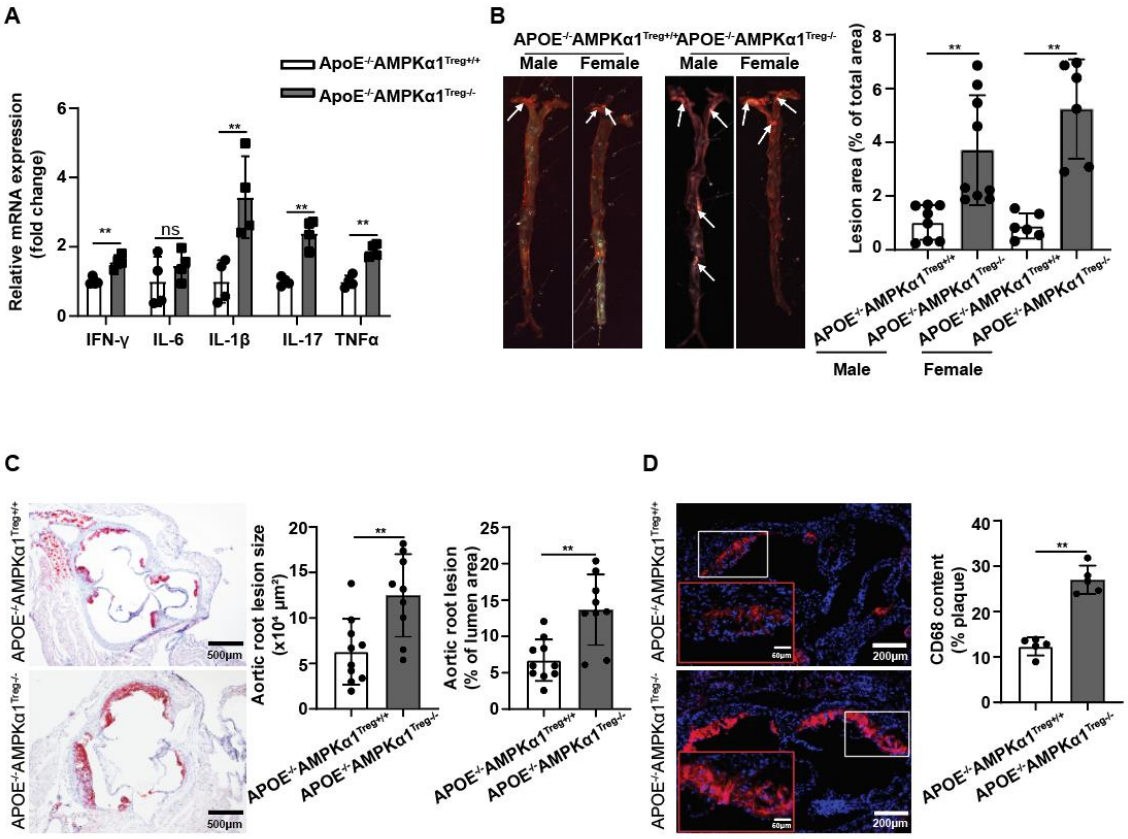

Figure 40. ***AMPKα1 in Tregs is required to prevent arterial inflammation and atherosclerosis.***
A, Relative mRNA level of indicated cytokines in the aorta tissues of 6-month-old ApoE$^{-/-}$Treg$^{AMPKα1+/+}$ and ApoE$^{-/-}$Treg$^{AMPKα1-/-}$ mice under chow diet condition (each sample is pooled by four mice aorta, n=4 in each group). B, Representative images and quantification of atherosclerotic plaque area by en face analysis of the aorta (n=8 in male ApoE$^{-/-}$AMPKα1$^{Treg+/+}$ mice, n=9 in male ApoE$^{-/-}$AMPKα1$^{Treg-/-}$ mice, n=7 in both female ApoE$^{-/-}$AMPKα1$^{Treg+/+}$ mice and ApoE$^{-/-}$AMPKα1$^{Treg-/-}$ mice). C, Representative images and quantification of atherosclerotic plaque size and % plaque is to lumen area by cross-sectional analysis of the aortic root (n=10 in ApoE$^{-/-}$AMPKα1$^{Treg+/+}$ group, n=9 ApoE$^{-/-}$AMPKα1$^{Treg-/-}$ group, Scale bar=500μm). D, Representative images and quantification of CD68 content among atherosclerotic plaque (n=5 in each group, Scale bar=200μm). Data are presented as mean±SD, ns p>0.05, *p<0.05, and **p<0.01 by Student *t* test.

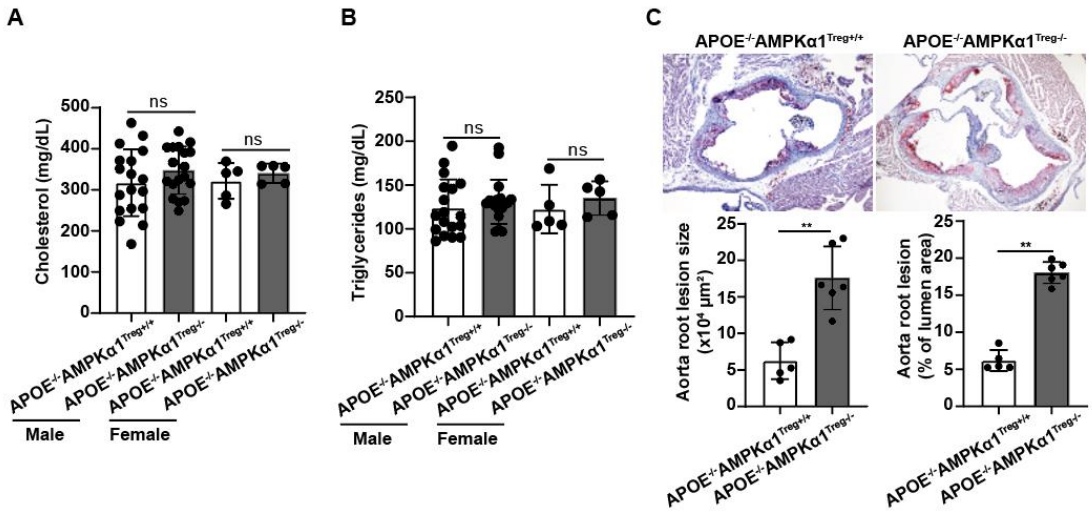

Figure 41. ***Deficiency of AMPKα1 in Tregs aggravates atherosclerosis in female ApoE-/- mice.***
A-B, Quantification of serum cholesterol (A) and triglycerides (B) level from 6-month-old ApoE$^{-/-}$Treg$^{AMPKα1+/+}$ and ApoE$^{-/-}$Treg$^{AMPKα1-/-}$ mice under chow diet condition (n=18 in each group). C, Representative oil red staining images and quantification of atherosclerotic plaque size and lesion area by cross-sectional analysis of the aortic root of female mice (n=5 in each group). Data are presented as mean±SD, ns $p>0.05$ and **$p<0.01$ by Students' *t* test.

4.4.10 Adoptive Transfer CA-AMPK Treg Ablates Atherosclerosis and Atherosclerotic Plaque Vulnerability

Given the essential role of AMPK in Treg in the development of atherosclerosis. We next investigated whether adoptive transfer CA-AMPK (constitutive active AMPK) Treg can prevent atherosclerosis development. We treated 8-week-old ApoE$^{-/-}$ mice with 12 weeks western diet and transferred GFP-Treg and GFP-CA AMPK Treg at the 8-week and the 10-week (**Figure 42A**). At the end of the treatment, GFP^{+} cells were still detected in the atherosclerotic aorta of recipient mice (**Figure 42B**), paralleled by a few cells detectable in the spleen (**Figure 42C**). Analyzed the T cells in the aorta, we found compared to non-Treg transfer group, adoptive transfer CA AMPK-Tregs but not GFP-Tregs significantly decreased the frequency of CD8^{+} T cells in the aorta (**Figure 42D and 42E**).

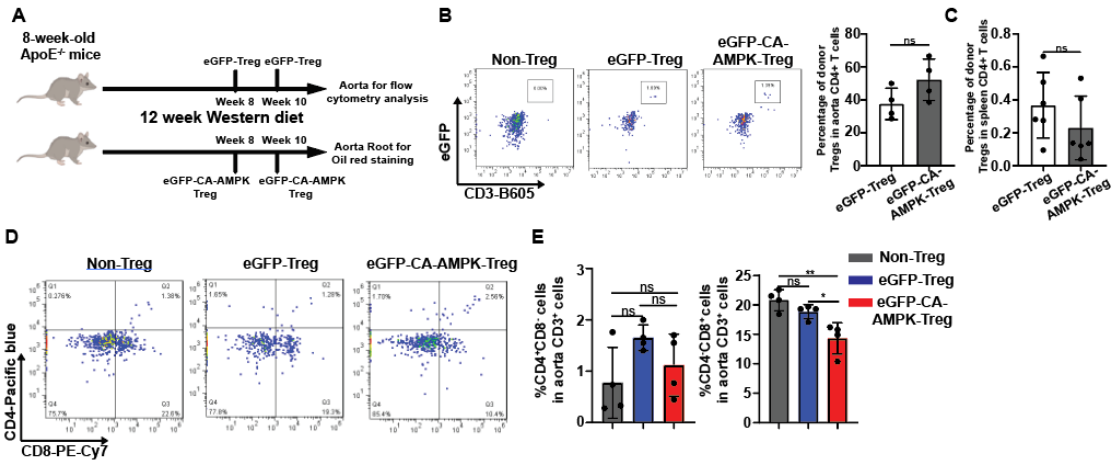

Figure 42. ***Adoptive transfer CA AMPK Treg prevent the infiltration of CD8+ T cells in aorta.***
A, Experiment designs and schematic diagram of adoptive Treg transfer experiment. Western diet feeding 8-week-old ApoE$^{-/-}$ mice received medium alone (non-Treg), GFP-Tregs or GFP-CA AMPK Tregs. B-C, The expression of donor Tregs in the aorta (B) (n=4/group) and spleen (C) (n=6/group) of recipient mice.D-E, Representative flow cytometry images (D) and quantification of CD4^{+}CD8- T cells and CD4^{-}CD8^{+} T cells frequency (E) (n=4/group). Data are presented as mean±SD, ns p>0.05, *p<0.05 and **p<0.01 by Students' *t* test (B and C) and one-way ANOVA (E).

Further analysis showed that treatment with CA AMPK-Tregs but not GFP-Tregs significant reduced macrophage content among the plaque areas (**Figure 43A and 43B**). Most importantly, adoptive transfer with CA AMPK-Tregs but not GFP-Tregs significantly decreased the plaque area at the aortic root compared to GFP-Tregs (**Figure 43C and 43D**). Furthermore, treatment with CA AMPK-Tregs also resulted in a significant increase in collagen content and reduced necrotic core compared to mice treated with GFP-Tregs. Of note, even though mice treated with GFP-Tregs also showed reduced necrotic core compared to untreated mice, the reduced fold was much less than that treated with CA AMPK Tregs (**Figure 43E and 43F**).

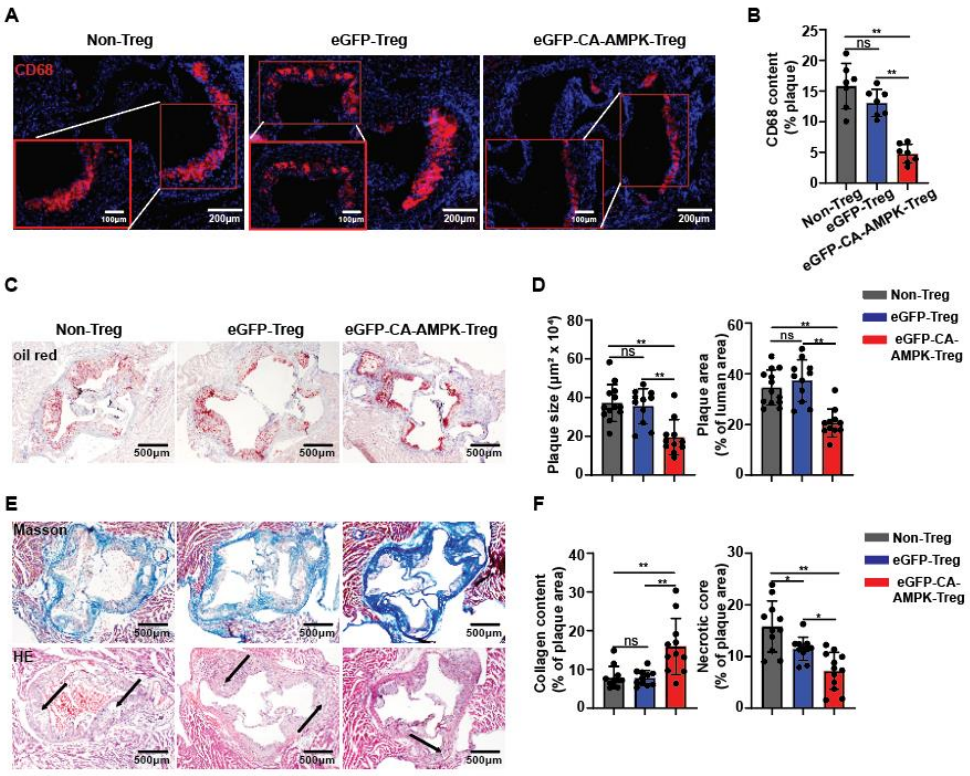

Figure 43. ***CA AMPK Treg treatment prevents atherosclerosis development and plaque vulnerability.*** A-B Representative IF images and quantification of CD68 content in plaque area (n=7/group).C-D, Representative oil red staining images and quantification of plaque size and plaque area (n=12/group). E-F, Representative Masson and H&E staining images and quantification of collagen content and necrotic core size (n=11/group). Data are presented as mean±SD, ns p>0.05, *p<0.05 and **p<0.01 by one-way ANOVA.

4.4.11 Adoptive Transfer of CA AMPK-Tregs Partially Restores the Immune Homeostasis in Western Diet-treated ApoE-/- Mice

Further analysis the T cell function in the spleen and peripheral lymph nodes, we found adoptive transfer of CA AMPK-Tregs can partially restores the disturbed immune homeostasis in western diet-fed ApoE$^{-/-}$ mice. Treatment with CA AMPK-Tregs, but not GFP-Tregs, increased naïve T cells (CD44^{low}CD62L^{high}) expression in both CD4^{+} T cells and CD8^{+} T cells in both peripheral lymph nodes and spleen. Meanwhile, treatment with CA AMPK-Tregs can also reduce the frequency of effector T cells (CD44^{high}CD62L^{low}) in CD8+ T cells (**Figure 44A-44D**). For IFNγ production, treatment with CA AMPK-Tregs showed mild effects on the production of IFNγ in CD4+ T cells (**Figure 44E-44F**). However, both GFP-Tregs and CA AMPK-Tregs treatment reduced the

production of IFNγ in CD8+ T cells. Compared to GFP-Tregs, CA AMPK-Tregs treatment showed stronger negative effects on IFNγ production in CD8+ T cells (**Figure 44G-44H**).

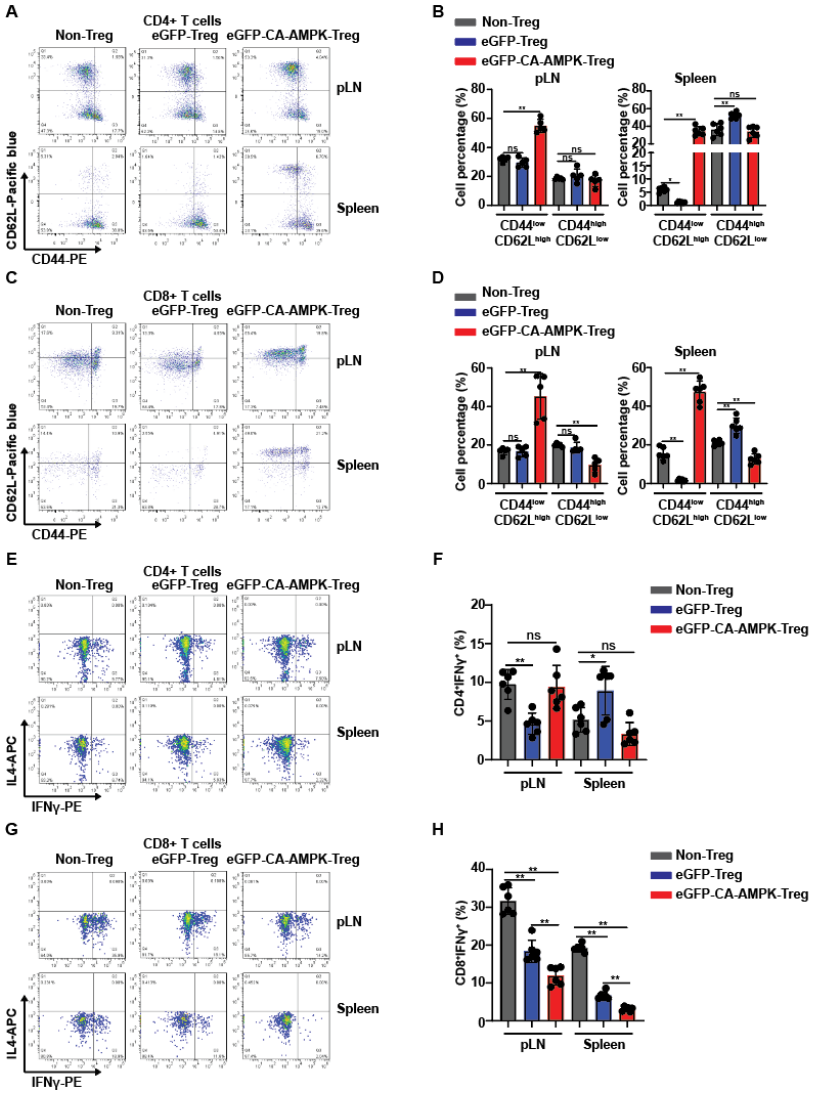

Figure 44*. Adoptive transfer CA AMPK-Tregs partially restores immune homeostasis in western diet feed ApoE-/- mice.*
A-D, Representative flow cytometry figures and quantification of naïve T cells and effector T cells in $CD4^+$ T cells (A and B) and $CD8^+$ T cells (C and D) in both peripheral lymph nodes (n=5/group) and spleen (n=6/group). E-H, Representative flow cytometry figures and quantification of IFNγ expression in CD4+ T cells (E and F) and CD8+ T cells (G and H) in both peripheral lymph nodes (n=5/group) and spleen (n=6/group). Data are presented as mean±SD, ns $p>0.05$, *$p<0.05$ and **$p<0.01$ by one-way ANOVA.

4.5 Discussion

In this study, we report that hypocholesterolemia-driven AMPK reduction promotes Tregs senescence with accentuated atherosclerosis in vivo. We first found spleen Tregs displayed

preferential upregulation of senescence-related markers than Tconv cells under hyperlipidemia conditions. In addition to splenocytes, we also observed significant induction of senescent Tregs in para-aorta lymph nodes and aorta tissues of $ApoE^{-/-}$ mice that received 16 weeks of western diet feeding. Compared with non-senescent Tregs, senescent Tregs were less efficient in suppressing arterial inflammation and atherosclerosis development. Mechanistically, senescent Tregs showed reduced functional suppression molecules and became more plasticity with upregulation of IFNγ. Furthermore, we discovered that AMPKα1 is required to restrain Treg senescence via suppressing ROS production, and deficiency of AMPKα1 is responsible for Treg senescence under hyperlipidemia conditions. Besides, deletion of AMPKα1 promoted Treg plasticity and disrupted immune homeostasis in $ApoE^{-/-}$ mice. Consequently, $ApoE^{-/-}$ mice with AMPKα1 deletion in Tregs displayed an upregulated arterial inflammation and aggregated atherosclerosis development within chow diet feeding. Our results indicate that AMPKα1 is the key molecular in Tregs in preventing senescence and Tregs plasticity.

Convention of physiological Tregs into pathological Tregs under hyperlipidemia conditions has been demonstrated to impair Tregs function and aggravate atherosclerosis progression(Ali et al., 2020; Butcher et al., 2016). However, the factors that mediate Tregs phenotype switching and dysfunctional during atherogenesis are still unclear. A recent study showed that Tregs became senescent with age and lost their immunosuppressive functions but produced inflammatory cytokines (Guo et al., 2020). However, whether and how senescent Tregs play their role in atherosclerosis is fully unknown. We discovered that hyperlipidemia promoted Tregs senescence in peripheral lymph organs and aorta tissues. Senescent Tregs were shown to be plastic and displayed less efficiency in suppressing vascular inflammation and atherosclerosis progression. By combining comprehensive *in vitro* and *in vivo* studies, we observed that AMPKα1 is required to prevent Tregs senescence via regulating ROS production both in age and hyperlipidemia conditions, and deficiency of AMPKα1 in Tregs promotes atherosclerosis development. Our findings suggest that hyperlipidemia skew Tregs into a dysfunctional senescent phenotype and

activation of AMPK prevents the formation of senescent Tregs, which restrain atherosclerosis progression.

Advanced atherosclerotic plaques contain senescent cells, which show deleterious effects at all stages of atherosclerosis via acquiring the senescence-associated secretory phenotype (SASP) (Gorenne et al., 2006; Minamino et al., 2002). Immunosenescence (immune cell senescence) plays an essential role in the initiation and progression of atherosclerosis (Childs et al., 2018; Song et al., 2020). Selective clearance of senescent cells via genetic or pharmacological methods reverses atherosclerosis progression (Childs et al., 2016). Tregs are also equally senescent during aging, but their roles in atherosclerosis are still unknown. Here, we demonstrated that Tregs are susceptible to hyperlipidemia to become senescent. These senescent Tregs displayed a less protective effect on arterial inflammation and atherosclerosis via downregulating Tregs function-related markers (CD25, GITR, ICOS, LAG3, Nrp1, PD1, Foxp3, and IL-10). An early study showed that gene expression of these Tregs function-related markers was normal in aged Tregs(Guo et al., 2020), which seems to contradict our observations. The reason could be due to the different stress conditions. Moreover, the comparison only happened on Tregs from young and aged mice, not the exact senescent Tregs ($C_{12}FDG^{high}$) and non-senescent Tregs ($C_{12}FDG^{low}$) in their study may be another reason caused this discrepancy. Our data suggest senescent Tregs can influence the proatherogenic processes through controlling Tregs function, which provides a novel immunotherapy target for atherosclerosis.

The plasticity of Tregs was defined by retaining Foxp3 expression but acquiring inflammatory factors of effector T cells, which are called Th-like Tregs (Shi and Chi, 2019). In response to pathological environments, Tregs may partially or fully assume plastic phenotypes and lose their immunosuppressive function (Sakaguchi et al., 2013; Smigiel et al., 2014). Hyperlipidemia-driven Treg plasticity is one of the primary reasons that leads to Tregs dysfunction during atherogenesis (Butcher et al., 2016; Gaddis et al., 2018). However, how hyperlipidemia leads to Treg plasticity and dysfunction is still unknown. Here, we uncovered hypercholesterolemia-induced senescent

Tregs acquired higher expression of IFNγ and were more likely to the convention to IFNγ+Tregs. IFNγ-producing Th1/Tregs were generated within the atherosclerotic aorta and are known as the significant phenotype of plastic Tregs (Butcher et al., 2016; Li et al., 2016a). Our data suggest that hypercholesterolemia-induced Tregs senescence is a potential mechanism for Tregs plasticity during atherosclerosis progression.

Besides Tregs plasticity, we also observed a significantly decreased Foxp3 expression in senescent Tregs, which means senescence may induce Tregs plasticity and disrupt Tregs stability. The plasticity and stability of Tregs are closely associated with each other. Unstable Tregs were shown to easily attain a Th1-like phenotype under pathological environments in islets (Zhou et al., 2009). Stable expression of Foxp3 inhibited the conversion of Tregs to IFNγ/TNFα-producing effector T cells(Oldenhove et al., 2009). Plasticity-promoting factors and plastic Tregs-related markers have also been known to participate in the stability regulation (Koch et al., 2012; Wang et al., 2011). In atherosclerosis, Tregs were reported to undergo both plasticity and instability(Ali et al., 2020). Therefore, further in-depth studies may shed new light on investigating whether senescence promotes Tregs instability during atherosclerosis via measuring the methylation status and mRNA level of the *Foxp3 (Toker et al., 2013)*.

AMPK has been reported to control the differentiation of Tregs by regulating lipid oxidation (Michalek et al., 2011). AMPK activation promotes the shift of Th17 cells to Tregs cells and stabilizes atherosclerotic plaque (Tian et al., 2017). Not only for Tregs differentiation, but we also observed that AMPKα1 is required to maintain Foxp3 protein stability and Tregs function (An et al., 2022; Zhu et al., 2021). Here we presented that a deficiency of AMPKα1 leads to Tregs senescence in young mice, identifying a novel role of AMPK in Tregs. The essential role of AMPKα1 in anti-Tregs senescence may explain why specific deletion of AMPKα1 in Tregs induced autoimmunity only in aged mice while not in young mice (Yang et al., 2017; Zhu et al., 2021).

Finally, we also demonstrated that AMPKα1 reduction is responsible for high cholesterol-induced Tregs senescence via gain- and loss- of function assay, suggesting the essential role of

AMPKα1 in Tregs senescence both in physiological and pathological conditions. Like senescent Tregs, AMPKα1-deficient Treg also showed decreased Foxp3 expression and increased plasticity, which impaired its protective effect on arterial inflammation and atherosclerosis progression. These findings offer AMPK a potential molecular target for atherosclerosis immunotherapy via modulating Tregs senescence.

In sum, we conclude that hyperlipidemia promotes Treg senescence to form plasticity and dysfunctional Tregs, which fails to prevent arterial inflammation and atherosclerosis. Degradation of AMPKα1 by hyperlipidemia leads to Tregs senescence and promotes atherosclerosis development. These findings identify the activation of AMPK as a novel method to prevent Tregs senescence, which is a novel immunotherapy target for atherosclerosis.

5 Conclusions and Perspectives

5.1 AMPK Maintains Tregs Function

Regulatory T cells (Tregs) are an indispensable constituent of the immune system, which are required to maintain immunological self-tolerance and tissue homeostasis (Josefowicz et al., 2012). Recent studies have witnessed Tregs-based immunotherapies to control physiological and pathological immune responses in clinical settings. In clinical trials, improved Treg numbers or their immunosuppressive activity have been used to treat autoimmune and other inflammatory diseases. (Ferreira et al., 2019). Moreover, reducing Tregs or their suppressive activity can be effective for evoking antitumor immune responses or enhancing antimicrobial immunity in chronic infection (Sakaguchi et al., 2020). Thus, a better understanding of the molecular mechanisms underlying Tregs survival and immunosuppressive function may benefit the development of novel immunotherapy strategies to modulate Treg function on inflammatory diseases and antitumor immunity.

In the first part of this dissertation, we found AMPK as a novel kinase which is required to the immunosuppressive function of Tregs in both *in vitro* and *in vivo* Treg function assays. The required role of AMPK in the regulation of Treg function prevent an age-dependent increase in autoinflammation. The role of AMPK in autoimmune disease has been demonstrated before as is shown that global deletion of AMPKα1 exacerbated experimental autoimmune encephalomyelitis (EAE) disease severity (Nath et al., 2009b). Moreover, activating AMPK can prevent autoimmune disease in animal models (Nath et al., 2009a; Zhang et al., 2022). In this dissertation, we found that mice with AMPKα1 global knockout spontaneously developed an autoimmune liver disease which can be recovered by adoptive Treg transfer from WT (*Prkaa1*+/+). This data indicates an essential role of AMPKα1 in Tregs in developing autoimmune liver disease. Indeed, we observed that the Treg-specific AMPKα1 deletion mice developed the autoimmune liver disease after 1-year-old, which means not only in Tregs but deficiency of AMPKα1 in other cells also contributes

to the development of autoimmune liver disease. Previous studies showed that activating AMPK by berberine in liver tissues could efficiently prevent autoimmune hepatitis (Wang et al., 2017). However, the hepatocyte specific AMPKα1 deficiency mice showed no obvious autoimmune phenotypes. Further experiments still need to investigate whether deletion of AMPKα1 in any other cell types such as conventional T cells, dendritic cells, or macrophages plays any role in developing autoimmune liver disease.

Multiple mechanisms have been proposed to mediate the immunosuppressive function of Tregs, such as expression of suppression-related cell surface molecules, production of immunosuppressive cytokines, and production of immune-suppressive metabolites. Cytotoxic T-lymphocyte antigen-4 (CTLA-4) is one of the essential cell surface molecules that controls the suppressive activity of Treg cells. CTLA-4 on the cell surface of Tregs impairs the maturation of APC via binding to CD80/CD86 (Walker and Sansom, 2011). CTLA-4 can not only compete CD80/CD86 binding with CD28 but also induce the deletion of CD80/86 via trans-endocytosis (Qureshi et al., 2011). In addition to CTLA-4, other immune checkpoint molecules, including ICOS, PD1, and LAG-3, are also highly expressed in activated Treg cells and inhibit the proliferation of effector T cells (Sasidharan Nair and Elkord, 2018).The expression of CD25 (high-affinity IL-2 receptor α-chain) on Tregs cells competes the IL-2 with effector T cells, limiting the proliferation or activation of IL-2. Foxp3+ Treg cells also utilize a wide range of inhibitory cytokines, such as TGF-β, IL-10, and IL-35, to perform inhibitory function (Collison et al., 2007; Huber and Schramm, 2006; Rubtsov et al., 2008). Moreover, Tregs cells can also produce perforin and granzyme to kill effector T cells (Cao et al., 2007). In tumor microenvironment (TME), we identified AMPK is required to maintain the expression of these function related molecules in Tregs, which is further support the indispensable role of AMPK in the regulation of Tregs function.

5.2 AMPK Controls Tregs Plasticity but not Stability

It is well established that Treg cells express the transcriptional factor Foxp3 and are stable

and long-lasting under physiological conditions. However, under some disease conditions, Tregs cells respond to environmental signals and display plastic differentiation and instability. Plasticity of Treg is characterized by retaining Foxp3 expression but gaining some features of helper T(Th) cells, including secretion of Th-related cytokines and expression of specific transcription factors in Th cells (Qiu et al., 2020). Instability of Tregs was described by loss of Foxp3 expression and becoming so-called ex-Tregs (Ali et al., 2020). Both plasticity and instability of Treg impair the suppressive capacity of these cells.

Th1-like Treg is the most widely reported subset of plastic Tregs due to the high expression of IFNγ, T-bet, and CXCR3 in Tregs cells(Zheng et al., 2011). Deficiency of deubiquitinase USP21 and E3 ligase VHL induced the reduction of FOXP3 protein level and the promotion of IFNγ in Treg cells in vivo(Lee et al., 2015a; Li et al., 2016b). Deficiency of IL-33 promotes the production of IFNγ in tumor infiltrated Tregs which promotes Tregs plasticity and tumor regression(Hatzioannou et al., 2020). Atherosclerosis environment drives Treg plasticity with accumulation of IFNγ^{+} Tregs in plaque area which impairs the protective effect of Tregs on arterial inflammation and atherosclerosis development. Though the plastic changes of Tregs have been widely reported, the mechanism behind this is still not clear. Our studies showed that activation of AMPK is required to restrain the plasticity of Tregs in both TME and atherosclerosis environments. And we also identified a novel mechanism that AMPK controls Treg plasticity via inhibiting the senescence of Tregs. Further studies working on the relationship between senescent Tregs and plastic Tregs in different animal models would achieve a comprehensive understanding of these plastic Treg subtypes.

As a specific transcription factor, stable expression of Foxp3 is required for the stability of Tregs(Nie et al., 2015). However, the reduction of Foxp3 under disease conditions promotes the expression of ex-Tregs. Several Foxp3 tracking mice have been generated to investigate the stability of Tregs(Miyao et al., 2012; Rubtsov et al., 2010; Zhou et al., 2009). Among them, the most widely used was the *Foxp3-IRES-YFP-Cre-loxp-td-RFP-loxp* mice model. In this mouse

model, Treg expresses both YFP and Cre recombinase under the control of the IRES element, which follows the *Foxp3* gene expression. The deletion of loxp sites that flank RFP by Cre recombinase mark Treg as red. The "current Tregs" display both yellow and red in this model. If Tregs become "ex Tregs," they lose YFP expression and only express RFP(Miyao et al., 2012). It has been demonstrated that 10-20% of total Tregs are unstable and switch to ex Tregs, and this ratio would increase in response to chronic inflammation(Zhou et al., 2009).

The stability of Tregs is tightly regulated by cellular metabolism. Different from conventional T cells (Tconv), Tregs are more likely to use oxidative phosphorylation (OXPHOS) but less reliant on glycolysis for energy production, which has a high expression of AMPK (Michalek et al., 2011). Glucose uptake impaires the function and stability of Tregs in the tumor microenvironment (TME), while lactate treatment prevents these destabilizing effects of high-glucose conditions(Kumagai et al., 2022). Inhibition of glycolysis promoted the induction of Foxp3 in response to TGF-β and IL-2 stimulation(Eleftheriadis et al., 2013). However, previous study indicates increased glycolysis promoted PI3K/Akt signaling and Treg proliferation(Gerriets et al., 2016). Thus, it is reasonable to speculate that high glycolysis promotes the proliferation of Treg cells. However, Tregs' stability and suppressive activity need to be balanced by other metabolic programs. Recent studies show great interest in regulating Treg stability by mitochondrial metabolism and OXPHOS. Deleting mitochondrial transcription factor A (Tfam) promoted the methylation in the TSDR of *the Foxp3* locus, which destabilized Foxp3 expression and impaired Treg suppressive function under inflammation conditions(Fu et al., 2019). Fatty acid oxidation (FAO) can degrade fatty acids to produce acetyl-CoA, which is involved in the mitochondrial tricarboxylic acid (TCA) cycle to regulate mitochondrial OXPHOS. Both short-chain fatty acids and acetyl-CoA can regulate Foxp3 protein acetylation and Treg stability(Smith et al., 2013; van Loosdregt et al., 2010). All these data suggest an indispensable role of OXPHOS for Treg stability and suppressive activity. As an essential energy modulator, AMPK has been widely demonstrated to regulate mitochondrial metabolism and OXPHOS(Rodriguez et al., 2021). However, our data showed that AMPK only

controls Foxp3 protein level while not affecting its mRNA expression. In both TME and normal conditions, deficiency of AMPK doesn't affect YFP expression. These data suggest that AMPK is essential to Treg plasticity but not stability. Further studies using *Prkaa1*$^{fl/fl}$ *Foxp3-IRES-YFP-Cre-loxp-td-RFP-loxp* mice can better understand the role of AMPK in the regulation of Treg stability in other disease model.

5.3 Stabilization of Foxp3 by AMPK

Foxp3 belongs to the Forkhead box (Fox) family, well conserved among mammals(Lam et al., 2013). In humans, the *Foxp3* gene locates on the X-chromosome at Xp11.23-Xq13.3, and mutation of Foxp3 leads to the immune dysregulation polyendocrinopathy enteropathy X-linked syndrome (IPEX)(Bennett et al., 2000; d'Hennezel et al., 2012). Foxp3 protein is about 431 amino acids and contains four functional domains, including a proline-rich N-terminal domain, zinc finger, leucine zipper, and Fork-head domain(Deng et al., 2020). The N-terminal region functions to suppress NFAT-mediated transcriptional signaling, the zinc finger and leucine zipper domain are required for the transcriptional functions of Foxp3, and the forkhead domain is essential for DNA binding and nuclear import(Lopes et al., 2006).

The expression and function of Foxp3 can be regulated in both transcriptional and post-transcriptional level. Transcriptionally, Foxp3 can be regulated by DNA methylation, histone modification, nucleosome positioning, and a series of cis-acting elements located on the promoter and the enhancer regions of the Foxp3 locus (Ohkura and Sakaguchi, 2020). Besides transcriptional regulation, Foxp3 expression is also highly regulated by post-translational modification (PTM), including phosphorylation, acetylation, methylation, O-GlcNAcylation, and ubiquitination.

Phosphorylation is a mechanism by which protein kinase binds to the serine (S), threonine (T), or tyrosine (Y) residue of a protein and controls protein stability and function. Several protein kinases have been documented to control Foxp3 expression via phosphorylation and

dephosphorylation mechanisms. Phosphorylation of Ser-19 and Thr-175 of Foxp3 by CDK2 decreased its protein stability and Treg function(Morawski et al., 2013). Under inflammation conditions, phosphorylation of Foxp3 at Ser-422 by PIM1 reduced its DNA binding activity while not affecting its protein stability(Li et al., 2014). Activation of NLK under TCR stimulation promoted the phosphorylation of Foxp3 at seven different sites and prevented its ubiquitination(Fleskens et al., 2019). Dephosphorylation of Foxp3 at Ser418 leads to impaired Treg function under TNFα treatment(Nie et al., 2013). Here, we identified AMPK as a novel kinase which can direct phosphorylates Foxp3 from the in vitro kinase assay. However, the phosphorylation site of Foxp3 by AMPK is still unclear. Further studies to determine the specific phosphorylate site of Foxp3 by AMPK can help us to better understand the relationship between AMPK and Foxp3.

In Treg cells, STUB1 (*CHIP*) is one of the major E3 ligases that directly ubiquitinate Foxp3. Under LPS or proinflammation stimulation, the expression of STUB1 was increased, leading to K48 polyubiquitination on Foxp3 at Lys-227, Lys-250, Lys-263, and Lys-268(Chen et al., 2013). Such ubiquitination decreased Foxp3 expression in a proteasome-dependent degradation and impaired Treg function(Chen et al., 2013).The ubiquitination process can be reversed by deubiquitinases (DUB), which remove ubiquitin tags from the substrate protein(Nijman et al., 2005). USP7 is the most well-known DUBs of Foxp3, which preserved Foxp3 homeostasis by removing K48-type polyubiquitination tags at Lys-249, Lys-251, Lys-263, Lys-267, and Lys-393(van Loosdregt et al., 2013). In this dissertation, we found deficiency of AMPKα1 increase STUB1 expression while not affecting the expression of USP7 in Tregs, which further promotes Foxp3 ubiquitination and degradation. Silencing STUB1 can partially reverse the Foxp3 protein level in AMPKα1-deficient Tregs, indicating an indenpensable function of STUB1 in the regulation of Foxp3 by AMPK. As an E3 ligase, STUB1 is known to regulate several proteins involved in multiple physiological and pathological processes, but mechanisms operating on the activity of STUB1 is still far more known(Paul and Ghosh, 2014). Therefore, further studies are still interesting to investigate the detail mechanisms on how AMPK regulate STUB1 in Tregs.

5.4 AMPK Controls the Function of Immunosuppressive Cells in TME

With the discovery of immune checkpoint inhibitors, immunotherapy has succeeded in clinical cancer treatment. Accumulation of large numbers of Tregs in tumor tissues hinders the efficacy of cancer immunotherapy due to their ability to suppress antitumor immune responses. A high ratio of Tregs cells to CD8+ T cells in the tumor microenvironment (TME) is correlated with poor prognosis(Fridman et al., 2012). Therefore, deletion of Tregs and suppression of Treg cell function are recognized as promising immunotherapy strategies.

An arduous task in the success of cancer immunotherapy is the selective depletion of tumor infiltrated Tregs or suppression of their immunosuppressive function. Thus, the identification of cell-intrinsic molecules that control Tregs' suppressive program could provide unique therapeutic strategies for tumor eradication. In the second part of the dissertation, we demonstrated that AMPK is also indispensable for the suppressive function of tumor infiltrated Tregs. Tumor exposed, AMPKα1-deficient Tregs are more plastic and reprogrammed to upregulate IFN-γ expression, thus preventing tumor development. Activation of AMPK has been shown to activate both antitumor and pro-tumor responses. Activation of AMPK by aerobic glycolysis in breast tumors promoted myeloid-derived suppressor cells (MDSC) expansion, promoting tumor progression (Li et al., 2018). Activation of AMPK has also been shown to promote cancer metastasis by adapting cancer cells to metabolic and oxidative stresses (Cai et al., 2020). In contrast to the immunosuppressive effects, stimulation of AMPK through Metformin induced phosphorylation and degradation of PD-L1, thereby promoting protective T-cell immunity (Cha et al., 2018). These studies suggest that the role of AMPK in tumor cells is dependent on the context.

For tumor-infiltrating immune cells, the role of AMPK is still controversial. The deficiency of AMPK in $CD8^+$ T cells suppresses their antitumor function, while conditional deletion of *Prkaa1* in MDSCs potentiated the antitumor T cell immunity (Rao et al., 2015a; Trillo-Tinoco et al., 2019). Not only for the MDSCs but AMPK has also been shown to regulate the immunosuppressive

phenotypes in macrophages and the restriction of effector T-cell expansion in tumors (Sag et al., 2008; Zhu et al., 2015). Our data showed an essential role of AMPK in tumor infiltrated Tregs; we hypothesize that condition deletion of AMPK in immunosuppressive cells could be a promising strategy for cancer immunotherapy.

5.5 Activation of AMPK as a Potential Therapeutic Target for Immunological Aging and Atherosclerosis

Age-associated diseases have become a health burden worldwide(Partridge et al., 2018). The immune system is greatly affected by aging, chronic inflammation (inflammaging), and immunosenescence. Aging is also one of the most substantial risk factors for the development of atherosclerosis. The immune cell senescence plays a pivotal role in the initiation and progression of atherosclerosis (Childs et al., 2016). As an important immune modulator, Tregs are also involved in the progression of atherosclerosis. However, whether and how the function of senescent Tregs is regulated during atherosclerosis is not known. In the third part of the dissertation, we found that hypercholesterolemia promotes Treg senescence via downregulation of the expression of AMPKα1. Senescent Tregs showed a minimal protective effect in atherosclerosis. This work revealed cellular senescence as a novel mechanism that controls Treg function during atherogenesis. Future studies to test if selectively removing senescent Treg cells by genetic or pharmacological means could be potential therapeutic strategies to treat atherosclerosis are warranted.

In the third part of the dissertation, we also observed a novel role of AMPK in regulating Treg senescence. The critical role of AMPK in the senescence of Tregs may explain why the Treg-specific AMPKα1 deletion mice develop autoimmune hepatitis only after 1-year-old. Tregs have been shown to senesce more severely than conventional T (Tconv) cells during aging. Aged Tregs have less protective efficiency in suppressing the Tconv cell aging phenotype and immunological aging(Guo et al., 2020). Further studies are needed to investigate whether constitutive activation

of AMPK in Tregs can be an effective way to treat immunological aging.

Finally, we found that AMPK regulates Treg senescence via maintaining ROS production. The cellular level of ROS is subject to tight regulation of cellular senescence and aging (Colavitti and Finkel, 2005). It has been shown that compared to Tconv cells, the ROS level is preferentially increased in Tregs regardless of age. This excessive ROS production impaired the proliferative capacity and function of aged Tregs (Guo et al., 2020). However, the specific mechanism of AMPK regulates ROS levels in Treg cells is still unclear. Given the essential role of the DCAF1/GSTP1 axis in regulating ROS and cellular senescence in Tregs cells, future studies on whether and how AMPK regulates DCAF1 expression in Tregs cells will provide valuable insights into the progression of Treg senescence. In addition, several other pathway, including PI3K/Akt/mTOR, DNA damage/p53 response, and inflammation, have also been shown to regulate cellular ROS generation (Ray et al., 2012). Therefore, it is of interest to investigate whether AMPK ameliorates Treg senescence and inflammation through these pathways.

5.6 Significance and Impacts

This dissertation has systemically established the essential roles of AMPK in regulatory T cells and AMPK downregulation in Tregs led to autoimmune diseases, cancer progression, and accelerated atherosclerosis. The main findings are as follow:

1. I discovered AMPK as a novel molecular required for Tregs' immunosuppressive function *in vitro* and *in vivo* experiments.
2. I determined the essential role of AMPK in tumor infiltrated Tregs and the potential therapeutic target of conditional deletion of AMPK in Tregs for cancer therapy.
3. I identified a novel role of AMPK in controlling Treg senescence and its therapeutic effects in atherosclerosis.
4. Overall, this dissertation has established a novel concept that the metabolic homeostasis plays an essential role in Tregs' stability, plasticity, and function.

6 References

Abdellatif, M., Sedej, S., Carmona-Gutierrez, D., Madeo, F., and Kroemer, G. (2018). Autophagy in Cardiovascular Aging. Circ Res *123*, 803-824.

Ait-Oufella, H., Salomon, B.L., Potteaux, S., Robertson, A.K., Gourdy, P., Zoll, J., Merval, R., Esposito, B., Cohen, J.L., Fisson, S.*, et al.* (2006). Natural regulatory T cells control the development of atherosclerosis in mice. Nat Med *12*, 178-180.

Akbar, A.N., Henson, S.M., and Lanna, A. (2016). Senescence of T Lymphocytes: Implications for Enhancing Human Immunity. Trends Immunol *37*, 866-876.

Ali, A.J., Makings, J., and Ley, K. (2020). Regulatory T Cell Stability and Plasticity in Atherosclerosis. Cells *9*.

Almeida, A., Cidad, P., Delgado-Esteban, M., Fernandez, E., Garcia-Nogales, P., and Bolanos, J.P. (2005). Inhibition of mitochondrial respiration by nitric oxide: its role in glucose metabolism and neuroprotection. J Neurosci Res *79*, 166-171.

An, J., Ding, Y., Yu, C., Li, J., You, S., Liu, Z., Song, P., and Zou, M.H. (2022). AMP-activated protein kinase alpha1 promotes tumor development via FOXP3 elevation in tumor-infiltrating Treg cells. iScience *25*, 103570.

Anding, A.L., and Baehrecke, E.H. (2017). Cleaning House: Selective Autophagy of Organelles. Dev Cell *41*, 10-22.

Aoki, C., Suzuki, K., Yanagi, K., Satoh, H., Niitani, M., and Aso, Y. (2012). Miglitol, an anti-diabetic drug, inhibits oxidative stress-induced apoptosis and mitochondrial ROS over-production in endothelial cells by enhancement of AMP-activated protein kinase. J Pharmacol Sci *120*, 121-128.

Apfeld, J., O'Connor, G., McDonagh, T., DiStefano, P.S., and Curtis, R. (2004). The AMP-activated protein kinase AAK-2 links energy levels and insulin-like signals to lifespan in C. elegans. Genes Dev *18*, 3004-3009.

Arvey, A., van der Veeken, J., Samstein, R.M., Feng, Y., Stamatoyannopoulos, J.A., and Rudensky, A.Y. (2014). Inflammation-induced repression of chromatin bound by the transcription factor Foxp3 in regulatory T cells. Nat Immunol *15*, 580-587.

Bacchetta, R., Barzaghi, F., and Roncarolo, M.G. (2018). From IPEX syndrome to FOXP3 mutation: a lesson on immune dysregulation. Ann N Y Acad Sci *1417*, 5-22.

Back, M., Yurdagul, A., Jr., Tabas, I., Oorni, K., and Kovanen, P.T. (2019). Inflammation and its resolution in atherosclerosis: mediators and therapeutic opportunities. Nat Rev Cardiol *16*, 389-406.

Barbi, J., Pardoll, D.M., and Pan, F. (2015). Ubiquitin-dependent regulation of Foxp3 and Treg function. Immunol Rev *266*, 27-45.

Bektas, A., Schurman, S.H., Gonzalez-Freire, M., Dunn, C.A., Singh, A.K., Macian, F., Cuervo, A.M., Sen, R., and Ferrucci, L. (2019). Age-associated changes in human CD4(+) T cells point to mitochondrial dysfunction consequent to impaired autophagy. Aging (Albany NY) *11*, 9234-9263.

Bennett, C.L., Christie, J., Ramsdell, F., Brunkow, M.E., Ferguson, P.J., Whitesell, L., Kelly, T.E., Saulsbury, F.T., Chance, P.F., and Ochs, H.D. (2001). The immune dysregulation, polyendocrinopathy, enteropathy, X-linked syndrome (IPEX) is caused by mutations of FOXP3. Nat Genet *27*, 20-21.

Bennett, C.L., Yoshioka, R., Kiyosawa, H., Barker, D.F., Fain, P.R., Shigeoka, A.O., and Chance, P.F. (2000).

X-Linked syndrome of polyendocrinopathy, immune dysfunction, and diarrhea maps to Xp11.23-Xq13.3. Am J Hum Genet *66*, 461-468.

Blagih, J., Coulombe, F., Vincent, E.E., Dupuy, F., Galicia-Vazquez, G., Yurchenko, E., Raissi, T.C., van der Windt, G.J., Viollet, B., Pearce, E.L.*, et al.* (2015). The energy sensor AMPK regulates T cell metabolic adaptation and effector responses in vivo. Immunity *42*, 41-54.

Bochtler, P., Riedl, P., Gomez, I., Schirmbeck, R., and Reimann, J. (2008). Local accumulation and activation of regulatory Foxp3+ CD4 T(R) cells accompanies the appearance of activated CD8 T cells in the liver. Hepatology *48*, 1954-1963.

Bonacina, F., Martini, E., Svecla, M., Nour, J., Cremonesi, M., Beretta, G., Moregola, A., Pellegatta, F., Zampoleri, V., Catapano, A.L.*, et al.* (2021). Adoptive transfer of CX3CR1 transduced-T regulatory cells improves homing to the atherosclerotic plaques and dampens atherosclerosis progression. Cardiovasc Res *117*, 2069-2082.

Bonney, K.M., Taylor, J.M., Thorp, E.B., Epting, C.L., and Engman, D.M. (2015). Depletion of regulatory T cells decreases cardiac parasitosis and inflammation in experimental Chagas disease. Parasitol Res *114*, 1167-1178.

Borst, J., Ahrends, T., Babala, N., Melief, C.J.M., and Kastenmuller, W. (2018). CD4(+) T cell help in cancer immunology and immunotherapy. Nat Rev Immunol *18*, 635-647.

Brieger, K., Schiavone, S., Miller, F.J., Jr., and Krause, K.H. (2012). Reactive oxygen species: from health to disease. Swiss Med Wkly *142*, w13659.

Burkewitz, K., Zhang, Y., and Mair, W.B. (2014). AMPK at the nexus of energetics and aging. Cell Metab *20*, 10-25.

Butcher, M.J., Filipowicz, A.R., Waseem, T.C., McGary, C.M., Crow, K.J., Magilnick, N., Boldin, M., Lundberg, P.S., and Galkina, E.V. (2016). Atherosclerosis-Driven Treg Plasticity Results in Formation of a Dysfunctional Subset of Plastic IFNgamma+ Th1/Tregs. Circ Res *119*, 1190-1203.

Cai, Z., Li, C.F., Han, F., Liu, C., Zhang, A., Hsu, C.C., Peng, D., Zhang, X., Jin, G., Rezaeian, A.H.*, et al.* (2020). Phosphorylation of PDHA by AMPK Drives TCA Cycle to Promote Cancer Metastasis. Mol Cell *80*, 263-278 e267.

Callender, L.A., Carroll, E.C., Beal, R.W.J., Chambers, E.S., Nourshargh, S., Akbar, A.N., and Henson, S.M. (2018). Human CD8(+) EMRA T cells display a senescence-associated secretory phenotype regulated by p38 MAPK. Aging Cell *17*.

Callender, L.A., Carroll, E.C., Bober, E.A., Akbar, A.N., Solito, E., and Henson, S.M. (2020). Mitochondrial mass governs the extent of human T cell senescence. Aging Cell *19*, e13067.

Cao, X., Cai, S.F., Fehniger, T.A., Song, J., Collins, L.I., Piwnica-Worms, D.R., and Ley, T.J. (2007). Granzyme B and perforin are important for regulatory T cell-mediated suppression of tumor clearance. Immunity *27*, 635-646.

Carey, T.E., Takahashi, T., Resnick, L.A., Oettgen, H.F., and Old, L.J. (1976). Cell surface antigens of human malignant melanoma: mixed hemadsorption assays for humoral immunity to cultured autologous melanoma cells. Proc Natl Acad Sci U S A *73*, 3278-3282.

Carling, D., Zammit, V.A., and Hardie, D.G. (1987). A common bicyclic protein kinase cascade inactivates the regulatory enzymes of fatty acid and cholesterol biosynthesis. FEBS Lett *223*, 217-222.

Cha, J.H., Yang, W.H., Xia, W., Wei, Y., Chan, L.C., Lim, S.O., Li, C.W., Kim, T., Chang, S.S., Lee, H.H.*, et*

al. (2018). Metformin Promotes Antitumor Immunity via Endoplasmic-Reticulum-Associated Degradation of PD-L1. Mol Cell *71*, 606-620 e607.

Chan, E.Y. (2009). mTORC1 phosphorylates the ULK1-mAtg13-FIP200 autophagy regulatory complex. Sci Signal *2*, pe51.

Chang, C.H., Curtis, J.D., Maggi, L.B., Jr., Faubert, B., Villarino, A.V., O'Sullivan, D., Huang, S.C., van der Windt, G.J., Blagih, J., Qiu, J.*, et al.* (2013). Posttranscriptional control of T cell effector function by aerobic glycolysis. Cell *153*, 1239-1251.

Chang, C.H., Qiu, J., O'Sullivan, D., Buck, M.D., Noguchi, T., Curtis, J.D., Chen, Q., Gindin, M., Gubin, M.M., van der Windt, G.J.*, et al.* (2015). Metabolic Competition in the Tumor Microenvironment Is a Driver of Cancer Progression. Cell *162*, 1229-1241.

Chavez, J.A., Roach, W.G., Keller, S.R., Lane, W.S., and Lienhard, G.E. (2008). Inhibition of GLUT4 translocation by Tbc1d1, a Rab GTPase-activating protein abundant in skeletal muscle, is partially relieved by AMP-activated protein kinase activation. J Biol Chem *283*, 9187-9195.

Chen, Z., Barbi, J., Bu, S., Yang, H.Y., Li, Z., Gao, Y., Jinasena, D., Fu, J., Lin, F., Chen, C.*, et al.* (2013). The ubiquitin ligase Stub1 negatively modulates regulatory T cell suppressive activity by promoting degradation of the transcription factor Foxp3. Immunity *39*, 272-285.

Cheung, P.C., Salt, I.P., Davies, S.P., Hardie, D.G., and Carling, D. (2000). Characterization of AMP-activated protein kinase gamma-subunit isoforms and their role in AMP binding. Biochem J *346 Pt 3*, 659-669.

Childs, B.G., Baker, D.J., Wijshake, T., Conover, C.A., Campisi, J., and van Deursen, J.M. (2016). Senescent intimal foam cells are deleterious at all stages of atherosclerosis. Science *354*, 472-477.

Childs, B.G., Li, H., and van Deursen, J.M. (2018). Senescent cells: a therapeutic target for cardiovascular disease. J Clin Invest *128*, 1217-1228.

Colavitti, R., and Finkel, T. (2005). Reactive oxygen species as mediators of cellular senescence. IUBMB Life *57*, 277-281.

Colin, S., Chinetti-Gbaguidi, G., and Staels, B. (2014). Macrophage phenotypes in atherosclerosis. Immunol Rev *262*, 153-166.

Collins, S.P., Reoma, J.L., Gamm, D.M., and Uhler, M.D. (2000). LKB1, a novel serine/threonine protein kinase and potential tumour suppressor, is phosphorylated by cAMP-dependent protein kinase (PKA) and prenylated in vivo. Biochem J *345 Pt 3*, 673-680.

Collison, L.W., Workman, C.J., Kuo, T.T., Boyd, K., Wang, Y., Vignali, K.M., Cross, R., Sehy, D., Blumberg, R.S., and Vignali, D.A. (2007). The inhibitory cytokine IL-35 contributes to regulatory T-cell function. Nature *450*, 566-569.

Cool, B., Zinker, B., Chiou, W., Kifle, L., Cao, N., Perham, M., Dickinson, R., Adler, A., Gagne, G., Iyengar, R.*, et al.* (2006). Identification and characterization of a small molecule AMPK activator that treats key components of type 2 diabetes and the metabolic syndrome. Cell Metab *3*, 403-416.

Cortez, J.T., Montauti, E., Shifrut, E., Gatchalian, J., Zhang, Y., Shaked, O., Xu, Y., Roth, T.L., Simeonov, D.R., Zhang, Y.*, et al.* (2020). CRISPR screen in regulatory T cells reveals modulators of Foxp3. Nature *582*, 416-420.

Costantini, E., D'Angelo, C., and Reale, M. (2018). The Role of Immunosenescence in Neurodegenerative Diseases. Mediators Inflamm *2018*, 6039171.

d'Hennezel, E., Bin Dhuban, K., Torgerson, T., and Piccirillo, C.A. (2012). The immunogenetics of immune dysregulation, polyendocrinopathy, enteropathy, X linked (IPEX) syndrome. J Med Genet *49*, 291-302.

Davies, S.P., Helps, N.R., Cohen, P.T., and Hardie, D.G. (1995). 5'-AMP inhibits dephosphorylation, as well as promoting phosphorylation, of the AMP-activated protein kinase. Studies using bacterially expressed human protein phosphatase-2C alpha and native bovine protein phosphatase-2AC. FEBS Lett *377*, 421-425.

Davies, S.P., Sim, A.T., and Hardie, D.G. (1990). Location and function of three sites phosphorylated on rat acetyl-CoA carboxylase by the AMP-activated protein kinase. Eur J Biochem *187*, 183-190.

Deeks, S.G., and Phillips, A.N. (2009). HIV infection, antiretroviral treatment, ageing, and non-AIDS related morbidity. BMJ *338*, a3172.

Deng, G., Nagai, Y., Xiao, Y., Li, Z., Dai, S., Ohtani, T., Banham, A., Li, B., Wu, S.L., Hancock, W.*, et al.* (2015). Pim-2 Kinase Influences Regulatory T Cell Function and Stability by Mediating Foxp3 Protein N-terminal Phosphorylation. J Biol Chem *290*, 20211-20220.

Deng, G., Song, X., and Greene, M.I. (2020). FoxP3 in Treg cell biology: a molecular and structural perspective. Clin Exp Immunol *199*, 255-262.

Desdin-Mico, G., Soto-Heredero, G., Aranda, J.F., Oller, J., Carrasco, E., Gabande-Rodriguez, E., Blanco, E.M., Alfranca, A., Cusso, L., Desco, M.*, et al.* (2020). T cells with dysfunctional mitochondria induce multimorbidity and premature senescence. Science *368*, 1371-1376.

Diestelhorst, J., Junge, N., Schlue, J., Falk, C.S., Manns, M.P., Baumann, U., Jaeckel, E., and Taubert, R. (2017). Pediatric autoimmune hepatitis shows a disproportionate decline of regulatory T cells in the liver and of IL-2 in the blood of patients undergoing therapy. PLoS One *12*, e0181107.

Egan, D.F., Chun, M.G., Vamos, M., Zou, H., Rong, J., Miller, C.J., Lou, H.J., Raveendra-Panickar, D., Yang, C.C., Sheffler, D.J.*, et al.* (2015). Small Molecule Inhibition of the Autophagy Kinase ULK1 and Identification of ULK1 Substrates. Mol Cell *59*, 285-297.

Egan, D.F., Shackelford, D.B., Mihaylova, M.M., Gelino, S., Kohnz, R.A., Mair, W., Vasquez, D.S., Joshi, A., Gwinn, D.M., Taylor, R.*, et al.* (2011). Phosphorylation of ULK1 (hATG1) by AMP-activated protein kinase connects energy sensing to mitophagy. Science *331*, 456-461.

Eichner, L.J., Brun, S.N., Herzig, S., Young, N.P., Curtis, S.D., Shackelford, D.B., Shokhirev, M.N., Leblanc, M., Vera, L.I., Hutchins, A.*, et al.* (2019). Genetic Analysis Reveals AMPK Is Required to Support Tumor Growth in Murine Kras-Dependent Lung Cancer Models. Cell Metab *29*, 285-302 e287.

Eichner, L.J., and Giguere, V. (2011). Estrogen related receptors (ERRs): a new dawn in transcriptional control of mitochondrial gene networks. Mitochondrion *11*, 544-552.

Eikawa, S., Nishida, M., Mizukami, S., Yamazaki, C., Nakayama, E., and Udono, H. (2015). Immune-mediated antitumor effect by type 2 diabetes drug, metformin. Proc Natl Acad Sci U S A *112*, 1809-1814.

Eiyama, A., and Okamoto, K. (2015). PINK1/Parkin-mediated mitophagy in mammalian cells. Curr Opin Cell Biol *33*, 95-101.

Eleftheriadis, T., Pissas, G., Karioti, A., Antoniadi, G., Antoniadis, N., Liakopoulos, V., and Stefanidis, I. (2013). Dichloroacetate at therapeutic concentration alters glucose metabolism and induces regulatory T-cell differentiation in alloreactive human lymphocytes. J Basic Clin Physiol Pharmacol

24, 271-276.

Fang, J., Yang, J., Wu, X., Zhang, G., Li, T., Wang, X., Zhang, H., Wang, C.C., Liu, G.H., and Wang, L. (2018). Metformin alleviates human cellular aging by upregulating the endoplasmic reticulum glutathione peroxidase 7. Aging Cell *17*, e12765.

Faubert, B., Boily, G., Izreig, S., Griss, T., Samborska, B., Dong, Z., Dupuy, F., Chambers, C., Fuerth, B.J., Viollet, B.*, et al.* (2013). AMPK is a negative regulator of the Warburg effect and suppresses tumor growth in vivo. Cell Metab *17*, 113-124.

Ferreira, L.M.R., Muller, Y.D., Bluestone, J.A., and Tang, Q. (2019). Next-generation regulatory T cell therapy. Nat Rev Drug Discov *18*, 749-769.

Ferri, S., Longhi, M.S., De Molo, C., Lalanne, C., Muratori, P., Granito, A., Hussain, M.J., Ma, Y., Lenzi, M., Mieli-Vergani, G.*, et al.* (2010). A multifaceted imbalance of T cells with regulatory function characterizes type 1 autoimmune hepatitis. Hepatology *52*, 999-1007.

Fleskens, V., Minutti, C.M., Wu, X., Wei, P., Pals, C., McCrae, J., Hemmers, S., Groenewold, V., Vos, H.J., Rudensky, A.*, et al.* (2019). Nemo-like Kinase Drives Foxp3 Stability and Is Critical for Maintenance of Immune Tolerance by Regulatory T Cells. Cell Rep *26*, 3600-3612 e3606.

Fogarty, S., Hawley, S.A., Green, K.A., Saner, N., Mustard, K.J., and Hardie, D.G. (2010). Calmodulin-dependent protein kinase kinase-beta activates AMPK without forming a stable complex: synergistic effects of Ca2+ and AMP. Biochem J *426*, 109-118.

Fontenot, J.D., Gavin, M.A., and Rudensky, A.Y. (2003). Foxp3 programs the development and function of CD4+CD25+ regulatory T cells. Nat Immunol *4*, 330-336.

Fridman, W.H., Pages, F., Sautes-Fridman, C., and Galon, J. (2012). The immune contexture in human tumours: impact on clinical outcome. Nat Rev Cancer *12*, 298-306.

Fu, Z., Ye, J., Dean, J.W., Bostick, J.W., Weinberg, S.E., Xiong, L., Oliff, K.N., Chen, Z.E., Avram, D., Chandel, N.S.*, et al.* (2019). Requirement of Mitochondrial Transcription Factor A in Tissue-Resident Regulatory T Cell Maintenance and Function. Cell Rep *28*, 159-171 e154.

Fujiwara, Y., Kawaguchi, Y., Fujimoto, T., Kanayama, N., Magari, M., and Tokumitsu, H. (2016). Differential AMP-activated Protein Kinase (AMPK) Recognition Mechanism of Ca2+/Calmodulin-dependent Protein Kinase Kinase Isoforms. J Biol Chem *291*, 13802-13808.

Fullerton, M.D., Galic, S., Marcinko, K., Sikkema, S., Pulinilkunnil, T., Chen, Z.P., O'Neill, H.M., Ford, R.J., Palanivel, R., O'Brien, M.*, et al.* (2013). Single phosphorylation sites in Acc1 and Acc2 regulate lipid homeostasis and the insulin-sensitizing effects of metformin. Nat Med *19*, 1649-1654.

Fulop, T., Larbi, A., Dupuis, G., Le Page, A., Frost, E.H., Cohen, A.A., Witkowski, J.M., and Franceschi, C. (2017). Immunosenescence and Inflamm-Aging As Two Sides of the Same Coin: Friends or Foes? Front Immunol *8*, 1960.

Funakoshi, M., Tsuda, M., Muramatsu, K., Hatsuda, H., Morishita, S., and Aigaki, T. (2011). A gain-of-function screen identifies wdb and lkb1 as lifespan-extending genes in Drosophila. Biochem Biophys Res Commun *405*, 667-672.

Gaddis, D.E., Padgett, L.E., Wu, R., McSkimming, C., Romines, V., Taylor, A.M., McNamara, C.A., Kronenberg, M., Crotty, S., Thomas, M.J.*, et al.* (2018). Apolipoprotein AI prevents regulatory to follicular helper T cell switching during atherosclerosis. Nat Commun *9*, 1095.

Garcia-Roves, P.M., Osler, M.E., Holmstrom, M.H., and Zierath, J.R. (2008). Gain-of-function R225Q

mutation in AMP-activated protein kinase gamma3 subunit increases mitochondrial biogenesis in glycolytic skeletal muscle. J Biol Chem *283*, 35724-35734.

Gerriets, V.A., Kishton, R.J., Johnson, M.O., Cohen, S., Siska, P.J., Nichols, A.G., Warmoes, M.O., de Cubas, A.A., MacIver, N.J., Locasale, J.W.*, et al.* (2016). Foxp3 and Toll-like receptor signaling balance Treg cell anabolic metabolism for suppression. Nat Immunol *17*, 1459-1466.

Gorenne, I., Kavurma, M., Scott, S., and Bennett, M. (2006). Vascular smooth muscle cell senescence in atherosclerosis. Cardiovasc Res *72*, 9-17.

Goronzy, J.J., and Weyand, C.M. (2012). Immune aging and autoimmunity. Cell Mol Life Sci *69*, 1615-1623.

Goronzy, J.J., and Weyand, C.M. (2019). Mechanisms underlying T cell ageing. Nat Rev Immunol *19*, 573-583.

Gotsman, I., Grabie, N., Gupta, R., Dacosta, R., MacConmara, M., Lederer, J., Sukhova, G., Witztum, J.L., Sharpe, A.H., and Lichtman, A.H. (2006). Impaired regulatory T-cell response and enhanced atherosclerosis in the absence of inducible costimulatory molecule. Circulation *114*, 2047-2055.

Gowans, G.J., Hawley, S.A., Ross, F.A., and Hardie, D.G. (2013). AMP is a true physiological regulator of AMP-activated protein kinase by both allosteric activation and enhancing net phosphorylation. Cell Metab *18*, 556-566.

Grahame-Clarke, C., Chan, N.N., Andrew, D., Ridgway, G.L., Betteridge, D.J., Emery, V., Colhoun, H.M., and Vallance, P. (2003). Human cytomegalovirus seropositivity is associated with impaired vascular function. Circulation *108*, 678-683.

Grant, C.R., Liberal, R., Holder, B.S., Cardone, J., Ma, Y., Robson, S.C., Mieli-Vergani, G., Vergani, D., and Longhi, M.S. (2014). Dysfunctional CD39(POS) regulatory T cells and aberrant control of T-helper type 17 cells in autoimmune hepatitis. Hepatology *59*, 1007-1015.

Greer, E.L., Dowlatshahi, D., Banko, M.R., Villen, J., Hoang, K., Blanchard, D., Gygi, S.P., and Brunet, A. (2007). An AMPK-FOXO pathway mediates longevity induced by a novel method of dietary restriction in C. elegans. Curr Biol *17*, 1646-1656.

Grootaert, M.O., da Costa Martins, P.A., Bitsch, N., Pintelon, I., De Meyer, G.R., Martinet, W., and Schrijvers, D.M. (2015). Defective autophagy in vascular smooth muscle cells accelerates senescence and promotes neointima formation and atherogenesis. Autophagy *11*, 2014-2032.

Grubeck-Loebenstein, B., Berger, P., Saurwein-Teissl, M., Zisterer, K., and Wick, G. (1998). No immunity for the elderly. Nat Med *4*, 870.

Guo, Z., Wang, G., Wu, B., Chou, W.C., Cheng, L., Zhou, C., Lou, J., Wu, D., Su, L., Zheng, J.*, et al.* (2020). DCAF1 regulates Treg senescence via the ROS axis during immunological aging. J Clin Invest *130*, 5893-5908.

Gutierrez-Salmeron, M., Garcia-Martinez, J.M., Martinez-Useros, J., Fernandez-Acenero, M.J., Viollet, B., Olivier, S., Chauhan, J., Lucena, S.R., De la Vieja, A., Goding, C.R.*, et al.* (2020). Paradoxical activation of AMPK by glucose drives selective EP300 activity in colorectal cancer. PLoS Biol *18*, e3000732.

Gwinn, D.M., Shackelford, D.B., Egan, D.F., Mihaylova, M.M., Mery, A., Vasquez, D.S., Turk, B.E., and Shaw, R.J. (2008). AMPK phosphorylation of raptor mediates a metabolic checkpoint. Mol Cell *30*, 214-226.

Hakim, F.T., Flomerfelt, F.A., Boyiadzis, M., and Gress, R.E. (2004). Aging, immunity and cancer. Curr Opin

Immunol *16*, 151-156.

Han, X., Tai, H., Wang, X., Wang, Z., Zhou, J., Wei, X., Ding, Y., Gong, H., Mo, C., Zhang, J.*, et al.* (2016). AMPK activation protects cells from oxidative stress-induced senescence via autophagic flux restoration and intracellular NAD(+) elevation. Aging Cell *15*, 416-427.

Han, Y., Liu, D., and Li, L. (2020). PD-1/PD-L1 pathway: current researches in cancer. Am J Cancer Res *10*, 727-742.

Handschin, C. (2016). Caloric restriction and exercise "mimetics": Ready for prime time? Pharmacol Res *103*, 158-166.

Hao, Z., Ma, Y., Wang, J., Fan, D., Han, C., Wang, Y., Ji, Y., and Wen, S. (2015). Hypoxia promotes AMP-activated protein kinase (AMPK) and induces apoptosis in mouse osteoblasts. Int J Clin Exp Pathol *8*, 4892-4902.

Hardie, D.G. (2007). AMP-activated/SNF1 protein kinases: conserved guardians of cellular energy. Nat Rev Mol Cell Biol *8*, 774-785.

Hardie, D.G. (2008). AMPK: a key regulator of energy balance in the single cell and the whole organism. Int J Obes (Lond) *32 Suppl 4*, S7-12.

Hardie, D.G. (2011). Adenosine monophosphate-activated protein kinase: a central regulator of metabolism with roles in diabetes, cancer, and viral infection. Cold Spring Harb Symp Quant Biol *76*, 155-164.

Hardie, D.G. (2015). Molecular Pathways: Is AMPK a Friend or a Foe in Cancer? Clin Cancer Res *21*, 3836-3840.

Hardie, D.G., and Carling, D. (1997). The AMP-activated protein kinase--fuel gauge of the mammalian cell? Eur J Biochem *246*, 259-273.

Hardie, D.G., Ross, F.A., and Hawley, S.A. (2012). AMPK: a nutrient and energy sensor that maintains energy homeostasis. Nat Rev Mol Cell Biol *13*, 251-262.

Hatziioannou, A., Alissafi, T., and Verginis, P. (2017). Myeloid-derived suppressor cells and T regulatory cells in tumors: unraveling the dark side of the force. J Leukoc Biol *102*, 407-421.

Hatzioannou, A., Banos, A., Sakelaropoulos, T., Fedonidis, C., Vidali, M.S., Kohne, M., Handler, K., Boon, L., Henriques, A., Koliaraki, V.*, et al.* (2020). An intrinsic role of IL-33 in Treg cell-mediated tumor immunoevasion. Nat Immunol *21*, 75-85.

Hawley, S.A., Boudeau, J., Reid, J.L., Mustard, K.J., Udd, L., Makela, T.P., Alessi, D.R., and Hardie, D.G. (2003). Complexes between the LKB1 tumor suppressor, STRAD alpha/beta and MO25 alpha/beta are upstream kinases in the AMP-activated protein kinase cascade. J Biol *2*, 28.

Hawley, S.A., Ross, F.A., Chevtzoff, C., Green, K.A., Evans, A., Fogarty, S., Towler, M.C., Brown, L.J., Ogunbayo, O.A., Evans, A.M.*, et al.* (2010). Use of cells expressing gamma subunit variants to identify diverse mechanisms of AMPK activation. Cell Metab *11*, 554-565.

Hawley, S.A., Selbert, M.A., Goldstein, E.G., Edelman, A.M., Carling, D., and Hardie, D.G. (1995). 5'-AMP activates the AMP-activated protein kinase cascade, and Ca2+/calmodulin activates the calmodulin-dependent protein kinase I cascade, via three independent mechanisms. J Biol Chem *270*, 27186-27191.

He, J., Shangguan, X., Zhou, W., Cao, Y., Zheng, Q., Tu, J., Hu, G., Liang, Z., Jiang, C., Deng, L.*, et al.* (2021). Glucose limitation activates AMPK coupled SENP1-Sirt3 signalling in mitochondria for T cell memory development. Nat Commun *12*, 4371.

He, N., Fan, W., Henriquez, B., Yu, R.T., Atkins, A.R., Liddle, C., Zheng, Y., Downes, M., and Evans, R.M. (2017). Metabolic control of regulatory T cell (Treg) survival and function by Lkb1. Proc Natl Acad Sci U S A *114*, 12542-12547.

Herrington, W., Lacey, B., Sherliker, P., Armitage, J., and Lewington, S. (2016). Epidemiology of Atherosclerosis and the Potential to Reduce the Global Burden of Atherothrombotic Disease. Circ Res *118*, 535-546.

Herzig, S., and Shaw, R.J. (2018). AMPK: guardian of metabolism and mitochondrial homeostasis. Nat Rev Mol Cell Biol *19*, 121-135.

Hinchy, E.C., Gruszczyk, A.V., Willows, R., Navaratnam, N., Hall, A.R., Bates, G., Bright, T.P., Krieg, T., Carling, D., and Murphy, M.P. (2018). Mitochondria-derived ROS activate AMP-activated protein kinase (AMPK) indirectly. J Biol Chem *293*, 17208-17217.

Hopkins, P.N., Toth, P.P., Ballantyne, C.M., Rader, D.J., and National Lipid Association Expert Panel on Familial, H. (2011). Familial hypercholesterolemias: prevalence, genetics, diagnosis and screening recommendations from the National Lipid Association Expert Panel on Familial Hypercholesterolemia. J Clin Lipidol *5*, S9-17.

Hori, S. (2014). Lineage stability and phenotypic plasticity of Foxp3(+) regulatory T cells. Immunol Rev *259*, 159-172.

Huber, S., and Schramm, C. (2006). TGF-beta and CD4+CD25+ regulatory T cells. Front Biosci *11*, 1014-1023.

Hudson, E.R., Pan, D.A., James, J., Lucocq, J.M., Hawley, S.A., Green, K.A., Baba, O., Terashima, T., and Hardie, D.G. (2003). A novel domain in AMP-activated protein kinase causes glycogen storage bodies similar to those seen in hereditary cardiac arrhythmias. Curr Biol *13*, 861-866.

Ido, Y., Duranton, A., Lan, F., Cacicedo, J.M., Chen, T.C., Breton, L., and Ruderman, N.B. (2012). Acute activation of AMP-activated protein kinase prevents H2O2-induced premature senescence in primary human keratinocytes. PLoS One *7*, e35092.

Inata, Y., Kikuchi, S., Samraj, R.S., Hake, P.W., O'Connor, M., Ledford, J.R., O'Connor, J., Lahni, P., Wolfe, V., Piraino, G.*, et al.* (2018). Autophagy and mitochondrial biogenesis impairment contribute to age-dependent liver injury in experimental sepsis: dysregulation of AMP-activated protein kinase pathway. FASEB J *32*, 728-741.

Inoki, K., Zhu, T., and Guan, K.L. (2003). TSC2 mediates cellular energy response to control cell growth and survival. Cell *115*, 577-590.

Jackson, S.H., Devadas, S., Kwon, J., Pinto, L.A., and Williams, M.S. (2004). T cells express a phagocyte-type NADPH oxidase that is activated after T cell receptor stimulation. Nat Immunol *5*, 818-827.

Johnson, J.L. (2007). Matrix metalloproteinases: influence on smooth muscle cells and atherosclerotic plaque stability. Expert Rev Cardiovasc Ther *5*, 265-282.

Jones, R.G., and Thompson, C.B. (2007). Revving the engine: signal transduction fuels T cell activation. Immunity *27*, 173-178.

Jorgensen, S.B., Viollet, B., Andreelli, F., Frosig, C., Birk, J.B., Schjerling, P., Vaulont, S., Richter, E.A., and Wojtaszewski, J.F. (2004). Knockout of the alpha2 but not alpha1 5'-AMP-activated protein kinase isoform abolishes 5-aminoimidazole-4-carboxamide-1-beta-4-ribofuranosidebut not contraction-induced glucose uptake in skeletal muscle. J Biol Chem *279*, 1070-1079.

Josefowicz, S.Z., Lu, L.F., and Rudensky, A.Y. (2012). Regulatory T cells: mechanisms of differentiation and function. Annu Rev Immunol *30*, 531-564.

Kahn, B.B., Alquier, T., Carling, D., and Hardie, D.G. (2005). AMP-activated protein kinase: ancient energy gauge provides clues to modern understanding of metabolism. Cell Metab *1*, 15-25.

Kaplan, R.C., Sinclair, E., Landay, A.L., Lurain, N., Sharrett, A.R., Gange, S.J., Xue, X., Hunt, P., Karim, R., Kern, D.M*., et al.* (2011). T cell activation and senescence predict subclinical carotid artery disease in HIV-infected women. J Infect Dis *203*, 452-463.

Kido, M., Watanabe, N., Okazaki, T., Akamatsu, T., Tanaka, J., Saga, K., Nishio, A., Honjo, T., and Chiba, T. (2008). Fatal autoimmune hepatitis induced by concurrent loss of naturally arising regulatory T cells and PD-1-mediated signaling. Gastroenterology *135*, 1333-1343.

Kim, J., Kim, Y.C., Fang, C., Russell, R.C., Kim, J.H., Fan, W., Liu, R., Zhong, Q., and Guan, K.L. (2013). Differential regulation of distinct Vps34 complexes by AMPK in nutrient stress and autophagy. Cell *152*, 290-303.

Kim, J., Kundu, M., Viollet, B., and Guan, K.L. (2011). AMPK and mTOR regulate autophagy through direct phosphorylation of Ulk1. Nat Cell Biol *13*, 132-141.

Kim, J.H., Park, J.M., Yea, K., Kim, H.W., Suh, P.G., and Ryu, S.H. (2010). Phospholipase D1 mediates AMP-activated protein kinase signaling for glucose uptake. PLoS One *5*, e9600.

Kishton, R.J., Barnes, C.E., Nichols, A.G., Cohen, S., Gerriets, V.A., Siska, P.J., Macintyre, A.N., Goraksha-Hicks, P., de Cubas, A.A., Liu, T*., et al.* (2016). AMPK Is Essential to Balance Glycolysis and Mitochondrial Metabolism to Control T-ALL Cell Stress and Survival. Cell Metab *23*, 649-662.

Koch, M.A., Thomas, K.R., Perdue, N.R., Smigiel, K.S., Srivastava, S., and Campbell, D.J. (2012). T-bet(+) Treg cells undergo abortive Th1 cell differentiation due to impaired expression of IL-12 receptor beta2. Immunity *37*, 501-510.

Konopka, A.R., and Miller, B.F. (2019). Taming expectations of metformin as a treatment to extend healthspan. Geroscience *41*, 101-108.

Krawczyk, C.M., Holowka, T., Sun, J., Blagih, J., Amiel, E., DeBerardinis, R.J., Cross, J.R., Jung, E., Thompson, C.B., Jones, R.G*., et al.* (2010). Toll-like receptor-induced changes in glycolytic metabolism regulate dendritic cell activation. Blood *115*, 4742-4749.

Krawitt, E.L. (2006). Autoimmune hepatitis. N Engl J Med *354*, 54-66.

Kuilman, T., Michaloglou, C., Mooi, W.J., and Peeper, D.S. (2010). The essence of senescence. Genes Dev *24*, 2463-2479.

Kuiper, E.M., Hansen, B.E., de Vries, R.A., den Ouden-Muller, J.W., van Ditzhuijsen, T.J., Haagsma, E.B., Houben, M.H., Witteman, B.J., van Erpecum, K.J., van Buuren, H.R*., et al.* (2009). Improved prognosis of patients with primary biliary cirrhosis that have a biochemical response to ursodeoxycholic acid. Gastroenterology *136*, 1281-1287.

Kukidome, D., Nishikawa, T., Sonoda, K., Imoto, K., Fujisawa, K., Yano, M., Motoshima, H., Taguchi, T., Matsumura, T., and Araki, E. (2006). Activation of AMP-activated protein kinase reduces hyperglycemia-induced mitochondrial reactive oxygen species production and promotes mitochondrial biogenesis in human umbilical vein endothelial cells. Diabetes *55*, 120-127.

Kumagai, S., Koyama, S., Itahashi, K., Tanegashima, T., Lin, Y.T., Togashi, Y., Kamada, T., Irie, T., Okumura, G., Kono, H*., et al.* (2022). Lactic acid promotes PD-1 expression in regulatory T cells in highly

glycolytic tumor microenvironments. Cancer Cell *40*, 201-218 e209.

Kumar, V., Patel, S., Tcyganov, E., and Gabrilovich, D.I. (2016). The Nature of Myeloid-Derived Suppressor Cells in the Tumor Microenvironment. Trends Immunol *37*, 208-220.

Lam, E.W., Brosens, J.J., Gomes, A.R., and Koo, C.Y. (2013). Forkhead box proteins: tuning forks for transcriptional harmony. Nat Rev Cancer *13*, 482-495.

Lapierre, P., Beland, K., Yang, R., and Alvarez, F. (2013). Adoptive transfer of ex vivo expanded regulatory T cells in an autoimmune hepatitis murine model restores peripheral tolerance. Hepatology *57*, 217-227.

Lapierre, P., and Lamarre, A. (2015). Regulatory T Cells in Autoimmune and Viral Chronic Hepatitis. J Immunol Res *2015*, 479703.

Le Bourg, E. (2009). Hormesis, aging and longevity. Biochim Biophys Acta *1790*, 1030-1039.

Lee, J.H., Elly, C., Park, Y., and Liu, Y.C. (2015a). E3 Ubiquitin Ligase VHL Regulates Hypoxia-Inducible Factor-1alpha to Maintain Regulatory T Cell Stability and Suppressive Capacity. Immunity *42*, 1062-1074.

Lee, J.H., Jang, H., Lee, S.M., Lee, J.E., Choi, J., Kim, T.W., Cho, E.J., and Youn, H.D. (2015b). ATP-citrate lyase regulates cellular senescence via an AMPK- and p53-dependent pathway. FEBS J *282*, 361-371.

Lee, S.Y., Moon, S.J., Kim, E.K., Seo, H.B., Yang, E.J., Son, H.J., Kim, J.K., Min, J.K., Park, S.H., and Cho, M.L. (2017). Metformin Suppresses Systemic Autoimmunity in Roquin(san/san) Mice through Inhibiting B Cell Differentiation into Plasma Cells via Regulation of AMPK/mTOR/STAT3. J Immunol *198*, 2661-2670.

Lee, Y.T., Lim, S.H., Lee, B., Kang, I., and Yeo, E.J. (2019). Compound C Inhibits B16-F1 Tumor Growth in a Syngeneic Mouse Model Via the Blockage of Cell Cycle Progression and Angiogenesis. Cancers (Basel) *11*.

Leon, M.L., and Zuckerman, S.H. (2005). Gamma interferon: a central mediator in atherosclerosis. Inflamm Res *54*, 395-411.

Lepez, A., Pirnay, T., Denanglaire, S., Perez-Morga, D., Vermeersch, M., Leo, O., and Andris, F. (2020). Long-term T cell fitness and proliferation is driven by AMPK-dependent regulation of reactive oxygen species. Sci Rep *10*, 21673.

Li, B., Samanta, A., Song, X., Iacono, K.T., Bembas, K., Tao, R., Basu, S., Riley, J.L., Hancock, W.W., Shen, Y.*, et al.* (2007). FOXP3 interactions with histone acetyltransferase and class II histone deacetylases are required for repression. Proc Natl Acad Sci U S A *104*, 4571-4576.

Li, C., Jiang, P., Wei, S., Xu, X., and Wang, J. (2020a). Regulatory T cells in tumor microenvironment: new mechanisms, potential therapeutic strategies and future prospects. Mol Cancer *19*, 116.

Li, J., McArdle, S., Gholami, A., Kimura, T., Wolf, D., Gerhardt, T., Miller, J., Weber, C., and Ley, K. (2016a). CCR5+T-bet+FoxP3+ Effector CD4 T Cells Drive Atherosclerosis. Circ Res *118*, 1540-1552.

Li, J., Wang, Y., Wang, Y., Wen, X., Ma, X.N., Chen, W., Huang, F., Kou, J., Qi, L.W., Liu, B.*, et al.* (2015). Pharmacological activation of AMPK prevents Drp1-mediated mitochondrial fission and alleviates endoplasmic reticulum stress-associated endothelial dysfunction. J Mol Cell Cardiol *86*, 62-74.

Li, W., Elshikha, A.S., Cornaby, C., Teng, X., Abboud, G., Brown, J., Zou, X., Zeumer-Spataro, L., Robusto, B., Choi, S.C.*, et al.* (2020b). T cells expressing the lupus susceptibility allele Pbx1d enhance

autoimmunity and atherosclerosis in dyslipidemic mice. JCI Insight *5*.

Li, W., Tanikawa, T., Kryczek, I., Xia, H., Li, G., Wu, K., Wei, S., Zhao, L., Vatan, L., Wen, B.*, et al.* (2018). Aerobic Glycolysis Controls Myeloid-Derived Suppressor Cells and Tumor Immunity via a Specific CEBPB Isoform in Triple-Negative Breast Cancer. Cell Metab *28*, 87-103 e106.

Li, Y., Lu, Y., Wang, S., Han, Z., Zhu, F., Ni, Y., Liang, R., Zhang, Y., Leng, Q., Wei, G.*, et al.* (2016b). USP21 prevents the generation of T-helper-1-like Treg cells. Nat Commun *7*, 13559.

Li, Z., Lin, F., Zhuo, C., Deng, G., Chen, Z., Yin, S., Gao, Z., Piccioni, M., Tsun, A., Cai, S.*, et al.* (2014). PIM1 kinase phosphorylates the human transcription factor FOXP3 at serine 422 to negatively regulate its activity under inflammation. J Biol Chem *289*, 26872-26881.

Libby, P., Buring, J.E., Badimon, L., Hansson, G.K., Deanfield, J., Bittencourt, M.S., Tokgozoglu, L., and Lewis, E.F. (2019). Atherosclerosis. Nat Rev Dis Primers *5*, 56.

Liberal, R., Grant, C.R., Longhi, M.S., Mieli-Vergani, G., and Vergani, D. (2015). Regulatory T cells: Mechanisms of suppression and impairment in autoimmune liver disease. IUBMB Life *67*, 88-97.

Liberal, R., Grant, C.R., Yuksel, M., Graham, J., Kalbasi, A., Ma, Y., Heneghan, M.A., Mieli-Vergani, G., Vergani, D., and Longhi, M.S. (2017). Regulatory T-cell conditioning endows activated effector T cells with suppressor function in autoimmune hepatitis/autoimmune sclerosing cholangitis. Hepatology *66*, 1570-1584.

Liberale, L., Montecucco, F., Tardif, J.C., Libby, P., and Camici, G.G. (2020). Inflamm-ageing: the role of inflammation in age-dependent cardiovascular disease. Eur Heart J *41*, 2974-2982.

Lim, S.A., Wei, J., Nguyen, T.M., Shi, H., Su, W., Palacios, G., Dhungana, Y., Chapman, N.M., Long, L., Saravia, J.*, et al.* (2021). Lipid signalling enforces functional specialization of Treg cells in tumours. Nature *591*, 306-311.

Lin, K., Dorman, J.B., Rodan, A., and Kenyon, C. (1997). daf-16: An HNF-3/forkhead family member that can function to double the life-span of Caenorhabditis elegans. Science *278*, 1319-1322.

Liu, B., Salgado, O.C., Singh, S., Hippen, K.L., Maynard, J.C., Burlingame, A.L., Ball, L.E., Blazar, B.R., Farrar, M.A., Hogquist, K.A.*, et al.* (2019). The lineage stability and suppressive program of regulatory T cells require protein O-GlcNAcylation. Nat Commun *10*, 354.

Liu, Y., Wang, L., Predina, J., Han, R., Beier, U.H., Wang, L.C., Kapoor, V., Bhatti, T.R., Akimova, T., Singhal, S.*, et al.* (2013). Inhibition of p300 impairs Foxp3(+) T regulatory cell function and promotes antitumor immunity. Nat Med *19*, 1173-1177.

Ljubicic, V., and Jasmin, B.J. (2013). AMP-activated protein kinase at the nexus of therapeutic skeletal muscle plasticity in Duchenne muscular dystrophy. Trends Mol Med *19*, 614-624.

Longhi, M.S., Ma, Y., Bogdanos, D.P., Cheeseman, P., Mieli-Vergani, G., and Vergani, D. (2004). Impairment of CD4(+)CD25(+) regulatory T-cells in autoimmune liver disease. J Hepatol *41*, 31-37.

Longhi, M.S., Mitry, R.R., Samyn, M., Scalori, A., Hussain, M.J., Quaglia, A., Mieli-Vergani, G., Ma, Y., and Vergani, D. (2009). Vigorous activation of monocytes in juvenile autoimmune liver disease escapes the control of regulatory T-cells. Hepatology *50*, 130-142.

Lopes, J.E., Torgerson, T.R., Schubert, L.A., Anover, S.D., Ocheltree, E.L., Ochs, H.D., and Ziegler, S.F. (2006). Analysis of FOXP3 reveals multiple domains required for its function as a transcriptional repressor. J Immunol *177*, 3133-3142.

Lu, X., Xuan, W., Li, J., Yao, H., Huang, C., and Li, J. (2021). AMPK protects against alcohol-induced liver

injury through UQCRC2 to up-regulate mitophagy. Autophagy *17*, 3622-3643.

Ma, E.H., Poffenberger, M.C., Wong, A.H., and Jones, R.G. (2017). The role of AMPK in T cell metabolism and function. Curr Opin Immunol *46*, 45-52.

MacIver, N.J., Blagih, J., Saucillo, D.C., Tonelli, L., Griss, T., Rathmell, J.C., and Jones, R.G. (2011). The liver kinase B1 is a central regulator of T cell development, activation, and metabolism. J Immunol *187*, 4187-4198.

Martin, F., Ladoire, S., Mignot, G., Apetoh, L., and Ghiringhelli, F. (2010). Human FOXP3 and cancer. Oncogene *29*, 4121-4129.

Matheu, A., Maraver, A., Klatt, P., Flores, I., Garcia-Cao, I., Borras, C., Flores, J.M., Vina, J., Blasco, M.A., and Serrano, M. (2007). Delayed ageing through damage protection by the Arf/p53 pathway. Nature *448*, 375-379.

Matthews, C., Gorenne, I., Scott, S., Figg, N., Kirkpatrick, P., Ritchie, A., Goddard, M., and Bennett, M. (2006). Vascular smooth muscle cells undergo telomere-based senescence in human atherosclerosis: effects of telomerase and oxidative stress. Circ Res *99*, 156-164.

Mayer, A., Denanglaire, S., Viollet, B., Leo, O., and Andris, F. (2008). AMP-activated protein kinase regulates lymphocyte responses to metabolic stress but is largely dispensable for immune cell development and function. Eur J Immunol *38*, 948-956.

Meley, D., Bauvy, C., Houben-Weerts, J.H., Dubbelhuis, P.F., Helmond, M.T., Codogno, P., and Meijer, A.J. (2006). AMP-activated protein kinase and the regulation of autophagic proteolysis. J Biol Chem *281*, 34870-34879.

Michalek, R.D., Gerriets, V.A., Jacobs, S.R., Macintyre, A.N., MacIver, N.J., Mason, E.F., Sullivan, S.A., Nichols, A.G., and Rathmell, J.C. (2011). Cutting edge: distinct glycolytic and lipid oxidative metabolic programs are essential for effector and regulatory CD4+ T cell subsets. J Immunol *186*, 3299-3303.

Mihaylova, M.M., Vasquez, D.S., Ravnskjaer, K., Denechaud, P.D., Yu, R.T., Alvarez, J.G., Downes, M., Evans, R.M., Montminy, M., and Shaw, R.J. (2011). Class IIa histone deacetylases are hormone-activated regulators of FOXO and mammalian glucose homeostasis. Cell *145*, 607-621.

Minamino, T., Miyauchi, H., Yoshida, T., Ishida, Y., Yoshida, H., and Komuro, I. (2002). Endothelial cell senescence in human atherosclerosis: role of telomere in endothelial dysfunction. Circulation *105*, 1541-1544.

Miyao, T., Floess, S., Setoguchi, R., Luche, H., Fehling, H.J., Waldmann, H., Huehn, J., and Hori, S. (2012). Plasticity of Foxp3(+) T cells reflects promiscuous Foxp3 expression in conventional T cells but not reprogramming of regulatory T cells. Immunity *36*, 262-275.

Morawski, P.A., Mehra, P., Chen, C., Bhatti, T., and Wells, A.D. (2013). Foxp3 protein stability is regulated by cyclin-dependent kinase 2. J Biol Chem *288*, 24494-24502.

Munoz-Espin, D., Canamero, M., Maraver, A., Gomez-Lopez, G., Contreras, J., Murillo-Cuesta, S., Rodriguez-Baeza, A., Varela-Nieto, I., Ruberte, J., Collado, M.*, et al.* (2013). Programmed cell senescence during mammalian embryonic development. Cell *155*, 1104-1118.

Munoz-Rojas, A.R., and Mathis, D. (2021). Tissue regulatory T cells: regulatory chameleons. Nat Rev Immunol *21*, 597-611.

Nakahata, Y., Sahar, S., Astarita, G., Kaluzova, M., and Sassone-Corsi, P. (2009). Circadian control of the

NAD+ salvage pathway by CLOCK-SIRT1. Science *324*, 654-657.

Nath, N., Khan, M., Paintlia, M.K., Singh, I., Hoda, M.N., and Giri, S. (2009a). Metformin attenuated the autoimmune disease of the central nervous system in animal models of multiple sclerosis. J Immunol *182*, 8005-8014.

Nath, N., Khan, M., Rattan, R., Mangalam, A., Makkar, R.S., de Meester, C., Bertrand, L., Singh, I., Chen, Y., Viollet, B.*, et al.* (2009b). Loss of AMPK exacerbates experimental autoimmune encephalomyelitis disease severity. Biochem Biophys Res Commun *386*, 16-20.

Ngoei, K.R.W., Langendorf, C.G., Ling, N.X.Y., Hoque, A., Varghese, S., Camerino, M.A., Walker, S.R., Bozikis, Y.E., Dite, T.A., Ovens, A.J.*, et al.* (2018). Structural Determinants for Small-Molecule Activation of Skeletal Muscle AMPK alpha2beta2gamma1 by the Glucose Importagog SC4. Cell Chem Biol *25*, 728-737 e729.

Niccoli, T., and Partridge, L. (2012). Ageing as a risk factor for disease. Curr Biol *22*, R741-752.

Nie, H., Zheng, Y., Li, R., Guo, T.B., He, D., Fang, L., Liu, X., Xiao, L., Chen, X., Wan, B.*, et al.* (2013). Phosphorylation of FOXP3 controls regulatory T cell function and is inhibited by TNF-alpha in rheumatoid arthritis. Nat Med *19*, 322-328.

Nie, J., Li, Y.Y., Zheng, S.G., Tsun, A., and Li, B. (2015). FOXP3(+) Treg Cells and Gender Bias in Autoimmune Diseases. Front Immunol *6*, 493.

Nijman, S.M., Luna-Vargas, M.P., Velds, A., Brummelkamp, T.R., Dirac, A.M., Sixma, T.K., and Bernards, R. (2005). A genomic and functional inventory of deubiquitinating enzymes. Cell *123*, 773-786.

Nordestgaard, B.G., Chapman, M.J., Humphries, S.E., Ginsberg, H.N., Masana, L., Descamps, O.S., Wiklund, O., Hegele, R.A., Raal, F.J., Defesche, J.C.*, et al.* (2013). Familial hypercholesterolaemia is underdiagnosed and undertreated in the general population: guidance for clinicians to prevent coronary heart disease: consensus statement of the European Atherosclerosis Society. Eur Heart J *34*, 3478-3490a.

Noto, H., Goto, A., Tsujimoto, T., and Noda, M. (2012). Cancer risk in diabetic patients treated with metformin: a systematic review and meta-analysis. PLoS One *7*, e33411.

O'Neill, H.M., Holloway, G.P., and Steinberg, G.R. (2013). AMPK regulation of fatty acid metabolism and mitochondrial biogenesis: implications for obesity. Mol Cell Endocrinol *366*, 135-151.

O'Neill, H.M., Maarbjerg, S.J., Crane, J.D., Jeppesen, J., Jorgensen, S.B., Schertzer, J.D., Shyroka, O., Kiens, B., van Denderen, B.J., Tarnopolsky, M.A.*, et al.* (2011). AMP-activated protein kinase (AMPK) beta1beta2 muscle null mice reveal an essential role for AMPK in maintaining mitochondrial content and glucose uptake during exercise. Proc Natl Acad Sci U S A *108*, 16092-16097.

O'Neill, L.A., and Hardie, D.G. (2013). Metabolism of inflammation limited by AMPK and pseudo-starvation. Nature *493*, 346-355.

Ohkura, N., and Sakaguchi, S. (2020). Transcriptional and epigenetic basis of Treg cell development and function: its genetic anomalies or variations in autoimmune diseases. Cell Res *30*, 465-474.

Ohue, Y., and Nishikawa, H. (2019). Regulatory T (Treg) cells in cancer: Can Treg cells be a new therapeutic target? Cancer Sci *110*, 2080-2089.

Oldenhove, G., Bouladoux, N., Wohlfert, E.A., Hall, J.A., Chou, D., Dos Santos, L., O'Brien, S., Blank, R., Lamb, E., Natarajan, S.*, et al.* (2009). Decrease of Foxp3+ Treg cell number and acquisition of

effector cell phenotype during lethal infection. Immunity *31*, 772-786.

Olson, N.C., Doyle, M.F., Jenny, N.S., Huber, S.A., Psaty, B.M., Kronmal, R.A., and Tracy, R.P. (2013). Decreased naive and increased memory CD4(+) T cells are associated with subclinical atherosclerosis: the multi-ethnic study of atherosclerosis. PLoS One *8*, e71498.

Ono, M. (2020). Control of regulatory T-cell differentiation and function by T-cell receptor signalling and Foxp3 transcription factor complexes. Immunology *160*, 24-37.

Overacre-Delgoffe, A.E., Chikina, M., Dadey, R.E., Yano, H., Brunazzi, E.A., Shayan, G., Horne, W., Moskovitz, J.M., Kolls, J.K., Sander, C.*, et al.* (2017). Interferon-gamma Drives Treg Fragility to Promote Anti-tumor Immunity. Cell *169*, 1130-1141 e1111.

Overacre-Delgoffe, A.E., and Vignali, D.A.A. (2018). Treg Fragility: A Prerequisite for Effective Antitumor Immunity? Cancer Immunol Res *6*, 882-887.

Partridge, L., Deelen, J., and Slagboom, P.E. (2018). Facing up to the global challenges of ageing. Nature *561*, 45-56.

Paul, I., and Ghosh, M.K. (2014). The E3 ligase CHIP: insights into its structure and regulation. Biomed Res Int *2014*, 918183.

Pawelec, G. (2014). Immunosenenescence: role of cytomegalovirus. Exp Gerontol *54*, 1-5.

Pearce, E.L., Walsh, M.C., Cejas, P.J., Harms, G.M., Shen, H., Wang, L.S., Jones, R.G., and Choi, Y. (2009). Enhancing CD8 T-cell memory by modulating fatty acid metabolism. Nature *460*, 103-107.

Peralta, S., Garcia, S., Yin, H.Y., Arguello, T., Diaz, F., and Moraes, C.T. (2016). Sustained AMPK activation improves muscle function in a mitochondrial myopathy mouse model by promoting muscle fiber regeneration. Hum Mol Genet *25*, 3178-3191.

Petty, A.J., and Yang, Y. (2017). Tumor-associated macrophages: implications in cancer immunotherapy. Immunotherapy *9*, 289-302.

Pinkosky, S.L., Scott, J.W., Desjardins, E.M., Smith, B.K., Day, E.A., Ford, R.J., Langendorf, C.G., Ling, N.X.Y., Nero, T.L., Loh, K.*, et al.* (2020). Long-chain fatty acyl-CoA esters regulate metabolism via allosteric control of AMPK beta1 isoforms. Nat Metab *2*, 873-881.

Qiang, W., Weiqiang, K., Qing, Z., Pengju, Z., and Yi, L. (2007). Aging impairs insulin-stimulated glucose uptake in rat skeletal muscle via suppressing AMPKalpha. Exp Mol Med *39*, 535-543.

Qiu, R., Zhou, L., Ma, Y., Zhou, L., Liang, T., Shi, L., Long, J., and Yuan, D. (2020). Regulatory T Cell Plasticity and Stability and Autoimmune Diseases. Clin Rev Allergy Immunol *58*, 52-70.

Qureshi, O.S., Zheng, Y., Nakamura, K., Attridge, K., Manzotti, C., Schmidt, E.M., Baker, J., Jeffery, L.E., Kaur, S., Briggs, Z.*, et al.* (2011). Trans-endocytosis of CD80 and CD86: a molecular basis for the cell-extrinsic function of CTLA-4. Science *332*, 600-603.

Rabinovitch, R.C., Samborska, B., Faubert, B., Ma, E.H., Gravel, S.P., Andrzejewski, S., Raissi, T.C., Pause, A., St-Pierre, J., and Jones, R.G. (2017). AMPK Maintains Cellular Metabolic Homeostasis through Regulation of Mitochondrial Reactive Oxygen Species. Cell Rep *21*, 1-9.

Rajamohan, F., Reyes, A.R., Frisbie, R.K., Hoth, L.R., Sahasrabudhe, P., Magyar, R., Landro, J.A., Withka, J.M., Caspers, N.L., Calabrese, M.F.*, et al.* (2016). Probing the enzyme kinetics, allosteric modulation and activation of alpha1- and alpha2-subunit-containing AMP-activated protein kinase (AMPK) heterotrimeric complexes by pharmacological and physiological activators. Biochem J *473*, 581-592.

Rao, E., Zhang, Y., Zhu, G., Hao, J., Persson, X.M., Egilmez, N.K., Suttles, J., and Li, B. (2015a). Deficiency of AMPK in CD8+ T cells suppresses their anti-tumor function by inducing protein phosphatase-mediated cell death. Oncotarget *6*, 7944-7958.

Rao, L.N., Ponnusamy, T., Philip, S., Mukhopadhyay, R., Kakkar, V.V., and Mundkur, L. (2015b). Hypercholesterolemia Induced Immune Response and Inflammation on Progression of Atherosclerosis in Apob(tm2Sgy) Ldlr(tm1Her)/J Mice. Lipids *50*, 785-797.

Ray, P.D., Huang, B.W., and Tsuji, Y. (2012). Reactive oxygen species (ROS) homeostasis and redox regulation in cellular signaling. Cell Signal *24*, 981-990.

Regulski, M.J. (2017). Cellular Senescence: What, Why, and How. Wounds *29*, 168-174.

Ren, H., Shao, Y., Wu, C., Ma, X., Lv, C., and Wang, Q. (2020). Metformin alleviates oxidative stress and enhances autophagy in diabetic kidney disease via AMPK/SIRT1-FoxO1 pathway. Mol Cell Endocrinol *500*, 110628.

Ren, Y., and Shen, H.M. (2019). Critical role of AMPK in redox regulation under glucose starvation. Redox Biol *25*, 101154.

Rodriguez, C., Munoz, M., Contreras, C., and Prieto, D. (2021). AMPK, metabolism, and vascular function. FEBS J *288*, 3746-3771.

Rolf, J., Zarrouk, M., Finlay, D.K., Foretz, M., Viollet, B., and Cantrell, D.A. (2013). AMPKalpha1: a glucose sensor that controls CD8 T-cell memory. Eur J Immunol *43*, 889-896.

Ross, F.A., MacKintosh, C., and Hardie, D.G. (2016). AMP-activated protein kinase: a cellular energy sensor that comes in 12 flavours. FEBS J *283*, 2987-3001.

Rubtsov, Y.P., Niec, R.E., Josefowicz, S., Li, L., Darce, J., Mathis, D., Benoist, C., and Rudensky, A.Y. (2010). Stability of the regulatory T cell lineage in vivo. Science *329*, 1667-1671.

Rubtsov, Y.P., Rasmussen, J.P., Chi, E.Y., Fontenot, J., Castelli, L., Ye, X., Treuting, P., Siewe, L., Roers, A., Henderson, W.R., Jr*., et al.* (2008). Regulatory T cell-derived interleukin-10 limits inflammation at environmental interfaces. Immunity *28*, 546-558.

Rudensky, A.Y. (2011). Regulatory T cells and Foxp3. Immunol Rev *241*, 260-268.

Sag, D., Carling, D., Stout, R.D., and Suttles, J. (2008). Adenosine 5'-monophosphate-activated protein kinase promotes macrophage polarization to an anti-inflammatory functional phenotype. J Immunol *181*, 8633-8641.

Sakaguchi, S. (2004). Naturally arising CD4+ regulatory t cells for immunologic self-tolerance and negative control of immune responses. Annu Rev Immunol *22*, 531-562.

Sakaguchi, S., Mikami, N., Wing, J.B., Tanaka, A., Ichiyama, K., and Ohkura, N. (2020). Regulatory T Cells and Human Disease. Annu Rev Immunol *38*, 541-566.

Sakaguchi, S., Miyara, M., Costantino, C.M., and Hafler, D.A. (2010). FOXP3+ regulatory T cells in the human immune system. Nat Rev Immunol *10*, 490-500.

Sakaguchi, S., Vignali, D.A., Rudensky, A.Y., Niec, R.E., and Waldmann, H. (2013). The plasticity and stability of regulatory T cells. Nat Rev Immunol *13*, 461-467.

Salminen, A., and Kaarniranta, K. (2012). AMP-activated protein kinase (AMPK) controls the aging process via an integrated signaling network. Ageing Res Rev *11*, 230-241.

Samani, N.J., Boultby, R., Butler, R., Thompson, J.R., and Goodall, A.H. (2001). Telomere shortening in atherosclerosis. Lancet *358*, 472-473.

Sarti, P., Forte, E., Giuffre, A., Mastronicola, D., Magnifico, M.C., and Arese, M. (2012). The Chemical Interplay between Nitric Oxide and Mitochondrial Cytochrome c Oxidase: Reactions, Effectors and Pathophysiology. Int J Cell Biol *2012*, 571067.

Sasidharan Nair, V., and Elkord, E. (2018). Immune checkpoint inhibitors in cancer therapy: a focus on T-regulatory cells. Immunol Cell Biol *96*, 21-33.

Scharping, N.E., Menk, A.V., Whetstone, R.D., Zeng, X., and Delgoffe, G.M. (2017). Efficacy of PD-1 Blockade Is Potentiated by Metformin-Induced Reduction of Tumor Hypoxia. Cancer Immunol Res *5*, 9-16.

Schisler, J.C., Rubel, C.E., Zhang, C., Lockyer, P., Cyr, D.M., and Patterson, C. (2013). CHIP protects against cardiac pressure overload through regulation of AMPK. J Clin Invest *123*, 3588-3599.

Shackelford, D.B., and Shaw, R.J. (2009). The LKB1-AMPK pathway: metabolism and growth control in tumour suppression. Nat Rev Cancer *9*, 563-575.

Shakeri, H., Lemmens, K., Gevaert, A.B., De Meyer, G.R.Y., and Segers, V.F.M. (2018). Cellular senescence links aging and diabetes in cardiovascular disease. Am J Physiol Heart Circ Physiol *315*, H448-H462.

Shao, Y., Yang, W.Y., Saaoud, F., Drummer, C.t., Sun, Y., Xu, K., Lu, Y., Shan, H., Shevach, E.M., Jiang, X.*, et al.* (2021). IL-35 promotes CD4+Foxp3+ Tregs and inhibits atherosclerosis via maintaining CCR5-amplified Treg-suppressive mechanisms. JCI Insight *6*.

Sharpless, N.E., and Sherr, C.J. (2015). Forging a signature of in vivo senescence. Nat Rev Cancer *15*, 397-408.

Shaw, R.J., Kosmatka, M., Bardeesy, N., Hurley, R.L., Witters, L.A., DePinho, R.A., and Cantley, L.C. (2004). The tumor suppressor LKB1 kinase directly activates AMP-activated kinase and regulates apoptosis in response to energy stress. Proc Natl Acad Sci U S A *101*, 3329-3335.

Shi, H., and Chi, H. (2019). Metabolic Control of Treg Cell Stability, Plasticity, and Tissue-Specific Heterogeneity. Front Immunol *10*, 2716.

Smigiel, K.S., Srivastava, S., Stolley, J.M., and Campbell, D.J. (2014). Regulatory T-cell homeostasis: steady-state maintenance and modulation during inflammation. Immunol Rev *259*, 40-59.

Smith, B.K., Marcinko, K., Desjardins, E.M., Lally, J.S., Ford, R.J., and Steinberg, G.R. (2016). Treatment of nonalcoholic fatty liver disease: role of AMPK. Am J Physiol Endocrinol Metab *311*, E730-E740.

Smith, P.M., Howitt, M.R., Panikov, N., Michaud, M., Gallini, C.A., Bohlooly, Y.M., Glickman, J.N., and Garrett, W.S. (2013). The microbial metabolites, short-chain fatty acids, regulate colonic Treg cell homeostasis. Science *341*, 569-573.

Son, S.M., Shin, H.J., Byun, J., Kook, S.Y., Moon, M., Chang, Y.J., and Mook-Jung, I. (2016). Metformin Facilitates Amyloid-beta Generation by beta- and gamma-Secretases via Autophagy Activation. J Alzheimers Dis *51*, 1197-1208.

Song, P., Zhao, Q., and Zou, M.H. (2020). Targeting senescent cells to attenuate cardiovascular disease progression. Ageing Res Rev *60*, 101072.

Soto-Gamez, A., and Demaria, M. (2017). Therapeutic interventions for aging: the case of cellular senescence. Drug Discov Today *22*, 786-795.

Stankowski, J.N., Zeiger, S.L., Cohen, E.L., DeFranco, D.B., Cai, J., and McLaughlin, B. (2011). C-terminus of heat shock cognate 70 interacting protein increases following stroke and impairs survival against

acute oxidative stress. Antioxid Redox Signal *14*, 1787-1801.

Stapleton, D., Mitchelhill, K.I., Gao, G., Widmer, J., Michell, B.J., Teh, T., House, C.M., Fernandez, C.S., Cox, T., Witters, L.A.*, et al.* (1996). Mammalian AMP-activated protein kinase subfamily. J Biol Chem *271*, 611-614.

Steinberg, G.R., and Carling, D. (2019). AMP-activated protein kinase: the current landscape for drug development. Nat Rev Drug Discov *18*, 527-551.

Steneberg, P., Lindahl, E., Dahl, U., Lidh, E., Straseviciene, J., Backlund, F., Kjellkvist, E., Berggren, E., Lundberg, I., Bergqvist, I.*, et al.* (2018). PAN-AMPK activator O304 improves glucose homeostasis and microvascular perfusion in mice and type 2 diabetes patients. JCI Insight *3*.

Stoneman, V., Braganza, D., Figg, N., Mercer, J., Lang, R., Goddard, M., and Bennett, M. (2007). Monocyte/macrophage suppression in CD11b diphtheria toxin receptor transgenic mice differentially affects atherogenesis and established plaques. Circ Res *100*, 884-893.

Sun, Y., Tian, T., Gao, J., Liu, X., Hou, H., Cao, R., Li, B., Quan, M., and Guo, L. (2016). Metformin ameliorates the development of experimental autoimmune encephalomyelitis by regulating T helper 17 and regulatory T cells in mice. J Neuroimmunol *292*, 58-67.

Suter, M., Riek, U., Tuerk, R., Schlattner, U., Wallimann, T., and Neumann, D. (2006). Dissecting the role of 5'-AMP for allosteric stimulation, activation, and deactivation of AMP-activated protein kinase. J Biol Chem *281*, 32207-32216.

Tamas, P., Hawley, S.A., Clarke, R.G., Mustard, K.J., Green, K., Hardie, D.G., and Cantrell, D.A. (2006). Regulation of the energy sensor AMP-activated protein kinase by antigen receptor and Ca2+ in T lymphocytes. J Exp Med *203*, 1665-1670.

Tan, H., Yang, K., Li, Y., Shaw, T.I., Wang, Y., Blanco, D.B., Wang, X., Cho, J.H., Wang, H., Rankin, S.*, et al.* (2017). Integrative Proteomics and Phosphoproteomics Profiling Reveals Dynamic Signaling Networks and Bioenergetics Pathways Underlying T Cell Activation. Immunity *46*, 488-503.

Tan, P., Wang, Y.J., Li, S., Wang, Y., He, J.Y., Chen, Y.Y., Deng, H.Q., Huang, W., Zhan, J.K., and Liu, Y.S. (2016). The PI3K/Akt/mTOR pathway regulates the replicative senescence of human VSMCs. Mol Cell Biochem *422*, 1-10.

Tanaka, A., and Sakaguchi, S. (2017). Regulatory T cells in cancer immunotherapy. Cell Res *27*, 109-118.

Thornton, C., Snowden, M.A., and Carling, D. (1998). Identification of a novel AMP-activated protein kinase beta subunit isoform that is highly expressed in skeletal muscle. J Biol Chem *273*, 12443-12450.

Tian, Y., Chen, T., Wu, Y., Yang, L., Wang, L., Fan, X., Zhang, W., Feng, J., Yu, H., Yang, Y.*, et al.* (2017). Pioglitazone stabilizes atherosclerotic plaque by regulating the Th17/Treg balance in AMPK-dependent mechanisms. Cardiovasc Diabetol *16*, 140.

Timilshina, M., You, Z., Lacher, S.M., Acharya, S., Jiang, L., Kang, Y., Kim, J.A., Chang, H.W., Kim, K.J., Park, B.*, et al.* (2019). Activation of Mevalonate Pathway via LKB1 Is Essential for Stability of Treg Cells. Cell Rep *27*, 2948-2961 e2947.

Toker, A., Engelbert, D., Garg, G., Polansky, J.K., Floess, S., Miyao, T., Baron, U., Duber, S., Geffers, R., Giehr, P.*, et al.* (2013). Active demethylation of the Foxp3 locus leads to the generation of stable regulatory T cells within the thymus. J Immunol *190*, 3180-3188.

Trillo-Tinoco, J., Sierra, R.A., Mohamed, E., Cao, Y., de Mingo-Pulido, A., Gilvary, D.L., Anadon, C.M., Costich, T.L., Wei, S., Flores, E.R.*, et al.* (2019). AMPK Alpha-1 Intrinsically Regulates the Function

and Differentiation of Tumor Myeloid-Derived Suppressor Cells. Cancer Res *79*, 5034-5047.

Trivedi, P.J., and Adams, D.H. (2013). Mucosal immunity in liver autoimmunity: a comprehensive review. J Autoimmun *46*, 97-111.

van Loosdregt, J., and Coffer, P.J. (2014). Post-translational modification networks regulating FOXP3 function. Trends Immunol *35*, 368-378.

van Loosdregt, J., Fleskens, V., Fu, J., Brenkman, A.B., Bekker, C.P., Pals, C.E., Meerding, J., Berkers, C.R., Barbi, J., Grone, A.*, et al.* (2013). Stabilization of the transcription factor Foxp3 by the deubiquitinase USP7 increases Treg-cell-suppressive capacity. Immunity *39*, 259-271.

van Loosdregt, J., Vercoulen, Y., Guichelaar, T., Gent, Y.Y., Beekman, J.M., van Beekum, O., Brenkman, A.B., Hijnen, D.J., Mutis, T., Kalkhoven, E.*, et al.* (2010). Regulation of Treg functionality by acetylation-mediated Foxp3 protein stabilization. Blood *115*, 965-974.

van Vliet, T., Varela-Eirin, M., Wang, B., Borghesan, M., Brandenburg, S.M., Franzin, R., Evangelou, K., Seelen, M., Gorgoulis, V., and Demaria, M. (2021). Physiological hypoxia restrains the senescence-associated secretory phenotype via AMPK-mediated mTOR suppression. Mol Cell *81*, 2041-2052 e2046.

Vara-Ciruelos, D., Dandapani, M., Russell, F.M., Grzes, K.M., Atrih, A., Foretz, M., Viollet, B., Lamont, D.J., Cantrell, D.A., and Hardie, D.G. (2019). Phenformin, But Not Metformin, Delays Development of T Cell Acute Lymphoblastic Leukemia/Lymphoma via Cell-Autonomous AMPK Activation. Cell Rep *27*, 690-698 e694.

Veiga-Parga, T., Sehrawat, S., and Rouse, B.T. (2013). Role of regulatory T cells during virus infection. Immunol Rev *255*, 182-196.

Viollet, B., Andreelli, F., Jorgensen, S.B., Perrin, C., Geloen, A., Flamez, D., Mu, J., Lenzner, C., Baud, O., Bennoun, M.*, et al.* (2003). The AMP-activated protein kinase alpha2 catalytic subunit controls whole-body insulin sensitivity. J Clin Invest *111*, 91-98.

Von Bertalanffy, L. (1950). The theory of open systems in physics and biology. Science *111*, 23-29.

Walker, L.S., and Sansom, D.M. (2011). The emerging role of CTLA4 as a cell-extrinsic regulator of T cell responses. Nat Rev Immunol *11*, 852-863.

Wang, B., Nie, J., Wu, L., Hu, Y., Wen, Z., Dong, L., Zou, M.H., Chen, C., and Wang, D.W. (2018). AMPKalpha2 Protects Against the Development of Heart Failure by Enhancing Mitophagy via PINK1 Phosphorylation. Circ Res *122*, 712-729.

Wang, J.C., and Bennett, M. (2012). Aging and atherosclerosis: mechanisms, functional consequences, and potential therapeutics for cellular senescence. Circ Res *111*, 245-259.

Wang, S., Liu, R., Yu, Q., Dong, L., Bi, Y., and Liu, G. (2019). Metabolic reprogramming of macrophages during infections and cancer. Cancer Lett *452*, 14-22.

Wang, S., Zhang, M., Liang, B., Xu, J., Xie, Z., Liu, C., Viollet, B., Yan, D., and Zou, M.H. (2010). AMPKalpha2 deletion causes aberrant expression and activation of NAD(P)H oxidase and consequent endothelial dysfunction in vivo: role of 26S proteasomes. Circ Res *106*, 1117-1128.

Wang, Y., Su, M.A., and Wan, Y.Y. (2011). An essential role of the transcription factor GATA-3 for the function of regulatory T cells. Immunity *35*, 337-348.

Wang, Y., Zhou, L., Li, Y., Guo, L., Zhou, Z., Xie, H., Hou, Y., and Wang, B. (2017). The Effects of Berberine on Concanavalin A-Induced Autoimmune Hepatitis (AIH) in Mice and the Adenosine 5'-

Monophosphate (AMP)-Activated Protein Kinase (AMPK) Pathway. Med Sci Monit *23*, 6150-6161.

Wang, Z., Wilson, W.A., Fujino, M.A., and Roach, P.J. (2001). Antagonistic controls of autophagy and glycogen accumulation by Snf1p, the yeast homolog of AMP-activated protein kinase, and the cyclin-dependent kinase Pho85p. Mol Cell Biol *21*, 5742-5752.

Watson, M.J., Vignali, P.D.A., Mullett, S.J., Overacre-Delgoffe, A.E., Peralta, R.M., Grebinoski, S., Menk, A.V., Rittenhouse, N.L., DePeaux, K., Whetstone, R.D*., et al.* (2021). Metabolic support of tumour-infiltrating regulatory T cells by lactic acid. Nature *591*, 645-651.

Weerasekara, V.K., Panek, D.J., Broadbent, D.G., Mortenson, J.B., Mathis, A.D., Logan, G.N., Prince, J.T., Thomson, D.M., Thompson, J.W., and Andersen, J.L. (2014). Metabolic-stress-induced rearrangement of the 14-3-3zeta interactome promotes autophagy via a ULK1- and AMPK-regulated 14-3-3zeta interaction with phosphorylated Atg9. Mol Cell Biol *34*, 4379-4388.

Wiley, C.D., Velarde, M.C., Lecot, P., Liu, S., Sarnoski, E.A., Freund, A., Shirakawa, K., Lim, H.W., Davis, S.S., Ramanathan, A*., et al.* (2016). Mitochondrial Dysfunction Induces Senescence with a Distinct Secretory Phenotype. Cell Metab *23*, 303-314.

Wing, J.B., Tanaka, A., and Sakaguchi, S. (2019). Human FOXP3(+) Regulatory T Cell Heterogeneity and Function in Autoimmunity and Cancer. Immunity *50*, 302-316.

Wolf, D., and Ley, K. (2019). Immunity and Inflammation in Atherosclerosis. Circ Res *124*, 315-327.

Woods, A., Johnstone, S.R., Dickerson, K., Leiper, F.C., Fryer, L.G., Neumann, D., Schlattner, U., Wallimann, T., Carlson, M., and Carling, D. (2003). LKB1 is the upstream kinase in the AMP-activated protein kinase cascade. Curr Biol *13*, 2004-2008.

Wu, C.M., Zheng, L., Wang, Q., and Hu, Y.W. (2020). The emerging role of cell senescence in atherosclerosis. Clin Chem Lab Med *59*, 27-38.

Wu, D., Luo, Y., Guo, W., Niu, Q., Xue, T., Yang, F., Sun, X., Chen, S., Liu, Y., Liu, J*., et al.* (2017). Lkb1 maintains Treg cell lineage identity. Nat Commun *8*, 15876.

Wu, N., Zheng, B., Shaywitz, A., Dagon, Y., Tower, C., Bellinger, G., Shen, C.H., Wen, J., Asara, J., McGraw, T.E*., et al.* (2013). AMPK-dependent degradation of TXNIP upon energy stress leads to enhanced glucose uptake via GLUT1. Mol Cell *49*, 1167-1175.

Wu, Z., Puigserver, P., Andersson, U., Zhang, C., Adelmant, G., Mootha, V., Troy, A., Cinti, S., Lowell, B., Scarpulla, R.C*., et al.* (1999). Mechanisms controlling mitochondrial biogenesis and respiration through the thermogenic coactivator PGC-1. Cell *98*, 115-124.

Xiao, B., Heath, R., Saiu, P., Leiper, F.C., Leone, P., Jing, C., Walker, P.A., Haire, L., Eccleston, J.F., Davis, C.T*., et al.* (2007). Structural basis for AMP binding to mammalian AMP-activated protein kinase. Nature *449*, 496-500.

Xiao, B., Sanders, M.J., Carmena, D., Bright, N.J., Haire, L.F., Underwood, E., Patel, B.R., Heath, R.B., Walker, P.A., Hallen, S*., et al.* (2013). Structural basis of AMPK regulation by small molecule activators. Nat Commun *4*, 3017.

Xie, Z., Zhang, J., Wu, J., Viollet, B., and Zou, M.H. (2008). Upregulation of mitochondrial uncoupling protein-2 by the AMP-activated protein kinase in endothelial cells attenuates oxidative stress in diabetes. Diabetes *57*, 3222-3230.

Xiong, Y., Wang, L., Di Giorgio, E., Akimova, T., Beier, U.H., Han, R., Trevisanut, M., Kalin, J.H., Cole, P.A., and Hancock, W.W. (2020). Inhibiting the coregulator CoREST impairs Foxp3+ Treg function and

promotes antitumor immunity. J Clin Invest *130*, 1830-1842.

Xu, F., Cui, W.Q., Wei, Y., Cui, J., Qiu, J., Hu, L.L., Gong, W.Y., Dong, J.C., and Liu, B.J. (2018). Astragaloside IV inhibits lung cancer progression and metastasis by modulating macrophage polarization through AMPK signaling. J Exp Clin Cancer Res *37*, 207.

Yan, Y., Zhou, X.E., Xu, H.E., and Melcher, K. (2018). Structure and Physiological Regulation of AMPK. Int J Mol Sci *19*.

Yang, J., Wei, P., Barbi, J., Huang, Q., Yang, E., Bai, Y., Nie, J., Gao, Y., Tao, J., Lu, Y.*, et al.* (2020). The deubiquitinase USP44 promotes Treg function during inflammation by preventing FOXP3 degradation. EMBO Rep *21*, e50308.

Yang, K., Blanco, D.B., Neale, G., Vogel, P., Avila, J., Clish, C.B., Wu, C., Shrestha, S., Rankin, S., Long, L.*, et al.* (2017). Homeostatic control of metabolic and functional fitness of Treg cells by LKB1 signalling. Nature *548*, 602-606.

Yin, Y., Li, X., Sha, X., Xi, H., Li, Y.F., Shao, Y., Mai, J., Virtue, A., Lopez-Pastrana, J., Meng, S.*, et al.* (2015). Early hyperlipidemia promotes endothelial activation via a caspase-1-sirtuin 1 pathway. Arterioscler Thromb Vasc Biol *35*, 804-816.

Yosef, R., Pilpel, N., Tokarsky-Amiel, R., Biran, A., Ovadya, Y., Cohen, S., Vadai, E., Dassa, L., Shahar, E., Condiotti, R.*, et al.* (2016). Directed elimination of senescent cells by inhibition of BCL-W and BCL-XL. Nat Commun *7*, 11190.

Younes, S.A., Talla, A., Pereira Ribeiro, S., Saidakova, E.V., Korolevskaya, L.B., Shmagel, K.V., Shive, C.L., Freeman, M.L., Panigrahi, S., Zweig, S.*, et al.* (2018). Cycling CD4+ T cells in HIV-infected immune nonresponders have mitochondrial dysfunction. J Clin Invest *128*, 5083-5094.

Yu, H., Huang, J., Liu, Y., Ai, G., Yan, W., Wang, X., and Ning, Q. (2010). IL-17 contributes to autoimmune hepatitis. J Huazhong Univ Sci Technolog Med Sci *30*, 443-446.

Yuan, X.L., Chen, L., Li, M.X., Dong, P., Xue, J., Wang, J., Zhang, T.T., Wang, X.A., Zhang, F.M., Ge, H.L.*, et al.* (2010). Elevated expression of Foxp3 in tumor-infiltrating Treg cells suppresses T-cell proliferation and contributes to gastric cancer progression in a COX-2-dependent manner. Clin Immunol *134*, 277-288.

Zappasodi, R., Serganova, I., Cohen, I.J., Maeda, M., Shindo, M., Senbabaoglu, Y., Watson, M.J., Leftin, A., Maniyar, R., Verma, S.*, et al.* (2021). CTLA-4 blockade drives loss of Treg stability in glycolysis-low tumours. Nature *591*, 652-658.

Zemanovic, S., Ivanov, M.V., Ivanova, L.V., Bhatnagar, A., Michalkiewicz, T., Teng, R.J., Kumar, S., Rathore, R., Pritchard, K.A., Jr., Konduri, G.G.*, et al.* (2018). Dynamic Phosphorylation of the C Terminus of Hsp70 Regulates the Mitochondrial Import of SOD2 and Redox Balance. Cell Rep *25*, 2605-2616 e2607.

Zhang, F., Bazzar, W., Alzrigat, M., and Larsson, L.G. (2021). Methods to Study Myc-Regulated Cellular Senescence: An Update. Methods Mol Biol *2318*, 241-254.

Zhang, J., Xie, Z., Dong, Y., Wang, S., Liu, C., and Zou, M.H. (2008). Identification of nitric oxide as an endogenous activator of the AMP-activated protein kinase in vascular endothelial cells. J Biol Chem *283*, 27452-27461.

Zhang, L., Chen, D., Tu, Y., Sang, T., Pan, T., Lin, H., Cai, C., Jin, X., Wu, F., Xu, L.*, et al.* (2022). Vitexin attenuates autoimmune hepatitis in mouse induced by syngeneic liver cytosolic proteins via

activation of AMPK/AKT/GSK-3beta/Nrf2 pathway. Eur J Pharmacol *917*, 174720.

Zhang, Z., Li, F., Tian, Y., Cao, L., Gao, Q., Zhang, C., Zhang, K., Shen, C., Ping, Y., Maimela, N.R., *et al.* (2020). Metformin Enhances the Antitumor Activity of CD8(+) T Lymphocytes via the AMPK-miR-107-Eomes-PD-1 Pathway. J Immunol *204*, 2575-2588.

Zhao, L., Tang, Y., You, Z., Wang, Q., Liang, S., Han, X., Qiu, D., Wei, J., Liu, Y., Shen, L., *et al.* (2011). Interleukin-17 contributes to the pathogenesis of autoimmune hepatitis through inducing hepatic interleukin-6 expression. PLoS One *6*, e18909.

Zhao, Y., Hu, X., Liu, Y., Dong, S., Wen, Z., He, W., Zhang, S., Huang, Q., and Shi, M. (2017). ROS signaling under metabolic stress: cross-talk between AMPK and AKT pathway. Mol Cancer *16*, 79.

Zheng, J., Liu, Y., Qin, G., Lam, K.T., Guan, J., Xiang, Z., Lewis, D.B., Lau, Y.L., and Tu, W. (2011). Generation of human Th1-like regulatory CD4+ T cells by an intrinsic IFN-gamma- and T-bet-dependent pathway. Eur J Immunol *41*, 128-139.

Zheng, Y., Delgoffe, G.M., Meyer, C.F., Chan, W., and Powell, J.D. (2009). Anergic T cells are metabolically anergic. J Immunol *183*, 6095-6101.

Zhou, X., Bailey-Bucktrout, S.L., Jeker, L.T., Penaranda, C., Martinez-Llordella, M., Ashby, M., Nakayama, M., Rosenthal, W., and Bluestone, J.A. (2009). Instability of the transcription factor Foxp3 leads to the generation of pathogenic memory T cells in vivo. Nat Immunol *10*, 1000-1007.

Zhu, H., Liu, Z., An, J., Zhang, M., Qiu, Y., and Zou, M.H. (2021). Activation of AMPKalpha1 is essential for regulatory T cell function and autoimmune liver disease prevention. Cell Mol Immunol *18*, 2609-2617.

Zhu, W., and Liu, S. (2020). The role of human cytomegalovirus in atherosclerosis: a systematic review. Acta Biochim Biophys Sin (Shanghai) *52*, 339-353.

Zhu, Y.P., Brown, J.R., Sag, D., Zhang, L., and Suttles, J. (2015). Adenosine 5'-monophosphate-activated protein kinase regulates IL-10-mediated anti-inflammatory signaling pathways in macrophages. J Immunol *194*, 584-594.

Zmijewski, J.W., Banerjee, S., Bae, H., Friggeri, A., Lazarowski, E.R., and Abraham, E. (2010). Exposure to hydrogen peroxide induces oxidation and activation of AMP-activated protein kinase. J Biol Chem *285*, 33154-33164.

Zou, M.H., Hou, X.Y., Shi, C.M., Kirkpatick, S., Liu, F., Goldman, M.H., and Cohen, R.A. (2003). Activation of 5'-AMP-activated kinase is mediated through c-Src and phosphoinositide 3-kinase activity during hypoxia-reoxygenation of bovine aortic endothelial cells. Role of peroxynitrite. J Biol Chem *278*, 34003-34010.

7 Vitae

Junqing An

Georgia State University
Institute for Biomedical Sciences
e-mail: jan14@student.gsu.edu

Positions and Employment

2017-2022	**Georgia State University, Atlanta, Georgia, U.S.** Research Assistant
2015-2017	**China Agriculture University, Beijing, China** Research Assistant, Department of Basic Veterinary Medicine

Education

2017-2022	**Georgia State University, Atlanta, Georgia, U.S.** Ph.D., Translational Biomedical Sciences
2015-2017	**China Agriculture University, Beijing, China** MS, College of Veterinary Medicine
2010-2015	**Northwest A&F University, Shanxi, China** BS, College of Veterinary Medicine

Honors and Awards

2015-2017	Graduate Student Assistant Scholarships from College of Veterinary Medicine. (China Agriculture University, Beijing, China)
2016	National Scholarship for Graduate Student, China Agriculture University, China
2017-2021	Doctoral Scholarship of China Scholarship Council

Publications

1. **An J**, Ding Y, Yu C, Li J, You S, Liu Z, Song P, Zou MH. AMP-activated protein kinase alpha1 promotes tumor development via FOXP3 elevation in tumor-infiltrating Treg cells. iScience. 2021 Dec 4;25(1):103570.
2. Zhu H*, Liu Z*, **An J***, Zhang M, Qiu Y, Zou MH. Activation of AMPKα1 is essential for regulatory T cell function and autoimmune liver disease prevention. Cell Mol Immunol. 2021 Dec;18(12):2609-2617. (* equal contribution)

3. **An J**, Zhao X, Wang Y, Noriega J, Gewirtz AT, Zou J. Western-style diet impedes colonization and clearance of Citrobacter rodentium. PLoS Pathog. 2021 Apr 5;17(4): e1009497.
4. Song P, **An J**, Zou MH. Immune Clearance of Senescent Cells to Combat Ageing and Chronic Diseases. Cells. 2020 Mar 10;9(3):671.
5. Ding Y, Han Y, Lu Q, **An J**, Zhu H, Xie Z, Song P, Zou MH. Peroxynitrite-Mediated SIRT (Sirtuin)-1 Inactivation Contributes to Nicotine-Induced Arterial Stiffness in Mice. Arterioscler Thromb Vasc Biol. 2019 Jul;39(7):1419-1431.
6. Tian J, Shi R, Xiao P, Liu T, She R, Wu Q, **An J**, Hao W, Soomro M. Hepatitis E Virus Induces Brain Injury Probably Associated With Mitochondrial Apoptosis. Front Cell Infect Microbiol. 2019 Dec 20; 9:433.
7. Tian J, Shi R, Liu T, She R, Wu Q, **An J**, Hao W, Soomro MH. Brain Infection by Hepatitis E Virus Probably via Damage of the Blood-Brain Barrier Due to Alterations of Tight Junction Proteins. Front Cell Infect Microbiol. 2019 Mar 19; 9:52.
8. **An J**, Liu T, She R, Wu Q, Tian J, Shi R, Hao W, Ren X, Yang Y, Lu Y, Yang Y, Wu Y. Replication of hepatitis E virus in the ovary and promotion of oocyte apoptosis in rabbits infected with HEV-4. Oncotarget. 2017 Dec 17;9(4):4475-4484.
9. Wu Q, **An J**, She R, Shi R, Hao W, Soomro M, Yuan X, Yang J, Wang J. Detection of Genotype 4 Swine Hepatitis E Virus in Systemic Tissues in Cross-Species Infected Rabbits. PLoS One. 2017 Jan 27;12(1): e0171277.
10. Tang J, Wu Q, Tang X, Shi R, Suo J, Huang G, **An J**, Wang J, Yang J, Hao W, She R, Suo X. Development of a vivo rabbit ligated intestinal Loop Model for HCMV infection. J Anim Sci Biotechnol. 2016 Dec 13; 7:69.